UiT

THE ARCTIC UNIVERSITY OF NORWAY

Faculty of Science and Technology

Octaiodoporphyrin and Octaiodocorrole: Isolation of a *Cis* Porphyrin Tautomer

—

Ivar Kristian Thomassen

A dissertation for the degree of Philosophiae Doctor – May 2018

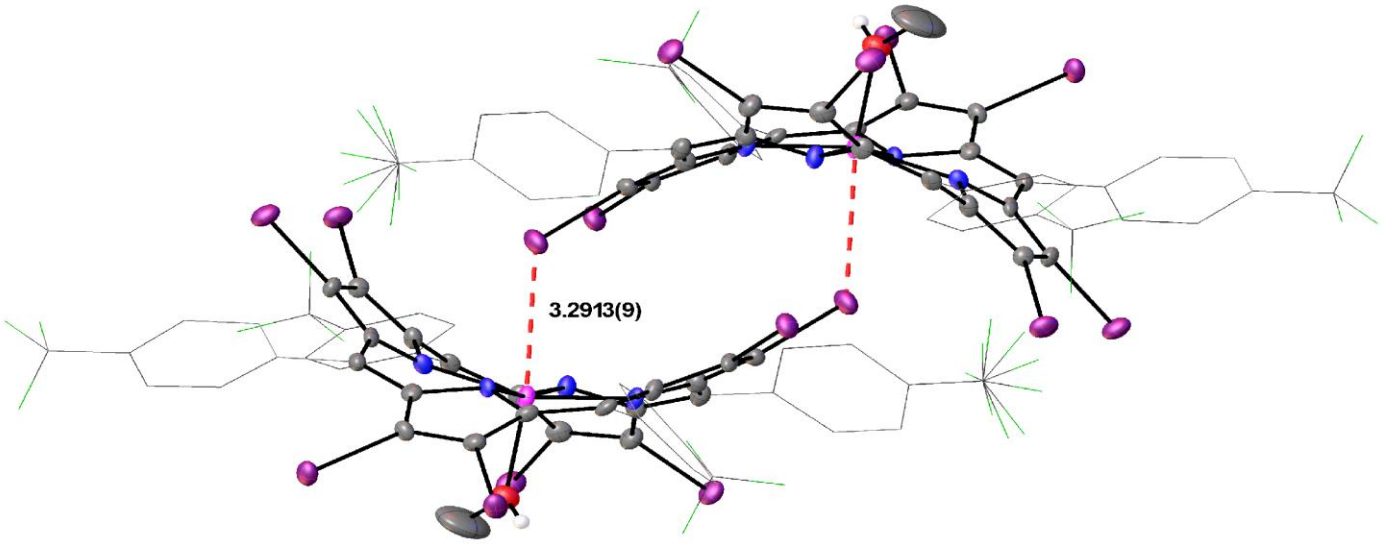

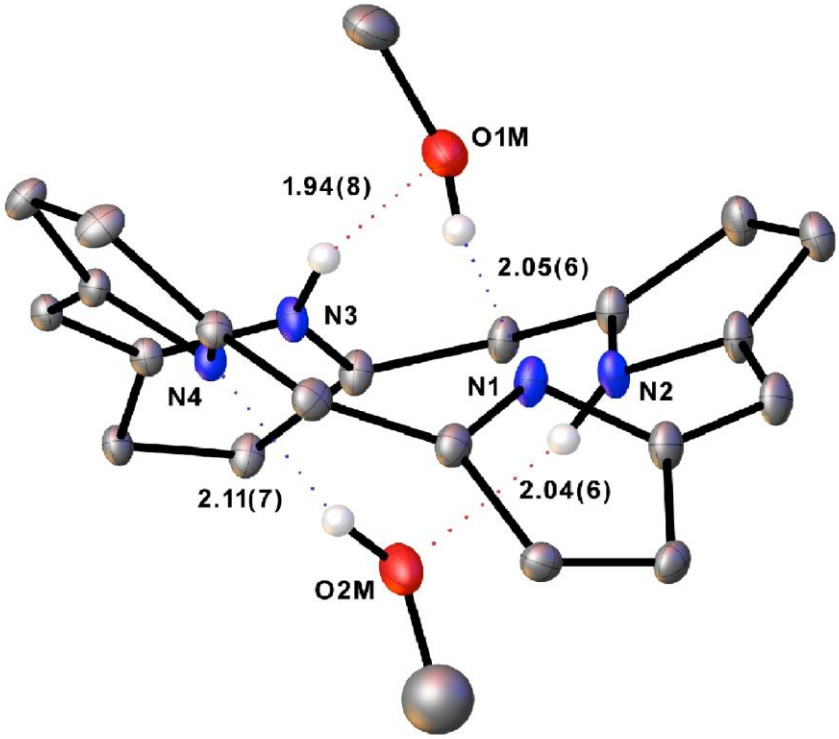

UNIVERSITY OF TROMSØ

A dissertation for the degree of Philosophiae Doctor

Octaiodoporphyrin and Octaiodocorrole: Isolation of a *Cis* Porphyrin Tautomer

Ivar Kristian Thomassen

Department of Chemistry

Faculty of Science and Technology

UiT – The Arctic University of Norway

Tromsø, Norway

Acknowledgements

I would like to express my deepest gratitude and appreciation to my advisor and friend Prof. Abhik Ghosh for giving me the opportunity to conduct the research described herein, and for letting me pursue my exuberant ideas. His guidance and expertise has assisted and motivated me greatly during these past four years, and has sparked a keen interest for porphyrin and corrole chemistry within me.

My sincere thanks also go to the senior researchers in our group, Dr. Abraham Alemayehu and Dr. Thomas Kolle, for their unfaltering support and willingness to share their wealth of expertise. They are truly some of my best friends, and I have shared many wonderful conversations and laughs with them. I also want to extend my deepest thanks to my fellow group members, with whom I have also become close friends with during my years as a PhD fellow – Simon, Rune, Hans-Kristian, Sumit, Hugo, Jan and Harald. We have shared many laughs and great conversations, and together imbibed more beers than I can count!

I am also profoundly grateful to Prof. Tore Lejon, for introducing me to the wonders of chemistry when I was still working towards my BSc. I also wish to thank Truls, Jostein, Fred and Arnfinn for their help with spectroscopic analyses and administrative tasks, and for their friendship. I also wish to thank Yngve for his friendship during my years at the fourth floor of the Department of Chemistry.

I also wish to thank our collaborators, Dr. Laura J. McCormick, Dr. Kevin J Gagnon, Dr. Hugo Vasquez-Lima, and Prof. Sergey Borisov for their specific contributions to aspects of this work.

Lastly, I wish to thank my family, in particular my girlfriend Emilie, and friends for their steadfast support and encouragement.

Ivar Kristian Thomassen
Tromsø, May 14, 2018.

Preface

Iodinated aromatics are excellent starting materials for further elaboration via transition-metal-catalyzed cross-coupling reactions such as the Suzuki, Heck, Stille, Kumada, Negishi, Hiyama and Sonogashira reactions. The synthetic potential of *β*-polyiodinated or octaiodinated porphyrins and corroles may thus be considerable. *β*-Iodinated porphyrins and corroles are expected to be more reactive compared with their *β*-brominated congeners, thus potentially allowing for new reactivity.

As part of my doctoral studies, I have synthesized and characterized the first examples of both *β*-octaiodinated porphyrins (**Paper A**) and *β*-octaiodinated corroles (**Paper C**). The syntheses required careful optimization, which ultimately led to products that were characterized by single-crystal X-ray structure determinations. Thus, Ni, Cu, and Zn *β*-octaiodoporphyrins and a Cu *β*-octaiodocorrole were synthesized and structurally characterized.

I was also intrigued by the highly electron-rich character of Ir(III) corroles and their propensity to readily undergo *β*-octabromination. Unfortunately, experiments aimed at polyiodination of six-coordinate Ir corroles failed to engender pure compounds within the time available to me. Nevertheless, several six-coordinate Ir(III) corroles with different nitrogen axial ligands were synthesized, of which three were structurally characterized. The phosphorescence behavior of a series of Ir(III) corroles was examined, but no major variation was found among the compounds examined.

While work on Ir(III) corroles was in progress, a fellow group member (Dr. Kolle E. Thomas) reported unambiguous structural evidence of the first *cis* tautomer of a free-base porphyrin in the form of the dihydrate of a highly saddled free-base *β*-heptakis(trifluoromethyl)-*meso*-tetraarylporphyrin. I was intrigued by the question whether additional *cis* tautomeric structures might eventuate when other highly saddled porphyrins are crystallized from appropriate amphiprotic solvents. This proved to be a long and tedious venture, but I was ultimately rewarded with discovering a second example of a *cis* porphyrin tautomer, this time in the form of a doubly hydrated, highly saddled, free-base *β*-octaiodoporphyrin (**Paper B**).

I was happy to steer the direction of my research entirely according to my own curiosity, with full support of my advisor and in the spirit of academic freedom embodied by the Research Council of Norway's FRIPRO program, which supported me. This meant that I

did not get a chance to investigate the synthetic potential of the polyiodinated macrocycles that I had synthesized. Other groups meanwhile have confirmed the considerable synthetic utility of polyiodinated porphyrinoid systems.

The main body of the thesis consists of three introductory chapters on (1) Introduction to Porphyrins and Corroles, (2) Synthesis of Porphyrins and Corroles, and (3) Functionalization of Porphyrins and Corroles, followed by brief introductions to and copies of my papers, and a report on my work on Ir(III) corroles.

Table of Contents

Chapter 7 – Synthesis, Characterization and Photophysical Properties of a Series of Six-Coordinated Iridium(III) Corroles.

List of Abbreviations

AcOH	acetic acid
BuLi	butyl lithium
Cod	cyclooctadiene
CV	cyclic voltammogram
DCM	dichloromethane
DDQ	2,3-dichloro-5,6-dicyano-1,4-benzoquinone
DMA	dimethylacetamide
DMAP	4-(dimethylamino)pyridine
DMSO	dimethyl sulfoxide
DPM	dipyrromethane
EtOAc	ethyl acetate
H_2	hydrogen gas (diatomic)
HOMO	highest occupied molecular orbital
IR	infrared spectroscopy
LUMO	lowest unoccupied molecular orbital
MeCN	acetonitrile
MeOH	methanol
NBS	*N*-bromosuccinimide
NCS	*N*-chlorosuccinimide
NIH	1,3-diiodo-5,5-dimethylhydantoin
NIS	*N*-iodosuccinimide
NMR	nuclear magnetic resonance
PDT	photodynamic therapy
Py	pyridine
r.t.	room temperature
SET	single electron transfer
TFA	trifluoroacetic acid
Tma	trimethylamine
TPC	5,10,15-triphenylcorrole
TPFPC	5,10,15-tris(pentafluorophenyl)corrole
TPFPP	5,10,15,20-tetrakis(pentafluorophenyl)porphyrin

TPP	5,10,15,20-tetraphenylporphyrin
UV-vis	ultraviolet-visible spectroscopy

Chapter 1 – Introduction to Porphyrins and Corroles

1.1. General structure and properties of porphyrins

Porphyrins are brightly colored tetrapyrrolic macrocyclic compounds that occur widely in biological systems. The word porphyrin derives from the ancient Greek word πορφύρα (porphyra), which translates to "purple", the color of a typical uncomplexed porphyrin. Hemes are iron-coordinated porphyrins found in many proteins, which are called hemoproteins that play a critical role in a multitude of bioprocesses. Their key biological functions include oxygen transport and storage (hemo- and myoglobin), dioxygen activation and utilization (cytochrome P-450 and cytochrome oxidase), electron transport (cytochromes *b* and *c*), gas sensing (FixL, CooA and soluble guanylate cyclase), detoxification, signal transduction, microRNA (ribonucleic acid) processing and circadian clock management.[1-3] The green pigments responsible for the photosynthesis in plants and certain photosynthetic organisms, chlorophylls and bacteriochlorophylls, contains a magnesium coordinated to modified porphyrins called chlorin/bacteriochlorin (**Figure 1**). Chlorins are essentially porphyrins where one of the pyrrolic double bonds have been reduced.

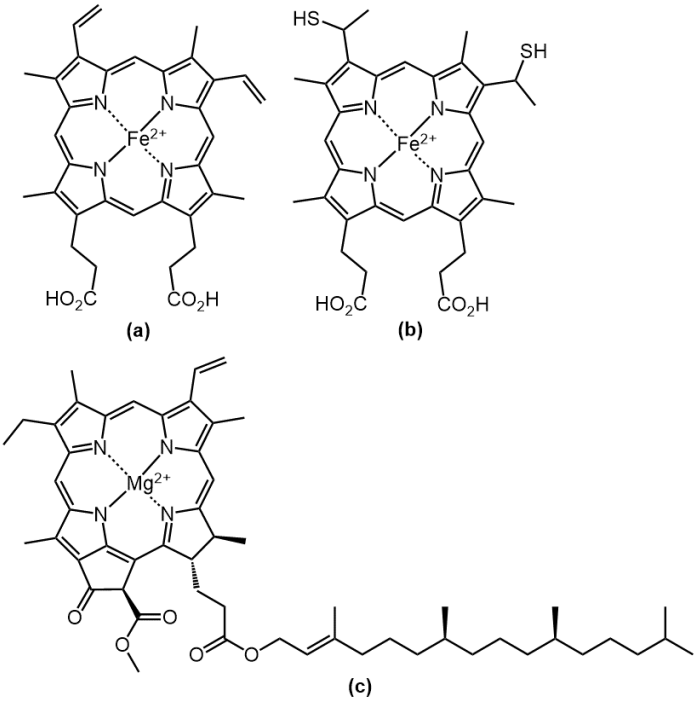

Figure 1. (a) Structure of heme *b* found in hemo- and myoglobin. (b) Structure of heme *c* found in cytochrome *c*. (c) Structure of chlorophyll *a* found in plants and photosynthetic organisms.

The four pyrrole rings of a porphyrin are bridged by four methine (=CH-) groups. The pyrrole carbons adjacent to the nitrogens are referred to as α-carbons, while the outer pyrrole carbons are called β-carbons. The methine carbons are called *meso*-carbons. Unsubstituted porphyrin or porphine has been widely studied theoretically, but is rather insoluble and therefore of limited interest to experimentalists (**Figure 2**).[4] Porphyrins are clearly aromatic compounds and their aromaticity is often simply represented as arising out of an [18]-annulene substructure (Figure 2). More sophisticated theoretical treatments suggest a somewhat different picture that includes the entire macrocyclic skeleton, but the simple picture should be sufficient for the present discussion.[5] The aromaticity manifests itself both in the significant stability of porphyrins and in their intense colors and strong near-UV absorption.

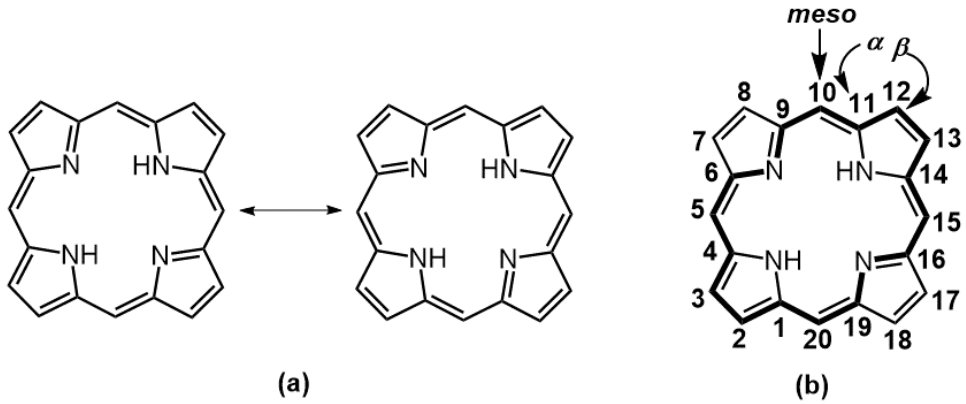

Figure 2. (a) Resonance structures of porphine. (b) Nomenclature and IUPAC atom numbering of porphyrins, the [18]-annulene substructure is marked in bold.

Neutral free-base (nonmetalated) porphyrins are amphoteric, which means the core nitrogens may be either protonated or deprotonated. Deprotonated (dianionic) porphyrins are, as we have already seen, effective ligands. Thus, metal complexes of such compounds exist for a vast majority of the metals and semi-metals (**Figure 3**).[6,7]

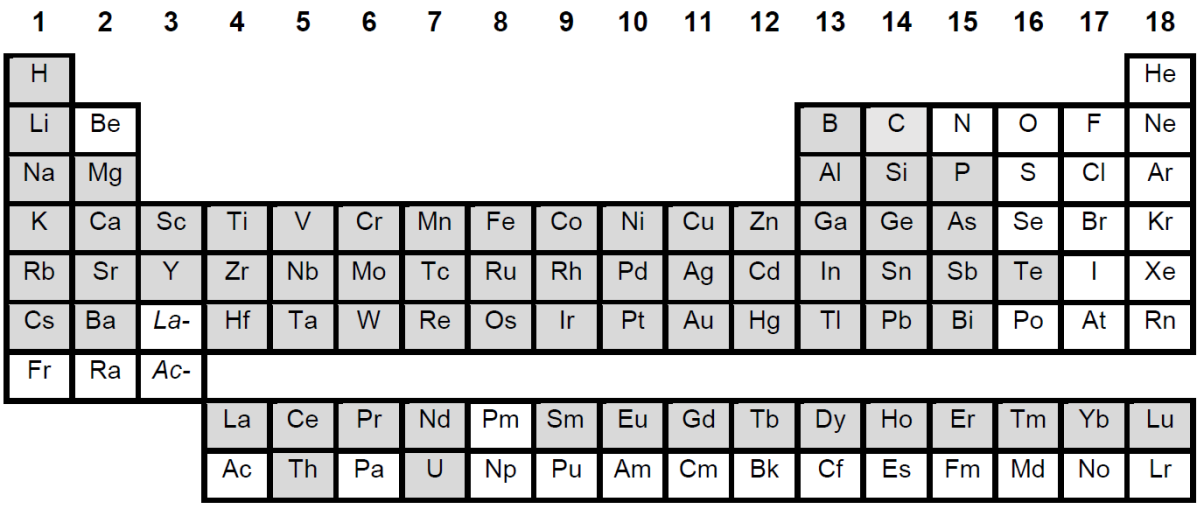

Figure 3. The periodic table of the porphyrins. Greyed elements indicate that the corresponding metalloporphyrin has been successfully synthesized.

Porphyrins are part of a much larger group of macrocycles known as porphyrinoids, which share structural, electronic, and optical characteristics to various extent. Examples include *N*-confused porphyrins,[8] heteroatom-substituted porphyrins,[9] cyclic oligopyrroles,[10] reduced porphyrins[11] (porphyrinogens, chlorins, bacteriochlorins, isobacteriochlorins), oxidized porphyrins,[12] expanded porphyrins[13,14] (penta-, hexa-, heptaphyrins, etc.) and contracted porphyrins[14-16] (triphyrins, subporphyrins, corroles, etc.). A selection of different porphyrinoids are depicted in **Figure 4**.

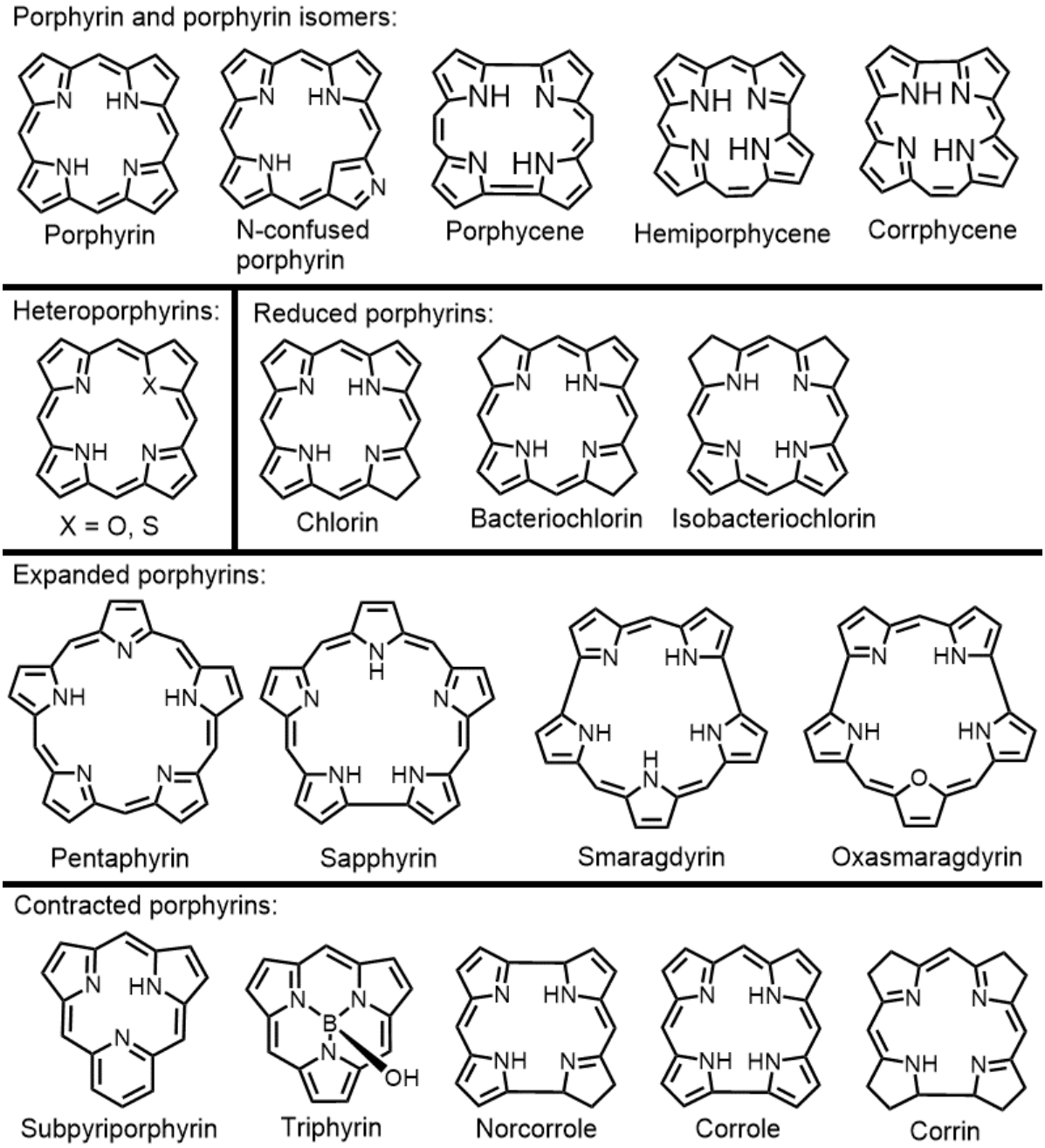

Figure 4. Examples of porphyrinoids.

1.2. General structure and properties of corroles

Amongst the porphyrinoids depicted in the preceding figure, corroles have been of particular interest in recent years due to their interesting coordination chemistry. Corroles are structurally similar to porphyrins, but lack one *meso*-carbon compared to their porphyrin analogues. While preserving aromaticity, this structural difference translates not only to a smaller molecular core but also three NH protons instead of the two that are found in porphyrins (**Figure 5**). The fully deprotonated corrole(3–) ligand can stabilize a variety of

transition metals in unusually high oxidation states. However, many formally high-valent metallocorroles are noninnocent, where the metal has a normal oxidation state and the corrole itself is partially or fully oxidized.[17,18]

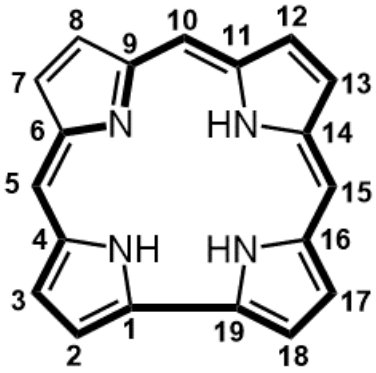

Figure 5. General structure of corroles with IUPAC numbering and the [18]-annulene structure in bold.

Unsurprisingly, like porphyrins, corroles are generally also vividly colored. No naturally occurring corroles have been observed to date. The name corrole, however, derives from corrin, itself a contraction of “contracted porphyrin", which is the macrocycle present in the cobalt-containing cofactor B_{12} (**Figure 6**). The intriguing photophysical and electronic properties, the ability to bind metals in various oxidation states, the ability to adopt different conformations, and the possibility of modulating desired properties through structural modifications, has made porphyrins and corroles useful for many different applications. These applications include catalysis (chemical and biomimetic), gas sensing, as dye sensitized solar cells, as photosensitizers in photodynamic therapy, as near infrared dyes, as optical materials and in nonlinear optics, and in supramolecular chemistry among others.[19-28]

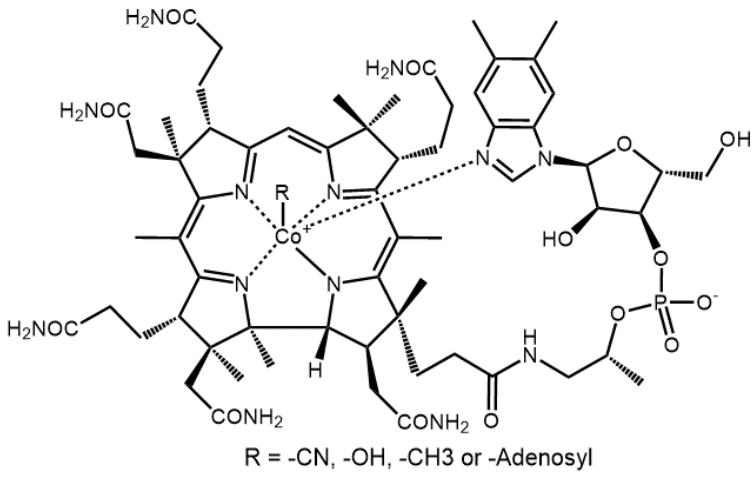

Figure 6. The general structure of cobalamin (vitamin B_{12}).

1.3. Nonplanarity in porphyrins

As aromatic compounds, porphyrins are expected to exhibit a planar conformation. Indeed, some of them are planar, but others adopt nonplanar conformations, usually as a result of one or more of the following factors:[29,30]

- Binding of an excessively small or large metal ion with a size mismatch to the porphyrin.
- Steric or electronic effects involving an axial or nitrogen bound ligand.
- Protonation of core nitrogens.
- Bulky substituents at the *meso*- and/or *β*-carbons causing the porphyrin to contort due to steric effects.

The four main types of nonplanar porphyrins (**Figure 7**) have been classified as being either domed, waved, ruffled or saddled (and combinations thereof).[31,32]

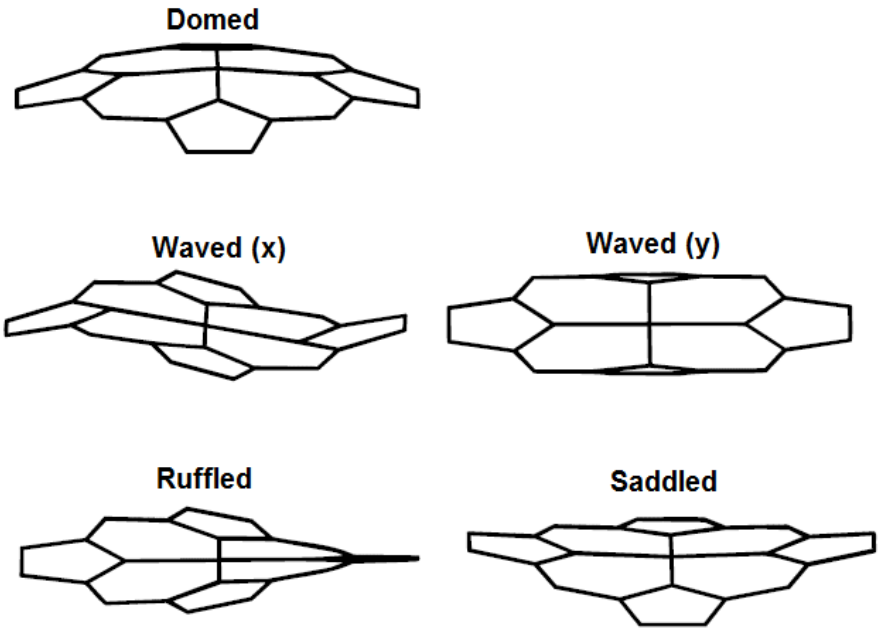

Figure 7. The nonplanar conformations of porphyrins. Adapted with permission from ref 32. Copyright 1998 Elsevier.

Domed conformations are often a result of the porphyrin coordinating a large metal ion, causing the metal to displace above the mean porphyrin plane while the *β*-carbons will be displaced below. Examples of porphyrins with domed conformations include *β*-octaethyl-5,10,15,20-tetrakis(nitro)porphyrinatothallium(III) (Tl[$(CH_2CH_3)_8$T*p*NO_2P])[33] and 5,10,15,20-tetrakis(*n*-Pr)porphyrinatolead(II) (Pb[TPrP]).[34] Porphyrins coordinated to other large metal ions like cadmium(II)[35] and bismuth(II)[36] have also been shown to exhibit domed conformations.

The uncommon waved conformation is characterized by the tilting of a pair of opposite pyrrole rings above or below the mean plane of the porphyrin, while the pair of opposite pyrroles are relatively unaffected. Examples of porphyrins with waved conformations are 5,10,15,20-tetrakis(2-thienylporphyrinato)zinc(II) (Zn[T(2-thienyl)P])[37] and *β*-octakis(4-fluorophenyl)-5,10,15,20-tetrakis(pentafluorophenyl)porphyrin (H_2[(*p*FP)$_8$TPFPP]).[38]

A ruffled conformation typically is observed when a pophyrin coordinates to a very small ion. Examples of this scenario include nickel porphyrins,[39] phosphorus(V) porphyrins[40] and certain low-spin iron(III) porphyrins,[41] causing the ring to contract and thus distort when the metal binds to the core nitrogens. Bulky substituents at the *meso*-carbons are also known to promote ruffled conformations. Examples include derivatives of *meso*-tetraisopropyl- and tetrakis(t-butyl)porphyrin.[42-44]

Saddling is characterized by alternate tilting of the pyrrole rings above and below the mean porphyrin plane. Saddling is mostly commonly observed for sterically hindered dodecasubstituted porphyrins such as *β*-octabromo-*meso*-tetraarylporphyrins and dodecaarylporphyrins.[45,46] In **Chapter 4** and **Paper A**, I will report *β*-octaiodo-*meso*-tetraarylporphyrins, which are some of the most saddled porphyrin derivatives reported to date. The degree of ruffling or saddling is determined from the dihedral angles. The angle at which two planes intersect is defined as the dihedral angle. For porphyrins and corroles, the planes are defined by two sets of three atoms, where two of the atoms are common (**Figure 8**).

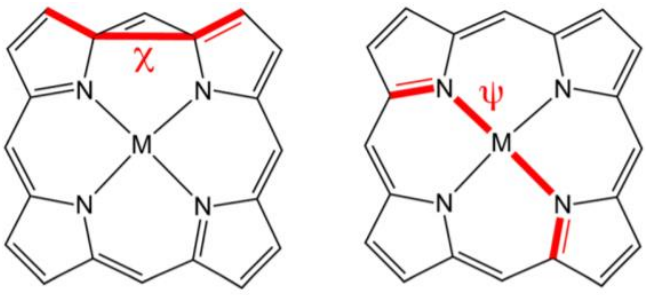

Figure 8. Ruffling (χ) and saddling (ψ) dihedrals.

1.4. Nonplanarity in corroles

The classification used for nonplanar porphyrins may also be applied for corroles. Corroles, however, do not display the same structural diversity as porphyrins do because of the increased ring strain. In essence, almost all metallocorroles are either planar or mildly

domed.[18] Curiously enough, some metallocorroles such as bis-trimethylamino-*β*-octabromo-5,10,15-tris(pentafluorophenylcorrolato)iridium(III) (Ir[Br_8TPFPC]tma_2)[47] and *β*-octabromo-5,10,15-tris(4-nitrophenylcorrolato)cobalt(III) (Co[Br_8TNO_2PC])[48] are essentially still planar even with considerable steric crowding. Free-base corroles on the other hands display pronounced nonplanar distortions. The crystal structure of the free-base corrole from the preceding example (*β*-octabromo-5,10,15-tris(pentafluorophenyl)corrole) exhibits strong nonplanar distortions. Dispersion-corrected DFT calculations has revealed that the main driving force behind these distortions is most likely related to steric effects between internal NH protons, as the presence of additional *β*-substituents only marginally adds to the effect.[49]

There are numerous examples of domed corroles reported. Examples include oxo-complexes of Mo(V), Tc(V) and Re(V), in addition to nitrido-complexes of Os(VI) and Ru(VI).[50-54]

Copper corroles are inherently saddled because of orbital interactions between corrole π-orbitals and metal d-orbitals. While peripheral steric crowding enhance this inherent nonplanar distortion,[55] the distortion is pronounced even in the absence of peripheral substituents. This inherent property can be explained in terms of a noninnocent corrole ligand with an overall electronic structure best described as a Cu(II)-corrole$^{\bullet 2-}$.[56] The only known example of a metallocorrole other than a copper corrole displaying strong saddling is *β*-octabromo-5,10,15-tris(4-methylphenylcorrolato)gold(II/III) (Ag[Br_8T*p*MePC]),[57] seemingly also because of a noninnocent corrole ligand. Interestingly, unhindered copper porphyrins with electron-donating substituents are also reported to be saddled.[58] Slight saddling has also been observed for other metallocorroles such as 5,10,15-tris(4-methylphenylcorrolato)silver(III) (Ag[T*p*MePC])[59] and chloro-*β*-octamethyl-5,10,15-tris(phenylcorrolato)iron(III) (Fe[OMTPC]Cl).[60] In **Chapter 6** and **Paper C**, I will report an example of a strongly saddled copper-*β*-octaiodo-*meso*-tetraarylcorrole.

So far, the wave conformation has not yet been observed for corroles. Theoretical calculations indicate that the ruffled conformation in corroles is energetically unfavorable, and as such only mild ruffling could be expected.[61] One of the few ruffled corroles reported to date, dimethoxo-*β*-heptabromo-5,10,15-tris(4-methylphenyl)corrolato]phosphorus(V) (P[Br_7T*p*MePC]$(OCH_3)_2$),[62] is known to exhibit mild ruffling.

1.5. NH tautomerism in porphyrins and corroles

Ever since the correct structural formula for the porphyrin nucleus was proposed and later proven,[63] it became apparent that NH tautomerism, which involves the migration of NH protons in the central cavity of the macrocycle, is a possibility (**Figure 9**). Based on simple analytical techniques such as ultraviolet-visible spectroscopy (UV-vis) and infrared spectroscopy (IR) it was eventually proposed that the *trans* tautomer was the major porphyrin tautomer. This makes sense from a steric point of view, as one would assume the central protons to position themselves as far away from each other as possible to minimize electrostatic repulsion. This notion was later proven using various analytical techniques such as solution- and solid-state nuclear magnetic resonance (NMR), laser induced fluorescence spectroscopy (LIF) and finally X-ray crystallography.[64] The interconversion between *trans* tautomers is rapid at room temperature and proceeds via the higher energy intermittent *cis* tautomer. It is now generally accepted, both theoretically and experimentally, that the tautomerization proceeds via consecutive single electron transfers, predominantly by direct electron tunneling between donor and acceptor.[65]

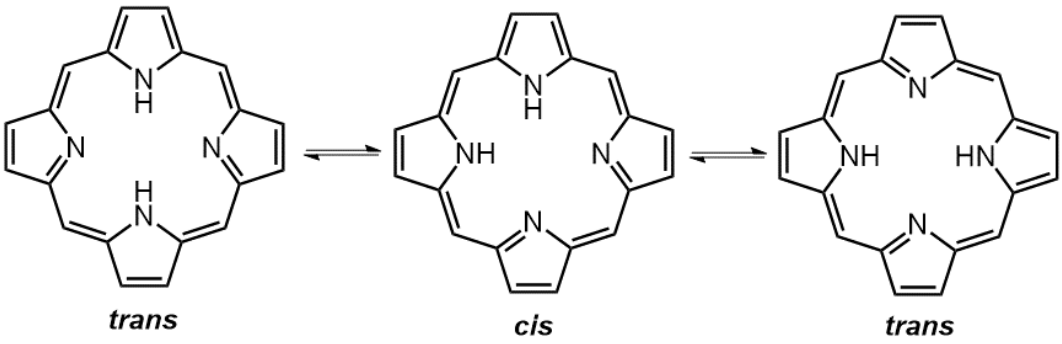

Figure 9. NH tautomerism in porphyrins.

NH tautomerism has also been documented for a number of other porphyrinoids. For example, for *N*-confused porphyrins, a tautomer with three central hydrogens predominates in nonpolar solvents, while one with two central hydrogens and an external NH hydrogen prevails in polar solvents (**Figure 10**).[66]

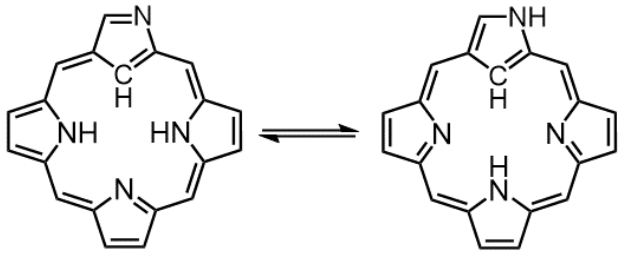

Figure 10. NH tautomerism in *N*-confused porphyrins.

Corroles also exhibit tautomers of comparable stability (**Figure 11**). For corroles with symmetrical A_3 or A_2B frameworks, only two tautomers are possible, while unsymmetrical corroles (ABC) engender four possible tautomers.[67] Given the nonplanarity resulting from electrostatic interactions between pyrrolic NH protons in a free-base corrole, the tautomers would be chiral as well. It is doubtful, however, that the enantiomers can be resolved.[49]

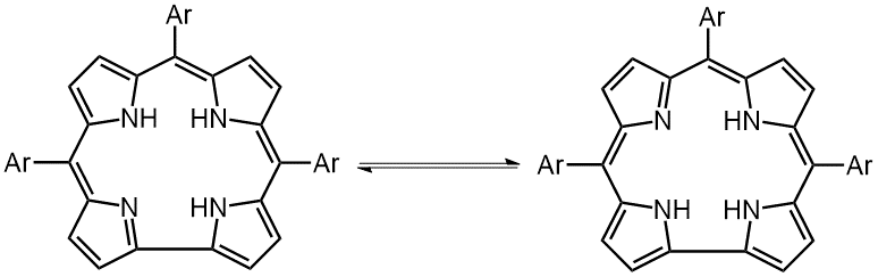

Figure 11. NH tautomerization in free-base corroles.

The study of proton transfer tautomerism in porphyrins and related macrocycles is of great interest because of their biological relevance. In **Chapter 5** and **Paper B**, I will report the structure of a stable *cis* tautomer of a sterically hindered free-base porphyrin, the long-sought intermediate of porphyrin tautomerism.

1.6. Electronic absorption spectra of porphyins and corroles

The conjugated π-system of porphyrins and corroles gives rise to strong absorptions in the near-UV and visible regions of the electromagnetic spectrum. A porphyrin or corrole generally produces a strong Soret (B) band in the near ultraviolet (~ 400 nm) and two to four weaker Q-bands absorbing in the visible region (~ 500-700 nm). **Figure 12** shows the UV-vis spectrum of free-base tetraphenylporphyrin (H_2[TPP]) while **Figure 13** shows the UV-vis spectrum of free-base triphenylcorrole (H_3[TPC]).

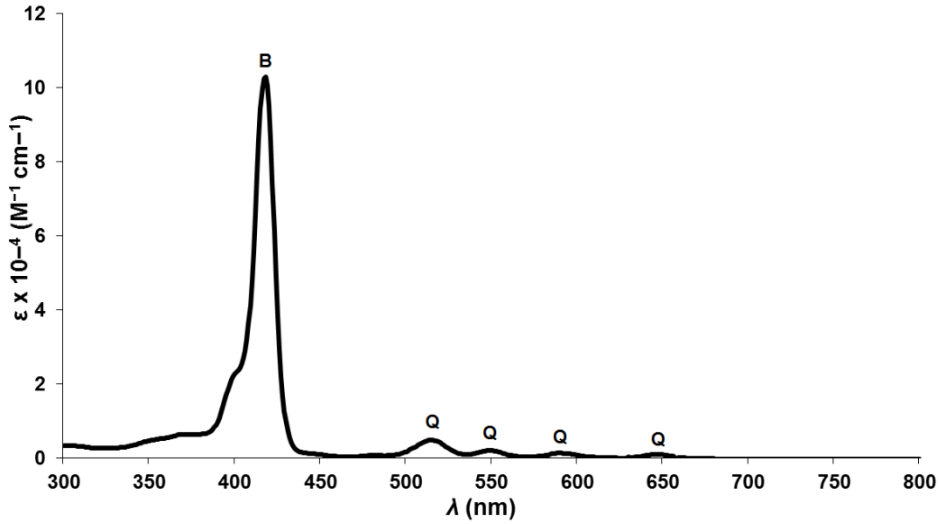

Figure 12. UV-vis spectrum of H_2[TPP].

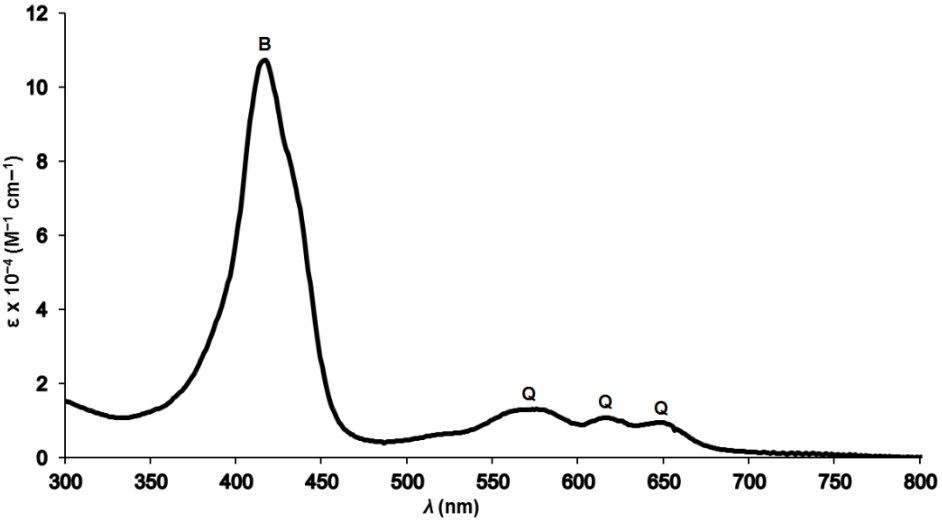

Figure 13. UV-vis spectrum of H_3[TPC].

Peripheral *β*- and *meso*-substitutions of the macrocycle or metal coordination, may lead to red- (bathochromic) or blue- (hypsochromic) shifted Soret and Q-bands in the UV-vis spectrum. Metal coordination typically also reduces the number of Q-bands as the molecule attains higher symmetry. **Figure 14** illustrates increasingly bathochromically shifted Soret and Q bands with increasing size of *β*-substituents for a series of nickel(II) *β*-octasubstituted porphyrins.

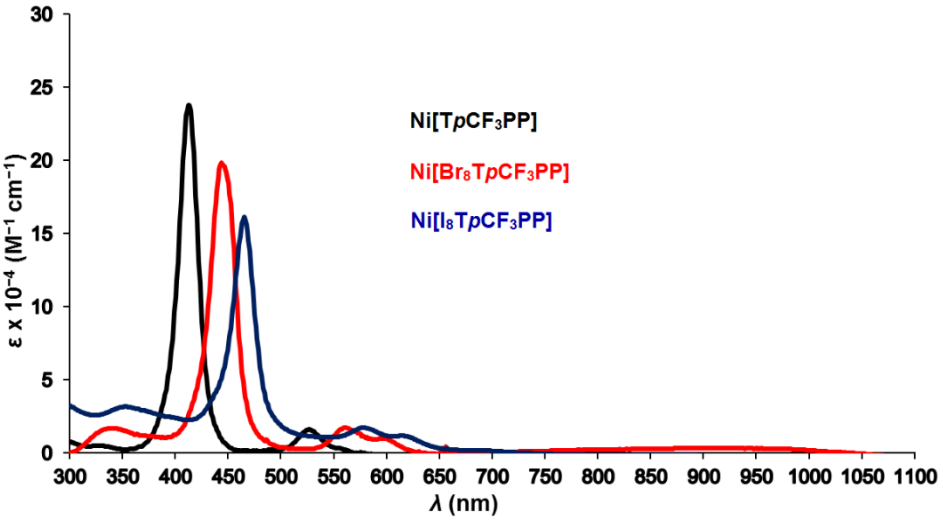

Figure 14. UV-vis spectra of Ni[T*p*CF_3PP], Ni[Br_8T*p*CF_3PP], and Ni[I_8T*p*CF_3PP].

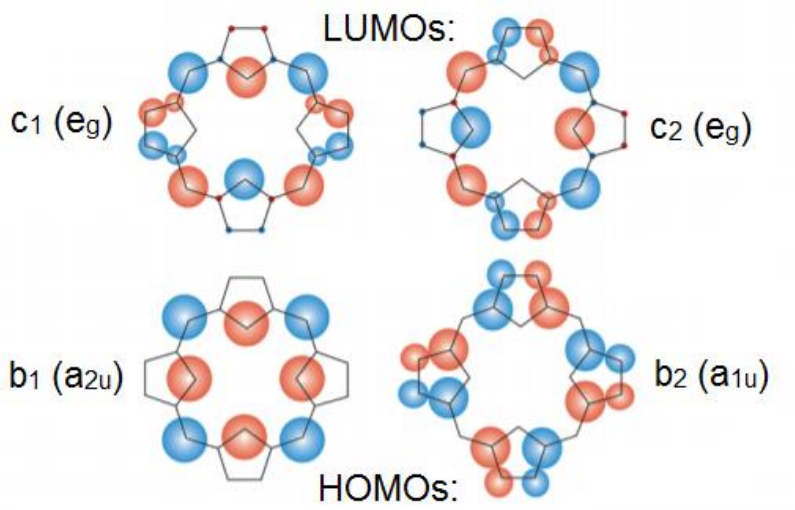

Figure 15. Gouterman's four orbital model for porphyrins (D_{4h}). Adapted with permission from ref 68. Copyright 2014 Royal Society of Chemistry.

The absorptions observed in the UV-vis spectra for porphyrins (D_{4h} symmetry) can be rationalized using Gouterman's "four orbital model". In this model the absorptions arise from electronic transitions between two sets of frontier orbitals – two degenerate HOMOs, denoted b_1 (a_{2u}) and b_2 (a_{1u}), and two degenerate LUMOs, c_1 (e_g) and c_2 (e_g) (**Figure 15**).[68] The relative size of the circles in the model signifies the orbital coefficient, which is the contribution from individual atomic orbitals making up the molecular orbital. As might be expected, the metal and the substituents on the porphyrin ring (*meso*- and *β*-substituents) affect the energies of the electronic transitions. Transitions between these molecular orbitals result in two pairs of

degenerate excited states, (both of ^1E_u symmetry), which corresponds to the lowest-energy Q band and the higher-energy Soret or B-band. The energy levels and associated electronic transitions of a porphyrin are schematically depicted in **Figure 16**.

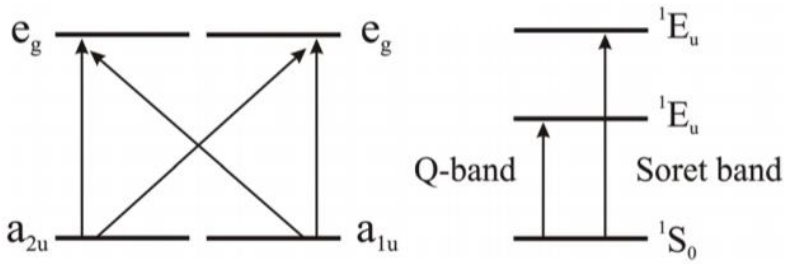

Figure 16. Porphyrin energy levels and electronic transitions. Adapted with permission from ref 68. Copyright 2014 Royal Society of Chemistry.

Quantum chemical calculations have shown that the "four orbital model" can also be applied for corroles.[69,70] Corroles have lower symmetry (C_{2v}) compared to porphyrins so the porphyrin a_{1u} and a_{2u} HOMOs transform as a_2 and b_1 for a corrole, while the porphyrin e_g LUMOs also split into b_1 and a_2 corrole LUMOs. The shapes of corrole frontier MOs remain qualitatively similar to those of porphyrins.

1.7. Fluorescence and phosphorescence in porphyrins and corroles

Porphyrin-type molecules exhibit a rich array of photophysical properties, of which fluorescence and phosphorescence are the two most important. Photophysical properties are generally schematically represented by a Jablonski diagram, in which the states are ordered vertically by energy and horizontally by spin multiplicity. A simplified Jablonski diagram is illustrated in **Figure 17**. Nonradiative transitions are indicated by squiggly arrows and radiative transitions by straight arrows. For typical aromatic molecules, light absorption typically occurs in about 1 fs, while fluorescence emission occurs on a time scale of about 10 ns. The significant lifetime of the fluorescent state allows for vibrational relaxation and, accordingly, the fluorescence emission nearly always has a lower energy than the absorption, the difference in energy (typically expressed in nm) is known as the Stokes shift. The singlet excited state may also transition to a triplet state, which typically has lower energy, in a process called intersystem crossing. Intersystem crossing is greatly accelerated in systems with large spin-orbit coupling, such as in heavy element compounds. Intersystem crossing may be followed by phosphorescence, which refers to the decay of the triplet state to the

singlet ground state. Because of its spin-forbidden nature, phosphorescence is much slower than fluorescence, with a time scale ranging from hundreds of μs to days or even longer.[71]

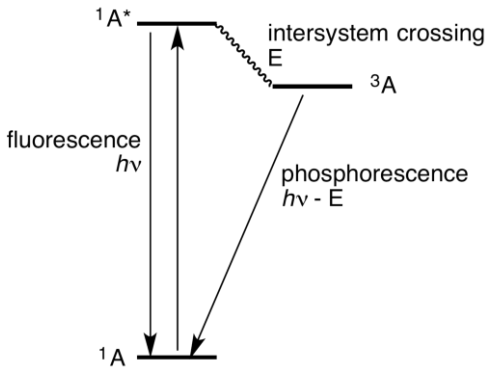

Figure 17. A simplified Jablonski diagram showing the excitation of a molecule from its singlet ground state (^1A) to its singlet excited state ($^1A^*$) followed by intersystem crossing to the triplet state (^3A) that relaxes to the ground state by phosphorescence. (Reproduced from the Wikipedia)

Fluorescence in porphyrins and corroles is generally limited to the free bases and closed-shell metal and nonmetal complexes.[72] Typical examples of fluorescent porphyrins are H_2[TPP] and Zn[TPP].[73-75] **Figure 18** depicts the fluorescence spectrum of H_2[TPP], showing emission in the red. Free-base *meso*-triarylcorroles typically display stronger fluorescence than analogous free-base porphyrins,[18] while certain Ga(III) and Al(III) corroles exhibit even brighter fluorescence than free-base corroles.[76]

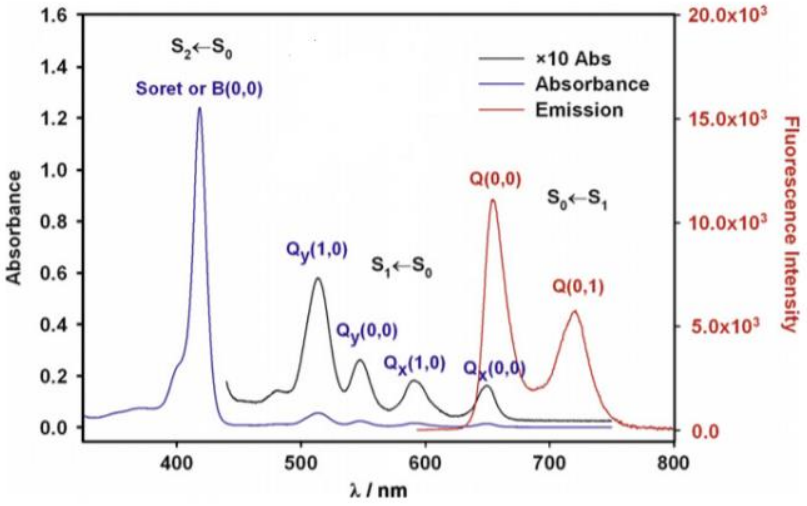

Figure 18. Absorption and emission spectra of H_2[TPP] (λ_{ex} = 418 nm) showing fluorescent emission (red). Adapted with permission from ref 74. Copyright 2008 Elsevier.

Classic examples metalloporphyrins exhibiting phosphorescence under ambient conditions include Pd(II) or Pt(II) porphyrins. Other examples include Ir(III) and even certain Zn(II) porphyrins.[77-79] As for Ir(III) porphyrins, phosphorescence has also been observed for Ir(III) corroles (**Figure 19**), as well as for Au(III) and Os(VI)-nitrido corroles.[80-82] The phosphorescence of Ir(III) corroles is also one of the key studies of **Chapter 7**, where a series of six-coordinate Ir(III) corroles with different axial ligands were prepared, characterized and analyzed.

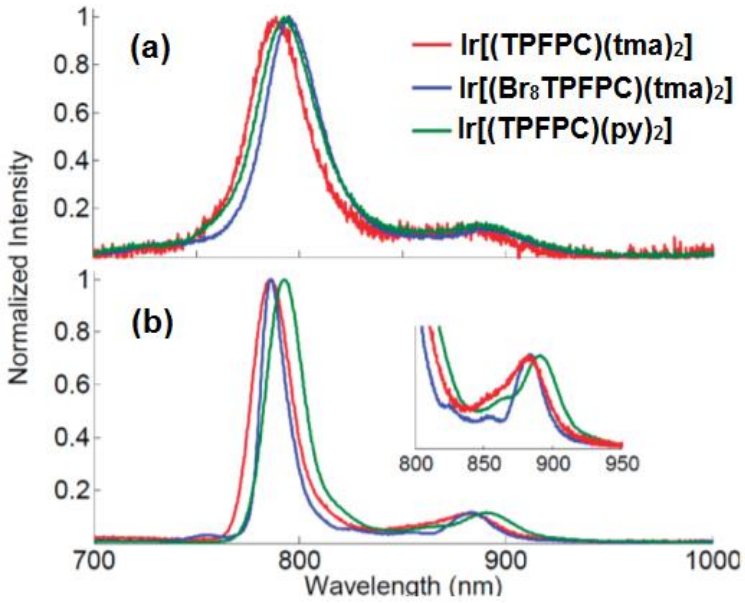

Figure 19. Emission spectra of iridium corroles (λ_{ex} = 496.5 nm) at (a) 298 K and (b) 77 K. Adapted with permission from ref 82. Copyright 2010 American Chemical Society

The ability of porphyrins and corroles to exhibit strong fluorescence and ambient-temperature phosphorescence, in addition to the highly tunable properties by chemical functionalization of the macrocycles, makes them ideal for a number of biomedical applications, particularly fluorescence imaging/microscopy, photodynamic therapy (PDT),[23,83] and oxygen sensing.[84,85]

Chapter 2 – Synthesis of Porphyrins and Corroles

2.1. Synthesis of porphyrins

H. Fischer prepared the first porphyrins in 1929 by heating dipyrromethene salts with different organic acids to prepare many different porphyrins, albeit in meager yields (**Figure 20**).[86] In 1935, Rothemund reported a one-pot porphyrin procedure in which pyrrole was reacted with gaseous acetaldehyde or with formaldehyde in methanol. The mixture was either kept stirring for weeks, heated under reflux for 15-24 hours, or heated in a sealed tube at 85-90°C for 10-24 hours to produce porphine or tetramethylporphine.[87] The procedure was later found to be compatible with other aldehydes such as propionaldehyde, *n*-butyraldehyde, benzaldehyde and furfural.[88] In 1941, Rothemund modified the procedure to prepare H_2[TPP] and what he believed to be its *cis* tautomer; the latter was later found to be tetraphenylchlorin.[89] The modified procedure consisted of heating pyrrole and benzaldehyde in sealed vessels containing pyridine at 220°C for 48 hours. A slightly modified procedure was later used to prepare a wide variety of *meso*-tetraarylporphyrins.[90]

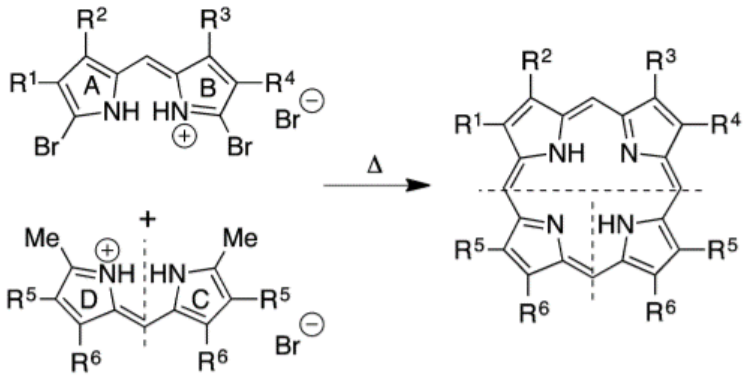

Figure 20. Fischer porphyrin synthesis starting from dipyrromethene salts. Adapted with permission from ref 91. Copyright 2016 Royal Society of Chemistry.

In 1960, F. MacDonald reported a procedure where formyl-substituted dipyrromethanes could be cyclized to porphyrins in the presence of an acid catalyst (**Figure 21**).[91] The conditions were much milder than in Fischer's procedure, and they subsequently laid the groundwork for the next half-decade of unsymmetrical porphyrin synthesis.

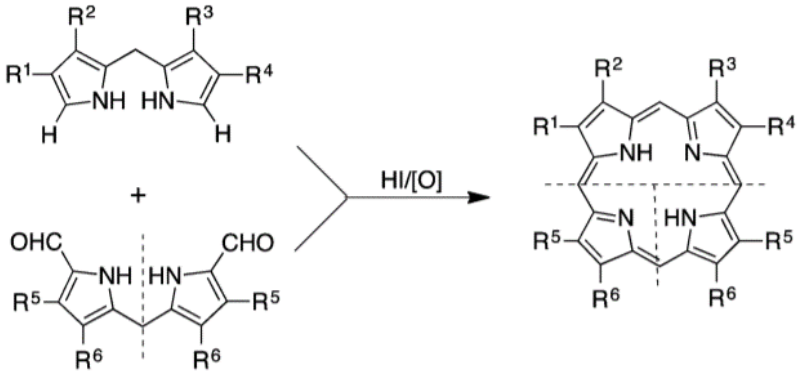

Figure 21. The MacDonald "2 + 2" method for synthesizing porphyrins from formyl-substituted dipyrromethanes. Adapted with permission from ref 91. Copyright 2016 Royal Society of Chemistry.

The one-pot procedure for synthesizing tetraarylporphyrins devised by Rothemund in the 1940s had several limitations such as low yield (4 – 5 %) and long reaction times (24 – 48 hours). After some mechanistic studies, Adler and co-workers reported a greatly improved procedure for synthesizing tetraarylporphyrins. In this procedure, equal amounts of pyrrole and an aromatic aldehyde were dissolved in acetic acid and refluxed for 6 – 8 hours to give the corresponding tetraarylporphyrin after purification (**Figure 22**). Yields for H_2[TPP] were reported to be 40 to 50 %.[92] In the following years, they optimized the procedure in terms of reaction time and convenience by substituting the acetic acid with propionic acid. After 30 minutes in refluxing propionic acid, the porphyrin would generally crystallize from the solution upon cooling, and could simply be filtered to give H_2[TPP] in 20 % yield.[93] This procedure has since been known as the Adler-Longo porphyrin synthesis.

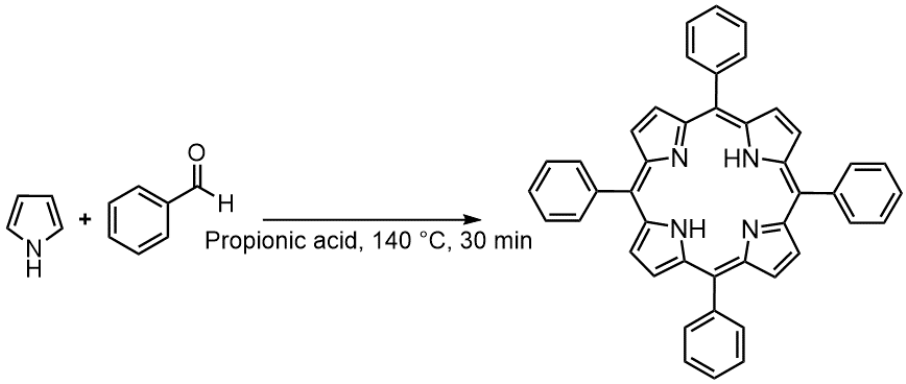

Figure 22. The Adler-Longo porphyrin synthesis.

The Adler-Longo method also has certain drawbacks, for example the procedure leads to significant tetraphenylchlorin contamination and is limited to aldehydes without sensitive functional groups, because of the harsh reaction conditions.

During the 1960s, cyclisation of *b*-oxobilanes and *b*-bilenes and oxidative cyclisation of *a*,*c*-biladienes were used to synthesize many unsymmetrical porphyrins (some examples can be seen in **Figure 23**).[91] In section 2.1, we shall see that *a*,*c*-biladienes were also used later to synthesize the first corroles.

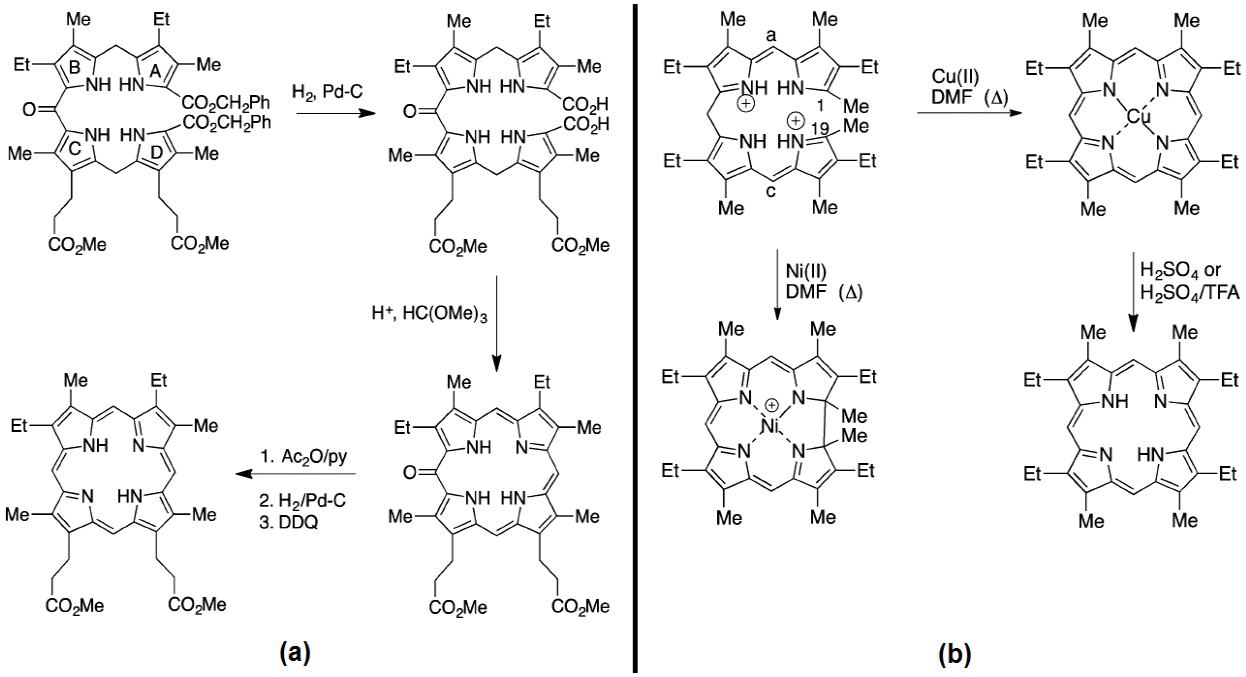

Figure 23. (a) Porphyrin synthesis via cyclisation of *b*-oxobilane. (b) Porphyrin synthesis via oxidative cyclisation of *a*,*c*-biladiene. Adapted with permission from ref 91. Copyright 2016 Royal Society of Chemistry.

One of the great advances in porphyrin synthesis came in 1986 when Lindsey reported a new procedure for pyrrole-aldehyde condensation. The procedure is mild, clean, gives unprecedentedly high yields, and tolerates a wide variety of functional groups (**Figure 24**).[94] The Lindsey method is a one-pot reaction with two steps. In the first step, equimolar amounts of pyrrole and aldehyde (10^{-2} M) are dissolved in anhydrous DCM under a nitrogen atmosphere. A catalytic amount (10^{-3} M) of $BF_3{\cdot}Et_2O$ or TFA is then added and the solution is left to stir until the reversible reaction is in equilibrium (1 hour). In the second step *p*-chloranil

(1 hour, reflux) or DDQ (5 min, r.t.) is used to oxidize the intermediate porphyrinogen to the porphyrin. The purification is straightforward and yields relatively pure porphyrin.
The most obvious disadvantage of the Lindsey procedure is the rather small concentrations of reagents employed. A multi-gram scale preparation is inconvenient because of the large volume of chlorinated solvent required. Lindsey later published a modified procedure where larger concentrations of pyrrole and aldehyde (10^{-1} M) were condensed using a higher concentration of boron trifluoride etherate (10^{-2} M).[95]

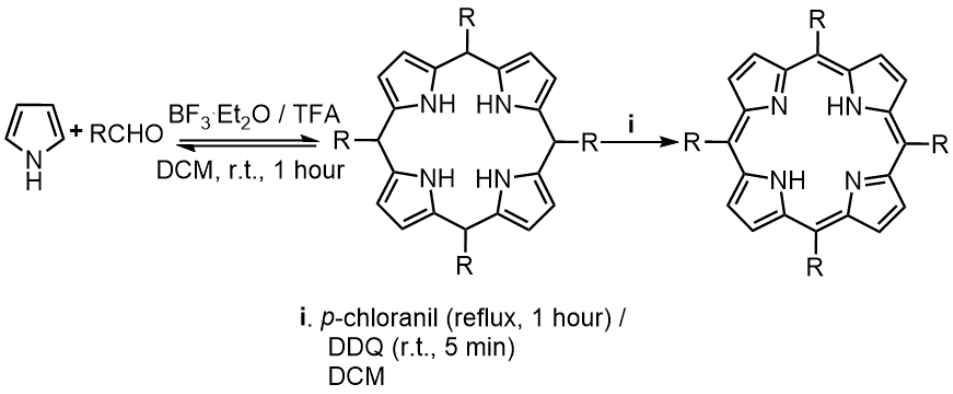

Figure 24. The Lindsey porphyrin synthesis.

Momenteau developed an interesting variety of the MacDonald "2 + 2" method in 1996. The synthesis involves acid catalyzed cyclisation of tripyrranes with 1-*H*-pyrrole-2,5-dicarbaldehyde (**Figure 25**).[96]

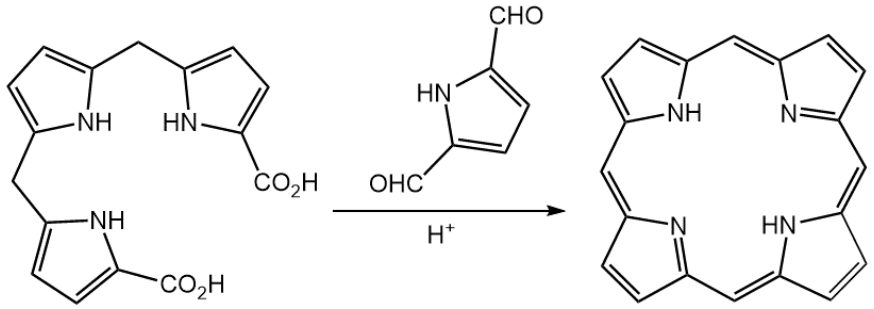

Figure 25. The MacDonald "3 +1" method as devised by Momenteau (substituents not shown).

Another noteworthy porphyrin synthesis employs higher-valent transition metal salts to synthesize tetraarylporphyrins in higher yields than those typically obtained by the Lindsey procedure. The reaction is thought to proceed by a radical mechanism (**Figure 26**).[97]

Other methods worth mentioning are microwave-assisted synthesis of porphyrins with corresponding microwave assisted metal insertion,[98] using ionic liquids[99] and solvent-free conditions.[100]

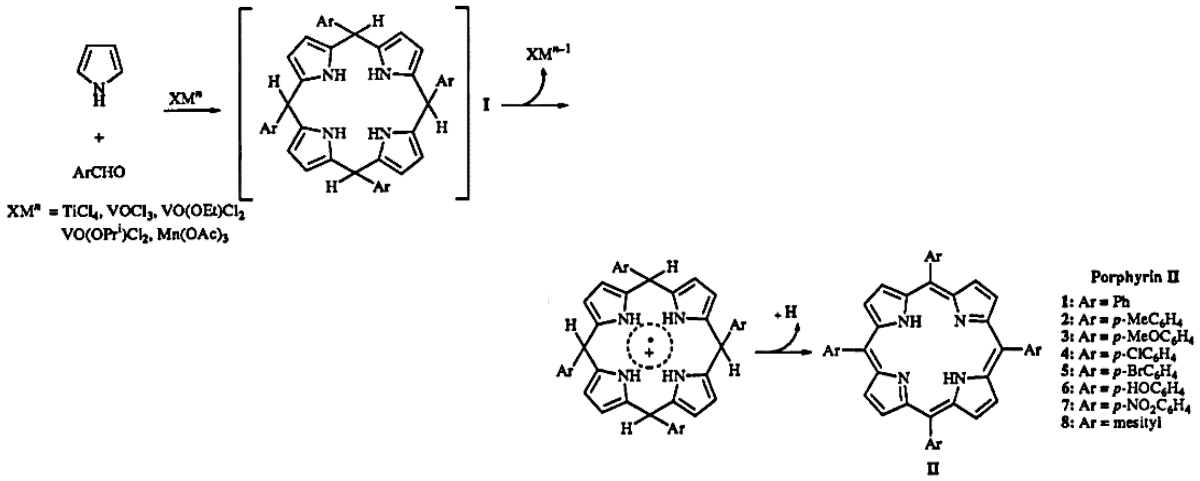

Figure 26. Synthesis of tetraarylporphyrins by high-valent metal salts. Adapted with permission from ref 97. Copyright 1969 Royal Society of Chemistry.

2.2. Synthesis of corroles

Johnson and Kay synthesized the first corroles in 1965 by photocyclisation of *a,c*-biladiene dihydrobromides in alkaline methanol solutions (**Figure 27**).[101] The methodology was later expanded to include cobalt assisted cyclisation of *a,c*-biladienes to the corresponding cobalt corroles and acidic condensations of dipyrromethanes and dipyrroles followed by complexation to cobalt.[102] The oxidative metal-assisted cyclisations of *a,c*-biladienes was later used to prepare iron, manganese and rhodium metallocorroles.[103]

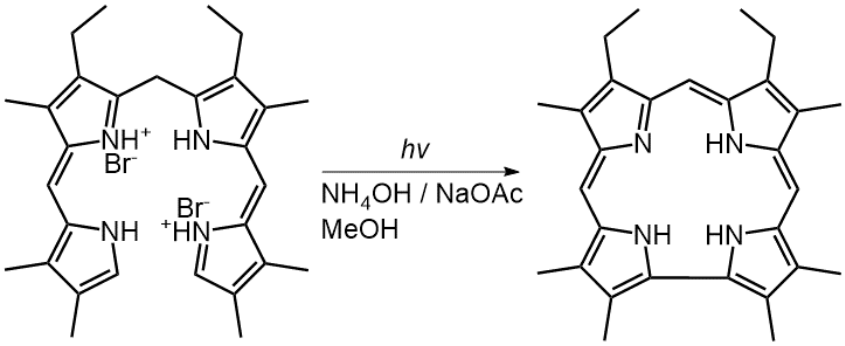

Figure 27. Photocyclisation of *a,c*-biladienes to corroles.

Ring contractions of porphyrins to the corresponding corroles have also been observed. In one example, rhenium insertion to an electron deficient porphyrin, 5,10,15,20-tetrakis(trifluoromethyl)porphyrin, instead led to the metallocorrole (**Figure 28**). It was postulated that the rhenium salt utilized in the reaction, reduced the porphyrin *via* a cyclopropane intermediate to the analogous corrole through detrifluoromethylation and ring contraction.[104]

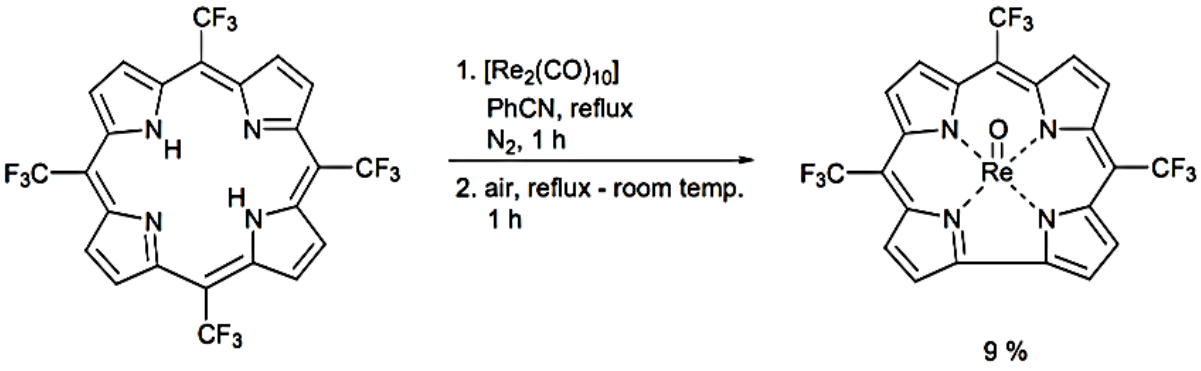

Figure 28. Rhenium-assisted ring contraction of a porphyrin to a corrole. Adapted with permission from ref 104. Copyright 1969 Royal Society of Chemistry.

Apart from a few odd examples, corroles received little attention and were mostly considered by-products of porphyrin synthesis until the end of the millennium. The first direct syntheses of A_3 free-base corroles from pyrrole and aldehyde were reported in 1999 by two different groups, the Gross and Paolesse groups (**Figure 29**). The one-pot synthesis reported by Paolesse was in essence a modified Rothemund reaction, where reaction conditions had been fine-tuned to increase the yield of triphenylcorrole (H_3[TPC]) relative to tetraphenylporphyrin (H_2[TPP]). Pyrrole and benzaldehyde (3 : 1 molar ratio) were refluxed in acetic acid for 4 hours, after which purification led to a 6 % yield of H_3[TPC] along with an equal amount of H_2[TPP].[105]

Gross's method, on the other hand, was a solvent-free, solid-supported, one-pot corrole synthesis. Equimolar amounts of pyrrole and pentafluorobenzaldehyde were adsorbed on basic alumina and subsequently heated for 4 hours at 100°C. After removal of the solid support, the reaction mixture was oxidized with DDQ and purified. By this method, Gross prepared tetrapentafluorophenylcorrole (H_3[TPFPC]) in a then-unprecedented 11 % yield.[106] Gross's method was thought to only work with aldehydes bearing strongly electron-withdrawing substituents, but it was later found that the method also works for electron-rich

aldehydes, although with comparably lower yields.[107] It was also assumed that Gross's method does not require any acid catalyst, but it has since been discovered that trace acid present with the aldehydes acts as the catalyst.[108]

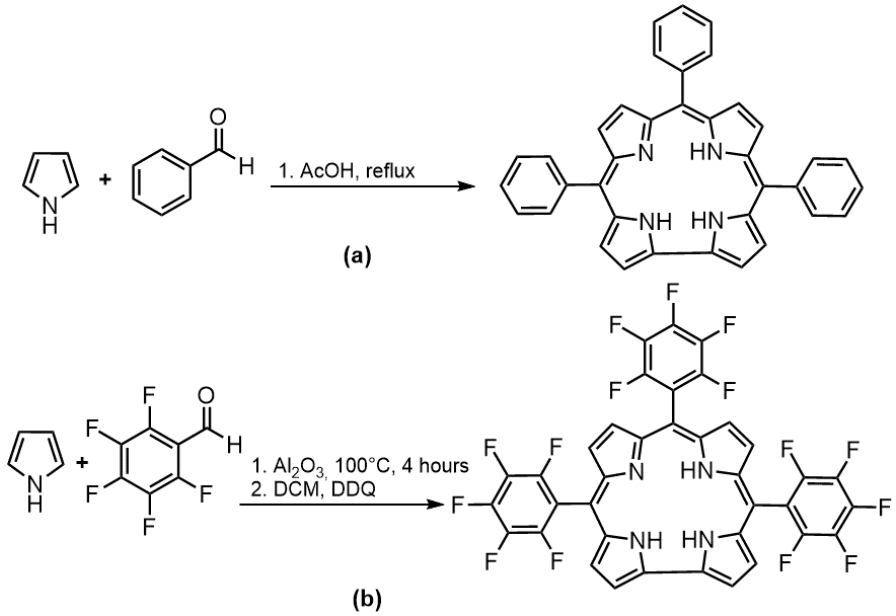

Figure 29. (a) One-pot free-base A_3 corrole synthesis by Paolesse. (b) One-pot free-base A_3 corrole synthesis by Gross.

Shortly afterwards, a two-step, one-pot method for synthesizing *trans*-A_2B corroles by MacDonald type (2+ 2) condensations of equimolar amounts of dipyrromethanes and electron-withdrawing aldehydes was reported by Gryko *et al*. Like Gross's method, this method does not require a catalyst and is reliant on a second step for the irreversible oxidation to corrole.[109] An optimized procedure, applicable to a wide range of different aldehydes and with higher yields, was published the same year. In the new procedure dipyrromethane and aldehyde (2:1 molar ratio) was dissolved in dichloromethane with added TFA, and stirred for 5 hours (**Figure 30**). It was found that sterically hindered DPMs required less TFA than unhindered ones. Oxidation with DDQ and subsequent purification gave a whole range of different corroles in yields ranging from 6 – 25 %.[110]

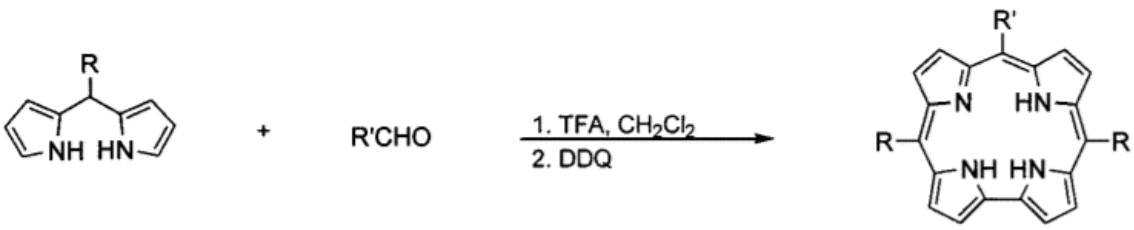

Figure 30. Condensation of DPMs and aldehydes to *trans*-A_2B corroles. Adapted with permission from ref 109. Copyright 2001 American Chemical Society.

The following year, Gryko also published a two-step general procedure for the preparation of ABC corroles by reaction of dicarbinoldipyrromethanes and pyrrole (1:50 or 1:145 molar ratio) in the presence of TFA or $BF_3{\cdot}Et_2O$.[111] The bilanes formed in the reaction was oxidized by DDQ and purified to obtain the ABC-type corroles (**Figure 31**). The method is also applicable for synthesizing *trans*-A_2B corroles in respectable yields. Gryko and co-workers soon reported a refined procedure for the preparation of A_3 and *trans*-A_2B corroles, following a lengthy optimization study conducted on a large number of different aldehydes. Three general sets of reaction conditions were prescribed depending on the reactivity and steric bulk of the aldehydes employed in the study.[112]

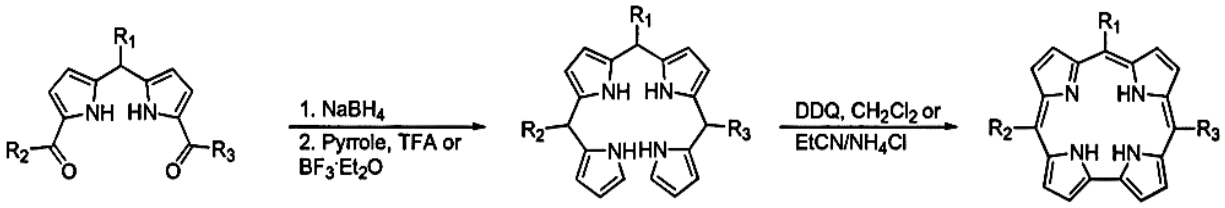

Figure 31. Condensation of dicarbinol-DPMs and pyrrole to ABC corroles. Adapted with permission from ref 111. Copyright 2002 American Chemical Society.

The possibility of dipyrromethane formation in water inspired the Gryko group to devise what has now become the bread and butter technique for A_3 and *trans*-A_2B corrole preparation (**Figures 32 and 33**).[113] They determined that by modulating the solvent ratios, such that the bilane precipitated instead of forming higher oligomers, they could increase the yield drastically. By optimizing the different reaction parameters such as the molar ratio of reactants, different solvent combinations, reaction time, and acid and oxidant concentration, they devised general reaction conditions that were applicable to a wide range of aldehydes. For the preparation of A_3 corroles, the procedure involves mixing pyrrole and aldehyde (2:1 molar ratio) in a water/methanol mixture (1:1) and stirring for three hours. Extraction and purification of the bilane followed by oxidation in *p*-chloranil and subsequent column chromatography afforded the corroles in yields ranging from 20 - 30 %.

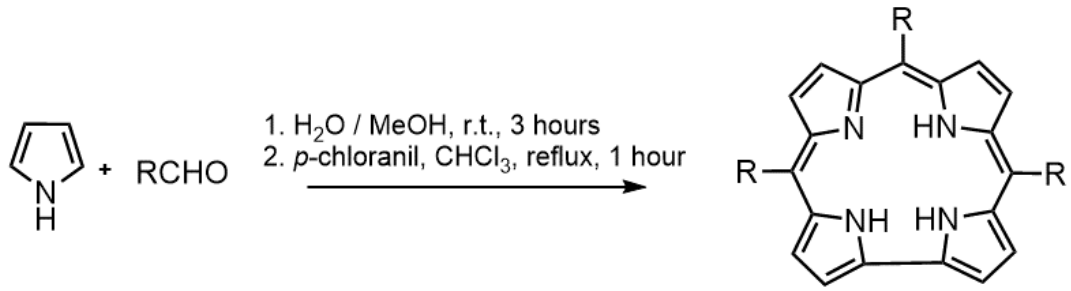

Figure 32. Gryko's method for synthesizing corroles from pyrroles and aldehydes.

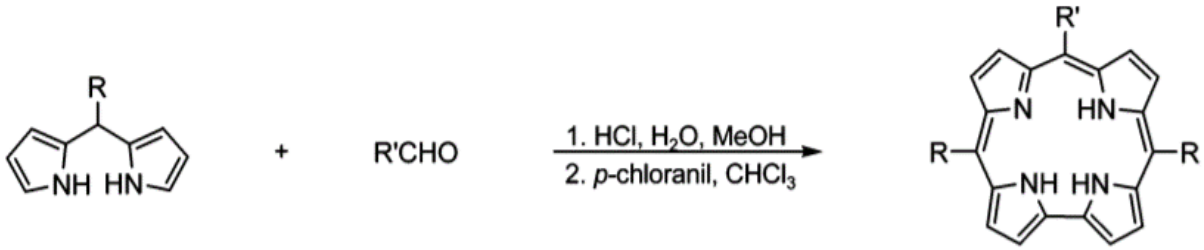

Figure 33. Gryko's method for synthesizing corroles from DPMs and aldehydes. Adapted with permission from ref 112. Copyright 2006 American Chemical Society.

More recent corrole syntheses include synthesis of (i) *cis*-A_2B corroles using MacDonald type "2 +2" condensations of monocarbinol-DPMs and dipyrromethanes,[114] (ii) microwave-assisted corrole synthesis,[115] (iii) and the use of ionic liquids.[116]

Chapter 3 – Functionalization of Porphyrins and Corroles

A wide range of reactions have been exploited to accomplish functionalizations and structural modifications of porhyrins and corroles. While a full review is impractical for reasons of space,[117,118] a brief overview is presented here as background to my own contributions. Some of the major approaches include:

- Functionalization of the nitrogens via metalation, demetallation and *N*-alkylation.
- Functionalization of the periphery via electrophilic aromatic substitutions such as halogenation, formylation, carboxylation, nitration, sulfo-/chlorosulfonation, borylation, fluoroalkylation, and aminomethylation, as well as by other reactions such as hydrogenation and Diels-Alder cycloadditions.
- Post-functionalization of peripheral substituents via nucleophilic aromatic substitution, metal-catalyzed cross-couplings (Suzuki-Miyaura, Sonogashira, Heck, Buchwald-Hartwig, Stille, etc.), oxidations and reductions, Wittig reactions, etc.

Most relevant to this work are functionalizations of the *β*-positions on porphyrins and corroles. In principle, *β*-positions on porphyrins and corroles can be functionalized by typical electrophilic aromatic substitution reactions either on the pyrrole, prior to macrocyclization, or on the macrocycle itself. Although the latter is more common, both approaches are represented in this thesis. *β*-Iodination has been intentionally left out of this chapter, as it will be discussed in depth in **Chapters 4 and 6**, where the first syntheses of *β*-octaiodoporphyrin and *β*-octaiodocorrole derivatives are described.

3.1. Formylation

The Vilsmeier-Haack reagent, dimethylformamide and phosphoryl chloride (DMF/$POCl_3$), provides a convenient route to *β*-formylated porphyrins and corroles. For porphyrins with open *meso* positions, the reaction can be made regioselective for *β*-carbons as opposed to the more reactive *meso* carbons via the use of a sterically hindered Vilsmeier reagent such as *N*,*N*-diisobutylformamide/$POCl_3$[119] or by using trimethyl orthoformate in TFA.[120] Interestingly, the reaction of these reagents with triphenylphosphine-(octamethylcorrolato)cobalt(III) (Co[OMC]PPh_3) led to 3- and 3,17-formylated metallocorroles;[121] most likely via oxidation of two methyl-groups.[102] Gross and co-workers also formylated the gallium-complex of TPFPC using the same conditions, which resulted in the 2- and 2,17-formylated species (**Figure 34**).[122]

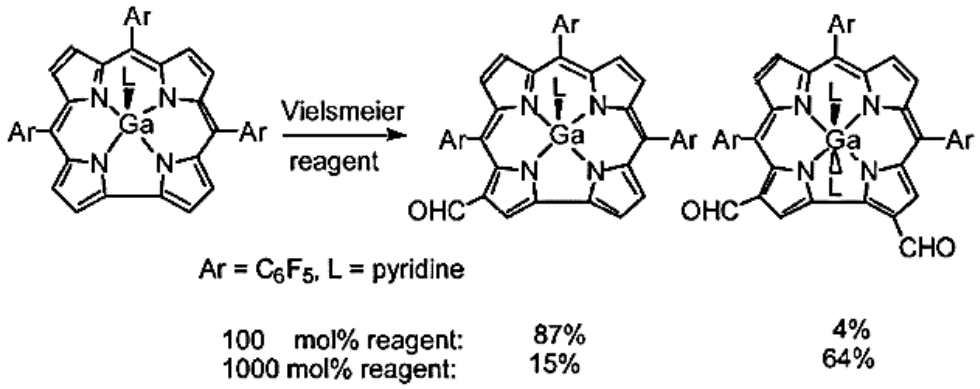

Figure 34. *β*-formylation of a gallium corrole. Adapted with permission from ref 122. Copyright 2002 American Chemical Society.

3.2. Carboxylation

Direct *β*-carboxylation has at the time of writing not been reported for porphyrins. If such moieties are desired, there are many other available options for acquiring them (e.g. during synthesis or by post-functionalization). A couple of examples include asymmetric synthesis[123] and oxidation of *β*-formylated porphyrins to the corresponding *β*-carboxylated porphyrins (**Figure 35**).[124]

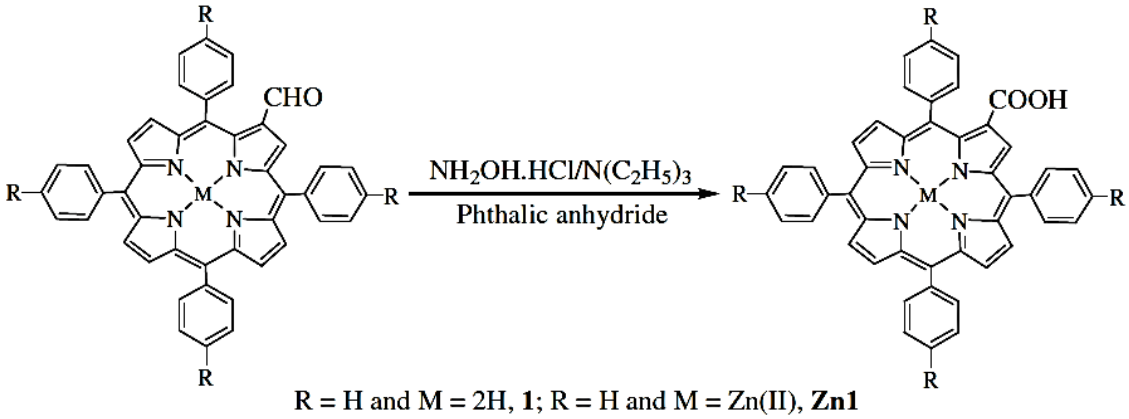

Figure 35. Synthesis of *β*-carboxy tetraarylporphyrins. Adapted with permission from ref 124. Copyright 2010 Elsevier.

A single example of the direct *β*-carboxylation of a gallium corrole was reported by the Gross group, but the method involves the use of highly toxic phosgene for the carboxylation (**Figure 36**).[125]

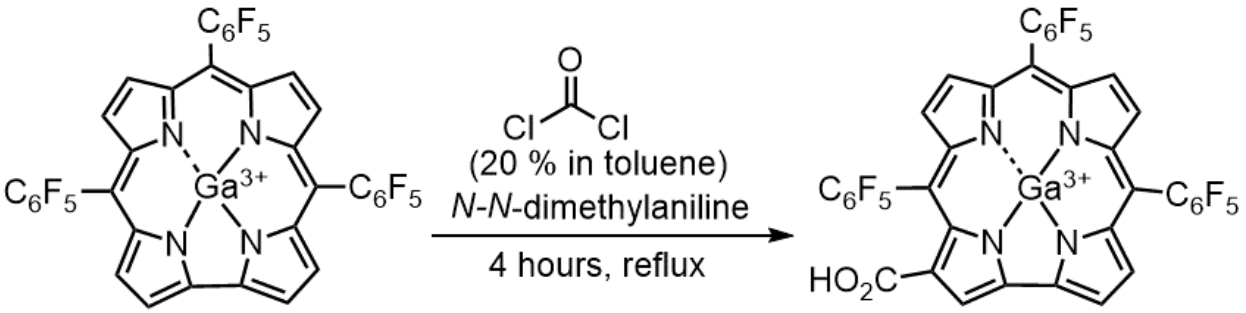

Figure 36. Direct *β*-monocarboxylation of a gallium corrole.

3.3. Nitration

β-Nitration of porphyrins and corroles can be achieved in numerous ways. Nitration using typical conditions such as fuming nitric acid on Zn[TPP] gave a regiomeric mixture of the *β*-di-nitrated metalloporphyrin,[126] while the same conditions applied to free-base 5,10,15,20-tetrakis(dichlorophenyl)porphyrin (H_2[TDCPP]) primarily gave the *β*-hexanitrated porphyrin (**Figure 37**).[127] A related procedure employing red fuming nitric acid, triflic acid and triflic anhydride was later used to successfully octanitrate Zn[TDCPP].[128] Treatment of several metalloporphyrins with nitrogen dioxide led to *β*-mononitration for the porphyrins complexed to the more electronegative metals (Cu, Ni and Pd), while it induced *meso*-attack on the more electropositive metal complexes (Mg, Zn, Fe and Co).[129] *β*-Mononitration of zinc porphyrins has also been achieved using iodine and silver nitrite in DCM/MeCN generated in situ via the porphyrin π-cation radicals.[130]

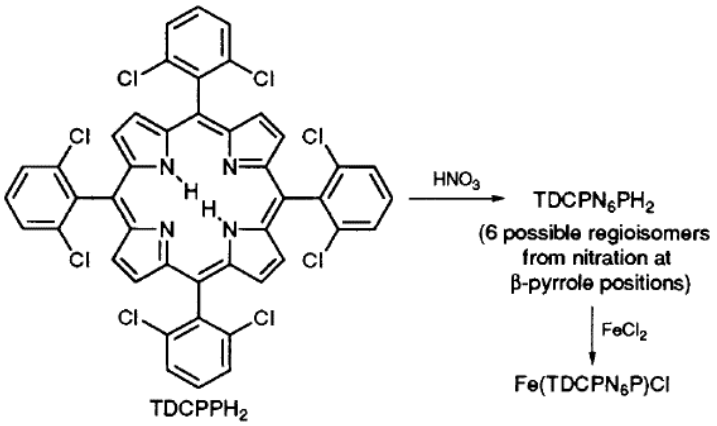

Figure 37. *β*-Hexanitration of a free-base porhyrin using fuming nitric acid. Adapted with permission from ref 127. Copyright 1969 Royal Society of Chemistry.

Nitration of corroles is not as straightforward as for porphyrins. The use of fuming nitric acid and nitrogen dioxide leads to decomposition of the corrole macrocycle instead of affording nitration.[117] Current progress in this area primarily involves the use of $NaNO_2$ as the nitration agent. Gross and co-workers first nitrated the gallium complex of TPFPC using $NaNO_2$ in the presence of a one-electron oxidant, yielding a mixture of the *β*-mono-, di- and trinitrated corrole.[122] Paolesse and co-workers later reported using $AgNO_2$ for the regioselective preparation of a *β*-mononitrated silver corrole directly from the free-base corrole.[131] The Paolesse group has since explored the field further and one of their latest protocols for nitration is based on the use of $NaNO_2$ as the nitration reagent and $AgNO_2$ as the oxidant. Careful adjustment of the molar ratios of reactants allowed for the regioselective *β*-mono and di-nitration of selected free-base and metallocorroles (**Figure 38**).[132,133]

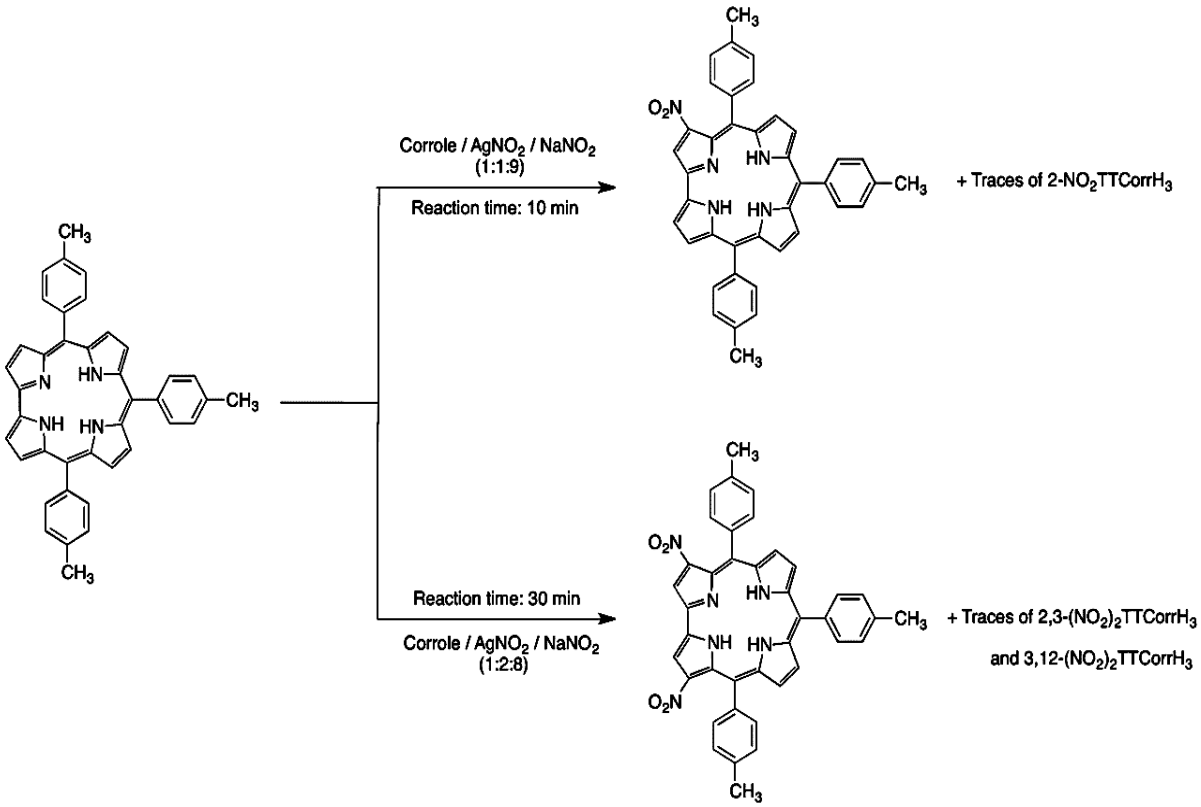

Figure 38. Regioselective *β*-nitration of a free-base corrole. Adapted with permission from ref 132. Copyright 2012 American Chemical Society.

3.4. Sulfo-/chlorosulfonation

Sulfonations or chlorosulfonations of *meso*-arylporphyrins predominantly lead to substitution on the *meso* aryl groups.[134,135] In one example, sulfonation of 5,15-diphenylporphyrin using concentrated sulfuric acid yielded mixtures of products displaying substitutions of both phenyl *para* positions and *β*-positions.[136]

β-Sulfonation of corroles has been achieved by the Gross group by stirring H_3[TPFPC] in concentrated sulfuric acid at room temperature (**Figure 39**). The reaction proved very regioselective, and despite many possible outcomes, only generated two isomers, 2,17- and 3,17-bis(sulfonic acid), in a 9 to 1 ratio.[137] Chlorosulfonation of the same corrole gave a quantitative yield of the *β*-2,17-(chlorosulfonyl) corrole.[138] Recently, Paolesse published a study investigating the effects of chlorosulfonation on H_3[TPC], which resulted in *β*-mono and disubstituted corroles. The main product, however, was the *β*-2-(chlorosulfonyl) corrole.[139]

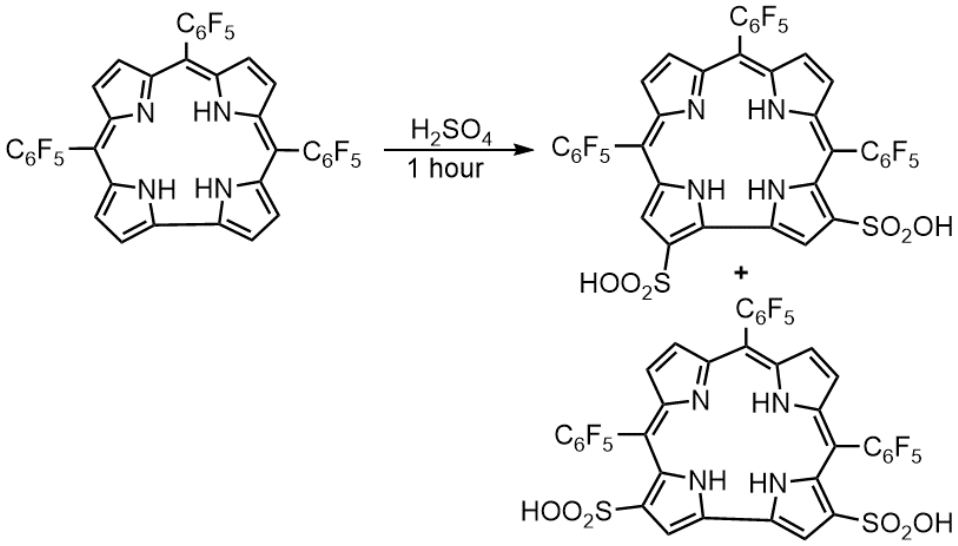

Figure 39. Preparation of *β*-sulfonic acid corroles using sulfuric acid at ambient temperature.

3.5. Borylation

Peripheral borylation of *β*-carbons has been achieved through typical metal-catalyzed cross-coupling schemes (**Figure 40**)[140,141] and more recently via iridium-catalyzed C-H bond activation. The latter protocol is versatile and applies to both porphyrins and corroles (**Figure 41**).[142,143] Porphyrin or corrole is reacted with bis(pinacolato)diborane and a catalytic amount of Ir[(cod)OMe]$_2$ in the presence of 4,4'-di-*tert*-butyl-2,2'-bipyridyl (dtbpy) to produce *β*-monoborylated corroles or *β*-mono, di-, tri- or tertborylated porphyrin. Some of these borylated products have been utilized in transition-metal-catalyzed cross-coupling reactions to prepare porphyrin-porphyrin and corrole-porhyrin *β-β* linked dimers, while others were used for introducing *β*-hydroxyl moieties through oxidation of the boryl group.

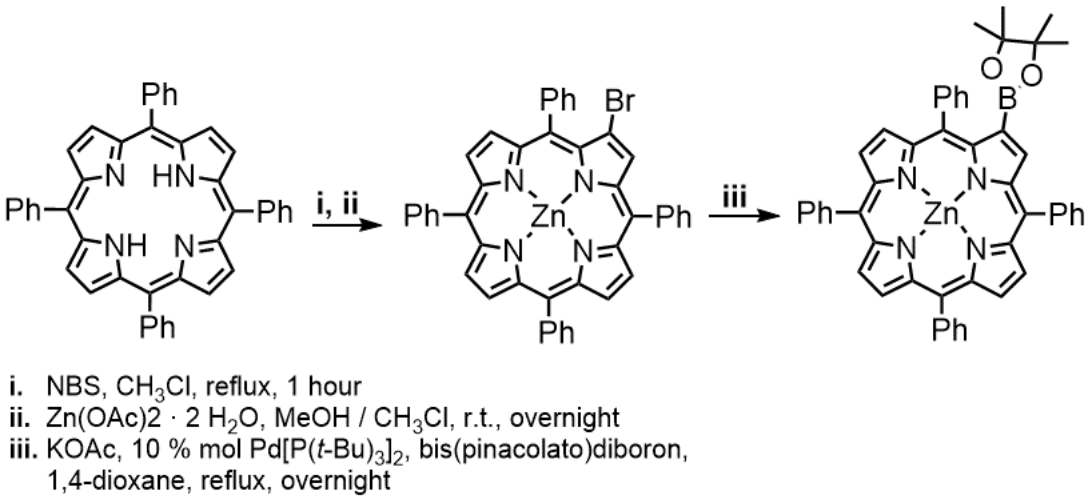

Figure 40. Synthesis of a *β*-monoborylated porphyrin via metal-catalyzed cross-coupling.

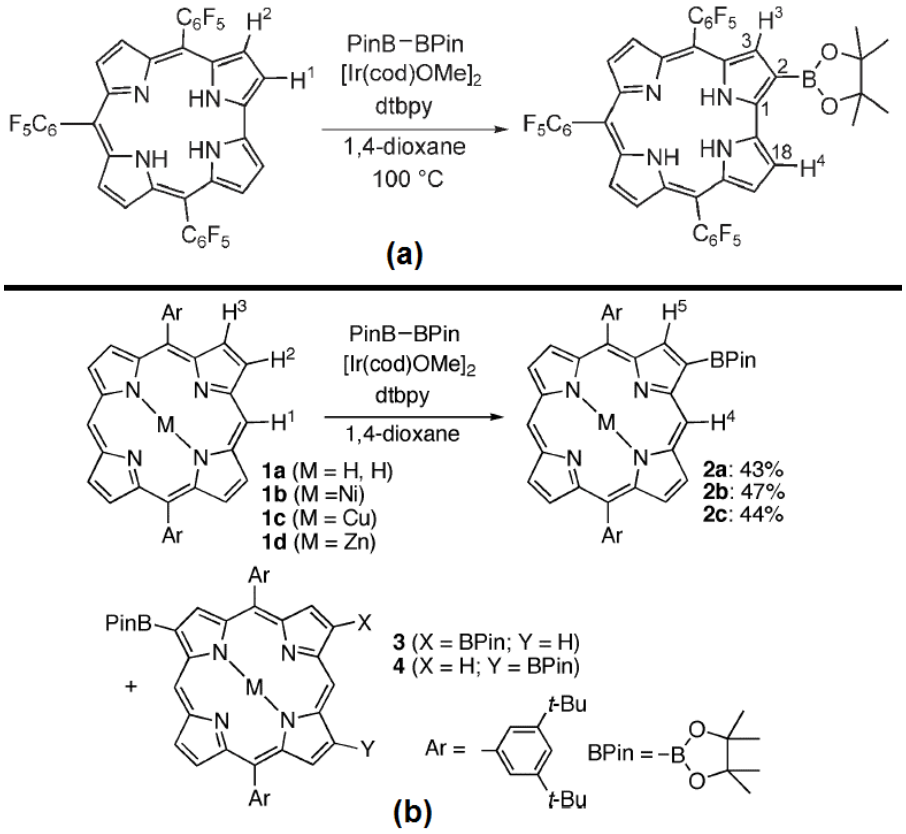

Figure 41. (a) Iridium-catalyzed borylation of corroles. Adapted with permission from ref 143. Copyright 2005 John Wiley and Sons. (b) Iridium-catalyzed borylation of porphyrins. Adapted with permission from ref 142. Copyright 2005 American Chemical Society.

3.6. Perfluoroalkylation

Methods for the preparation of *β*-perfluoroalkylated porphyrins include condensations of mono-perfluoroalkylated pyrroles[144] and substitutions of existing functionalities such as bromine via nucleophilic trifluoromethylation[145] or metal-catalyzed cross-coupling reactions.[146] Direct *β*-monoperfluoroalkylation of various free-base tetraarylporphyrins has been achieved using perfluoroalkyl iodides in the presence of sodium dithionite ($Na_2S_2O_4$)/sodium bicarbonate ($NaHCO_3$) in a DMSO-DCM mixture (**Figure 42**).[147] A slightly modified procedure has been shown to facilitate both *meso*- and *β*-perfluoroalkylation on free-base and zinc complexes of 5,15-diphenylporphyrin.[148] The procedure was also used to synthesize, depending on the solvents employed, *β*-perfluoroalkylated metallochlorins and metalloporphyrins in the presence of copper powder. It was hypothesized that a SET mechanism was at play in the formation of *β*-perfluoroalkylated chlorins, while perfluoroalkylcopper intermediates facilitated the formation of *β*-perfluoroalkylated porphyrins.[149] This protocol has since been adapted to also allow for *β*-perfluoroalkylation of H_3[TPFPC] and the preparation of fluorinated ring fused corroles using *α*,*ω*-diiodoperfluoroalkanes ($I(CF_2)_{3/4}I$).[150]

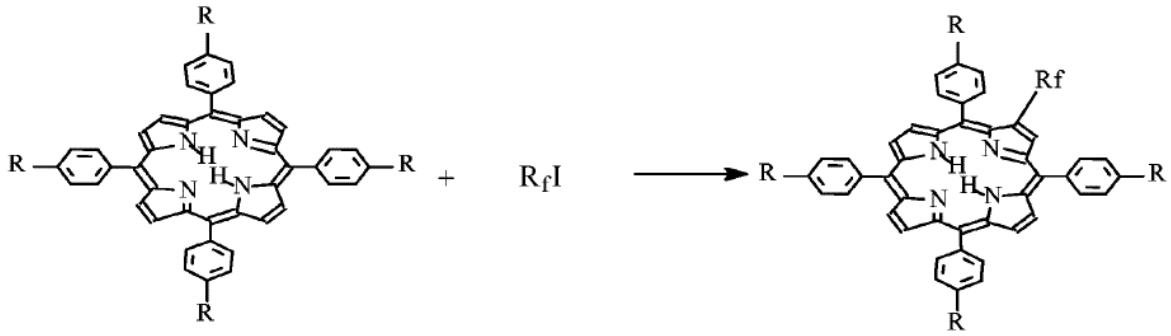

Figure 42. Direct *β*-perfluoroalkylations of free-base porphyrins. Adapted with permission from ref 147. Copyright 2003 American Chemical Society.

3.7. Aminomethylation

The available literature on peripheral aminomethylations on porphyrins is scarce. Bis(*N*,*N*-dimethylamino)methane has been found to be an effective reagent for the aminomethylation of the vinyl and carbon-carbon double bond in the enol groups of metal-free methylpheophorbide *a* (chlorophyll *a* derivative),[151] while tetrakis(4-aminomethylphenyl)porphyrin has been synthesized from a pre-functionalized aldehyde.[152] There are no reports of direct *β*-aminomethylations of porphyrins for the time being. Unexpectedly, during experiments aimed at synthesizing cycloadducts from pyridine-tris-5,10,15(pentafluorophenylcorrolato)gallium(III) (Ga[TPFPC]py) using paraformaldehyde and sarcosine, two *β*-aminomethylated corrole isomers were obtained instead (**Figure 43**).[153]

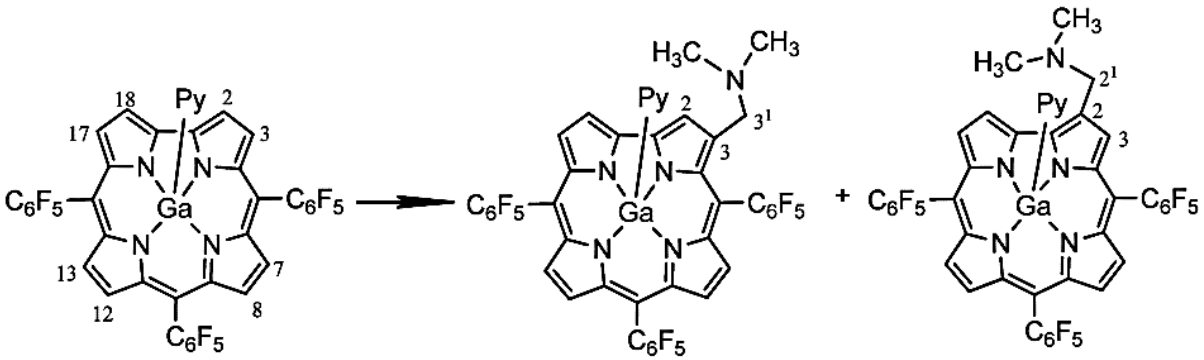

Figure 43. *β*-aminomethylated corrole isomers obtained from the reaction of Ga[TPFPC]py with paraformaldehyde and sarcosine. Adapted with permission from ref 153. Copyright 2012 John Wiley and Sons.

3.8. Hydrogenation

The reaction of 5,10,15,20-tetrakis(pentafluorophenyl)porphyrin (H_2[TPFPP]) using Pd/C and H_2 in different solvent mixtures and in the presence or absence of trimethylamine, led to the formation of chlorins, bacteriochlorins and isobacteriochlorins in varying ratios.[154] In contrast, catalytic hydrogenation of uroporphyrin conducted in a methanol/water mixture gave the corresponding porphyrinogen.[11] Dihydrogen donors such as diimides generated from *p*-toluenesulfonylhydrazine have also been employed for hydrogenations of porphyrin *β*-*β* double bonds, leading to chlorins, bacteriochlorins and isobacteriochlorins (**Figure 44**).[155,156] The reaction of H_3[TPFPC] with *p*-toluenesulfonylhydrazine and potassium carbonate in pyridine at 110 °C for 2 hours results in the selective formation of the 7,8-dihydrocorrole. Interestingly, the 2,3-dihydrocorrole isomer is not formed in this reaction (**Figure 45**).[157]

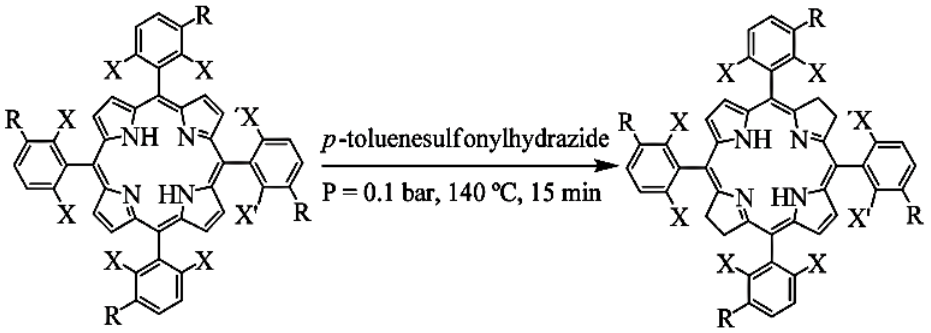

1a-d

2a-d

Entry	Compound	X	X′	R	Yield
1	**2a**	F	F	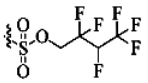	84%
2	**2b**	F	F	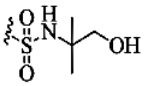	87%
3	**2c**	F	F	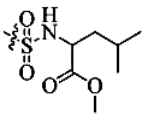	80%
4	**2d**	F	F	H	60%

Figure 44. Hydrogenation of porphyrins via diimides to bacteriochlorins. Adapted with permission from ref 156. Copyright 2012 Royal Society of Chemistry.

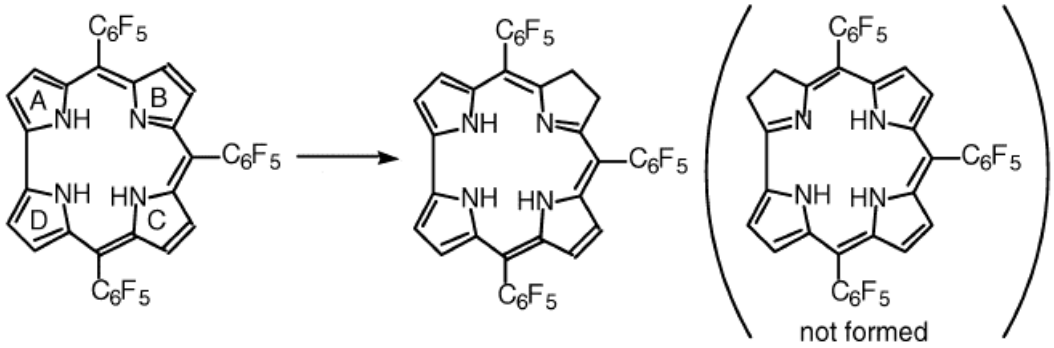

Figure 45. Hydrogenation of H_3[TPFPC] via diimides to the 7,8-dihydrocorrole. Adapted with permission from ref 157. Copyright 2002 Elsevier.

3.9. Cycloadditions

An extensive study on porphyrins has revealed that they participate in many different cycloadditions acting as either the 2π or the 4π component, i.e., as either the diene or dienophile in [4 + 2] cycloadditions or as the 1,3-dipole or dipolarophile in dipolar cycloadditions.[158] The same group also conducted a similar study on H_3[TPFPC] and determined that it also could react as both the 2π or 4π component, in both [4 + 2] cycloadditions and in thermal [4 + 4] cycloadditions, depending on temperature and reaction time (**Figure 46**).[159]

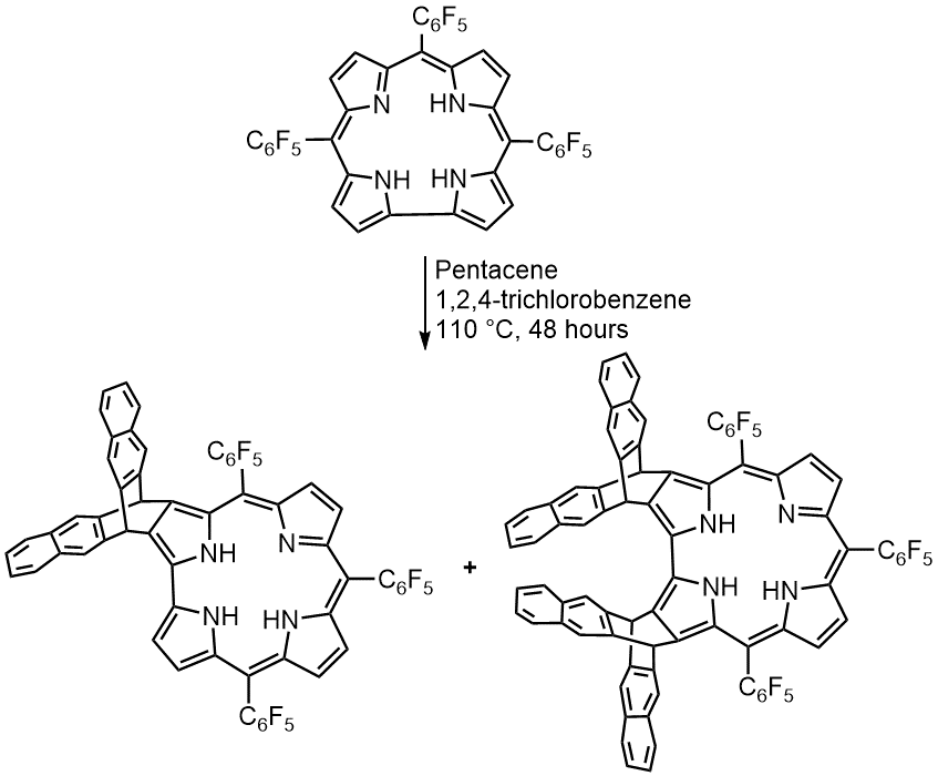

Figure 46. [4 + 2] cycloaddition products obtained from the reaction of pentacene and H_3[TPFPC].

3.10. Fluorination

β-Fluorinated porphyrins and corroles are relatively rare, in large part due to the inconvenience of obtaining such compounds. No direct protocol for *β*-fluorination exists for obtaining these compounds, and therefore all synthetic methods rely on the condensation of a fluorinated pyrrole and an aldehyde. Ogoshi *et al*. prepared the first *β*-tetrafluorinated porphyrin in 2 % yield by tetramerization of 3-methyl-4-fluoro-3-methylpyrrole-2-carboxylic acid, which had been prepared by a tedious multi-step protocol.[160] Other early syntheses include the preparation of 1-fluoro-1-methylmesoporphyrin-IX via a MacDonald type “2 + 2”

condensation of dipyrromethenes and copper-mediated cyclization of an *a,c*-difluorobiladiene (**Figure 47**).[161]

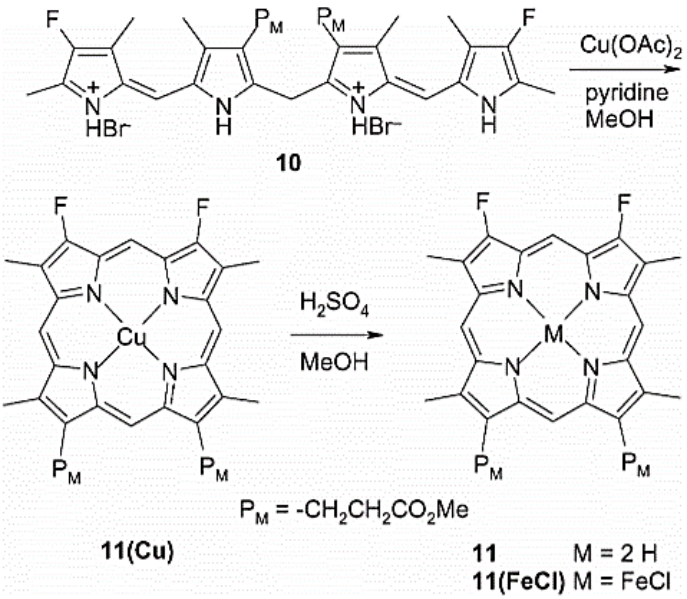

Figure 47. Synthesis of a *β*-fluorinated porphyrin via an *a,c*-difluorobiladiene. Adapted with permission from ref 161. Copyright 2008 John Wiley and Sons.

Coincidentally, the first *β*-octafluorinated porphyrins were simultaneously reported in 1997 by two different groups, both utilizing 3,4-difluoropyrrole, an aromatic aldehyde and typical Lindsey conditions (**Figure 48**).[162,163] An easier and more straightforward procedure for synthesizing 3,4-difluoropyrrole was published in 1998 and is still today the most widely used protocol.[164] However, quite recently, a much simplified procedure involving the double lithiation of the readily accessible 1-triisopropylsilyl-3,4-dibromopyrrole and subsequent reaction with *N*-fluorobenzenesulfonimide (NFSI), leading to the *N*-protected 3,4-difluoropyrrole was reported.[165]

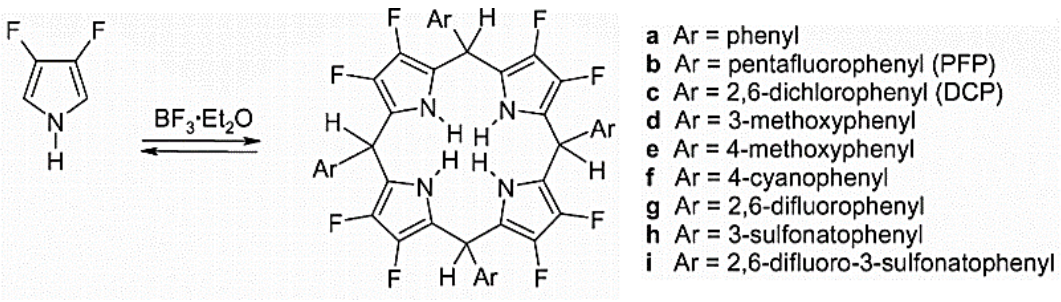

Figure 48. Synthesis of *β*-octafluorinated porphyrins via 3,4-difluoropyrrole. Adapted with permission from ref 161. Copyright 2008 John Wiley and Sons.

The first synthesis of a *β*-octafluorinated corrole, and also the first perfluorinated corrole, was reported in 2006 by Chang *et al*., and utilized 3,4-difluoropyrrole under solvent-free conditions.[166] Shortly thereafter, Ghosh and co-workers synthesized several other *β*-octafluoro tetraarylcorroles using the same conditions (**Figure 49**).[167] More recently, *β*-octafluorocorroles have also been synthesized from 3,4-difluoropyrroles using modified Lindsey conditions.[168]

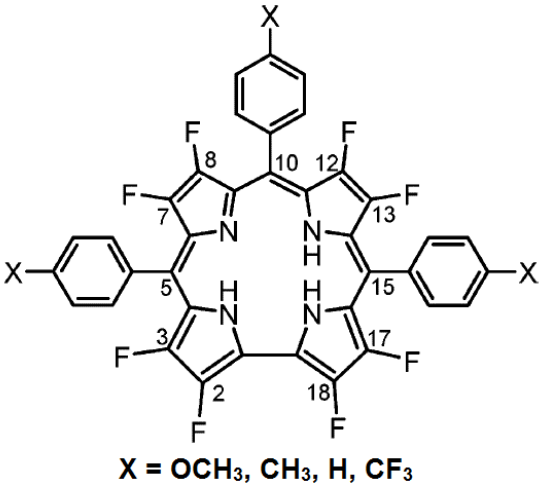

Figure 49. *β*-octafluoro tetraarylcorroles synthesized by the Ghosh group. Adapted with permission from ref 167. Copyright 2003 American Chemical Society.

3.11. Chlorination

The first synthesis of *β*-octachlorinated porphyrins was accomplished by the slow bubbling of chlorine gas through a hot (140 °C) *o*-dichlorobenzene solution of 5,10,15,20-tetrakis(2,6-dichlorophenylporphyinatio)iron(III) (Fe[2,6-TDCPP]) and anhydrous iron chloride. Treatment of chloro-5,10,15,20-tetrakis(pentachlorophenylporphyrinato)iron(III) (Fe[TPCPP]Cl) under the same conditions gave the corresponding perchlorinated metalloporphyrin (**Figure 50**). In addition, it was found that the reaction of Ni[TPP] with just over 8 equivalents of *N*-chlorosuccinimide (NCS) in hot (140 °C) *o*-dichlorobenzene readily yielded the *β*-octachlorinated nickel porphyrin, which could then be demetallated to the free base.[169] Reactions of NCS with free-base 5,10,15,20-tetrakis(2,6-dimethoxyphenyl)porphyrin unexpectedly resulted in the chlorination of both the *β*-positions and the 3- and 5-positions on the phenyl ring, giving a highly chlorinated porphyrin.[170] More recent syntheses have used an excess thionyl chloride ($SOCl_2$) as the chlorination agent.[171,172]

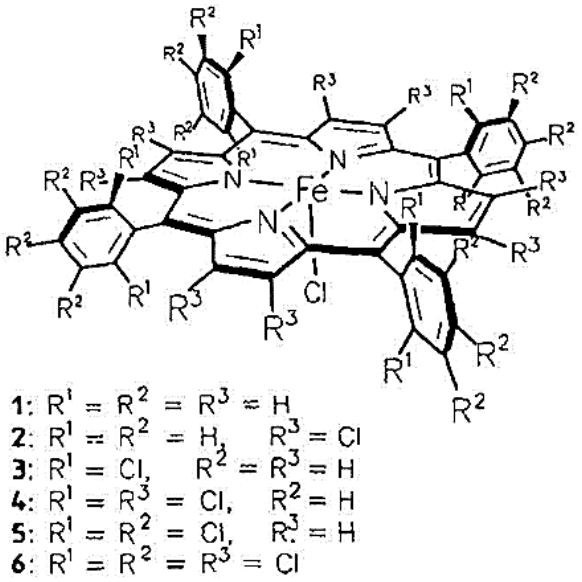

Figure 50. Products obtained by *β*-chlorination of iron porphyrins. Adapted with permission from ref 169. Copyright 2003 John Wiley and Sons.

Maes *et al*. synthesized the first *β*-octachlorinated corrole using the conditions devised by Dolphin *et al*. for porphyrins. The copper complex of 5,15-bis(mesityl)-10-(2,6-dichloropyrimidin-5-yl)corrole was treated with excess NCS in hot *o*-dichlorobenzene to yield the corresponding *β*-octachlorinated copper corrole, which could then be demetallated to the free-base *β*-octachlorocorrole (**Figure 51**).[173] Gross and co-workers prepared bis-pyridine-*β*-octachloro-5,10,15-tris(pentafluorophenylcorrolato)cobalt(III) (Co[Cl_8TPFPC]py_2) by bubbling chlorine gas through a solution of benzene and the parent metallocorrole, followed by the addition of pyridine and $NaBH_4$.[174]

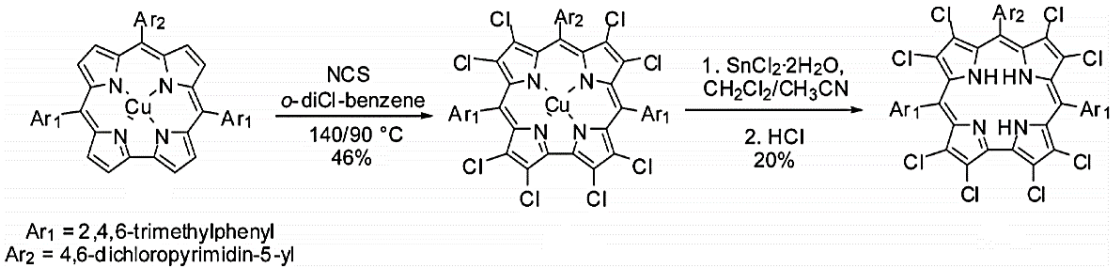

Figure 51. Synthesis and demetallation protocol for a copper corrole. Adapted with permission from ref 173. Copyright 2008 Royal Society of Chemistry.

3.12. Bromination

β-Bromination of porphyrins and corroles is commonly done with liquid bromine or *N*-bromosuccinimide (NBS). Methods developed by the Traylor and Krishnan groups laid the groundwork for much of the research in this area. Traylor reported the successful *β*-octabromination of 5,10,15,20-tetrakis(2,6-dichlorophenylporphyrinato)zinc(II) using NBS in refluxing carbon tetrachloride,[175] while the Krishnan group later accomplished the *β*-octabromination of Cu[TPP] using liquid bromine in a chloroform/carbon tetrachloride solution at ambient temperature. The copper complex was demetallated and the resulting free base was used to prepare several additional *β*-octabrominated metalloporphyrins (**Figure 52**).[176] A more recent publication details the use of 3,4-dibromopyrrole and aromatic aldehydes for the preparation of free-base *β*-octabromo porphyrins by standard Lindsey conditions, eliminating the need for copper insertion and subsequent demetallation (**Figure 53**).[177]

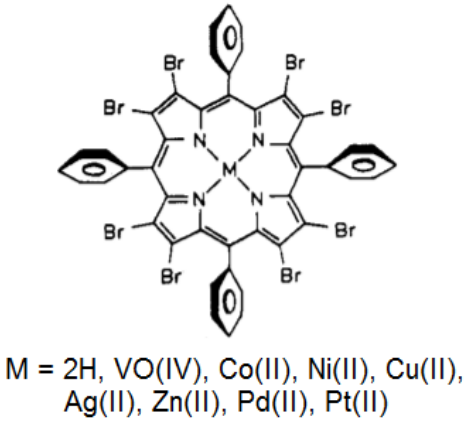

Figure 52. *β*-octabrominated free-base and metalloporphyrins prepared by Krishnan *et al*. Adapted with permission from ref 176. Copyright 1991 American Chemical Society.

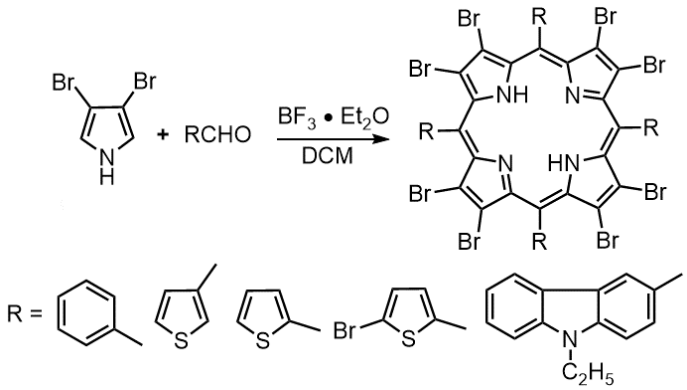

Figure 53. Synthesis of *β*-octabrominated porphyrins from 3,4-dibromopyrrole.

Paolesse reported the initial formation of a *β*-octabrominated isocorrole from the reaction of TPC and an excess NBS in chloroform at ambient temperature. The isocorrole formation was hypothesized to occur due to steric strain induced by the central NH protons, causing one of the protons to migrate to the 10-*meso* carbon. Cobalt complexation of the isocorroles using cobalt(II)acetate and triphenylphosphine led to re-aromatization and the corresponding cobalt *β*-octabromocorroles.[48] Another group found that by controlling the amount of NBS carefully, it was possible to regioselectively obtain *β*-di-, tri- and tetrabrominated corroles in good yields. The *β*-mono-brominated corrole, however, was obtained as an inseparable mixture of two isomers.[150] Paolesse found that by reacting either the free-base isocorrole or the silver complex of 3-NO_2-T*p*MePC with NBS in chloroform, the *β*-monobrominated 2-Br or 3-Br isomer could be obtained, respectively. The driving force behind the regioselective formation of the 2-Br isomer is thought to be the isocorrole intermediate (**Figure 54**).[178] Paolesse has since published many similar studies.[179,180] Gross and co-workers have also reported several *β*-octabrominated metal complexes of TPFPC prepared by both NBS and liquid bromine.[181-183] Quite recently, Ghosh and co-workers reported a simplified procedure for the purification of *β*-octabromocorroles, and the synthesis of previously inaccessible sterically hindered 5,10,15-tris(2,6-dichlorophenyl)corrole. In the modified procedure, crystallization is utilized in lieu of tedious column chromatography for a wide range of *β*-octabromo derivatives.[184]

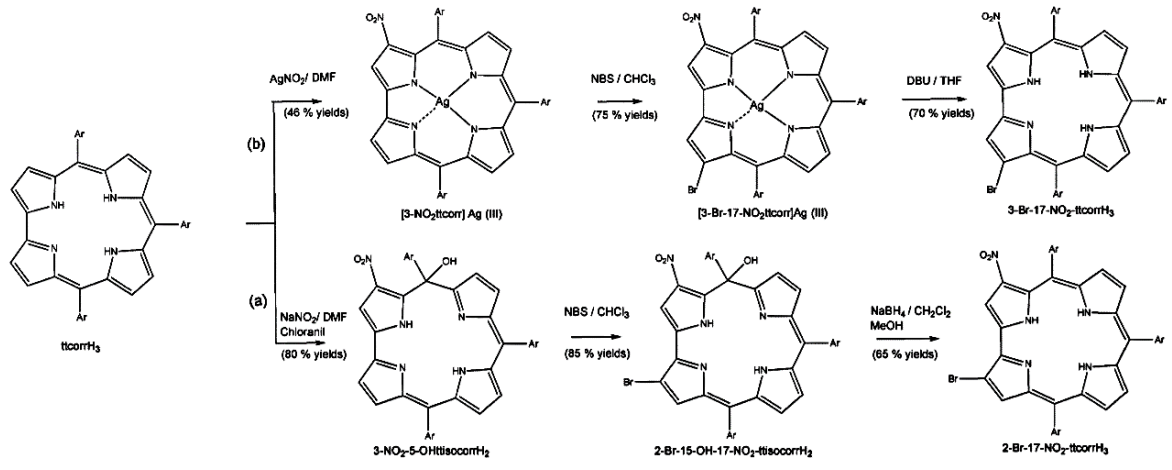

Figure 54. Different reaction pathways for the bromination of 3-NO_2-T*p*MePC derivatives. Adapted with permission from ref 178. Copyright 2011 Royal Society of Chemistry.

3.13. Alkylation

We have already seen a few examples of *β*-alkylated porphyrins and corroles synthesized by various methods based on pre-alkylated reactants prior to macrocyclization. Examples include the Fischer and MacDonald (2 + 2) and (3 + 1) syntheses and condensations of alkyl-substituted *b*-bilenes, *b*-oxobilanes, *a*,*c*-biladienes, DPMs and pyrroles. Attempts at direct alkylations of porphyrins using nucleophiles such as organolithiums or Grignard reagents preferentially lead to attack on *meso*-positions and formation of chlorins through subsequent *β*-attacks.[185] In one study, reaction of chloro-*N*-phenyl-5,10,15,20-tetrakis(phenylporphyrinato)zinc(II) with butyl- and methyllitium led to monobutylated and monomethylated porphyrin, respectively (**Figure 55**). The reaction was thought to proceed via nucleophilic addition to the *β*-*β* double bond.[186]

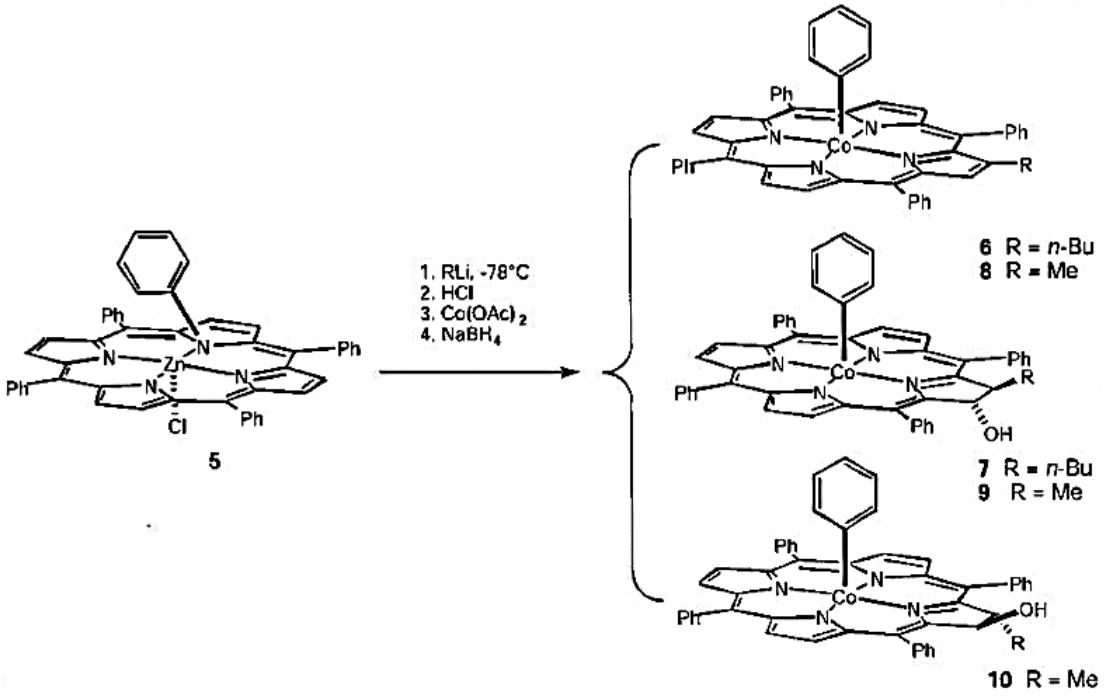

Figure 55. Direct *β*-alkylation of a metalloporphyrin. Adapted with permission from ref 186. Copyright 1999 John Wiley and Sons.

3.14. Arylation

Like alkylation, *β*-arylation of porphyrins and corroles can be accomplished via condensations of pre-arylated pyrroles[187-190] with aldehydes, or by transition-metal-catalyzed cross-couplings on the brominated macrocycles.[191,192] In an important development, a protocol for the regioselective, direct *β*-di-arylation of 5,10,15-tris(3,5-di-*tert*-butylphenylporphyrinato)nickel(II) has been reported by Osuka and coworkers.[193]

Metalloporphyrins and different aryl halides were reacted in the presence of pivalic acid, potassium carbonate, catalytic amounts of palladium acetate and a bulky ligand (DavePhos) in DMA (**Figure 56**). Applying the same procedure to 5,10,15-tris(3,5-di-*tert*-butylphenyl)-20-(formylporphyrinato)nickel(II) displayed similar regioselectivity, albeit with slower reaction rates.[194] No similar protocol has been reported for corroles yet.

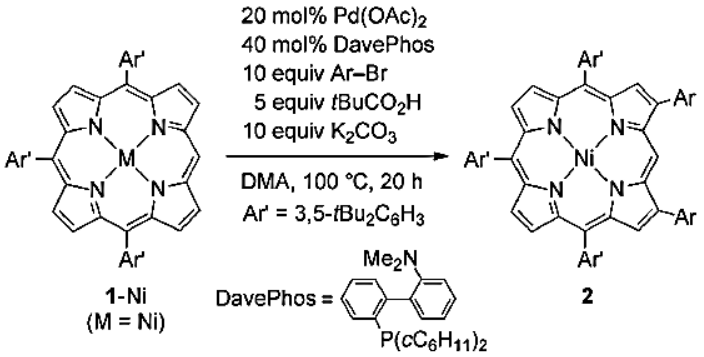

Entry	Ar	2	Yield[a] [%]
1	C_6H_5	**2a**	76
2	2-MeC_6H_4	**2b**	71
3	3-MeC_6H_4	**2c**	81
4	4-MeC_6H_4	**2d**	79
5	3,5-$Me_2C_6H_3$	**2e**	80
6	2-naphthyl	**2f**	84
7	3-$MeOC_6H_4$	**2g**	72
8	4-$MeOC_6H_4$	**2h**	8
9	4-$Me_2NC_6H_4$	**2i**	32
10	4-$EtO_2CC_6H_4$	**2j**	28
11	4-$O_2NC_6H_4$	**2k**	3

Figure 56. Scope of the palladium-catalyzed direct *β*-arylation of porphyrins. Adapted with permission from ref 193. Copyright 2011 John Wiley and Sons.

Chapter 4. Introduction to Paper A: Octaiodoporphyrin.

Porphyrins enjoy applications in diverse fields as solar cells,[22] photodynamic therapy,[23,83] NIR dyes,[25] nonlinear optics,[26] gas sensing,[84] catalysis,[195] and light emitting materials[196] among others. The ease of modulating properties through chemical transformations of the macrocycle is undoubtedly a major factor underlying the versatility of the compounds, and as such, the functionalization of porphyrins has been extensively studied.[197] Of great importance are *β*-octabrominated porphyrins, in large part due to the ease of replacing the bromines by other functionalities through typical organometallic reactions.[118] The most extensively developed of these reactions is the Suzuki-Miyaura cross-coupling, which is the palladium-catalyzed cross-coupling of an aryl halide with a boronic acid or ester (**Figure 57**).[198] The reaction proceeds via oxidative addition of Pd(0) to the aryl halide, resulting in an organopalladium(II)-complex (**A**). The complex reacts with base to form (**B**), which reacts through transmetalation with a boronate complex to produce (**C**). Reductive elimination of the cross-coupled species (**D**) restores the Pd(0) catalyst.

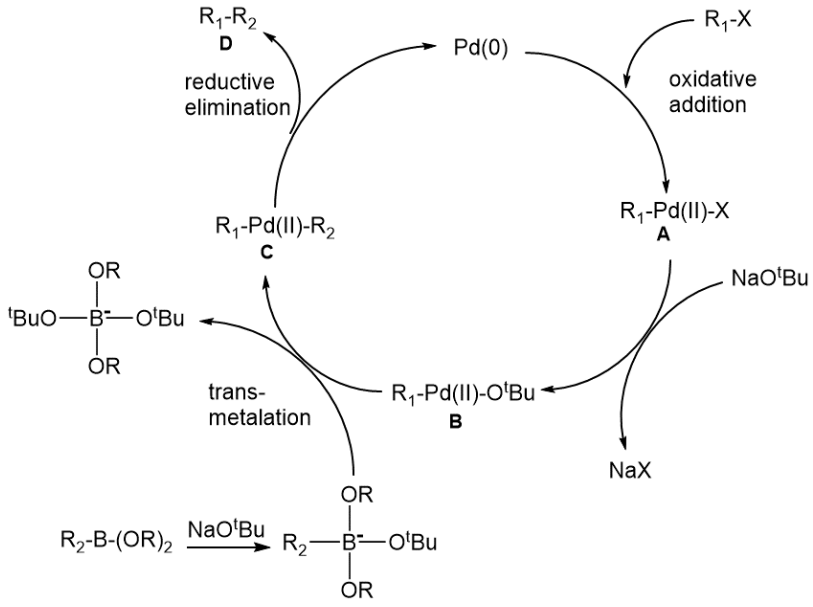

Figure 57. Catalytic cycle depicting the mechanism of the Suzuki-Miyaura cross-coupling reaction.

It is commonly accepted that the rate-determining step in the Suzuki-Miyaura reaction is the oxidative addition step, and the rate of reaction depends on the bond dissociation energy of the carbon-halogen bond. The relative rate of reaction thus typically proceeds in the order of R−I > R−Br > R−Cl > R−F.[199] In addition, there are numerous similar transition-metal-

catalyzed cross-coupling reactions including the Heck-,[200] Stille-,[201] Kumada-,[202] Negishi-,[203] Hiyama-[204] and Sonogashira reactions,[205] enabling a wide array of different functionalizations.

The idea of synthesizing a *β*-octaiodoporphyrin, which would be more reactive and might permit reactions that are impossible with *β*-octabromoporphyrins, intrigued me. From my literature searches, it became evident that despite almost 100 years of porphyrin research, not a single example of a *β*-octaiodinated porphyrin has been reported. In fact, very few iodinated porphyrin species have been reported at all. The few examples I encountered included the mono- and diiodination of a 5,15-diphenylporphyrin using bis(trifluoroacetoxy-)-iodobenzene-iodine in chloroform/pyridine. This led to a regiomeric mixture where the first iodination happens at one of the free *meso* positions, and the second happens at one of the *β*-positions. On applying the same conditions to a 5,15-diarylporphyrin with bulky aryl groups (3,4,5-trimethoxyphenyl), diiodination happens selectively at the free *meso*-positions. The zinc-complex of this porphyrin was subsequently used successfully in a Sonogashira-type coupling to produce the *meso*-5,15(phenyl)-10,20-(diethynyl)porphyrin.[197] There is a similar example of the synthesis of a porphyrin bearing iodine in the *meso*-position,[206] and of others where iodine is situated on the phenyl rings,[207,208] but *β*-iodination is almost unprecedented.[209] Inspired by the absence of *β*-polyiodoporphyrin derivatives, I set my sights on the synthesis of *β*-octaiodoporphyrin. Direct *β*-iodination seemed unpromising, since electrophilic iodination is generally rather sluggish compared to electrophilic bromination or chlorination. My efforts instead focused on synthesizing 3,4-diiodopyrrole for subsequent condensation to the *β*-octaiodinated porphyrin. An early synthesis of 3,4-diiodopyrrole was achieved using a bulky *N*-protecting group (triisopropylsilyl or TIPS) to direct the electrophilic attack. However, the protocol relied on using stoichiometric amounts of highly toxic mercuric acetate and iodine.[210] I decided to utilize the 1-TIPS-pyrrole for obtaining regioselective iodination, but started searching for a new iodination protocol. NIS worked reasonably for my purpose, but the reaction proved time-consuming and led to mixtures of mono and diiodinated products. During my efforts to optimize the procedure, I found an old method for direct periodination of unactivated aromatics employing a mixture of iodine (I_2) and periodic acid (H_5IO_6) in concentrated sulfuric acid.[211] Initial experiments using this procedure led to nearly explosive sublimation of iodine. However, upon substituting the sulfuric acid for Et_2O or THF, the reaction was complete in one hour with good yields.

Finding the conditions that ultimately led to the *β*-octaiodinated porphyrin was a painfully long and troublesome affair involving adjustment of acid catalyst used, solvent,

aldehyde, amount and type of oxidant, reaction time and temperature. By careful optimizations of the parameters, I eventually found the conditions leading to exclusively *β*-octaiodinated porphyrin. Thus, condensation of 3,4-diiodopyrrole and 4-trifluoromethylbenzaldehyde using typical Lindsey conditions ($BF_3 \bullet Et_2O$ in DCM) at -10 °C resulted in a 10 % yield of the expected $H_2[I_8T\textit{p}CF_3PP]$ – the first *β*-octaiodoporphyrin. The free-base *β*-octaiodoporphyrin could be complexed to Ni(II), Cu(II) and Zn(II), and the products structurally characterized. The crystal structure of the Zn(II) complex exhibits the most saddled distortion of any simple metalloporphyrin, known to date.

β-Octaiodinated porphyrins have clear synthetic potential and may pave the way for novel and faster chemical transformations than analogous *β*-octabrominated porphyrins. Exploring these ligands by means of transition-metal-catalyzed cross-couplings remains a key goal for future research.

Chapter 5. Introduction to Paper B: Molecular Structure of a *β*-Octaiodo-*meso*-tetraarylporphyrin. A Rational Route to *Cis* Porphyrin Tautomers?

The location and dynamics of the central NH protons of porphyrins has been the subject of many in-depth studies over the years.[212] Early X-ray crystal structures[213-216] and ab initio calculations indicated a linear N−H···H−N arrangement, where each NH proton participates in symmetric, bifurcated hydrogen bonding with two adjacent nitrogen.[217-219] Subsequently, elaborate kinetic studies revealed that the NH tautomerism in free-base porphyrins occurs in a stepwise manner, most likely via a *cis* porphyrin tautomer.[220-223] Early density functional theory calculations confirmed that the *cis* tautomer is a true minimum-energy structure with exact C_{2v} symmetry in the absence of symmetry-lowering substituents. The calculations also indicated an energy of 7-8 kcal/mol for the *cis* tautomer relative to the ground-state *trans* tautomer.[65,224]

Interestingly, as early as 1941, Rothemund erroneously believed to have isolated the *cis* tautomer as a by-product of his eponymous tetraphenylporphyrin synthesis.[89] Later work showed that this product is actually tetraphenylchlorin. Aside from an *cis*-*N*,*N´*-dimethylated porphyrin,[225] no genuine *cis* porphyrin tautomer has been reported, until very recently.[226] Single crystal X-ray analysis of free-base *β*-heptakis(trifluoromethyl)-*meso*-tetrakis(4-fluorophenyl)porphyrin (H_2[$(CF_3)_7$T*p*FPP]), a compound synthesized by my colleague Dr. Kolle E. Thomas, revealed the first ever *cis* porphyrin structure. The unique stability of the *cis* tautomeric structure reflected the combined effects of strong macrocycle saddling, which relieved electrostatic repulsion between the two neighboring NH protons, and two polarization-enhanced transannular N−H···O−H···N hydrogen bond chains, each involving a molecule of water (**Figure 58**). DFT calculations indicated that the dihydrated *cis* tautomer should have a lower energy than the dihydrated *trans* tautomer by some 8.3 kcal/mol.

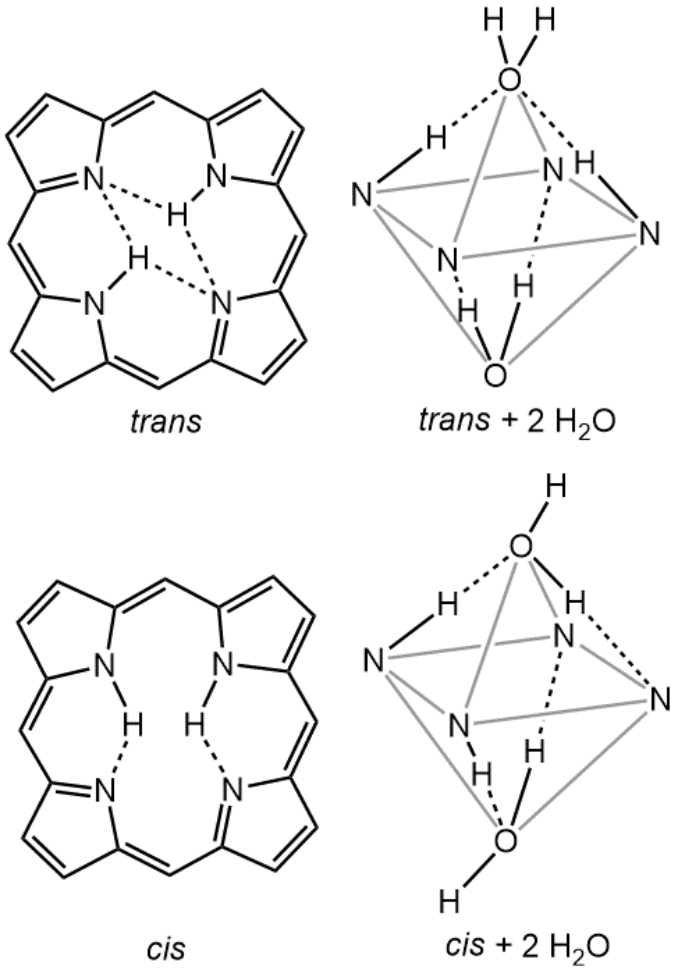

Figure 58. Potential hydrogen bond chains in *trans* and *cis* tautomers of a free-base porphyrin.

From water structure theory, we know that each water molecule can form up to four hydrogen bonds in a tetrahedral arrangement – two via the oxygen lone pairs and two via the hydrogens.[227,228] An important feature of hydrogen bonds is the so-called cooperative effect, which allows large clusters of hydrogen-bonded water to form. The essence of this effect is that a water molecule that acts as a hydrogen bond acceptor also becomes a better hydrogen bond donor. This effect is clearly displayed in cyclic water pentamers where the hydrogen bond network can be classified as either homodromic (donor-acceptor), antidromic (acceptor-acceptor), or heterodromic (donor-donor), depending on the orientation of the hydrogens (**Figure 59**). Homodromic networks, where the hydrogens all point in the same direction (clockwise or anticlockwise), are more stable than antidromic networks, where only some hydrogens point in a given direction. The heterodromic system is the least stable with only two hydrogens in a cooperative alignment. Studies of *β*-cyclodextrin has also revealed homodromic hydrogen-bonding networks within the cavity of the molecule (**Figure 60**).[229,230]

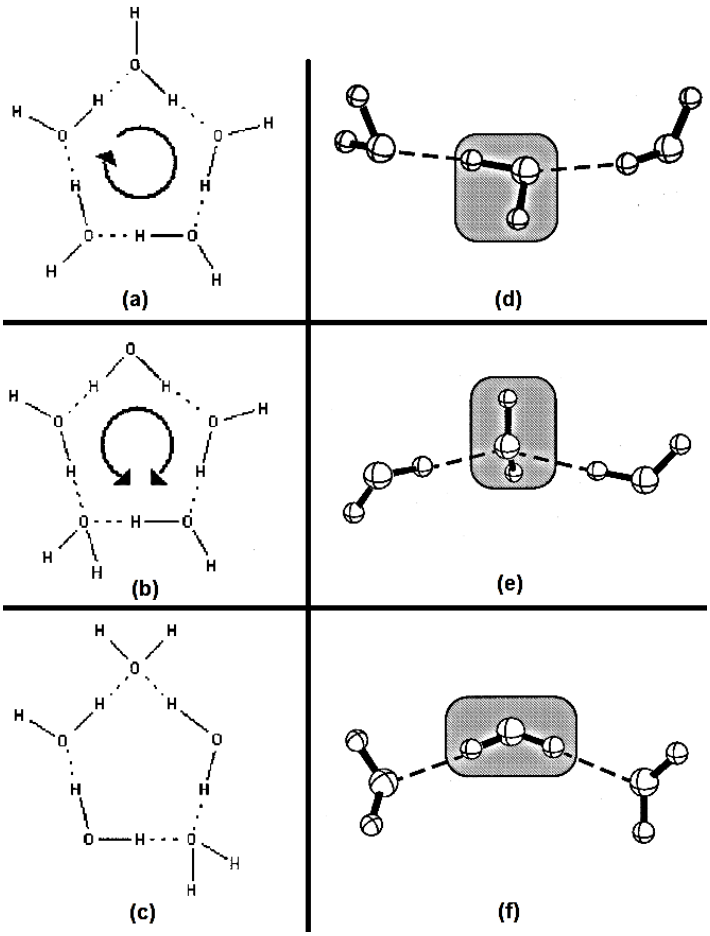

Figure 59. Arrangements of cyclic hydrogen bonds: (a) homodromic, (b) antidromic or (c) heterodromic. Adapted with permission from ref 227. Copyright 2010 John Wiley and Sons. Participation of individual water molecules as either (d) donor-acceptor, (e) acceptor-acceptor or (f) donor-donor. Adapted with permission from ref 228. Copyright 2000 Elsevier.

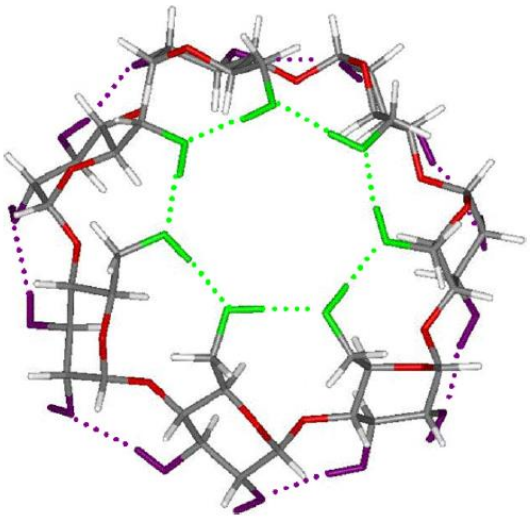

Figure 60. Calculated minimum energy homodromic hydrogen bonded network in *β*-cyclodextrin. Adapted with permission from ref 229. Copyright 2007 Elsevier.

The X-ray structure of the previously mentioned *cis* porphyrin tautomer shows two adjacent central NH protons pointing above and below the mean porphyrin plane.[226] Each NH proton acts as a hydrogen bond donor to a molecule of water, which in turn acts as a hydrogen bond donor to an opposite unprotonated nitrogen, forming homodirectional polarization-enhanced N−H···O−H···N hydrogen bond chains. The homodirectional hydrogen-bonded chains also explain the increased stability of the *cis* tautomer compared to the *trans* tautomer, for which a homodirectional hydrogen bond network is impossible. Although the structure fully made sense, the question remained whether the observed structure was just a one-off, or whether additional *cis* porphyrin tautomers would be discovered in the future. As it happens, I was destined to answer this question.

Crystallization of free-base *β*-octaiodoporphyrin was something I worked on continuously ever since we published our first synthetic paper on the subject (**Paper A**). I crystallized the free base porphyrin from a variety of different solvents, but every time the X-ray diffraction analysis proved inadequate in terms of quality. After numerous attempts over a year, I finally managed to obtain high-quality crystals by vapor diffusion of methanol into a concentrated toluene solution of the free-base porphyrin. The X-ray structure revealed only the second known example of a *cis* porphyrin tautomer. The details of the structure proved entirely analogous to the first one – namely a strongly saddled *cis β*-octaiodoporphyrin tautomer with a homodirectional N−H···O−H···N strap across each face. The only significant difference was that the bridging unit was a mixture of methanol and water.

Based on the two *cis* porphyrin structures, it seems likely that additional such structures might be discovered in the future. The requirements appear to be two-fold: a free-base porphyrin with a strongly saddled conformation due to steric factors and the presence of an amphiprotic solvent. Whether *β*-octabromoporphyrins and dodecaarylporphyrins might exhibit a *cis* tautomeric structure under suitable conditions remains a key question in this area.

Chapter 6. Introduction to Paper C: Synthesis and Molecular Structure of a Copper Octaiodocorrole.

Ever since the development of convenient and simple one-pot synthetic routes,[112,113] the chemistry of corroles has grown exponentially. Qualitatively, corroles share many of the same intriguing electronic, photophysical, metal-coordinating and catalytic properties of porphyrins; many details, however, are very different. The differences largely reflect two factors, a significantly smaller N_4 core than porphyrins and trianionic character (compared with dianionic porphyrins). In addition, corroles are generally more electron-rich and oxidation-prone than porphyrins. Corroles engender a variety of high oxidation state transition metal complexes.[18] However, because of the electron-richness of the ring, many of the complexes are noninnocent and have significant corrole dianion-radical character.

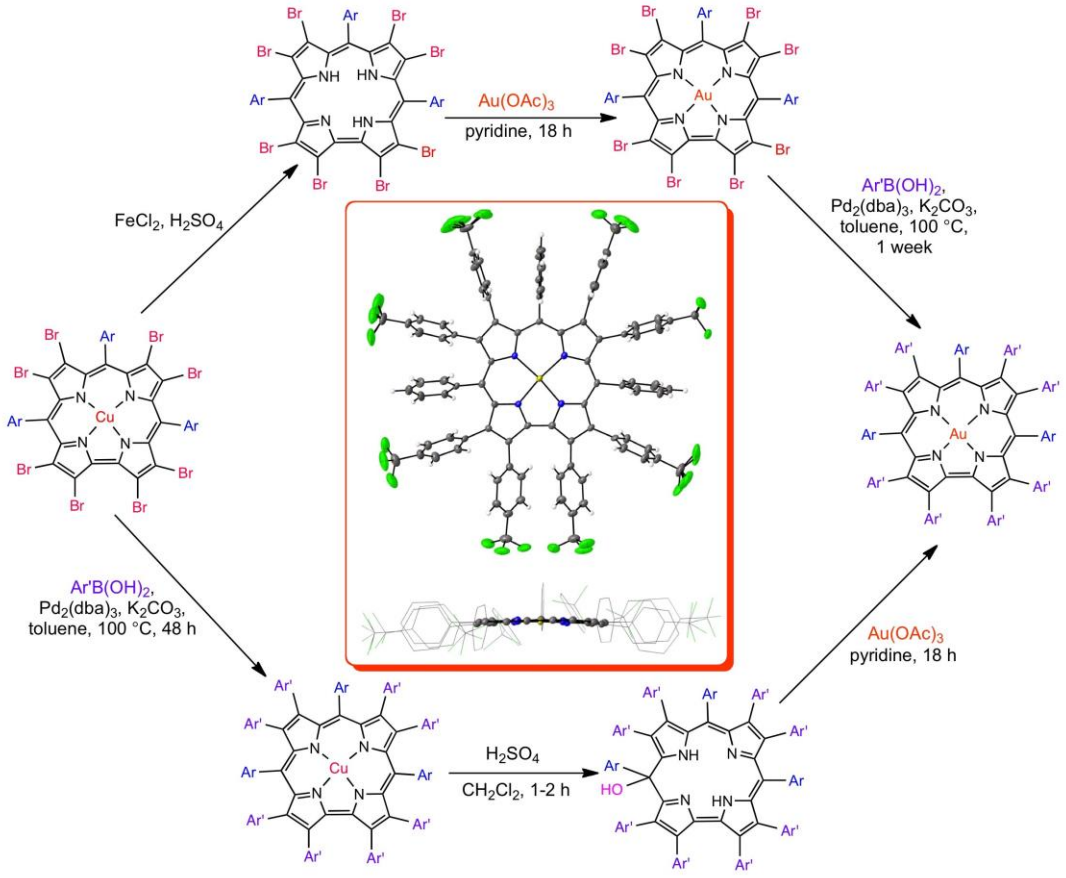

Figure 61. Two uses of *β*-octabromocorroles to synthesize Au undecaarylcorroles. Adapted with permission from ref 231. Copyright 2016 Elsevier.

As for porphyrins, *β*-octabromination of corroles affords a stepping stone to a plethora of available transition-metal-catalyzed transformations.[117] **Figure 61** provides a good illustration of this chemistry, which provided two routes to a gold undecaarylcorrole.[231] A series of undecasubstituted corroles were synthesized some time ago by Suzuki coupling on a *β*-octabrominated free-base corrole.[232] The reaction, however, took between 1½ and 2½ days to complete. The potential of a *β*-octaiodinated corrole would thus be immense, given the higher facility of the rate-limiting oxidative addition step in reactions like the Suzuki-Miyaura coupling.[199] Thus, I set out on a quest to synthesize an octaiodocorrole. The literature on the field was sparse, with only a handful of examples. Gross reported the partial *β*-tri- and tetraiodination of aluminum and gallium corroles using an excess of iodine and NIS, respectively (**Figure 62**). Reaction of the aluminum complex with 1,3-diiodo-5,5-dimethylhydantoin (NIH) also yielded the tetraiodinated species, albeit in lower yields.[233,234] Interestingly, all the iodines in the tetraiodinated aluminum species added regiselectively to two of the pyrrole rings (positions 2, 3, 17, and 18). They also applied the same protocol to cobalt corroles, in which case a mixture of *β*-tri- and tetraiodinated products were obtained. In this case as well, the iodines added regioselectively to the same two pyrrole rings.[235] Finally, they reported obtaining the *β*-tetraiodinated metallocorroles (Cu, Ag, Au) by a one-pot conversion of H_3[TPFPC] using a metal acetate and NIS in pyridine.[236] Paolesse has also prepared a *β*-diiodinated silver corrole complex by treatment with NIS in a dichloromethane/acetonitrile mixture.[180]

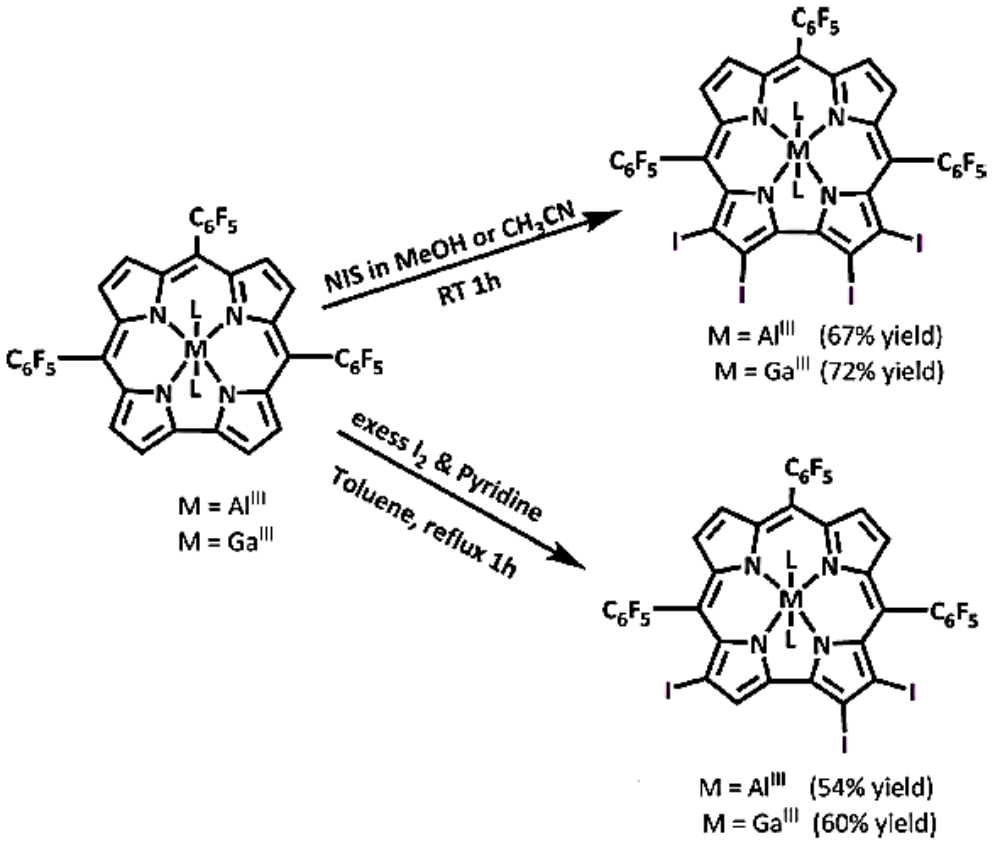

Figure 62. Two routes for obtaining partially *β*-iodinated Ga(III) and Al(III) corroles. Adapted with permission from ref 234. Copyright 2014 American Chemical Society.

My initial efforts to synthesize a *β*-octaiodocorrole focused on the utilization of 3,4-diiodopyrrole via a variety of different synthetic methods, which unfortunately resulted in only traces of the expected corroles. The attempted iodination of iridium corroles using NIS, led to mixtures of partially *β*-iodinated corroles and decomposition products. It occurred to me that copper corroles – known for their inherent saddling – might be better suited sterically to sustain *β*-octaiodination. I therefore prepared a series of copper corroles Cu[T*p*XPC], where X = OMe, Me and CF_3. Iodination using the same protocol I applied for the preparation of 1-TIPS-3,4-diiodopyrrole (**Paper A**),[237] proved too harsh and resulted in complete destruction of the corroles. Attempts at metal-halogen exchange of *β*-octabrominated copper corroles with BuLi or Rieke Magnesium[238] followed by the addition of suitable electrophiles like NIS, NIH and ICl were also fruitless. The interaction of Cu[T*p*OMePC] and Cu[T*p*MePC] with TFA-activated NIS failed, but Cu[T*p*CF_3PC] yielded the desired *β*-octaiodocorrole, albeit with significant amounts of inseparable impurities. Accordingly, I chose to examine the performance of another electron-deficient Cu corrole Cu[T*p*CNPC]. Stirring the said Cu corrole with an excess of NIS in the presence of TFA in 4:1

toluene/dicloromethane for several hours indeed produced moderate yields of the expected *β*-octaiodocorrole. By varying experimental conditions such as the amount of iodinating agent (10 – 100 eq.) and the solvent (acetonitrile, dichloromethane, toluene and mixtures thereof), I was able to zero in on a convenient protocol for preparing the *β*-octaiodinated corrole in yields of around 20 %. Crystals suitable for X-ray analysis were obtained by vapor diffusion of heptane into a concentrated solution of the corrole in *o*-dichlorobenzene, revealing the first example of a *β*-octaiodinated corrole. Future work will concentrate on developing additional, more general routes to these delicate compounds, and exploring their use as pre-cursors to other *β*-octafunctionalized corroles through transition-metal-catalyzed coupling reactions. Exploiting the stability and reactivity of Cu[T*p*CNPC] is also worth exploring vis-à-vis other synthetic transformations, perhaps for obtaining *β*-octafluorinated and *β*-octanitrated corroles under conditions that were previously deemed too harsh.

Chapter 7. Synthesis, Characterization and Photophysical Properties of a Series of Six-Coordinated Iridium(III) Corroles.

7.1. Introduction

Iridium(III) porphyrins exhibit a rich chemistry, particularly as catalysts of key transformations such as olefin cyclopropanation, four-electron reduction of dioxygen, hydrogen generation from water splitting, hydroxylation, insertions into S-H bonds, and C-O bond cleavage.[239-244] Iridium(III) porphyrins are also known to exhibit strong ambient-temperature phosphorescence with quantum yields of up to 30 %. These photophysical properties are tunable with regard to the axial ligands as iridium(III) porphyrins are typically six-coordinate, unlike their square-planar Pd(II) and Pt(II) counterparts, which are also known for their strong ambient-temperature phosphorescence.[78] Iridium was first inserted into corroles by Gray and co-workers with a view of replicating the strong room-temperature phosphorescence of iridium porphyrins. Iridium corroles were indeed found to exhibit ambient-temperature phosphorescence, with a more bathochromically shifted character than most other Ir(III) complexes and less impressive lifetimes and quantum yields.[82,245] In contrast to Ir(III) porphyrins, Ir(III) corroles are stabilized even by weakly donating axial ligands.[246] Furthermore, cyclic voltammetry has revealed Ir(III) corroles to be very electron rich, as Ir(II) is not electrochemically accessible and Ir(IV) is accessible only at low potentials.[47]

The relative rarity of iridium corroles in literature and their intriguing photophysical and electronic properties prompted me to investigate these compounds further, in particular, whether the electron rich character of Ir(III) corroles could be exploited to obtain novel *β*-octaiodinated corroles. For this purpose, a series of Ir(III) corroles, Ir[T*p*XPC]L_2, where T*p*XPC^{3-} is the trianion of *meso*-tris(*p*-X-phenyl)corrole, X = OMe, CH_3, H and CF_3 and L = trimethylamine (tma), pyridine (py), were prepared. For X = CF_3, Ir(III) complexes with L = 4-dimethylaminopyridine (dmap), 4-picolinic acid and isoquinoline were also prepared (**Figure 63**).

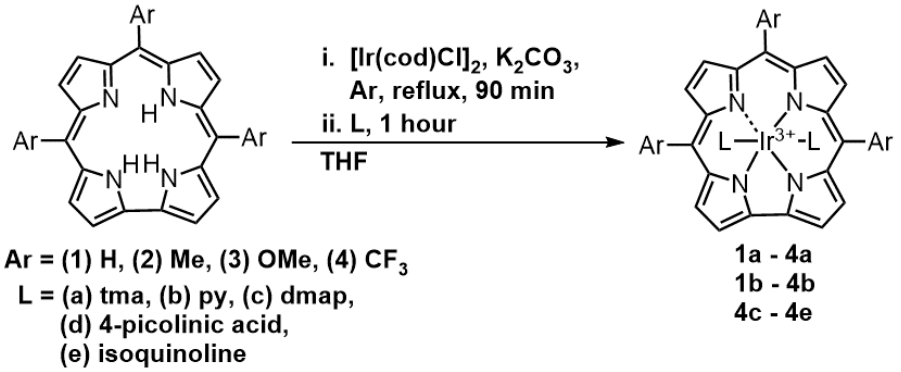

Figure 63. Synthesis of Ir(III) corroles.

Despite many attempts at iodinating the compounds using various electrophilic iodinating reagents (NIS, NIH, ICl), only complex mixtures of partially *β*-iodinated compounds (1-4 iodines) were observed. Nevertheless, the synthesis, purification and characterization of the new iridium corroles were not a complete waste of time. Armed with the fact that Ir(III) compounds tend to be phosphorescent, we also carried out a phosphorescence analysis on the most stable series – Ir[T*p*CF_3PC]L_2, where L = tma, py, dmap, 4-picolinic acid and isoquinoline. I wanted to see whether the phosphorescence varied among simple Ir(III) corroles and particularly whether the axial ligand would affect this. Somewhat disappointingly, all the compounds examined exhibited comparably weak phosphorescence in the NIR region. The complexes with pyridine and isoquinoline ligands displayed higher quantum yields, while the dmap complex exhibited a surprisingly long decaying component both at room temperature and at 77 K. Thus, to a large extent, the current work is a relatively small extension of our existing knowledge of Ir corroles. The remainder of the chapter describes the characterization of the various Ir corroles prepared.

7.2. Nuclear magnetic resonance spectroscopy

Most of the ^{1}H spectra display sharp resonances indicative of diamagnetism, while a few, in particular some *β*-Hs, show broadening. The latter is likely because of a non-optimal deuterated solvent, as the solubility varies greatly across the synthesized Ir(III) corroles. Furthermore, the tma protons resonate upfield at around −3 ppm, as is expected for a planar, aromatic macrocycle and small shielded ligands above and below. The same effect is seen on the *ortho*-protons of pyridine, 4-dimethylaminopyridine, 4-picolinic acid, and isoquinoline. Complete 1D ^{1}H-NMR spectra with assignments and supplementary 2D ^{1}H-NMR spectra can be found in the Supporting Information at the end of this Chapter.

7.3. Ultraviolet-visible spectroscopy

The UV-vis spectra for the six-coordinate Ir(III) corroles display intense and split Soret and Q bands, most likely reflecting ligand-to-metal charge transfer states.[47] The exact nature of the excited states still needs to be clarified. The UV-vis spectra of the new compounds synthesized are shown in **Figures 64 - 74**, while **Table 1** summarizes the absorption maxima.

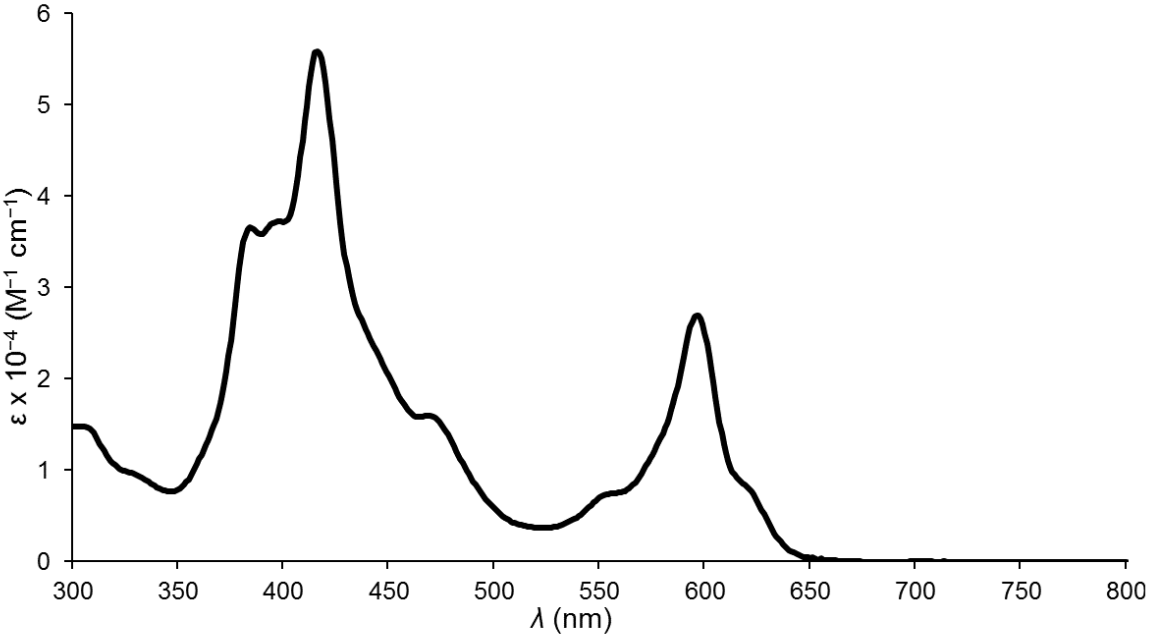

Figure 64. UV-vis spectrum of Ir[TPC]tma_2 (**1a**).

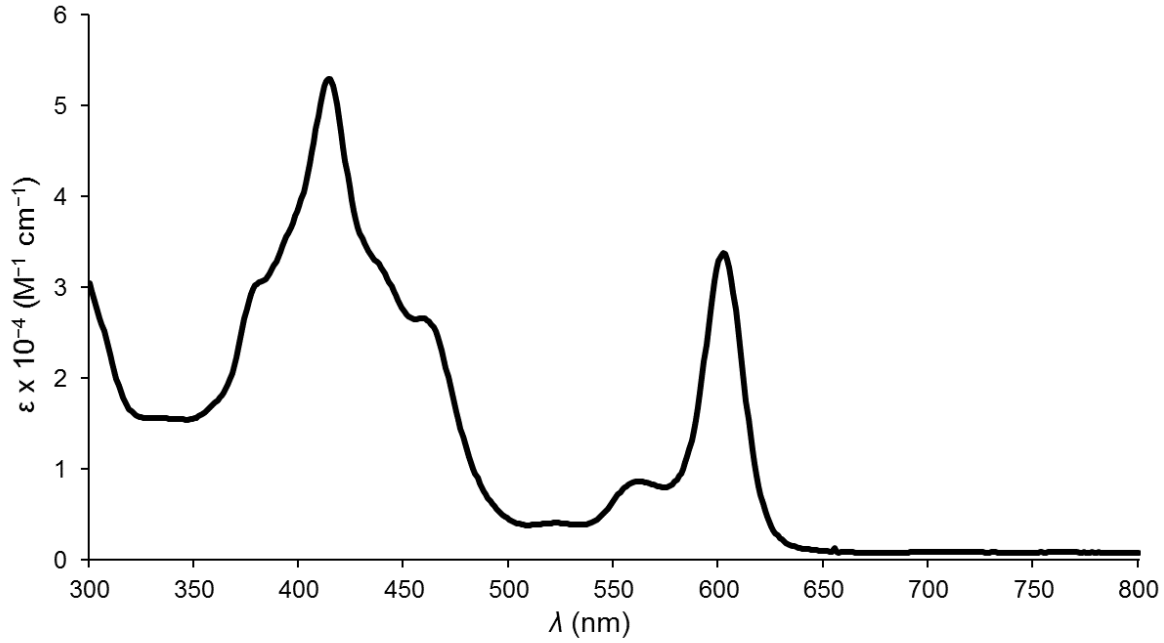

Figure 65. UV-vis spectrum of Ir[TPC]py_2 (**1b**).

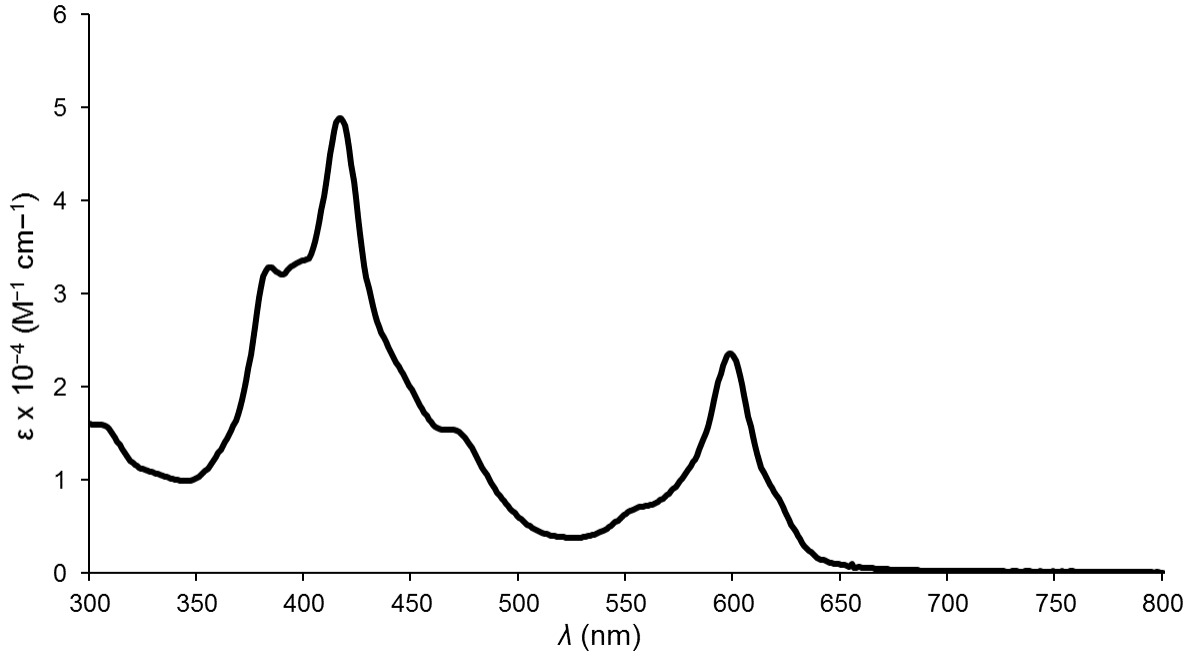

Figure 66. UV-vis spectrum of Ir[T*p*MePC]tma_2 (**2a**).

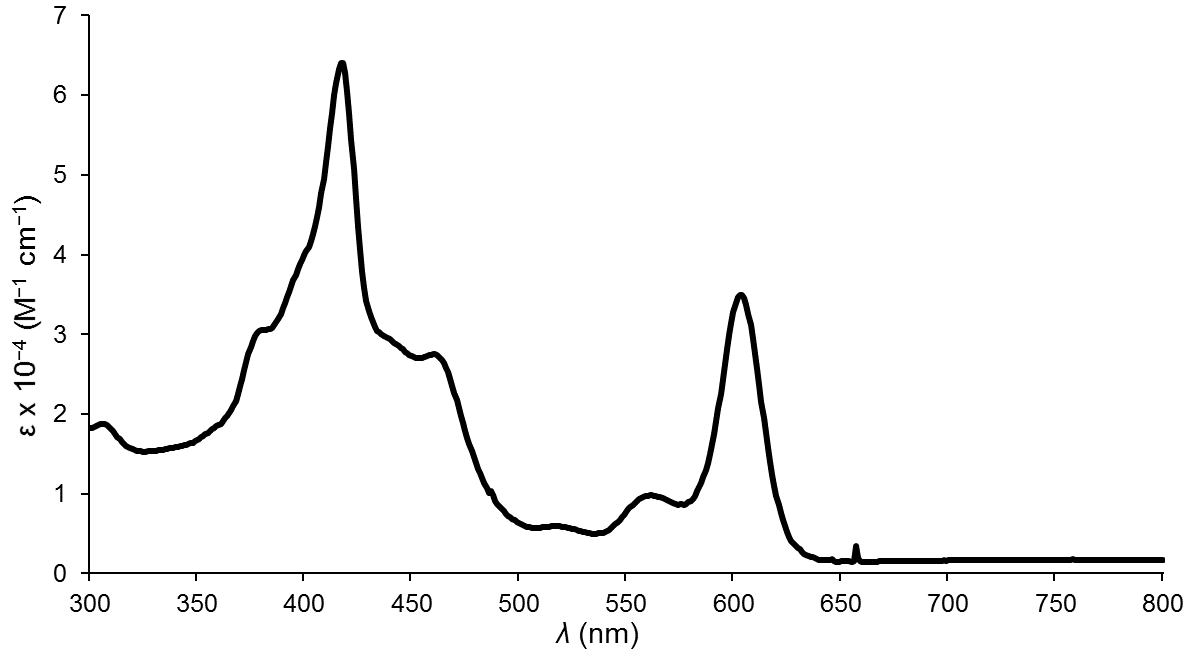

Figure 67. UV-vis spectrum of Ir[T*p*MePC]py_2 (**2b**).

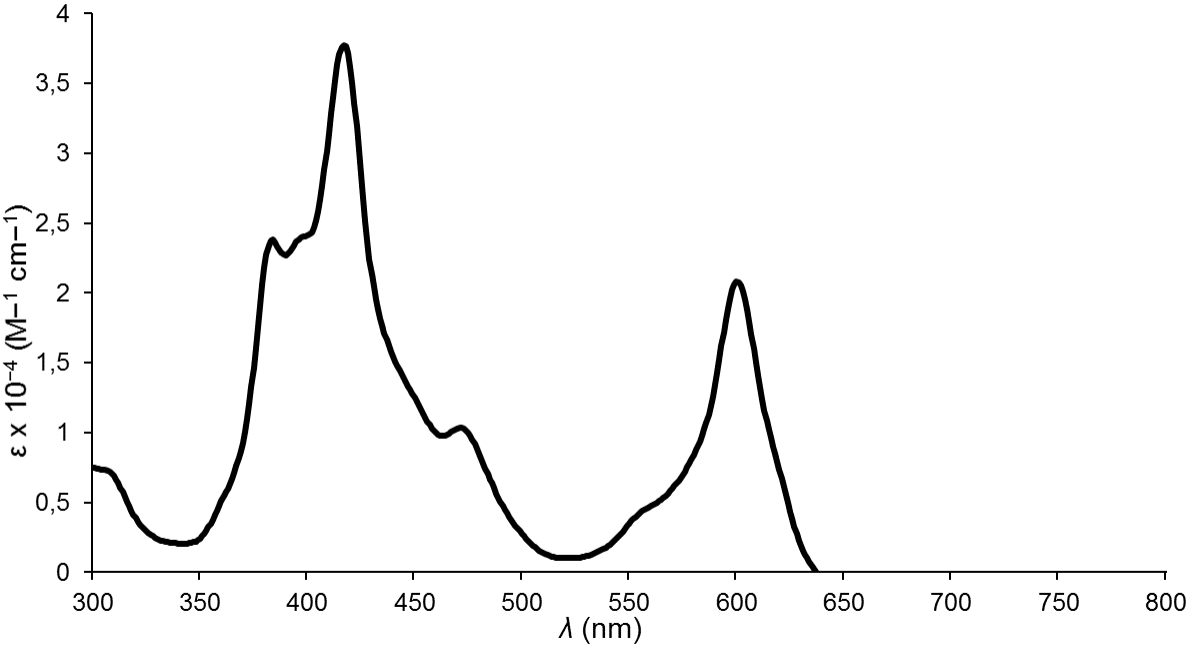

Figure 68. UV-vis spectrum of Ir[T*p*OMePC]tma_2 (**3a**).

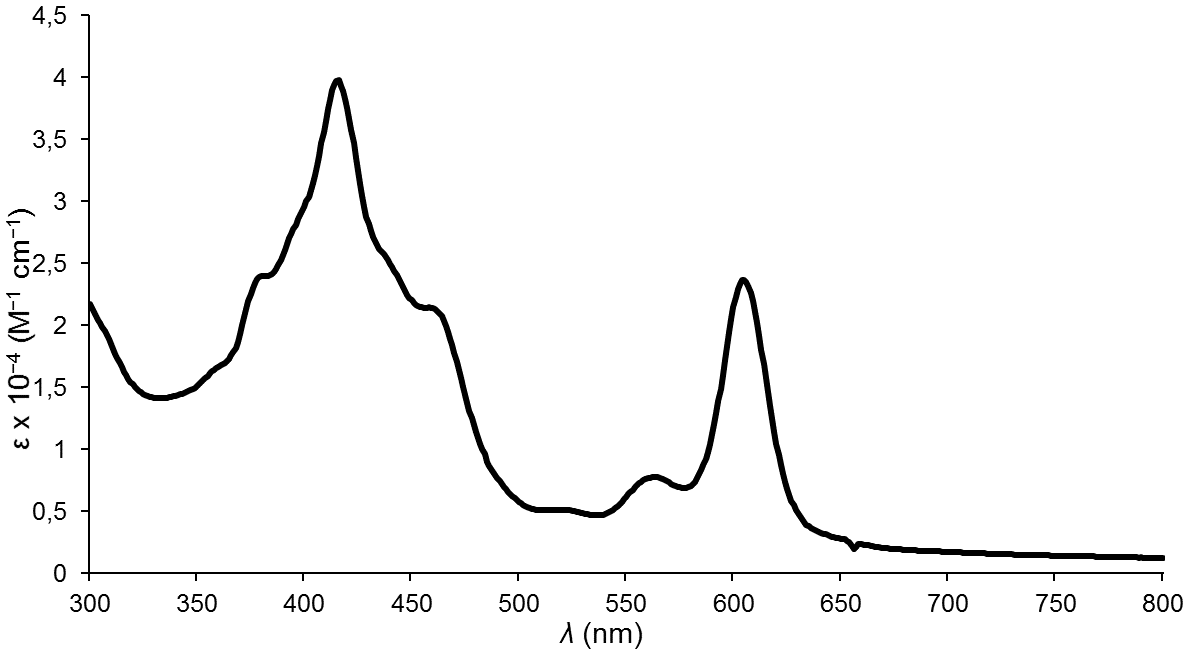

Figure 69. UV-vis spectrum of Ir[T*p*OMePC]py_2 (**3b**).

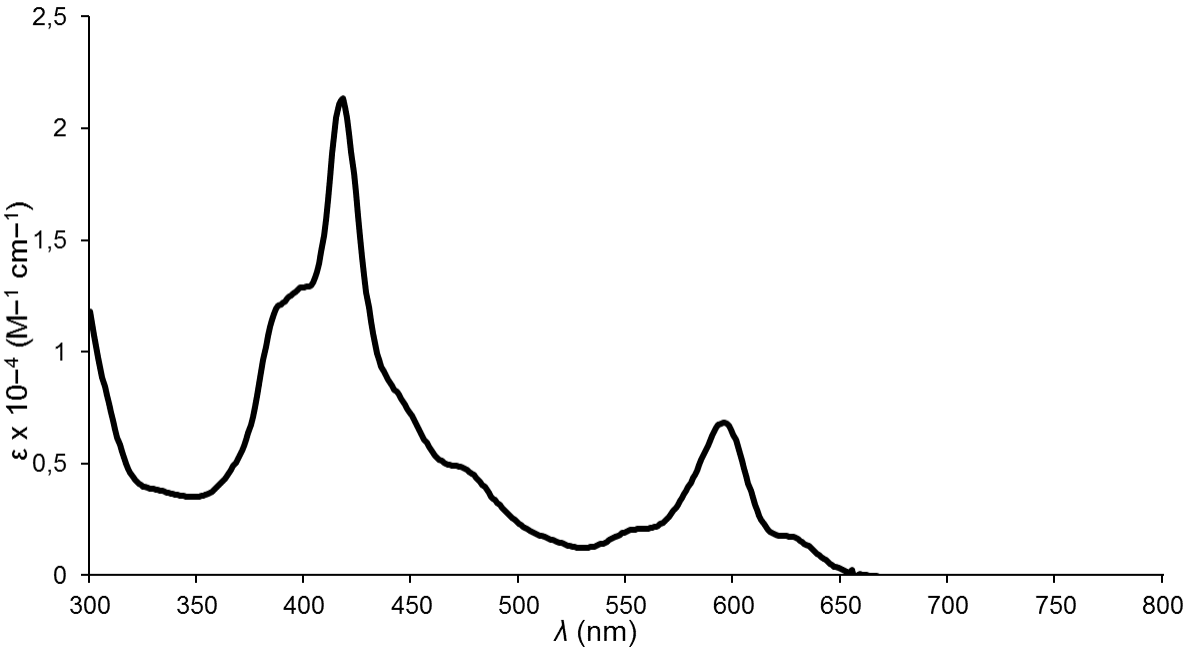

Figure 70. UV-vis spectrum of Ir[T*p*CF_3PC]tma_2 (**4a**).

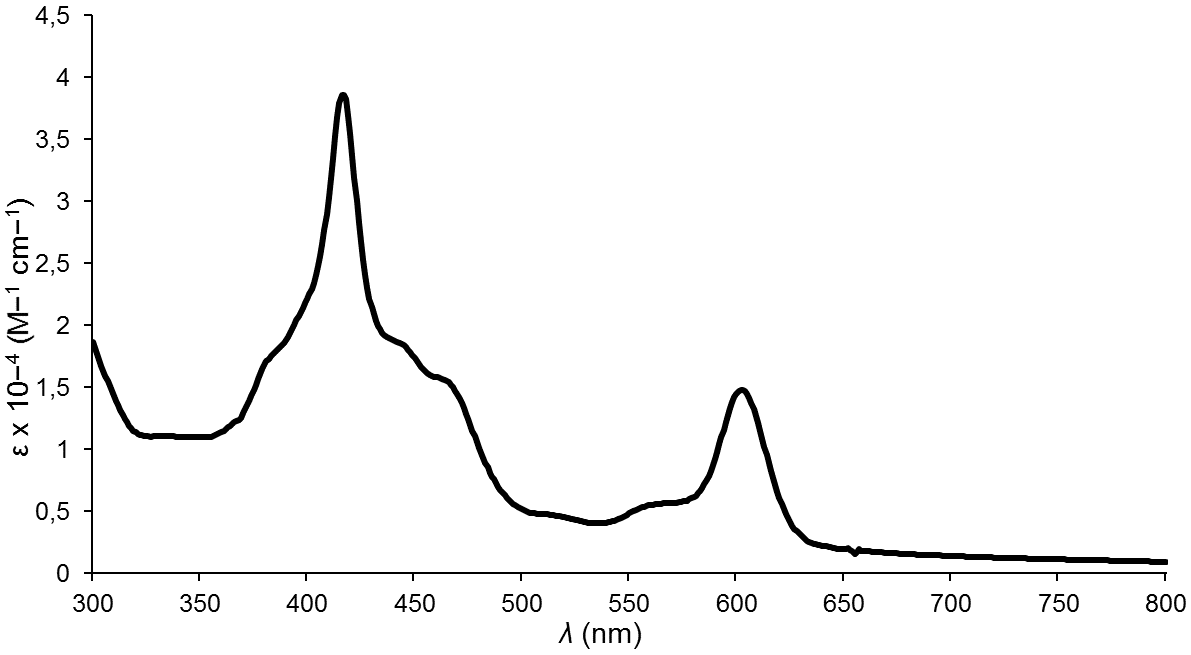

Figure 71. UV-vis spectrum of Ir[T*p*CF_3PC]py_2 (**4b**).

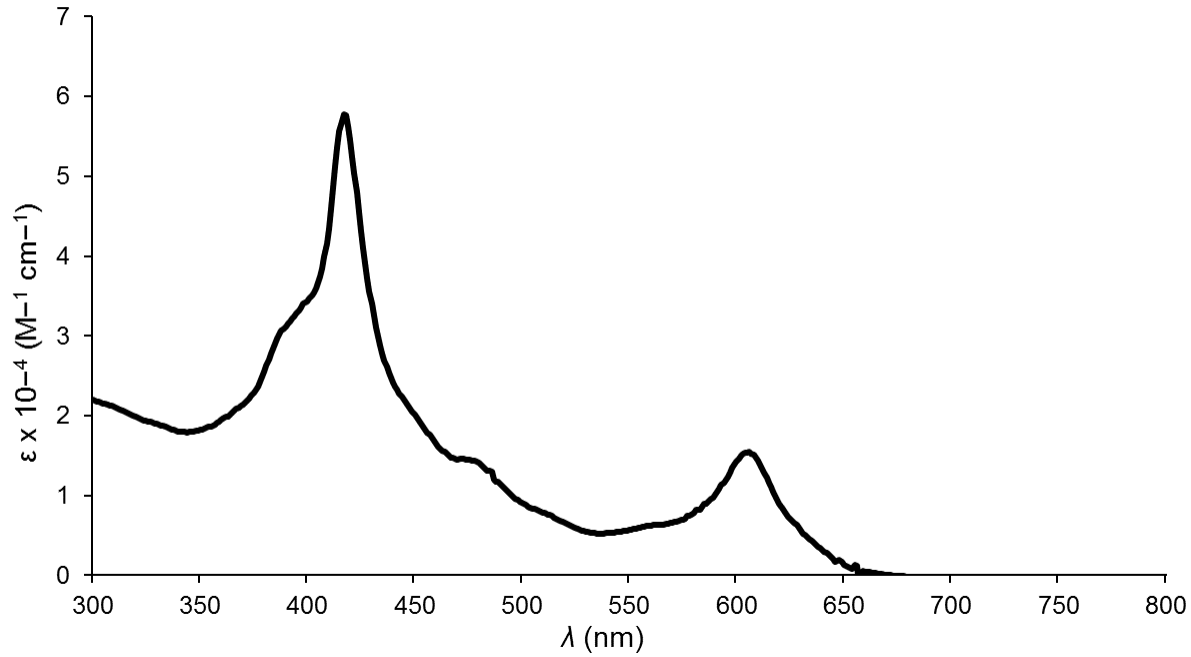

Figure 72. UV-vis spectrum of Ir[T*p*CF_3PC]$dmap_2$ (**4c**).

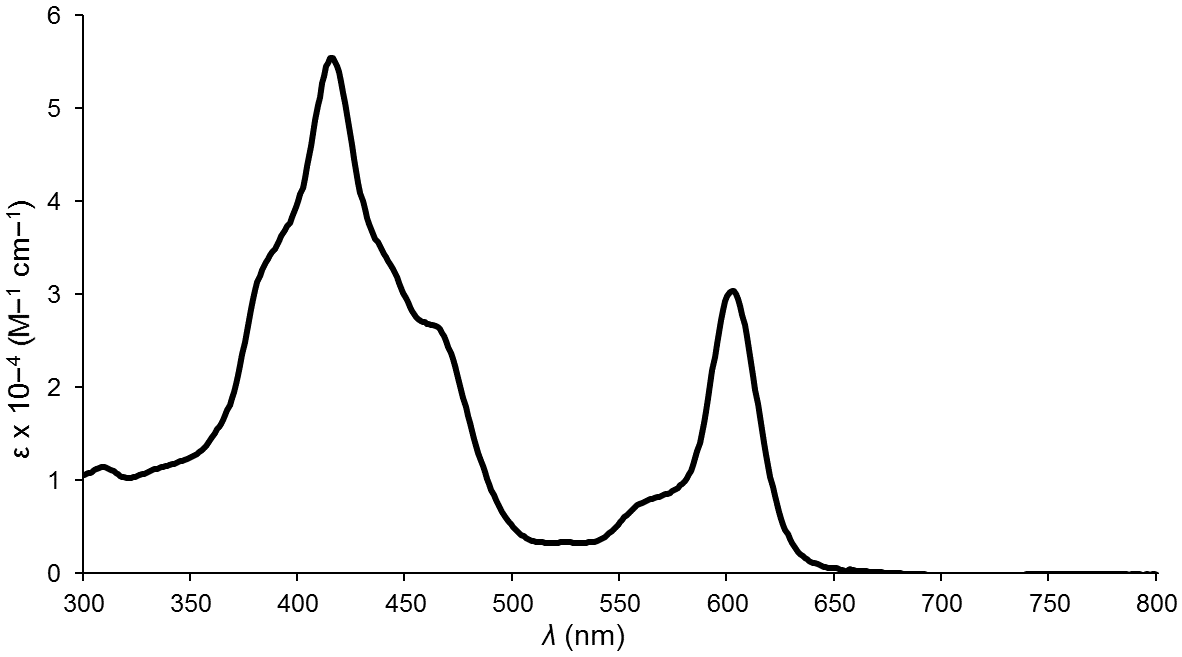

Figure 73. UV-vis spectrum of Ir[T*p*CF_3PC]4-picolinic $acid_2$ (**4d**).

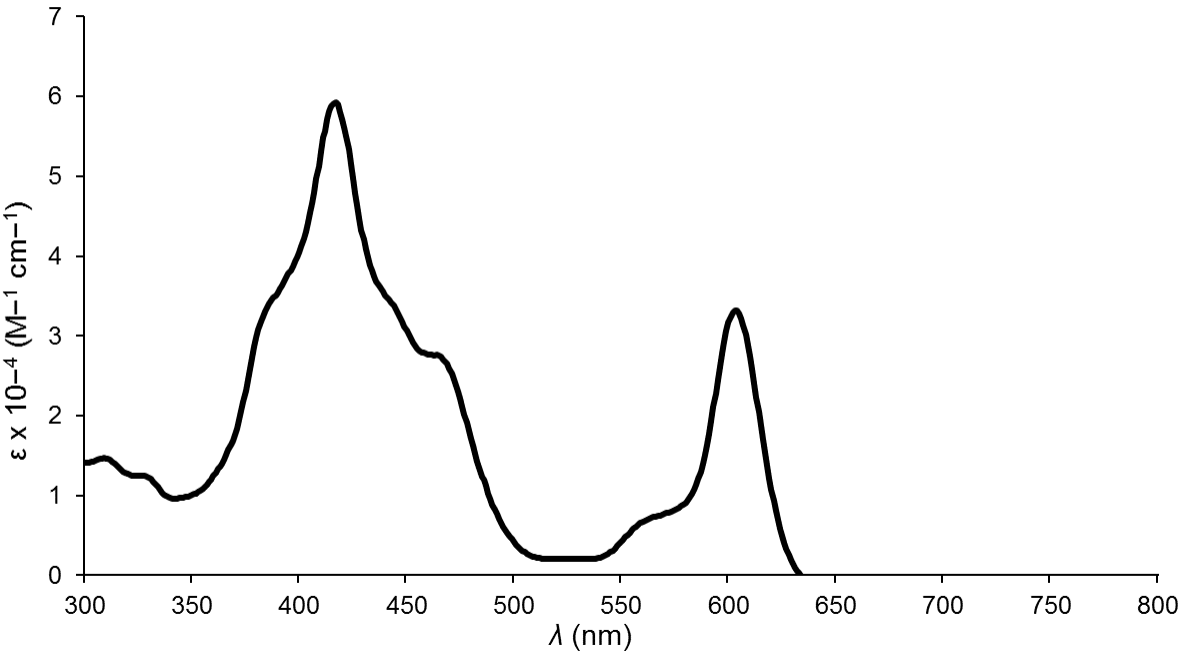

Figure 74. UV-vis spectrum of Ir[T*p*CF_3PC]$isoquinoline_2$ (**4e**).

Table 1. Absorption maxima (λ, nm) for Ir(III) corroles.

Complex	B_{max}	Q_{max}
Ir[TPC]tma_2	416	596
Ir[TPC]py_2	414	602
Ir[T*p*MePC]tma_2	417	598
Ir[T*p*MePC]py_2	417	603
Ir[T*p*OMePC]tma_2	417	600
Ir[T*p*OMePC]py_2	416	605
Ir[T*p*CF_3PC]tma_2	418	595
Ir[T*p*CF_3PC]py_2	416	602
Ir[T*p*CF_3PC]$dmap_2$	418	606
Ir[T*p*CF_3PC]4-picolinic $acid_2$	414	602
Ir[T*p*CF_3PC]$isoquinoline_2$	417	603

7.4. Electrochemistry

Cyclic voltammograms show two redox processes at positive potentials relative to SCE for all the synthesized corroles. Representative cyclic voltammograms are depicted in **Figure 75** and **Figure 76**, while **Table 2** summarizes the redox potentials. The first redox process may be tentatively assigned as a metal-centered oxidation (Ir^{III}/Ir^{IV}) based on literature precedence,[47] but the nature of the second oxidation is not clear. Ongoing spectroelectrochemical studies (which are not complete at this time) may shed some light on the exact nature of these redox processes. The absence of observable redox processes at negative potentials correlates well with previous literature and is indicative of the highly electron-rich character of these metallocorroles.[47]

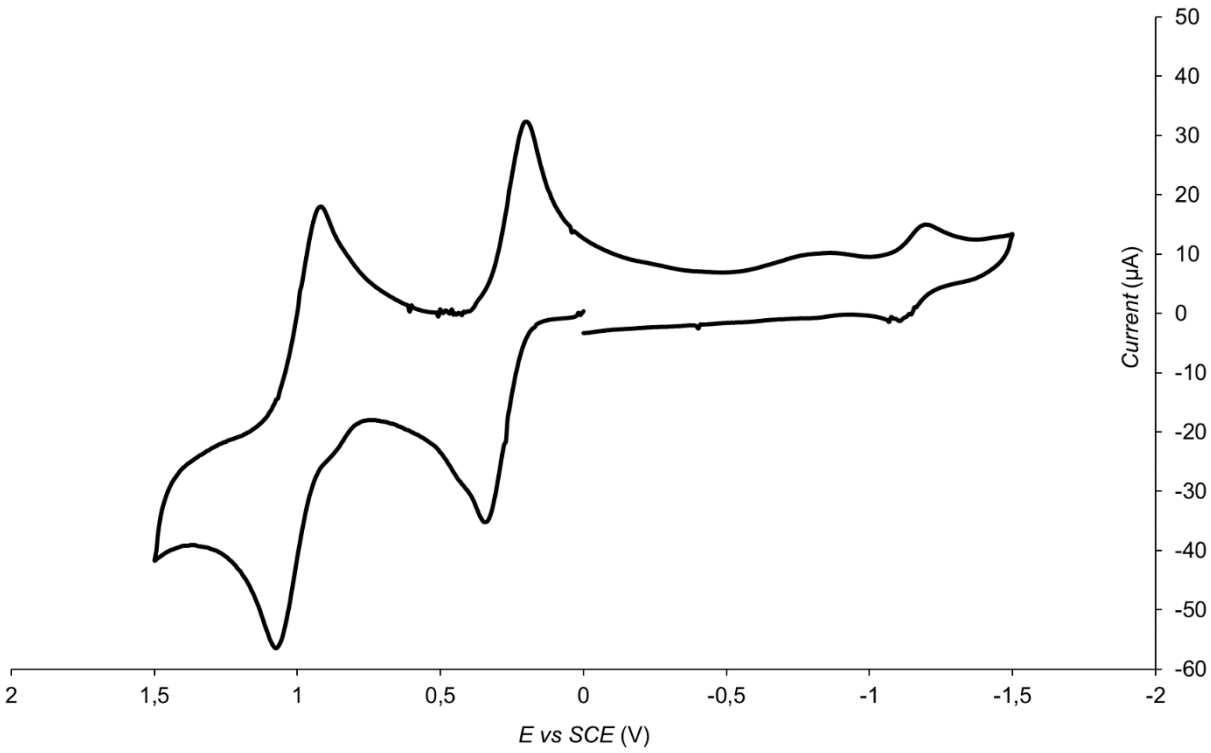

Figure 75. Cyclic voltammogram of Ir[TPC]py_2 (**1b**).

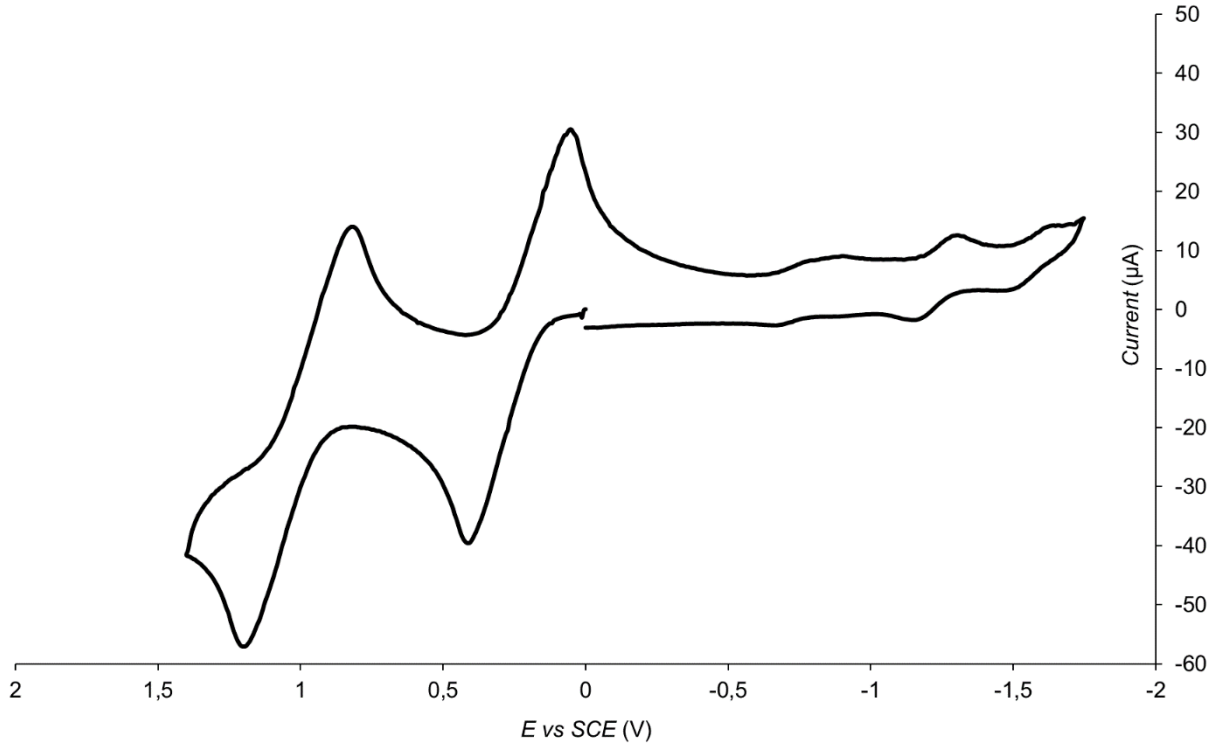

Figure 76. Cyclic voltammogram of Ir[T*p*MePC]py_2 (**2b**).

Table 2. List of redox potentials for Ir(III) corroles.

Complex	$E_{½ox1}$	$E_{½ox2}$
Ir[TPC]tma$_2$	0.31	1.09
Ir[TPC]py$_2$	0.28	1.00
Ir[T*p*MePC]tma$_2$	0.26	1.02
Ir[T*p*MePC]py$_2$	0.52	1.02
Ir[T*p*OMePC]tma$_2$	0.23	0.94
Ir[T*p*OMePC]py$_2$	0.20	0.89
Ir[T*p*CF$_3$PC]tma$_2$	0.44	1.18
Ir[T*p*CF$_3$PC]py$_2$	0.41	1.11

7.5. Absorption and emission spectroscopy

The emission spectra of the new Ir corroles were determined in the laboratory of Prof. Sergey M. Borisov at the Graz University of Technology in Austria. All the complexes were found to exhibit weak phosphorescence in the near-infrared part of the spectrum in anoxic solutions (**Figure 77**). The phosphorescence is almost quenched in the presence of molecular oxygen. The excitation spectra (**Figure 78**) match the absorption spectra very well. As expected, the emission spectra are much narrower at 77 K (**Figure 79**), which enables more precise determination of the triplet state energies from the edge of the emission spectra. The phosphorescence quantum yields are very weak, which makes their precise estimation challenging. Estimations indicate quantum yields of around 0.02 – 0.04 % at ambient temperature with about a 2-fold increase at 77 K. The phosphorescence of the bis-pyridine and bis-isoquinoline complexes were found to be stronger than that of bis-tma and bis-dmap complexes. Furthermore, the emission spectra for the bis-pyridine, isoquinoline, and 4-picolinic acid are almost identical (**Figure 77, Table 3**). The decay time profiles for these complexes are mono-exponential (**Figure 80**). The fits provide very similar values of ~ 5 μs at 295 K and ~ 10 μs at 77 K. Interestingly, in the case of the bis-dmap complex, a relatively long decaying component was observed both at ambient temperature and at 77 K.

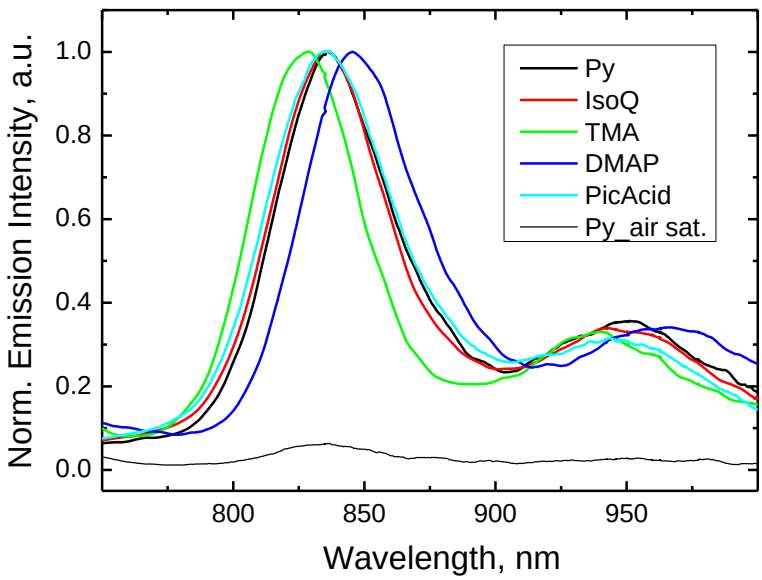

Figure 77. Emission spectra of selected Ir(III) corroles in solutions at 295 K. The bis-4-picolinic acid complex was measured in ethanol, all other complexes in toluene; λ_{ex} 595-605 nm in the maximum of the Q-band.

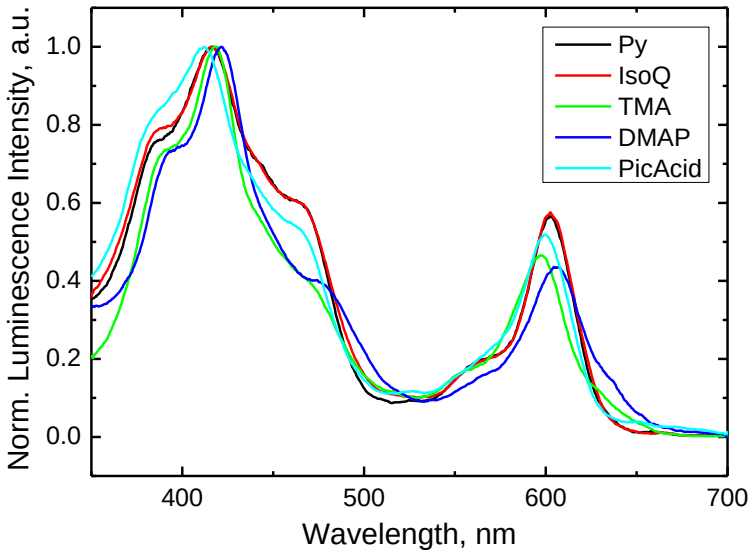

Figure 78. Excitation spectra of the Ir(III) corroles in anoxic solutions at 295 K. The bis-4-picolinic acid complex was measured in ethanol, all other complexes in toluene. The emission was detected in the maximum of the emission spectra. RG9 long-pass filter was used in the emission channel to eliminate the artefacts.

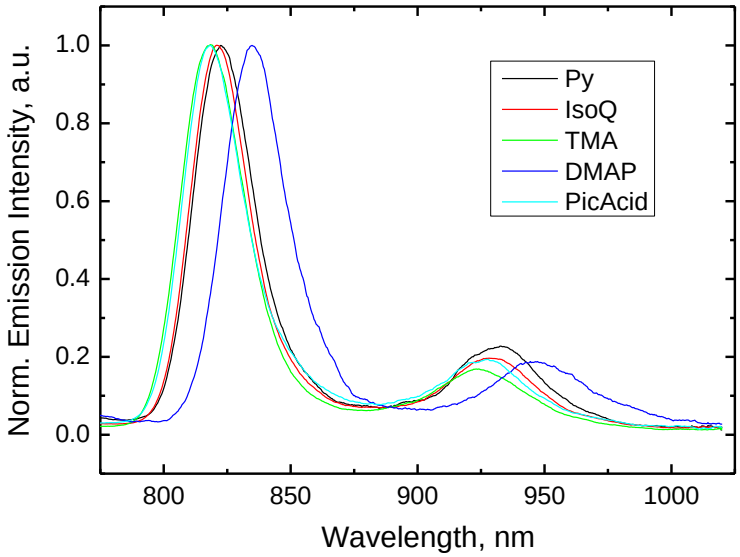

Figure 79. Emission spectra of the selected Ir(III) corroles in frozen glasses. The bis-4-picolinic acid complex was measured in 4:1 ethanol:methanol, while all other complexes in 2:3 toluene:tetrahydrofuran; λ_{ex} 595-605 nm in the maximum of the Q-band.

Table 3. Photophysical properties of Ir(III) corroles. [1]) In toluene for all complexes except Ir[T*p*CF_3PC]4-picolinic $acid_2$. [2]) In ethanol. [3]) In toluene/tetrahydrofuran (4:6 v/v) for all complexes except Ir[T*p*CF_3PC]4-picolinic $acid_2$. [4]) In ethanol/methanol (4:1 v/v). [5]) Estimated at the edge of the emission spectra and acquired at 77 K.

Complex	295 K(1)			77K(3)			
	$\lambda_{max,em}$, nm	τ, μs	QY, %	λ_{max} em, nm	τ, μs	QY, %	E_T, cm^{-1} (5)
Ir[T*p*CF_3PC)]py_2	836	5.6	~0.04	823	9.8	~0.04	12560
Ir[T*p*CF_3PC]$isoquinoline_2$	836	4.9	~0.04	821	10.4	~0.06	12560
Ir[T*p*CF_3PC]tma_2	828	0.6 (38%); 5.1 (62%)	~0.02	818	4.2	~0.06	12630
Ir[T*p*CF_3PC]$dmap_2$	846	2.3 (78%); 8.1 (22%)	~0.02	835	5.2 (61%); 36 (39%)	~0.03	12410
Ir[T*p*CF_3PC]4-picolinic $acid_2$	836(2)	4.8(2)	~0.02	818(4)	10.7(4)	~0.04	12630

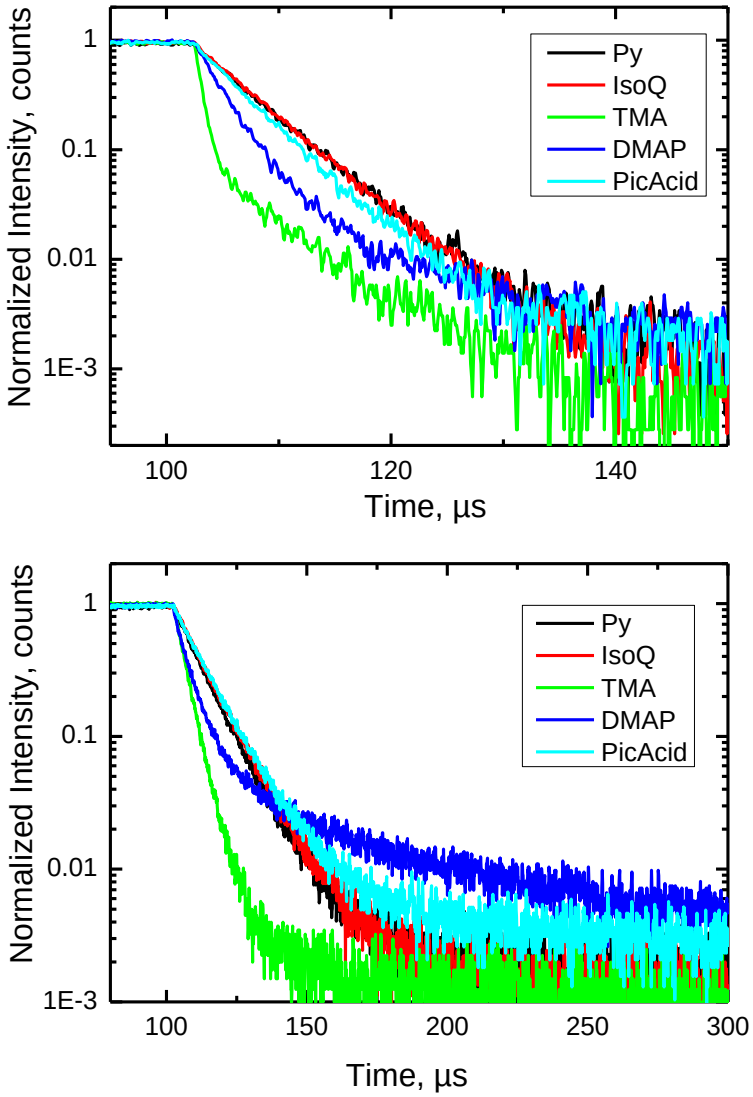

Figure 80. Phosphorescence decay for the selected Ir(III) corroles in anoxic solutions at 295 K (up) and in frozen glass at 77 K. The solvents are the same as stated in **Figure 77** and **Figure 79.**

7.6. X-ray crystallography

Single-crystal X-ray structure determinations were carried out for three six-coordinate Ir corroles – Ir[TPC]tma$_2$ (**1a**), Ir[T*p*MePC]tma$_2$ (**2a**), and Ir[T*p*CF$_3$PC]py$_2$ (**4b**). The analyses were carried out by our collaborator Dr. Laura J. McCormick at Beamline 11.3.1 at the Advanced Light Source at Lawrence Berkeley National Laboratory. Side and top views of these compounds are depicted in **Figure 81 - 83**, while crystallographic data for these compounds are presented in **Table 4**.

The metrical parameters of the structures are relatively unremarkable. The Ir-N distances involving the corrole are approximately 1.96 ± 0.02 Å and those involving the axial ligands are considerably longer at 2.066 Å for the bis-pyridine complex and 2.17 ± 0.03 Å for the bis-tma complex. These short equatorial Ir-N distances are a testament to the sterically constrained nature of the corrole macrocycle. Despite the steric mismatch between 5d transition metals and the corrole N_4 cavity, it is remarkable that the majority of 5d metallocorroles are quite rugged, both chemically and photochemically.

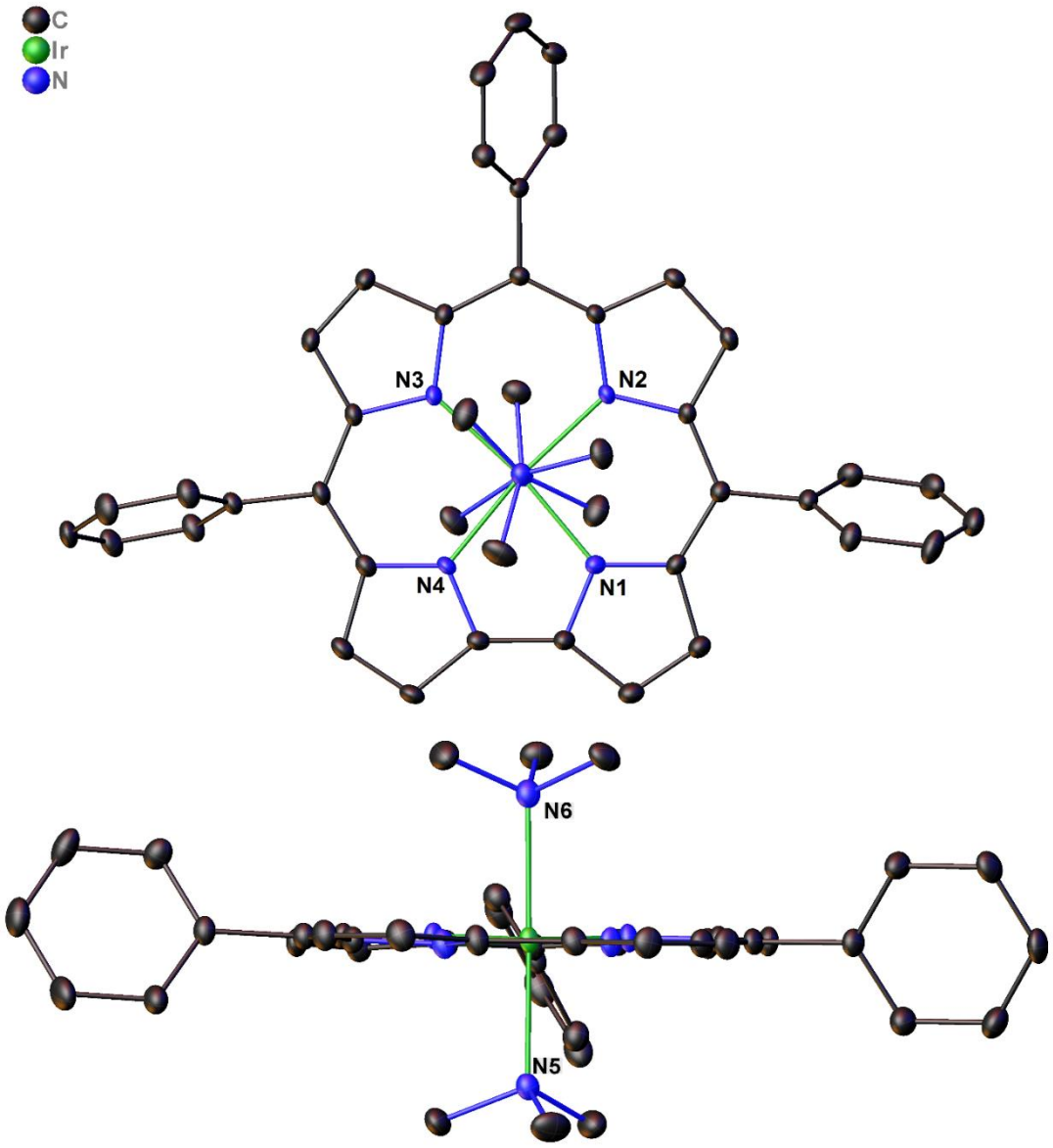

Figure 81. Top and side views of Ir[TPC]tma_2 (**1a**). Selected bond distances (Å) for labelled atoms: Ir-N1 1.9543(16), Ir-N2 1.9728(16), Ir-N3 1.9745(16), Ir-N4 1.9489(17), Ir-N5 2.1795(18), Ir-N6 2.1672(18).

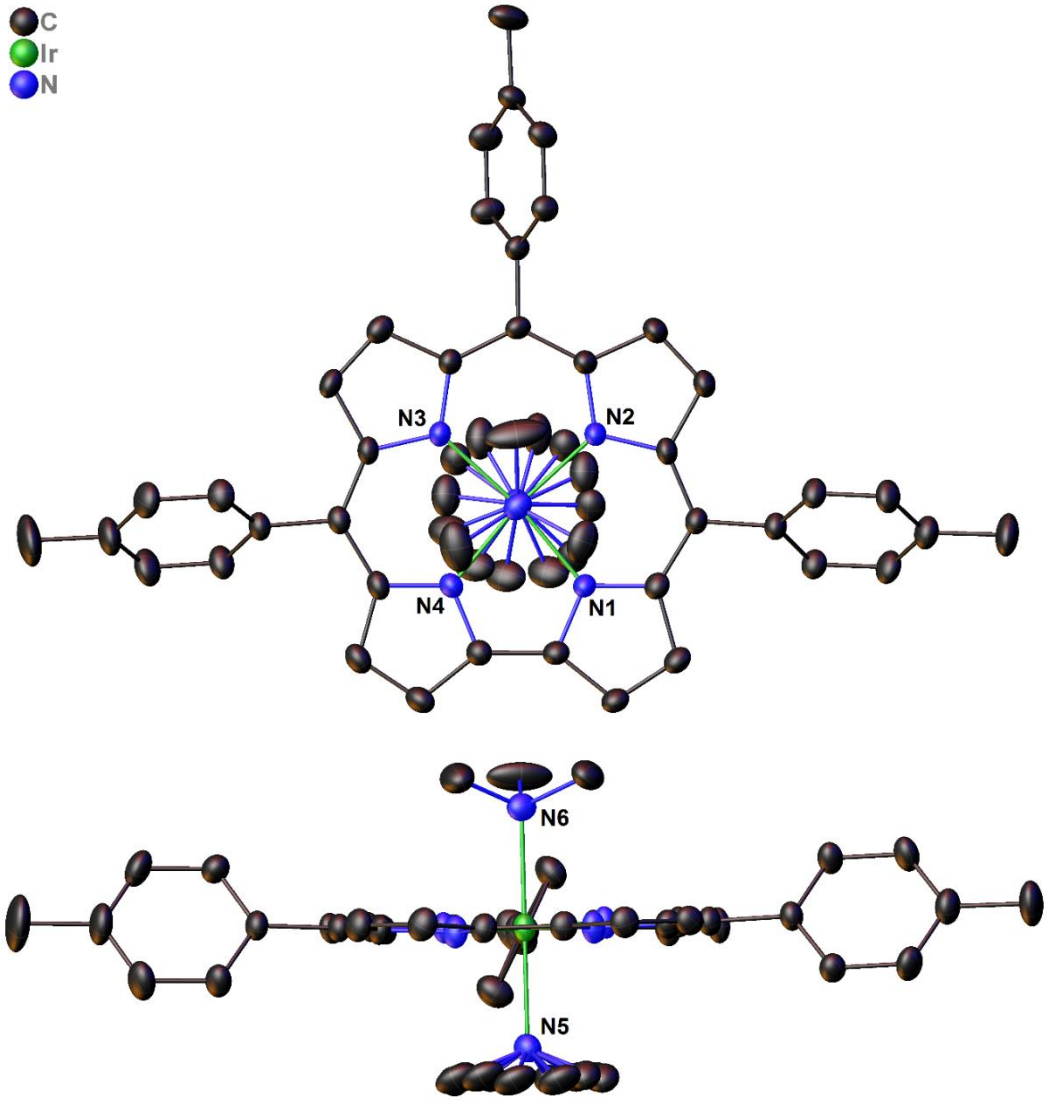

Figure 82. Top and side view of Ir[T*p*MePC]tma$_2$ (**2a**). Selected bond distances (Å) for labelled atoms: Ir-N1 1.953(2), Ir-N2 1.9746(19), Ir-N3 1.978(2), Ir-N4 1.948(2), Ir-N5 2.178(3), Ir-N6 2.176(3).

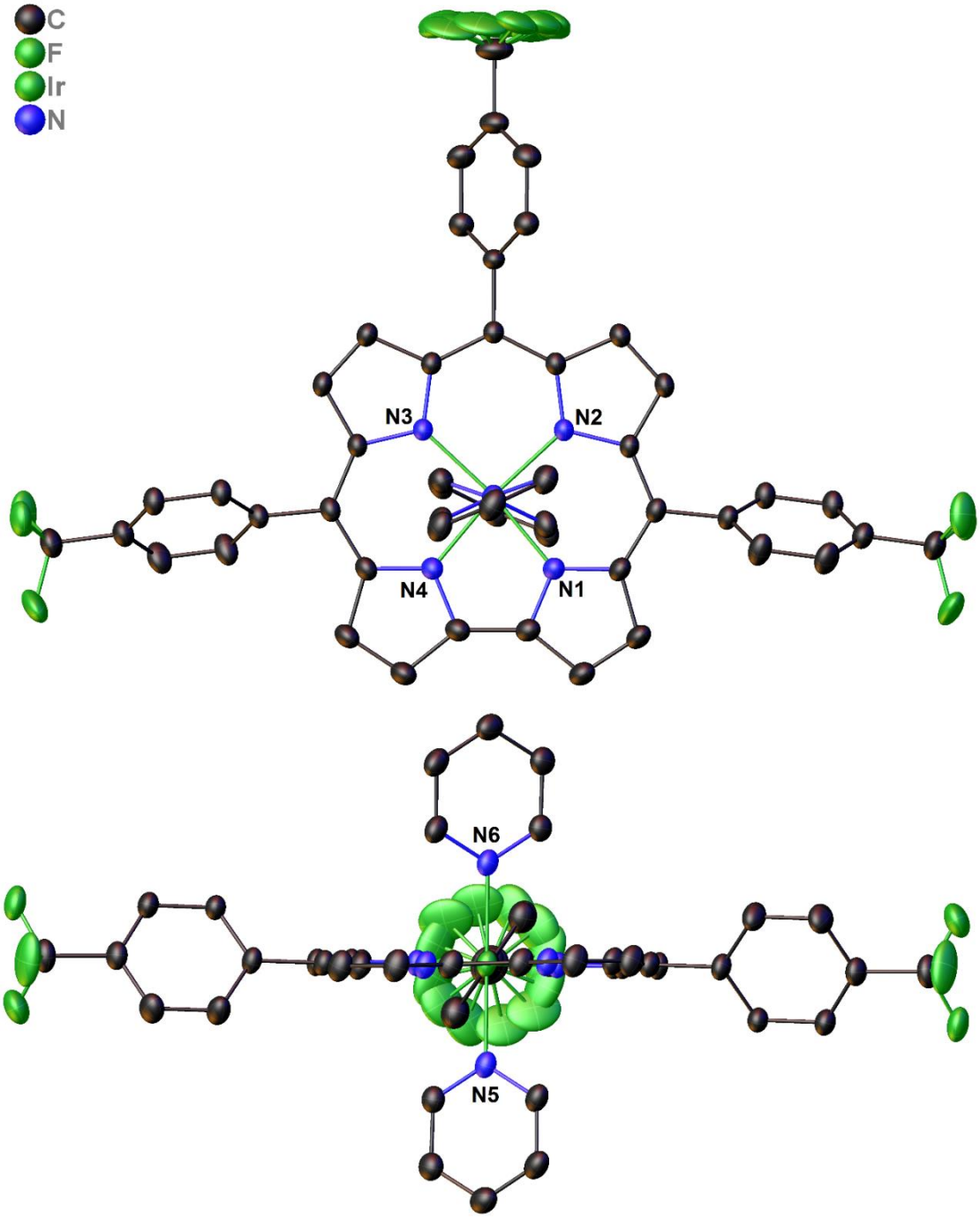

Figure 83. Top and side view of Ir[T*p*CF_3PC]py_2 (**4b**). Selected bond distances (Å) for labelled atoms: Ir-N1 1.946(2), Ir-N2 1.9702(18), Ir-N3 1.902(18), Ir-N4 1.946(2), Ir-N5 2.066(2), Ir-N6 2.066(2).

Table 4. Crystallographic data for Ir(III) corroles.

Compound	Ir^{III}[TPC]tma_2	Ir^{III}[T*p*MePC]tma_2	Ir^{III}[T*p*CF_3PC]py_2
Chemical formula	$C_{43}H_{41}IrN_6$	$C_{54.25}H_{66.25}IrN_6$	$C_{50}H_{30}F_9IrN_6$
Formula mass	834.02	994.58	1078.00
Crystal system	Monoclinic	Monoclinic	Monoclinic
Space group	P 2_1/n	P 2_1/n	C 2/c
λ [Å]	0.7749	0.7293	0.7749
a [Å]	11.4814(5)	12.8383(7)	18.1543(9)
b [Å]	21.7131(10)	15.3802(8)	16.8434(7)
c [Å]	13.7137(6)	24.6017(13)	14.2251(7)
α [º]	90	90	90
β [º]	94.371(2)	92.934(2)	112.321(2)
Υ [º]	90	90	90
Z	4	4	4
V [Å]	3408.8(3)	4851.4(4)	4023.8(3)
Temperature [K]	100(2)	150(2)	100(2)
Density [g cm^{-3}]	1.625	1.362	1.779
Meas. reflections	46872	91185	40581
Unique reflections	10433	16047	10326
Parameters	457	612	324
Restraints	0	52	6
R_{int}	0.0478	0.0599	0.0431
θ range [º]	1.919-33.659	3.206-64.748	1.867-41.256
R_1, wR_2 all data	0.0276, 0.0551	0.0407, 0.1113	0.0463, 0.0935
S (GooF) all data	1.049	0.828	1.039
Max/min res. dens. [e $Å^{-3}$]	1.123/-1.092	0.90/-1.74	3.436/-2.876

7.7. Conclusion

Eleven new Ir(III) corroles were synthesized and characterized by ^{1}H-NMR, mass spectrometry, UV-vis spectroscopy, and cyclic voltammetry, while three of the compounds also proved amenable to single-crystal X-ray structure determination. Five compounds were analyzed for phosphorescence, but unfortunately all were found to be rather weakly phosphorescent. Future work on the Ir(III) corroles will focus on determining the nature of electrochemical oxidation processes and exploring the corroles as precursors for obtaining *β*-polyiodo derivatives.

7.8. Experimental section

(a) Materials. Chloro(1,5-cyclooctadiene)iridium(I) dimer was obtained from Sigma-Aldrich. Silica gel 60 (0.04-0.063 mm particle size, 230-400 mesh, Merck) was employed for flash chromatography. Silica gel 60 preparative thin-layer chromatographic plates (20 cm x 20 cm, 0.5 mm thick, Merck) and aluminum oxide 60 preparative thin-layer chromatographic plates (20 cm x 20 cm, 1.5 mm thick, Merck) were used for final purification of all complexes. Unless otherwise mentioned, all other chemicals were obtained from Sigma-Aldrich.

(b) Instrumental methods. UV−visible spectra were recorded on an HP 8453 spectrophotometer. ^{1}H NMR spectra were recorded on a 400 MHz Bruker Avance III HD spectrometer equipped with a 5 mm BB/1H SmartProbe in $CDCl_3$ and referenced to residual $CHCl_3$ 7.26 ppm, C_6D_6 and referenced to residual C_6H_6 7.16 ppm, C_3D_6O and referenced to residual C_3H_6O 2.05 ppm or CD_3OD and referenced to residual CH_3OH 3.31 ppm. High-resolution electrospray-ionization (HR-ESI) mass spectra were recorded from methanolic solution on an LTQ Orbitrap XL spectrometer.

Cyclic voltammetry was performed at 298 K using an EG&G model 263A potentiostat with a three-electrode system, comprising a glassy carbon working electrode, a platinum wire counterelectrode, and a saturated calomel reference electrode (SCE), in CH_2Cl_2 (distilled from CaH_2) as solvent. The reference electrode was separated from the bulk solution by a fritted-glass bridge filled with the electrolyte solution. The electrolyte solution was purged with argon for several minutes, and electrochemical measurements were conducted under an argon blanket. All potentials are referenced to the SCE.

General procedure for the synthesis of Ir[T*p*XPC]L$_2$ (X = OMe, CH$_3$, H, CF$_3$, L = tma, py, dmap, 4-picolinic acid, isoquinoline). The free-base corroles were prepared according to previously reported procedures.[112,113] The iridium complexes were prepared according to a previously reported procedure with slight modifications.[47] Bis(1,5-cyclooctadiene)diiridium(I) dichloride (2 eq.) and potassium carbonate (10 eq.) was dissolved in an anhydrous solution of tetrahydrofuran (150 mL) containing the free-base corrole (~0.1 mmol, 1 eq.) The solution was degassed with argon for a few minutes and then brought to a reflux under inert atmosphere. After 1 hour and 30 minutes, tma *N*-oxide (15 eq.) was added all at once and the solution was left to reach room temperature (1 hour). In the case of compounds **1b** to **4b**, pyridine (15 eq.) was used instead of tma *N*-oxide, while for compounds **4c** to **4e**, 4-dimethylaminopyridine (15 eq.), 4-picolinic acid (15 eq.) and isoquinoline (15 eq.)

were used, respectively. The purification details and characterization for each case are as follows.

Ir[TPC]tma$_2$ (1a). The reaction mixture was evaporated to dryness on a rotary evaporator; the residue was dissolved in a small amount of dichloromethane and subjected to column chromatography (silica, CH_2Cl_2:hexanes, 1:1) followed by preparative thin-layer chromatography (silica, CH_2Cl_2:pentane, 1:1) to afford **1a** as a dichroic purple-green solid. Yield 37.5 mg (30 %). UV-vis (CH_2Cl_2): λ_{max} (nm) [ϵ x 10^{-4} ($M^{-1}cm^{-1}$)]: 384 (3.65, sh), 416 (5.58), 468 (1.59, sh), 596 (2.67). ^{1}H NMR (400 MHz, acetone-d_6, δ): 8.88 (d, *J* = 4.1 Hz, 2H, *β*-H), 8.62 (d, *J* = 4.7 Hz, 2H, *β*-H), 8.39 (d, *J* = 4.8 Hz, 2H, *β*-H), 8.24 – 8.19 (m, 4H, 5,15 -*o*-Ph), 8.15 – 8.11 (m, 2H, 10 -*o*-Ph), 8.01 (s, 2H, *β*-H), 7.78 (dt, *J* = 14.9, 7.5 Hz, 6H, 5,10,15 -*m*-Ph), 7.69 – 7.63 (m, 3H, 5,10,15 -*p*-Ph), -2.86 (s, 18H, tma-CH_3). MS (ESI): M^+ = 834.3017 (expt), 834.3019 (calcd for $IrC_{43}H_{41}N_6$).

Ir[TPC]py$_2$ (1b). The reaction mixture was evaporated to dryness on a rotary evaporator; the residue was dissolved in a small amount of dichloromethane and subjected to column chromatography (silica, CH_2Cl_2:hexanes, 1:1) followed by preparative thin-layer chromatography (silica, CH_2Cl_2:pentane, 1:1) to afford **1b** as a dichroic purple-green solid. Yield 83.4 mg (63.6 %). UV-vis (CH_2Cl_2): λ_{max} (nm) [ϵ x 10^{-4} ($M^{-1}cm^{-1}$)]: 414 (5.30), 459 (2.66, sh), 562 (0.86, sh), 602 (3.37). ^{1}H NMR (400 MHz, acetone-d_6, δ): 8.82 – 8.78 (m, 2H, *β*-H), 8.62 (dd, *J* = 4.8, 1.1 Hz, 2H, *β*-H), 8.38 (d, *J* = 4.7 Hz, 2H, *β*-H), 8.28 – 8.22 (m, 4H, 5,15 -*o*-Ph), 8.17 (d, *J* = 4.1 Hz, 2H, *β*-H), 8.05 – 8.00 (m, 2H, 10 -*o*-Ph), 7.77 (dd, *J* = 8.3, 6.8 Hz, 4H, 5,15 -*m*-Ph), 7.70 – 7.59 (m, 5H, 5,15 -*p*-Ph and 10 -*p*,*m*-Ph), 6.30 (tt, *J* = 7.6, 1.5 Hz, 2H, *p*-Py), 5.42 – 5.33 (m, 4H, *m*-Py), 1.85 (dt, *J* = 5.4, 1.5 Hz, 4H, *o*-Py). MS (ESI): M^+ = 874.2403 (expt), 874.2393 (calcd for $IrC_{47}H_{33}N_6$).

Ir[T*p*MePC]tma$_2$ (2a). The reaction mixture was evaporated to dryness on a rotary evaporator; the residue was dissolved in a small amount of dichloromethane and subjected to column chromatography (silica, CH_2Cl_2:hexanes, 1:1) followed by preparative thin-layer chromatography (silica, CH_2Cl_2:pentane, 1:2) to afford **2a** as a brightly green solid. Yield 75.7 mg (49.6 %). UV-vis (CH_2Cl_2): λ_{max} (nm) [ϵ x 10^{-4} ($M^{-1}cm^{-1}$)]: 384 (3.28, sh), 417 (4.88), 468 (1.54, sh), 598 (2.36). ^{1}H NMR (400 MHz, chloroform-*d*, δ): 8.88 – 8.82 (m, 2H, *β*-H), 8.66 (d, *J* = 4.7 Hz, 2H, *β*-H), 8.39 (d, *J* = 4.6 Hz, 2H, *β*-H), 8.03 (dd, *J* = 47.5, 7.5 Hz, 8H 5,10,15 -*o*-Ph + *β*-H, 8H), 7.57 (dd, *J* = 14.0, 7.6 Hz, 6H, 5,10,15 -*m*-Ph), 1.28 (s, 9H, Ph -*p*-CH_3), -2.88 (s, 18H, tma-CH_3). MS (ESI): M^+ = 876.3488 (expt), 876.3489 (calcd for $IrC_{46}H_{47}N_6$).

Ir[T*p*MePC]py$_2$ (2b). The reaction mixture was evaporated to dryness on a rotary evaporator; the residue was dissolved in a small amount of dichloromethane and subjected to column chromatography (silica, CH_2Cl_2:hexanes, 1:1) followed by preparative thin-layer chromatography (silica, CH_2Cl_2:pentane, 1:1) to afford **2b** as a dichroic purple-green solid. Yield 36 mg (30.1 %). UV-vis (CH_2Cl_2): λ_{max} (nm) [ϵ x 10^{-4} ($M^{-1}cm^{-1}$)]: 417 (6.40), 460 (2.75, sh), 562 (0.98, sh), 603 (3.49). ^{1}H NMR (400 MHz, benzene-d_6, δ): 9.14 (dd, *J* = 4.5, 3.0 Hz, 4H, *β*-H), 8.97 (d, *J* = 4.8 Hz, 2H, *β*-H), 8.80 (d, *J* = 4.2 Hz, 2H, *β*-H), 8.46 – 8.41 (m, 4H, 5,15 -*o*-Ph), 8.30 (d, *J* = 7.9 Hz, 2H, 10 -*o*-Ph), 7.42 (d, *J* = 7.7 Hz, 4H, 5,15 -*m*-Ph), 7.37 (d, *J* = 8.0 Hz, 2H, 10 -*m*-Ph), 4.79 (t, *J* = 7.6 Hz, 2H, *p*-Py), 4.17 – 4.11 (m, 4H, *m*-Py), 2.42 (d, *J* = 4.2 Hz, 9H, Ph -*p*-CH_3), 2.06 (dt, *J* = 5.3, 1.5 Hz, 4H, *o*-Py). MS (ESI): M^+ = 916.2873 (expt), 916.2863 (calcd for $IrC_{50}H_{39}N_6$).

Ir[T*p*OMePC]tma$_2$ (3a). The reaction mixture was evaporated to dryness on a rotary evaporator; the residue was dissolved in a small amount of dichloromethane and subjected to column chromatography (silica, CH_2Cl_2:hexanes, 1:1 followed by CH_2Cl_2 then CH_2Cl_2 :EtOAc, 9:1). Subsequent purification by preparative thin-layer chromatography (silica, EtOAc:CH_2Cl_2, 4:1) afforded **3a** as a brightly green solid.
Yield 35.2 mg (29.2 %). UV-vis (CH_2Cl_2): λ_{max} (nm) [ϵ x 10^{-4} ($M^{-1}cm^{-1}$)]: 384 (0.74, sh), 417 (1.05), 468 (0.36, sh), 600 (0.48). ^{1}H NMR (400 MHz, chloroform-*d*, δ): 8.89 (d, *J* = 3.8 Hz, 2H, *β*-H), 8.68 (d, *J* = 4.7 Hz, 2H, *β*-H), 8.32 (d, *J* = 4.6 Hz, 2H, *β*-H), 8.06 (d, *J* = 8.0 Hz, 4H, 5,15 -*o*-Ph), 7.92 (d, *J* = 7.9 Hz, 2H, 10 -*o*-Ph), 7.83 (s, 2H, *β*-H), 7.33 (dd, *J* = 11.7, 8.2 Hz, 6H, 5,10,15 -*m*-Ph), 4.09 (d, *J* = 3.6 Hz, 9H, Ph -*p*-OCH_3), -2.86 (s, 18H, tma-CH_3). MS (ESI): M^+ = 924.3358 (expt), 924.3336 (calcd for $IrC_{46}H_{47}O_3N_6$).

Ir[T*p*OMePC]py$_2$ (3b). The reaction mixture was evaporated to dryness on a rotary evaporator; the residue was dissolved in a small amount of dichloromethane and subjected to column chromatography (silica, CH_2Cl_2) followed by preparative thin-layer chromatography (silica, CH_2Cl_2) to afford **3b** as a brightly green solid.
Yield 31.2 mg (24.5 %). UV-vis (CH_2Cl_2): λ_{max} (nm) [ϵ x 10^{-4} ($M^{-1}cm^{-1}$)]: 416 (3.98), 458 (2.14, sh), 563 (0.77, sh), 605 (2.36). ^{1}H NMR (400 MHz, benzene-d_6, δ): 9.19 – 9.15 (m, 4H, 2 *β*-H), 8.98 (d, *J* = 4.9 Hz, 2H, *β*-H), 8.76 (s, 2H, *β*-H), 8.42 (d, *J* = 8.0 Hz, 4H, 5,15 -*o*-Ph), 8.08 (d, *J* = 8.5 Hz, 2H, 10 -*o*-Ph), 7.20 (d, *J* = 8.8 Hz, 4H, 5,15 -*m*-Ph), 7.11 – 7.07 (m, 2H, 10 -*m*-Ph), 4.81 (ddd, *J* = 7.7, 6.2, 1.5 Hz, 2H, *p*-Py), 4.20 – 4.16 (m, 4H, *m*-Py), 3.55 (d, *J* = 2.0 Hz, 9H, Ph -*p*-OCH_3), 2.11 – 2.07 (m, 4H, *o*-Py). MS (ESI): M^+ = 964.2724 (expt), 964.2711 (calcd for $IrC_{50}H_{39}O_3N_6$).

Ir[T*p*CF$_3$PC]tma$_2$ (4a). The reaction mixture was evaporated to dryness on a rotary evaporator; the residue was dissolved in a small amount of dichloromethane and subjected to column chromatography (silica, CH_2Cl_2:hexanes, 1:1) followed by preparative thin-layer chromatography (silica, CH_2Cl_2:pentane, 1:3) to afford **4a** as a dark green solid.
Yield 14.7 mg (11.8 %). UV-vis (CH_2Cl_2): λ_{max} (nm) [ϵ x 10^{-4} ($M^{-1}cm^{-1}$)]: 418 (2.13), 595 (0.68). ^{1}H NMR (400 MHz, chloroform-*d*, δ): 8.89 (d, *J* = 4.2 Hz, 2H, *β*-H), 8.64 (d, *J* = 4.8 Hz, 2H, *β*-H), 8.48 (d, *J* = 4.8 Hz, 2H, *β*-H), 8.38 (d, *J* = 7.8 Hz, 4H, 5,15 -*o*-Ph), 8.29 (d, *J* = 7.8 Hz, 2H, 10 -*o*-Ph), 8.20 (d, *J* = 4.2 Hz, 2H, *β*-H), 8.01 (d, *J* = 7.9 Hz, 4H, 5,15 -*m*-Ph), 7.98 (d, *J* = 7.9 Hz, 2H, 10 -*o*-Ph), -2.93 (s, 18H, tma-CH_3). MS (ESI): M^+ = 1038.2654 (expt), 1038.2641 (calcd for $IrC_{46}H_{38}F_9N_6$).

Ir[T*p*CF$_3$PC]py$_2$ (4b). The reaction mixture was evaporated to dryness on a rotary evaporator; the residue was dissolved in a small amount of dichloromethane and subjected to column chromatography (silica, CH_2Cl_2:hexanes, 1:1) followed by preparative thin-layer chromatography (silica, CH_2Cl_2:pentane, 1:2) to afford **4b** as a dark green solid.
Yield 16.3 mg (13.7 %). UV-vis (CH_2Cl_2): λ_{max} (nm) [ϵ x 10^{-4} ($M^{-1}cm^{-1}$)]: 416 (3.86), 602 (1.48). ^{1}H NMR (400 MHz, benzene-d_6, δ): 9.12 (d, *J* = 4.3 Hz, 2H, *β*-H), 8.90 (d, *J* = 4.8 Hz, 2H, *β*-H), 8.75 (d, *J* = 4.8 Hz, 2H, *β*-H), 8.54 (d, *J* = 4.3 Hz, 2H, *β*-H), 8.30 (d, *J* = 8.0 Hz, 4H, 5,15 -*o*-Ph), 8.23 (d, *J* = 7.9 Hz, 2H, 10 -*o*-Ph), 7.76 (dd, *J* = 8.1, 6.6 Hz, 6H, 5,10,15 -*m*-Ph), 4.84 (tt, *J* = 7.7, 1.5 Hz, 2H, *p*-Py), 4.23 – 4.17 (m, 4H, *m*-Py), 1.86 (dt, *J* = 5.6, 1.5 Hz, 4H, *o*-Py). MS (ESI): M^+ = 1078.2032 (expt), 1078.2015 (calcd for $IrC_{50}H_{30}F_9N_6$).

Ir[T*p*CF$_3$PC]dmap$_2$ (4c). The reaction mixture was evaporated to dryness on a rotary evaporator; the residue was dissolved in a small amount of dichloromethane and subjected to column chromatography (alumina, CH_2Cl_2:hexanes, 1:1) followed by preparative thin-layer chromatography (alumina, CH_2Cl_2:pentane, 1:1) to afford **4c** as a green solid.
Yield 31.7 mg (18.1 %). UV-vis (CH_2Cl_2): λ_{max} (nm) [ϵ x 10^{-4} ($M^{-1}cm^{-1}$)]: 418 (1.79), 606 (0.48). ^{1}H NMR (400 MHz, benzene-d_6, δ): 9.20 (d, *J* = 4.2 Hz, 2H, *β*-H), 8.99 (d, *J* = 4.8 Hz, 2H, *β*-H), 8.86 (d, *J* = 4.8 Hz, 2H, *β*-H), 8.60 (d, *J* = 4.2 Hz, 2H, *β*-H), 8.45 (d, *J* = 7.9 Hz, 4H, 5,15 -*o*-Ph), 8.40 (d, *J* = 7.9 Hz, 2H, 10 -*o*-Ph), 7.77 (dd, *J* = 8.3, 2.1 Hz, 6H, 5,10,15 -*m*-Ph), 3.57 – 3.52 (m, 4H, *m*-Py), 1.76 – 1.69 (m, 4H, *o*-Ph), 1.07 (s, 6H, *N*-CH_3), 1.00 (s, 6H, *N*-CH_3). MS (ESI): M^+ = 1164.2855 (expt), 1164.2860 (calcd for $IrC_{54}H_{40}F_9N_8$).

Ir[T*p*CF$_3$PC]4-picolinic acid$_2$ (4d). The reaction mixture was evaporated to dryness on a rotary evaporator; the residue was dissolved in a small amount of dichloromethane and subjected to column chromatography (alumina, CH_2Cl_2:EtOAc, 1:1) followed by preparative thin-layer chromatography (alumina, EtOAc:MeOH, 1:1) to afford **4d** as a green solid.

Yield 29.6 mg (40.1 %). UV-vis (CH_2Cl_2): λ_{max} (nm) [ϵ x 10^{-4} ($M^{-1}cm^{-1}$)]: 414 (1.71), 602 (0.94). ^{1}H NMR (400 MHz, methanol-d_4, δ): 8.88 (d, *J* = 4.2 Hz, 2H, *β*-H), 8.61 (d, *J* = 4.8 Hz, 2H, *β*-H), 8.43 – 8.41 (m, 6H, *β*-H + 5,15 -*o*-Ph), 8.28 (d, *J* = 8.0 Hz, 2H, 10 -*o*-Ph), 8.24 (d, *J* = 4.3 Hz, 2H, *β*-H), 8.08 – 8.03 (m, 4H, 5,15 -*m*-Ph), 7.99 (d, *J* = 7.9 Hz, 2H, 10 -*m*-Ph), 5.61 (d, *J* = 7.1 Hz, 4H, *m*-Py), 1.75 (d, *J* = 7.0 Hz, 4H, *o*-Py). MS (ESI): M^- = 1165.1729 (expt), 1165.1745 (calcd for $IrC_{52}H_{29}F_9N_6O_4$).

Ir[T*p*CF$_3$PC]isoquinoline$_2$ (4e). The reaction mixture was evaporated to dryness on a rotary evaporator; the residue was dissolved in a small amount of dichloromethane and subjected to column chromatography (silica, CH_2Cl_2:hexanes, 1:3) followed by preparative thin-layer chromatography (silica, CH_2Cl_2:hexanes, 1:3) to afford **4e** as a green solid. Yield 12.1 mg (7.9 %). UV-vis (CH_2Cl_2): λ_{max} (nm) [ϵ x 10^{-4} ($M^{-1}cm^{-1}$)]: 417 (1.82), 603 (1.02). ^{1}H NMR (400 MHz, chloroform-*d*, δ): 8.88 (d, *J* = 4.2 Hz, 2H, *β*-H), 8.69 (d, *J* = 4.8 Hz, 2H, *β*-H), 8.46 (d, *J* = 4.7 Hz, 2H, *β*-H), 8.43 (d, *J* = 7.9 Hz, 4H, 5,15 -*o*-Ph), 8.29 (s, 2H, *β*-H), 8.24 (d, *J* = 7.9 Hz, 2H, 10 -*o*-Ph), 8.05 – 7.99 (m, 4H, 5,15 -*m*-Ph), 7.93 (d, *J* = 7.9 Hz, 2H, 10 -*m*-Ph), 7.07 (ddd, *J* = 8.2, 6.9, 1.2 Hz, 2H, isoquinoline -C7), 6.93 (ddd, *J* = 8.2, 6.9, 1.1 Hz, 2H, isoquinoline -C6), 6.76 – 6.72 (m, 2H, isoquinoline -C8), 6.40 (d, *J* = 8.4 Hz, 2H, isoquinoline -C5), 5.58 – 5.54 (m, 2H, isoquinoline -C4), 2.36 (s, 2H, isoquinoline -C1), 1.68 (d, *J* = 6.9 Hz, 2H, isoquinoline -C3). MS (ESI): M^- = 1178.2351 (expt), 1178.2329 (calcd for $IrC_{58}H_{34}F_9N_6$).

X-ray structure determinations. X-ray data for **1a**, **2a** and **4b** were collected on beamline 11.3.1 at the Advanced Light Source, Lawrence Berkeley National Lab. Samples were mounted on MiTeGen kapton loops and placed in a 100(2) K (**1a, 4b**)/150(2) K (**2a**) nitrogen cold stream provided by an Oxford Cryostream 800 Plus low-temperature apparatus on the goniometer head of a Bruker D8 diffractometer equipped with a PHOTON100 CMOS detector operating in shutterless mode. Diffraction data were collected using synchrotron radiation monochromated using silicon(111) to a wavelength of 0.7293(1)Å (**2a**)/0.7749(1)Å (**1a**, **4b**). An approximate full-sphere of data was collected using a combination of φ and ω scans with scan speeds of one second per degree for the φ scans and one and three seconds per degree for the ω scans at 2θ = 0 and −45, respectively. The structures were solved by intrinsic phasing (SHELXT)[247] and refined by full-matrix least-squares on F2 (SHELXL-2014).[248] All non-hydrogen atoms were refined anisotropically. Hydrogen atoms were geometrically calculated and refined as riding atoms. Additional crystallographic information has been summarized in Table 4.

Supporting information

Synthesis, Characterization and Photophysical Properties of a Series of Six-Coordinated Iridium(III) Corroles.

Table of contents

^{1}H proton NMR spectra

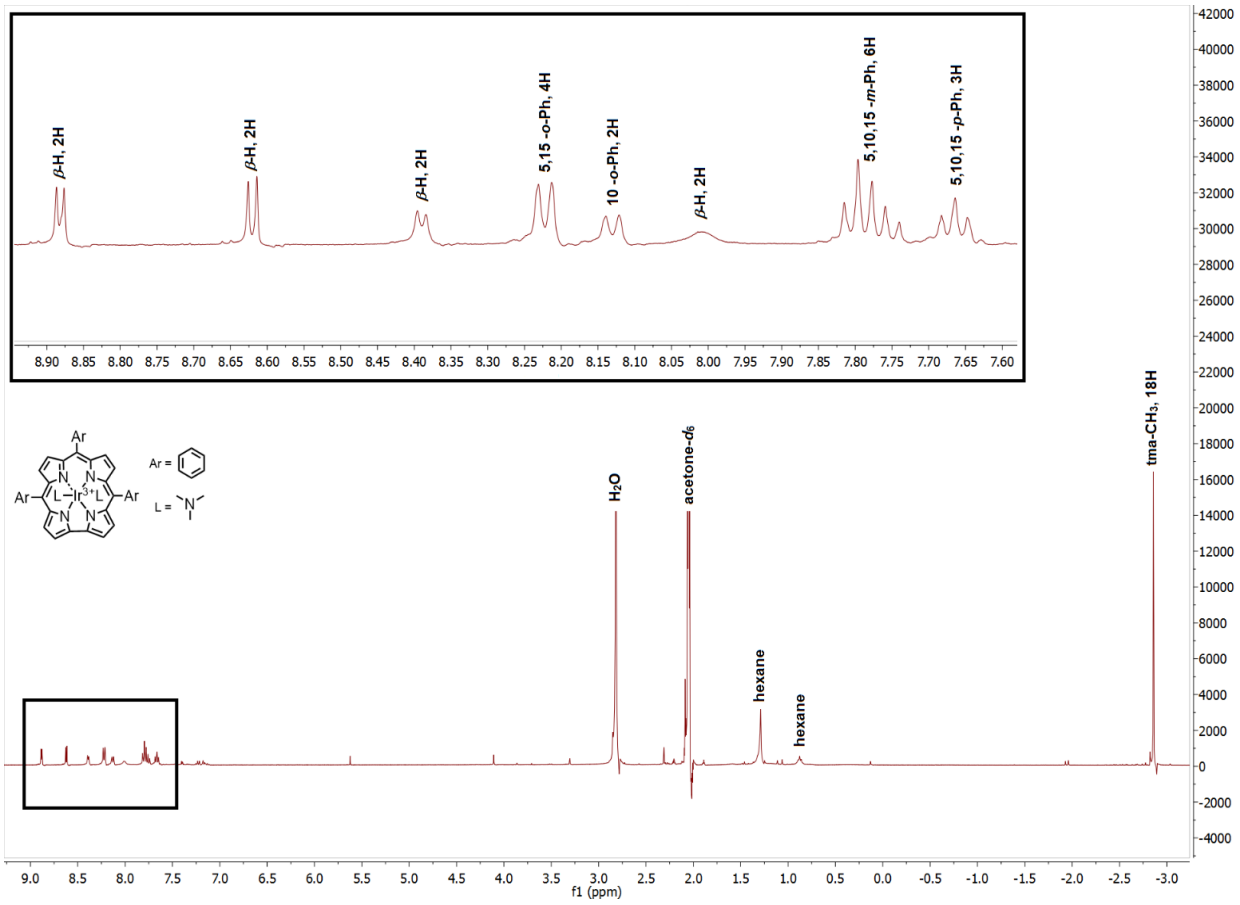

Figure S1. ^{1}H NMR spectrum of Ir[TPC]tma$_2$ (**1a**). (c) Expanded view of the aromatic area.

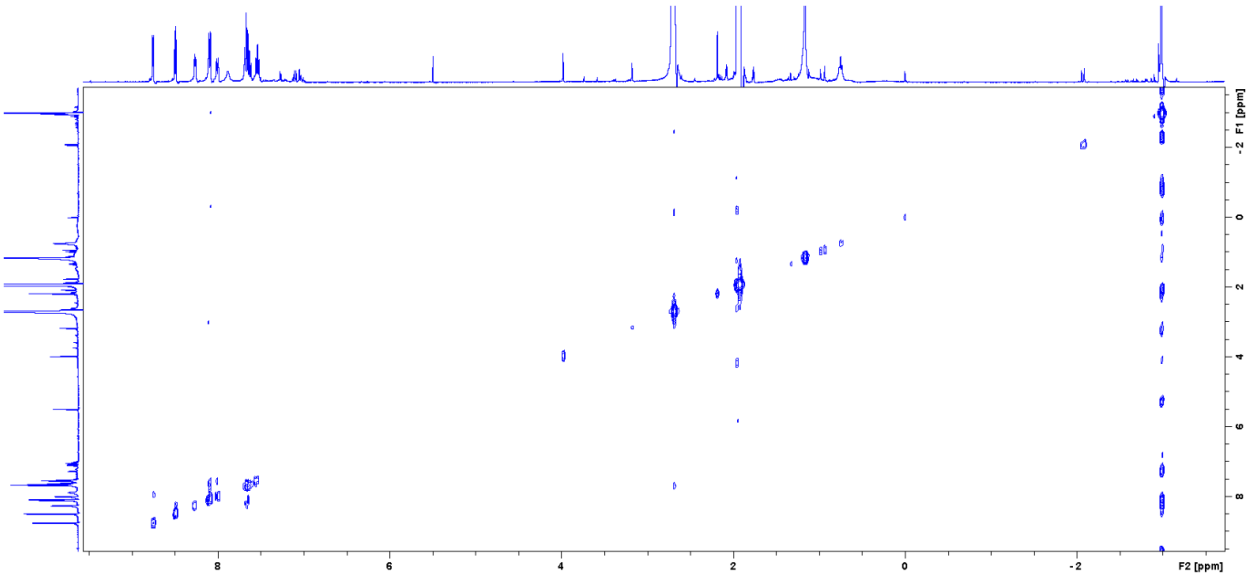

Figure S2. COSY spectrum of **1a**.

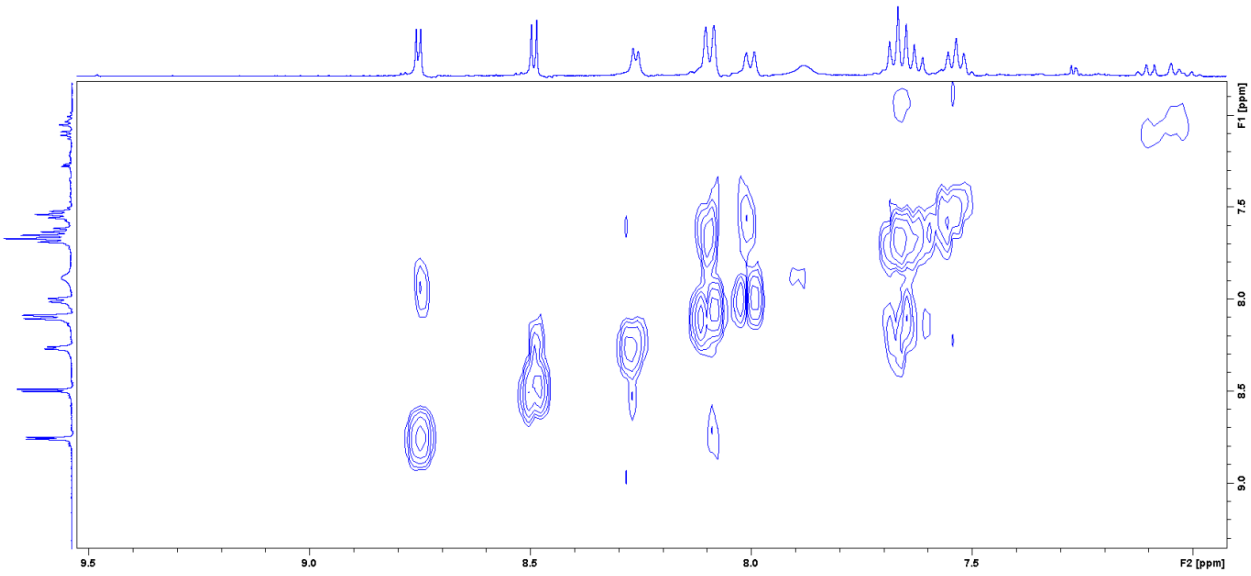

Figure S3. Expanded view of the aromatic area of **1a**.

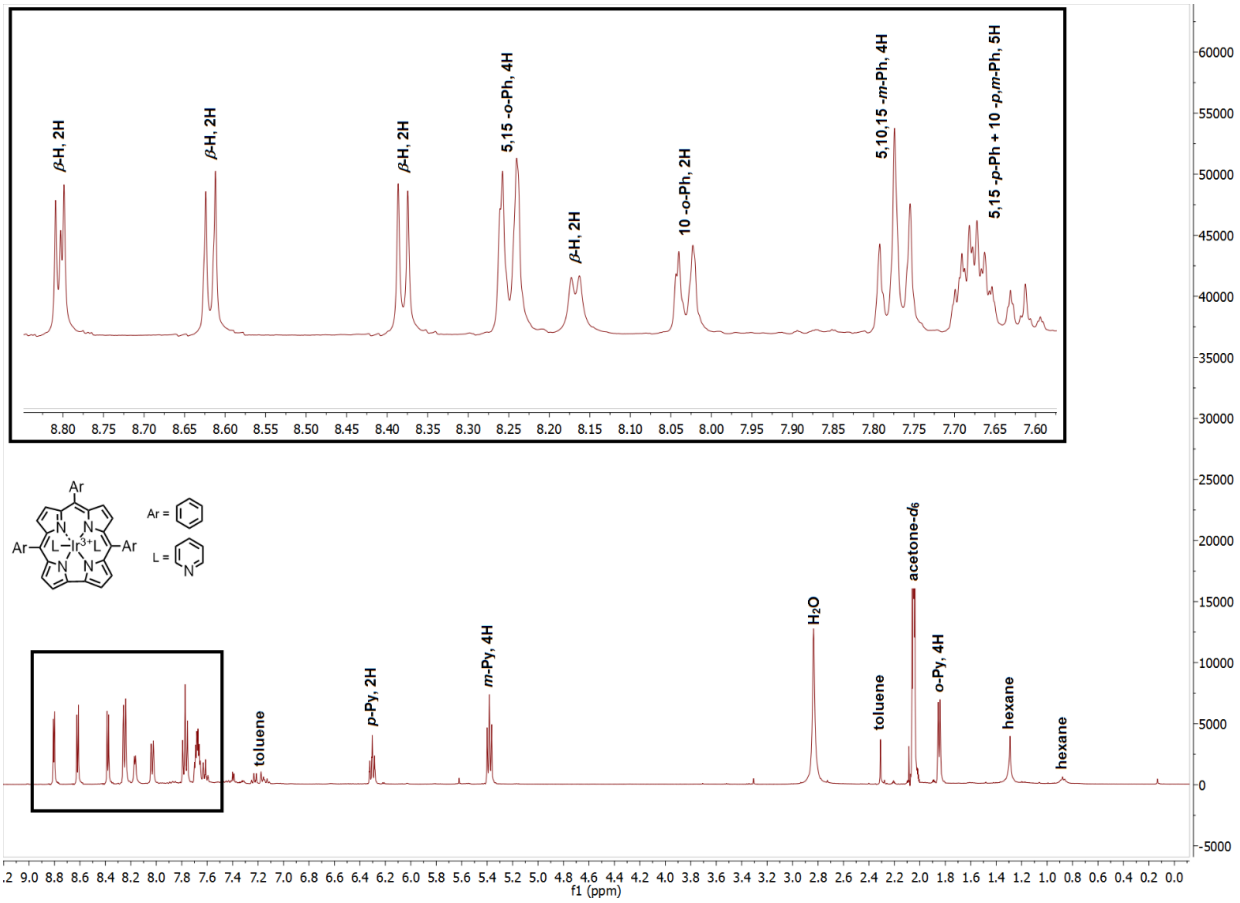

Figure S4. ^{1}H NMR spectrum of Ir[TPC]py$_2$ (**1b**).

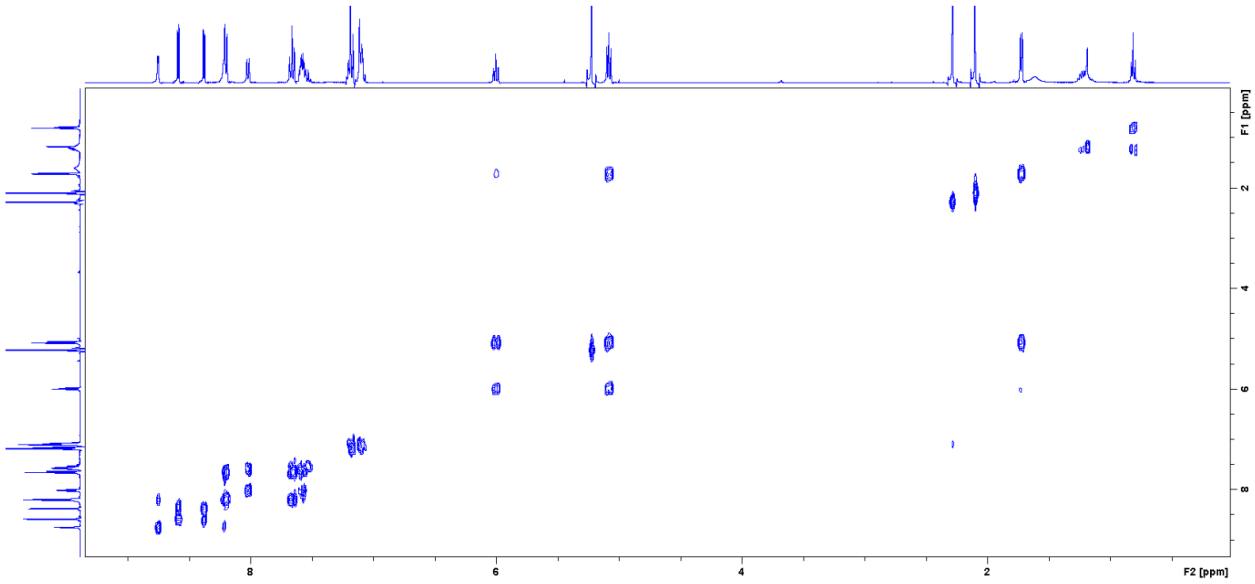

Figure S5. COSY spectrum of **1b**.

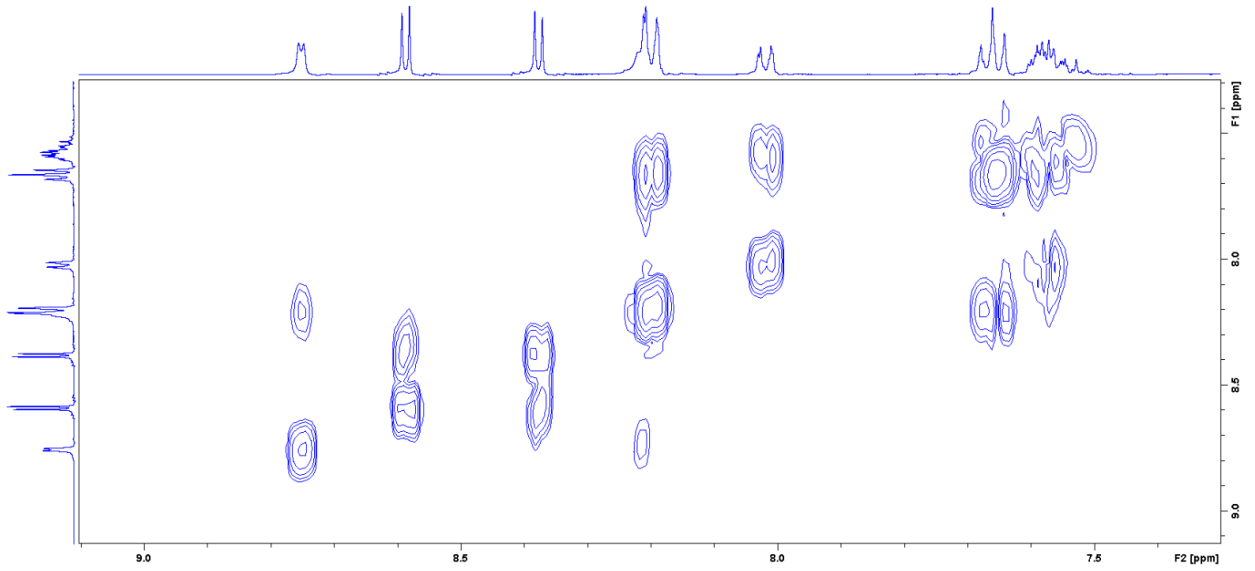

Figure S6. Expanded view of the aromatic area of **1b**.

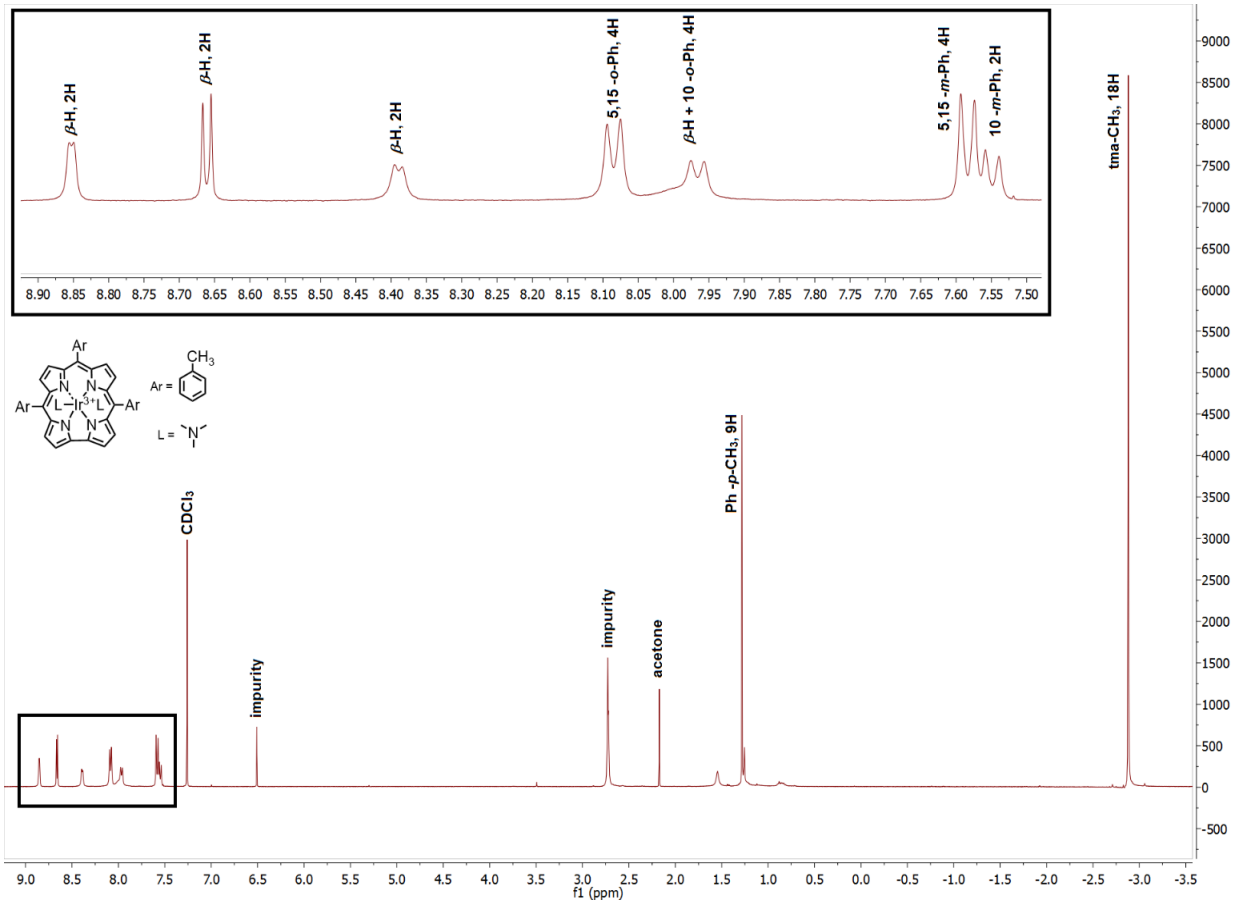

Figure S7. ^{1}H NMR spectrum of Ir[T*p*MePC]tma$_2$ (**2a**).

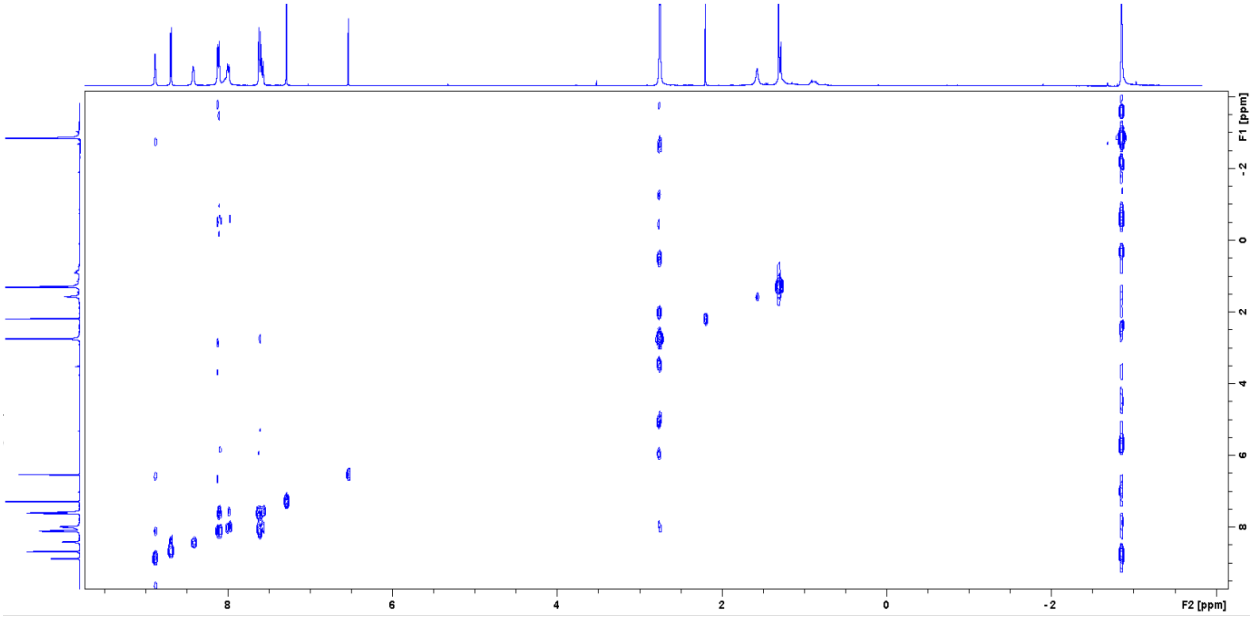

Figure S8. COSY spectrum of **2a**.

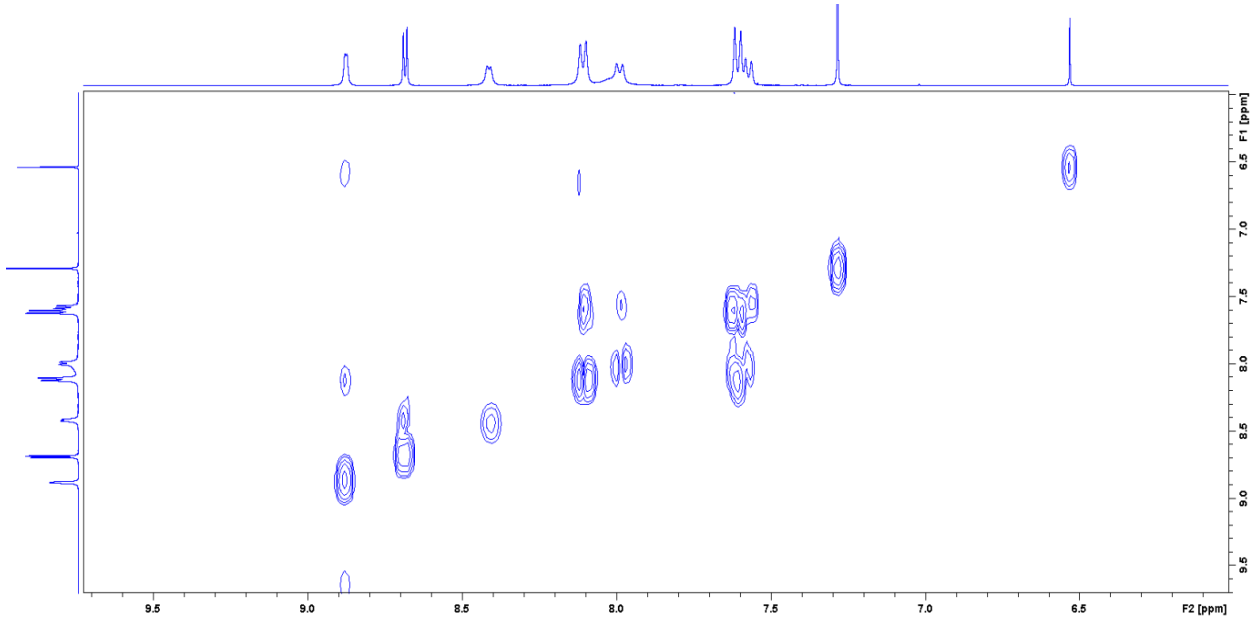

Figure S9. Expanded view of the aromatic area of **2b**.

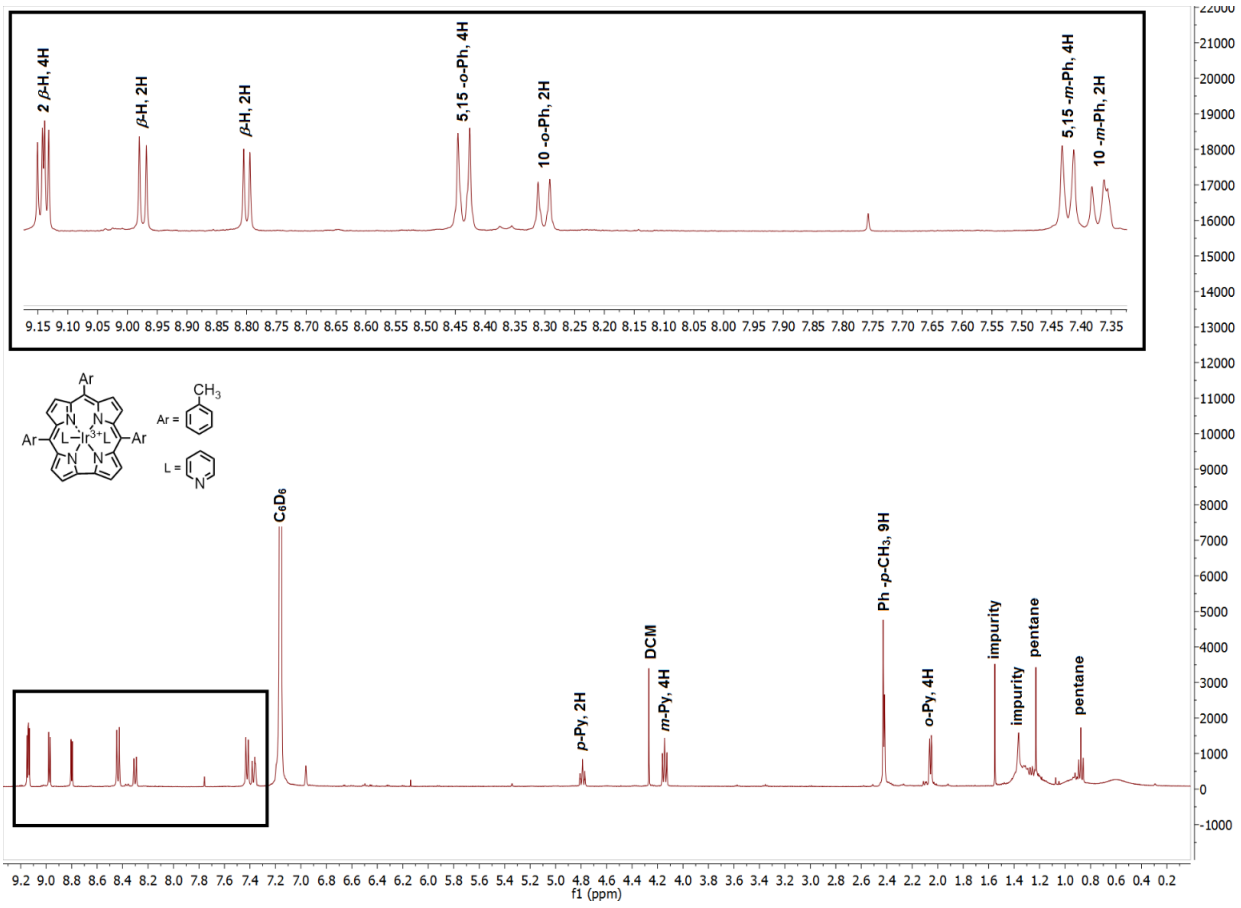

Figure S10. ^{1}H NMR spectrum of Ir[T*p*MePC]py$_2$ (**2b**).

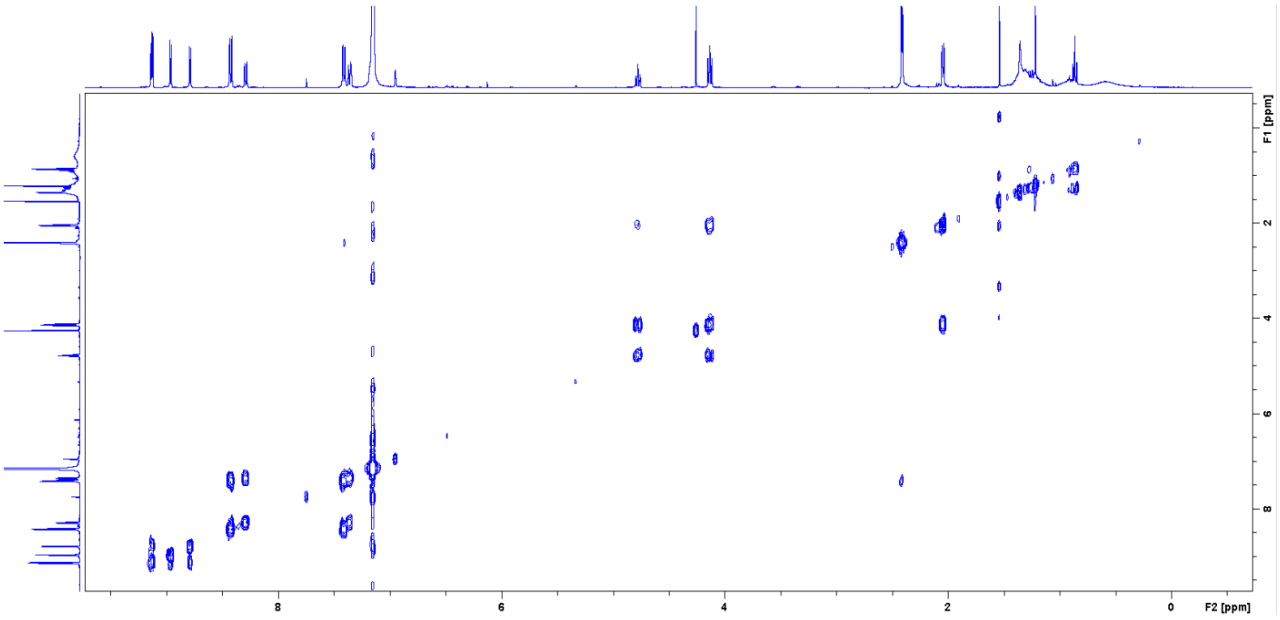

Figure S11. COSY spectrum of **2b**.

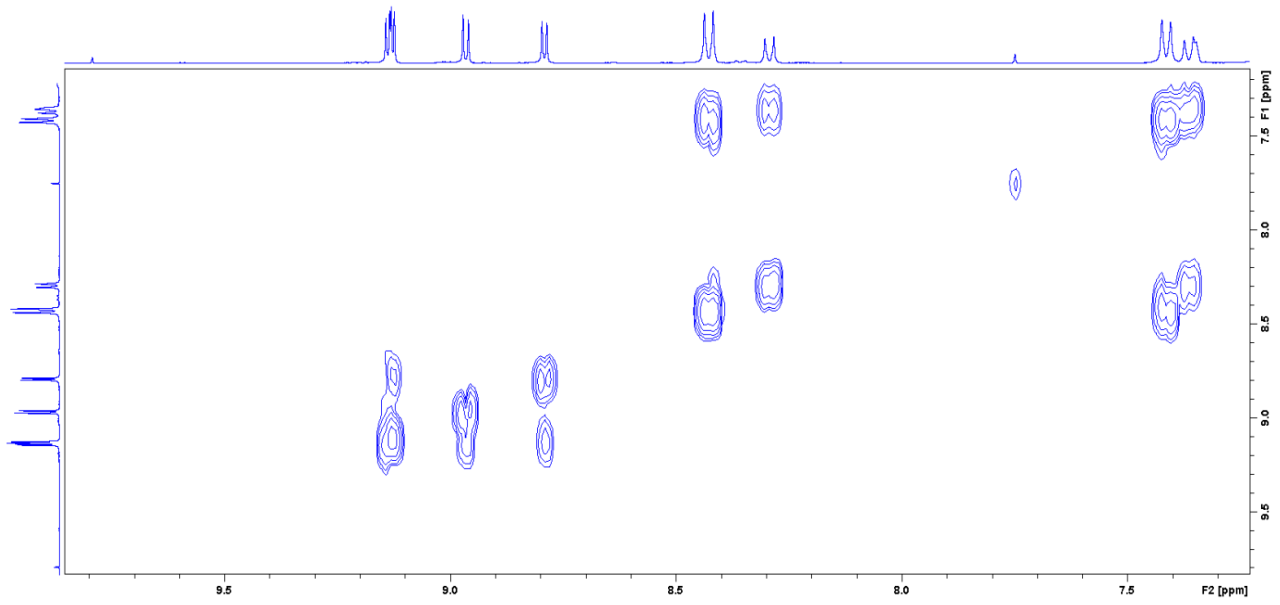

Figure S12. Expanded view of the aromatic area of **2b**.

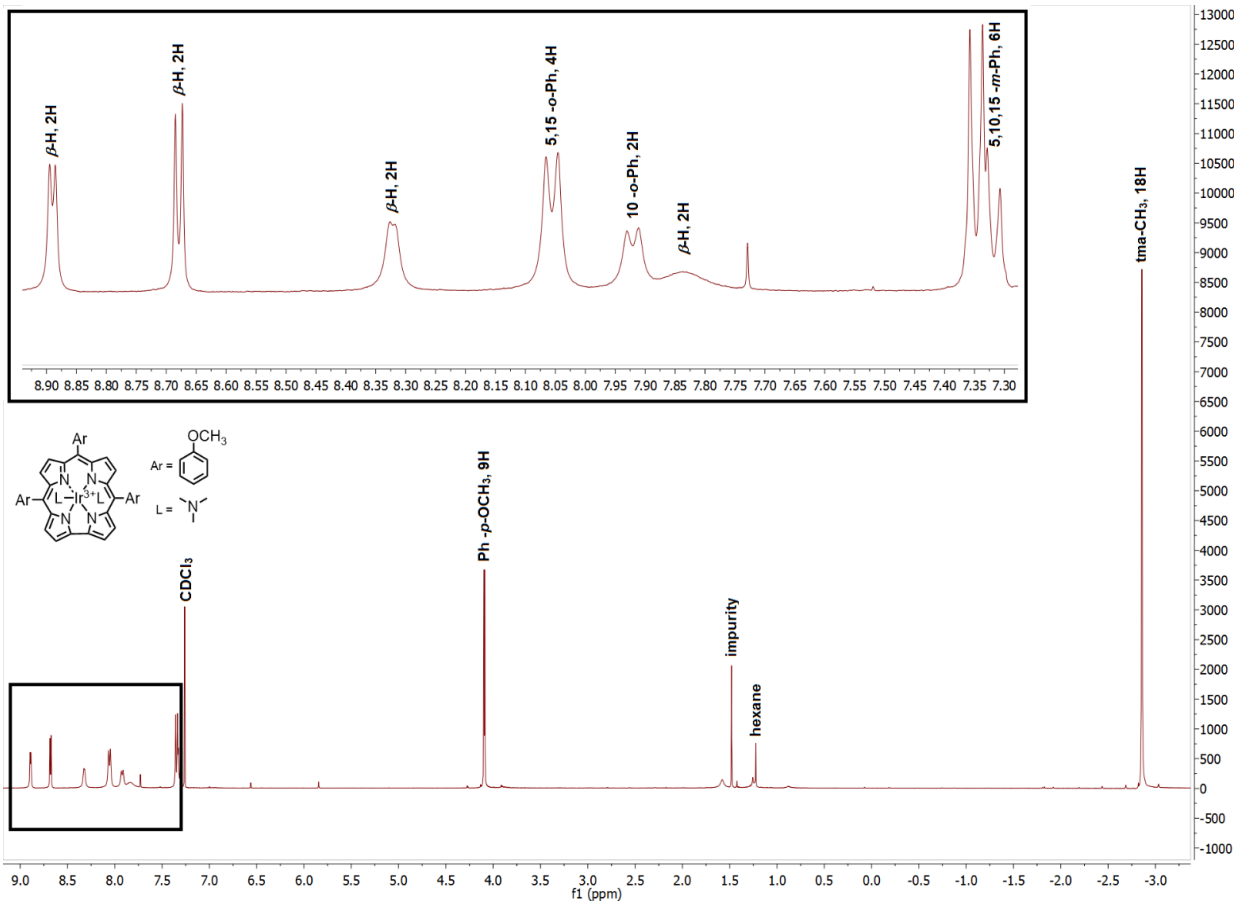

Figure S13. ^{1}H NMR spectrum of Ir[T*p*OMePC]tma$_2$ (**3a**).

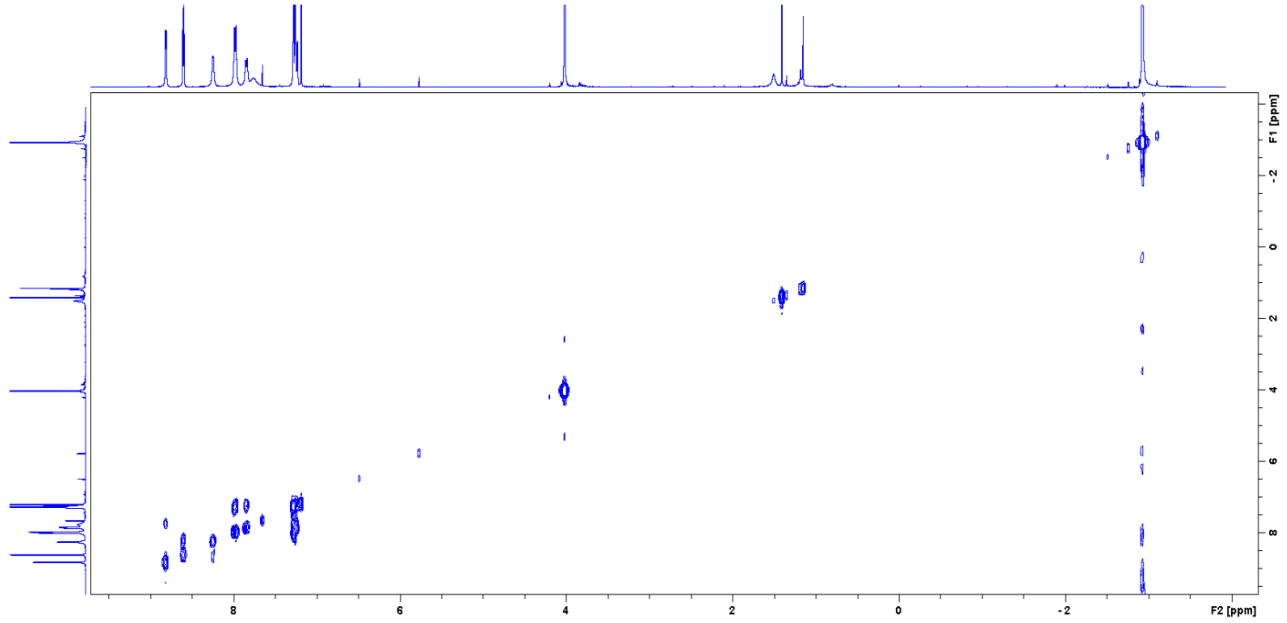

Figure S14. COSY spectrum of **3a**.

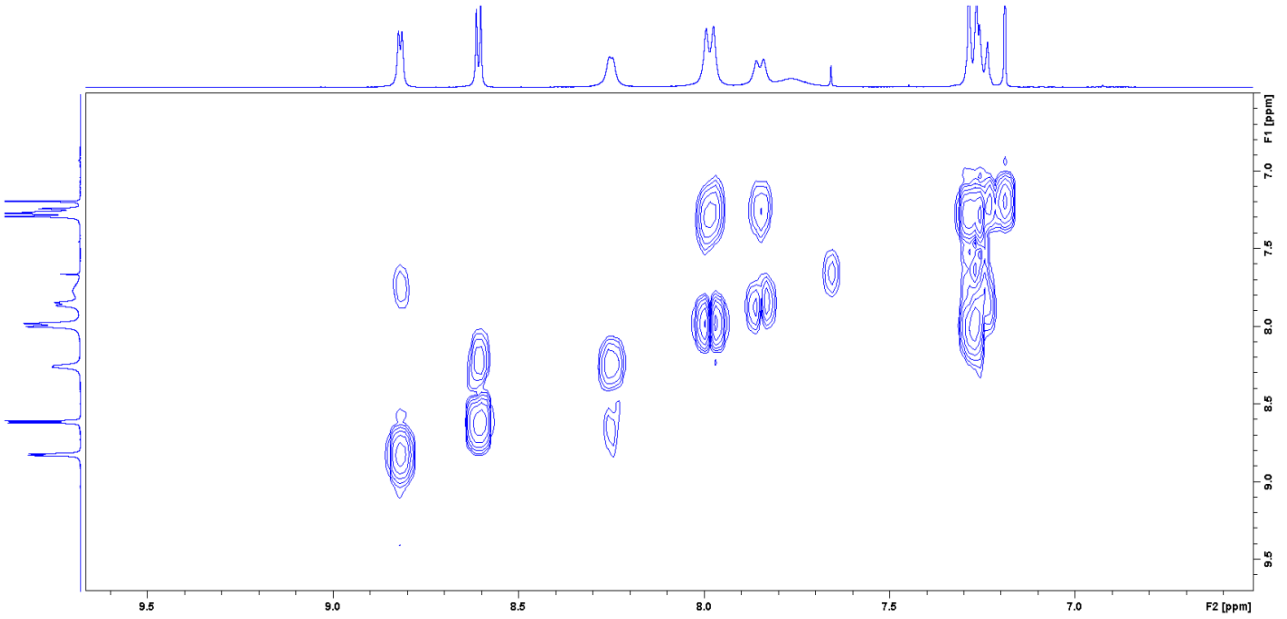

Figure S15. Expanded view of the aromatic area of **3a**.

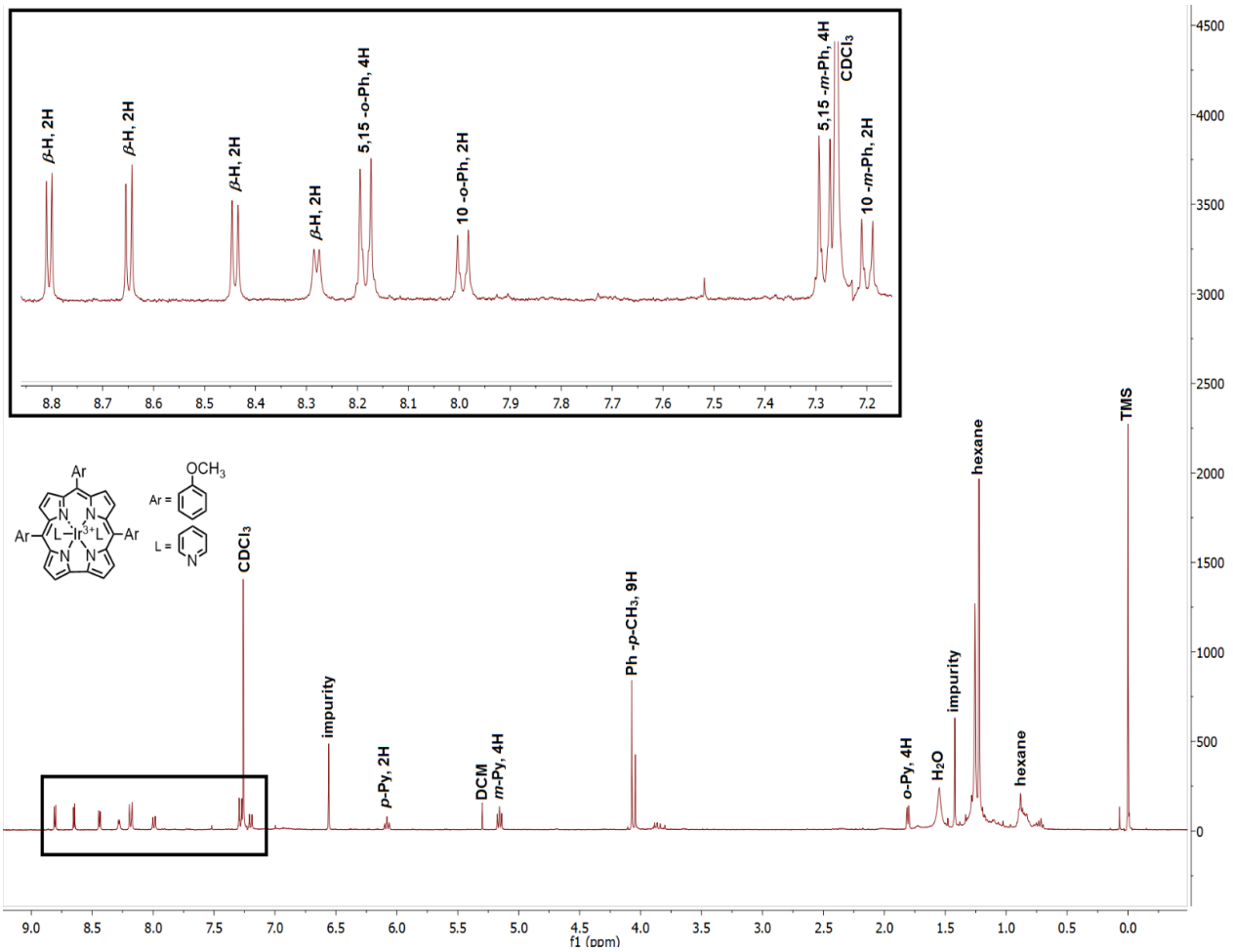

Figure S16. ^{1}H NMR spectrum of Ir[T*p*OMePC]py$_2$ (**3b**) in $CDCl_3$.

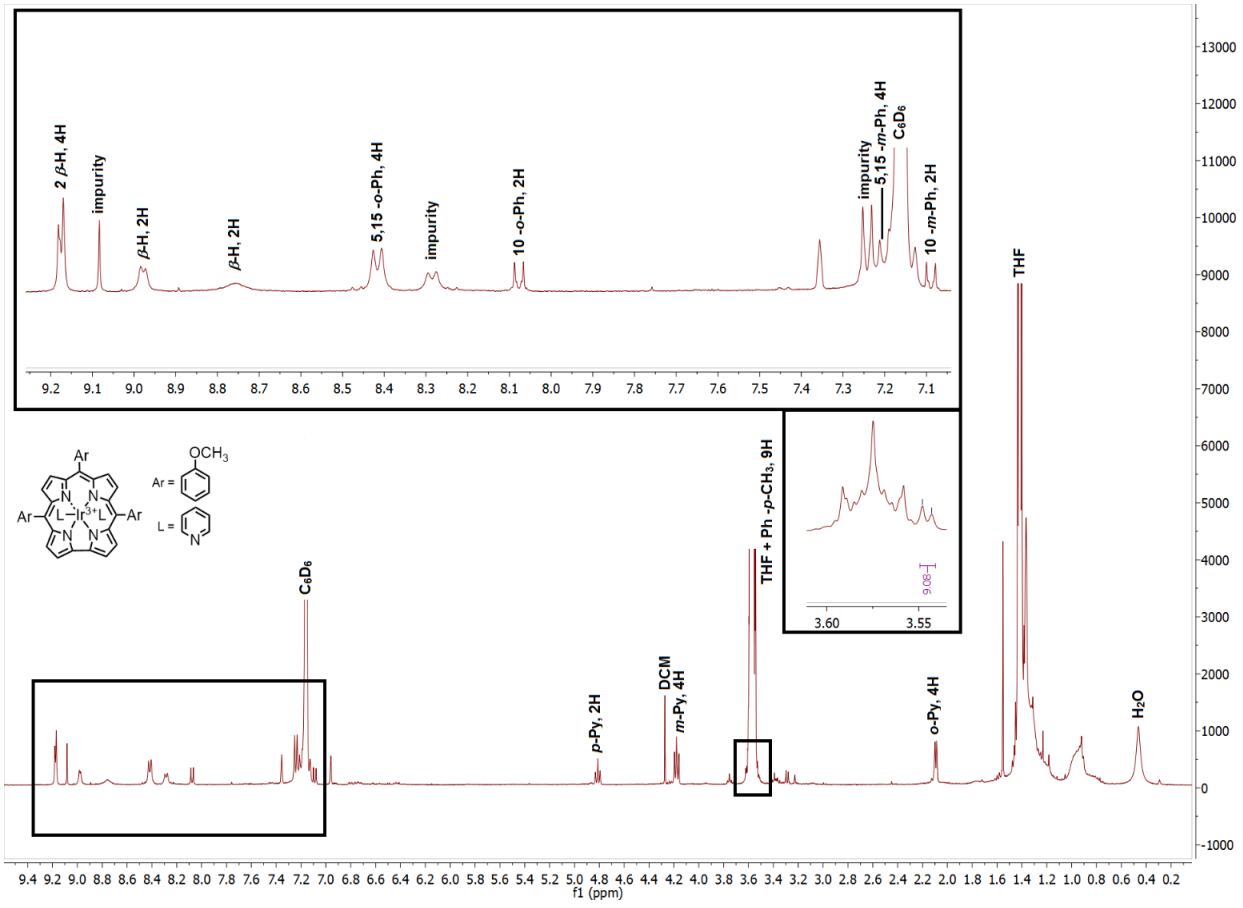

Figure S17. ^{1}H NMR spectrum of **3b** in C_6D_6.

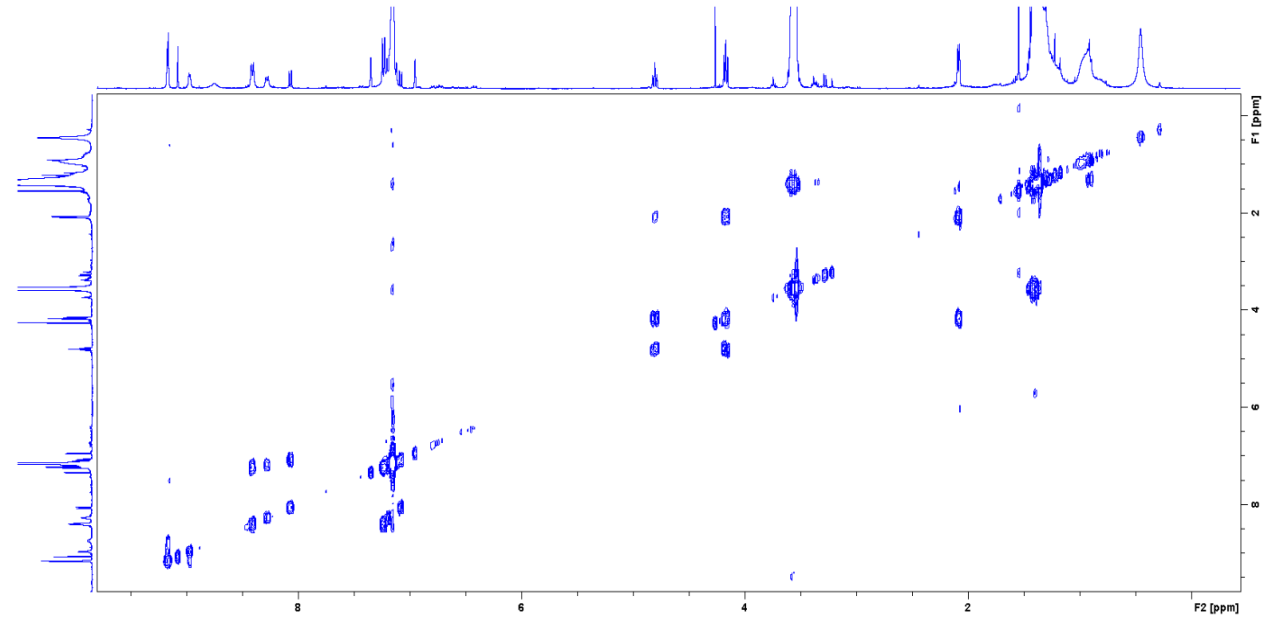

Figure S18. COSY spectrum of **3b**.

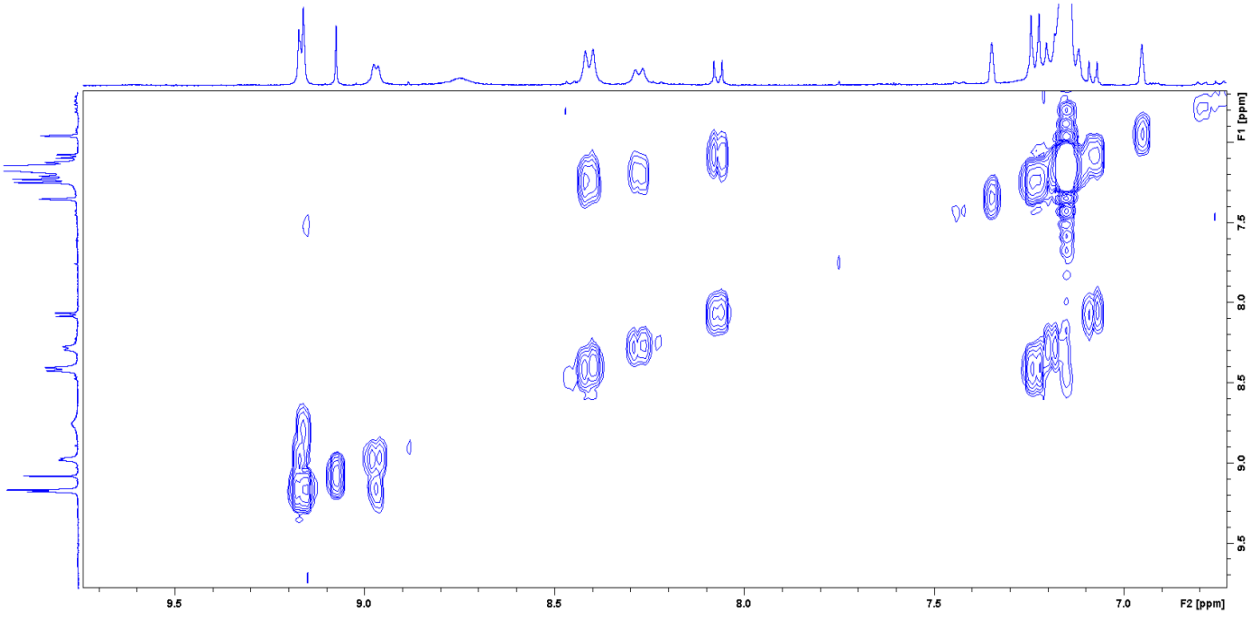

Figure S19. Expanded view of the aromatic area of **3b**.

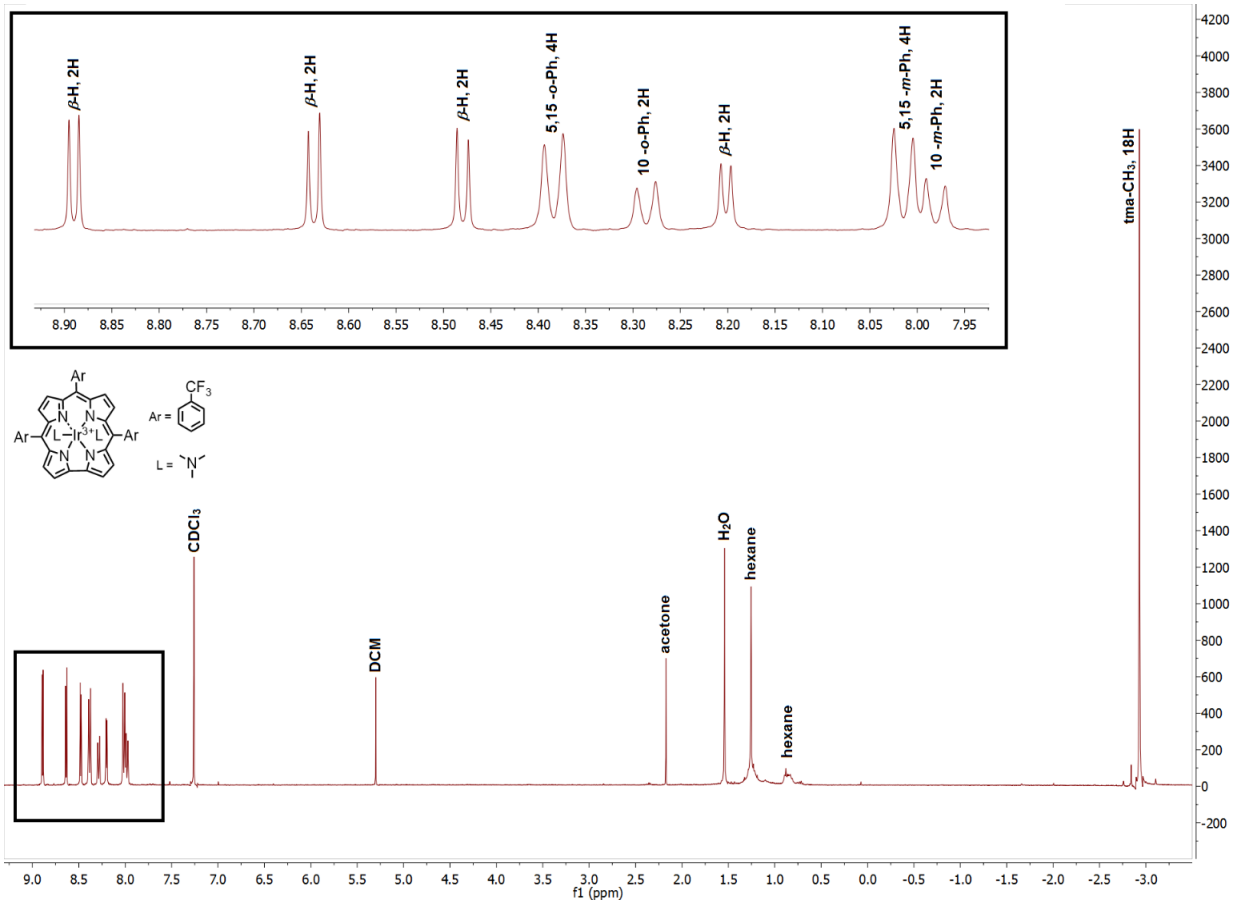

Figure S20. ^{1}H NMR spectrum of Ir[T*p*CF_3PC]tma_2 (**4a**).

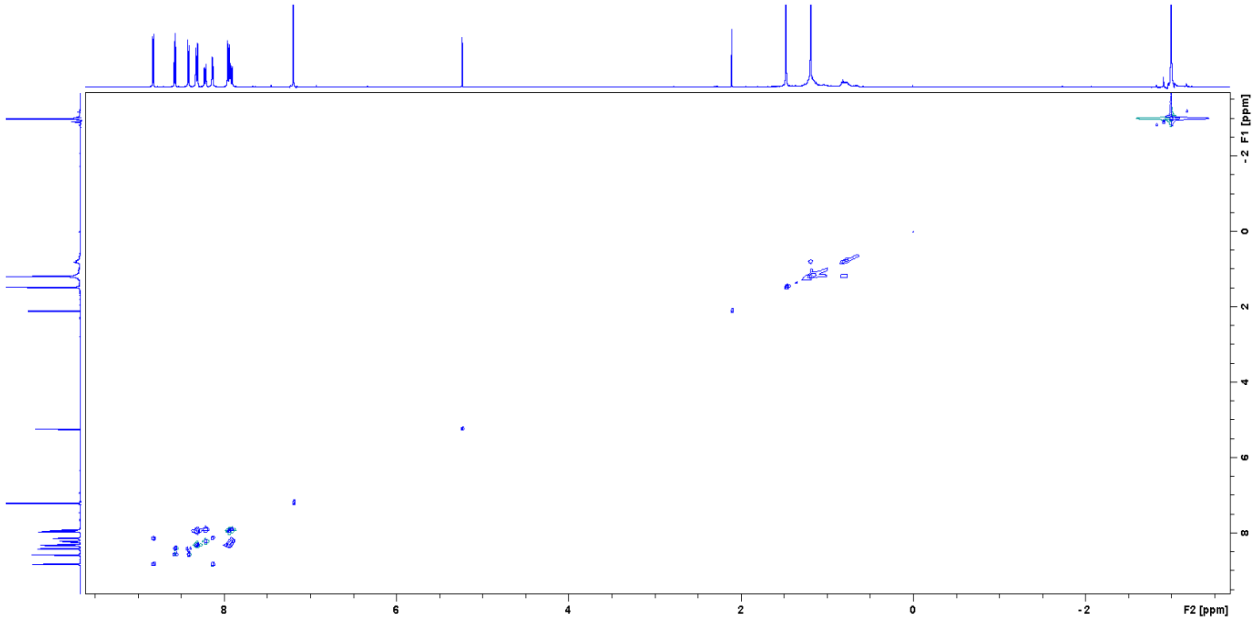

Figure S21. COSY spectrum of **4a**.

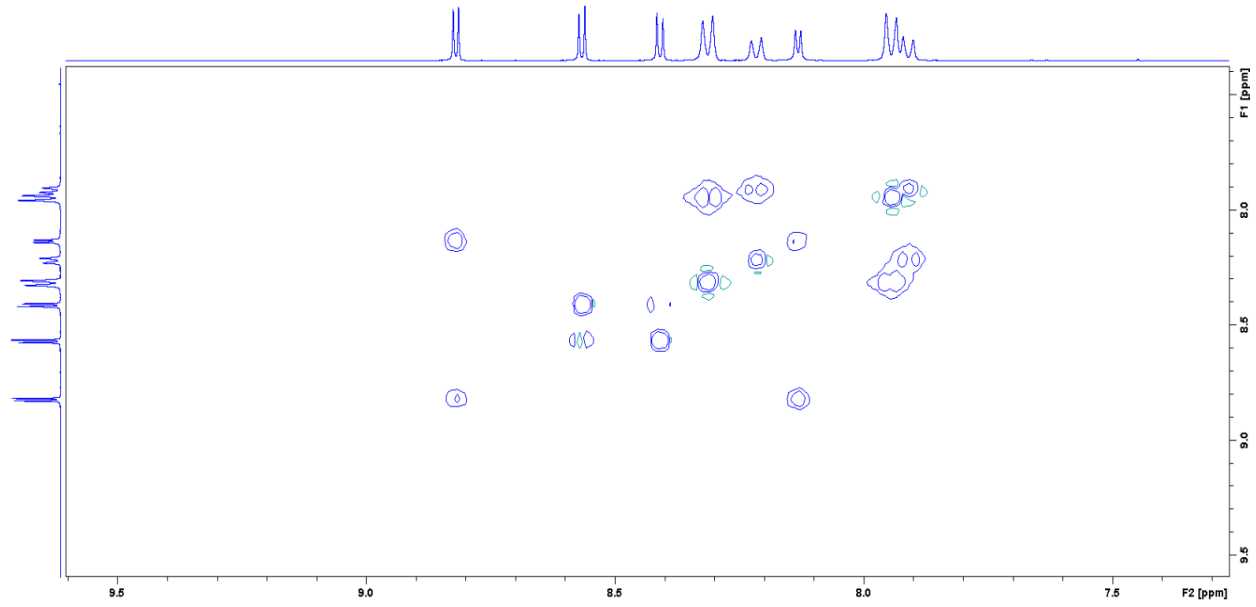

Figure S22. Expanded view of the aromatic area of **4a**.

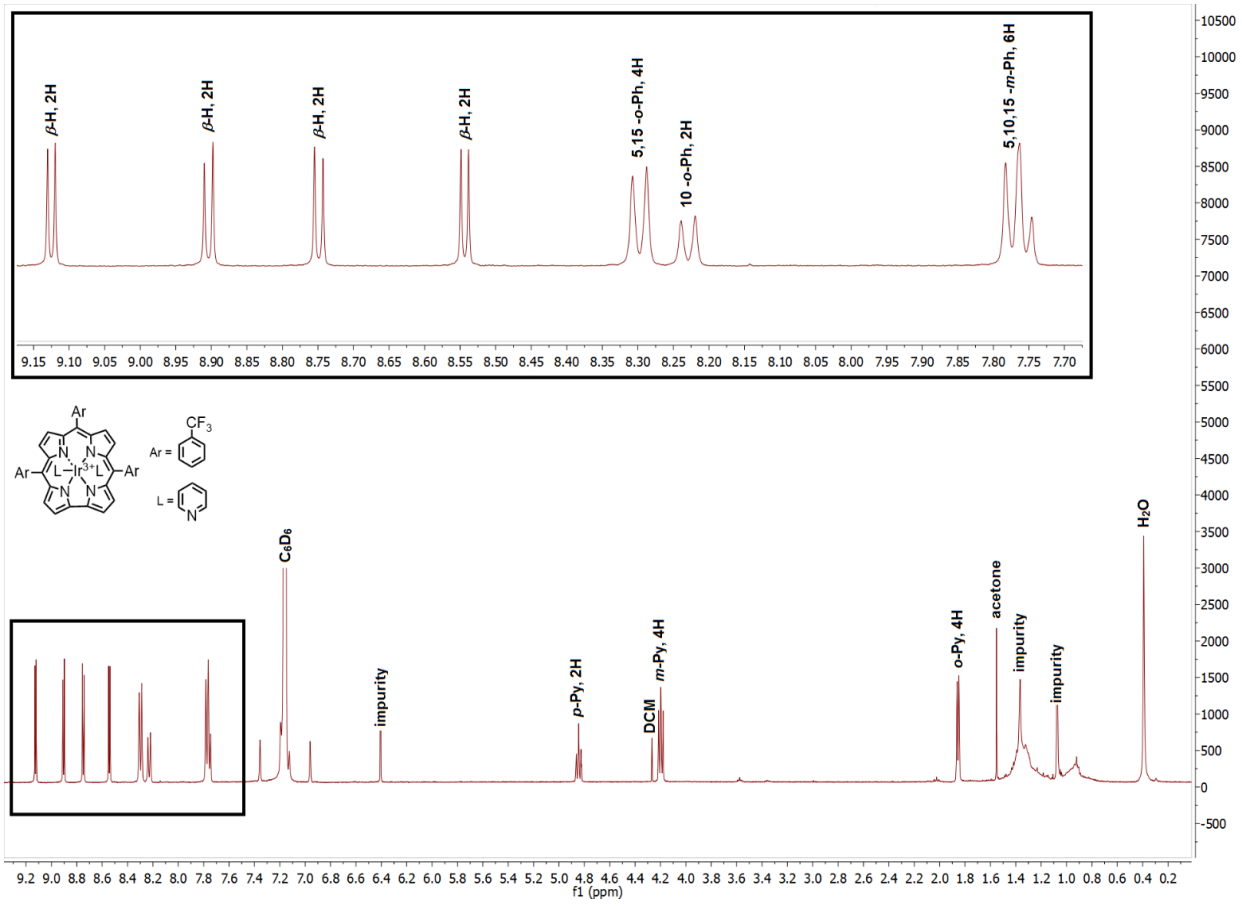

Figure S23. ^{1}H NMR spectrum of Ir[T*p*CF_3PC]py_2 (**4b**).

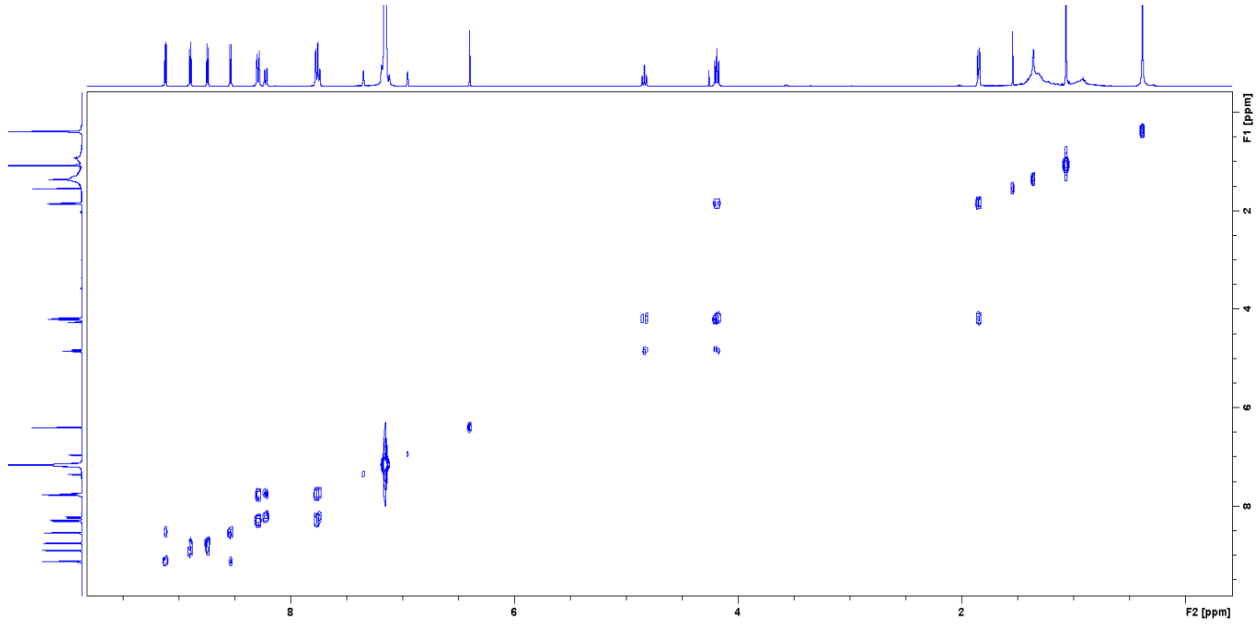

Figure S24. COSY spectrum of **4b**.

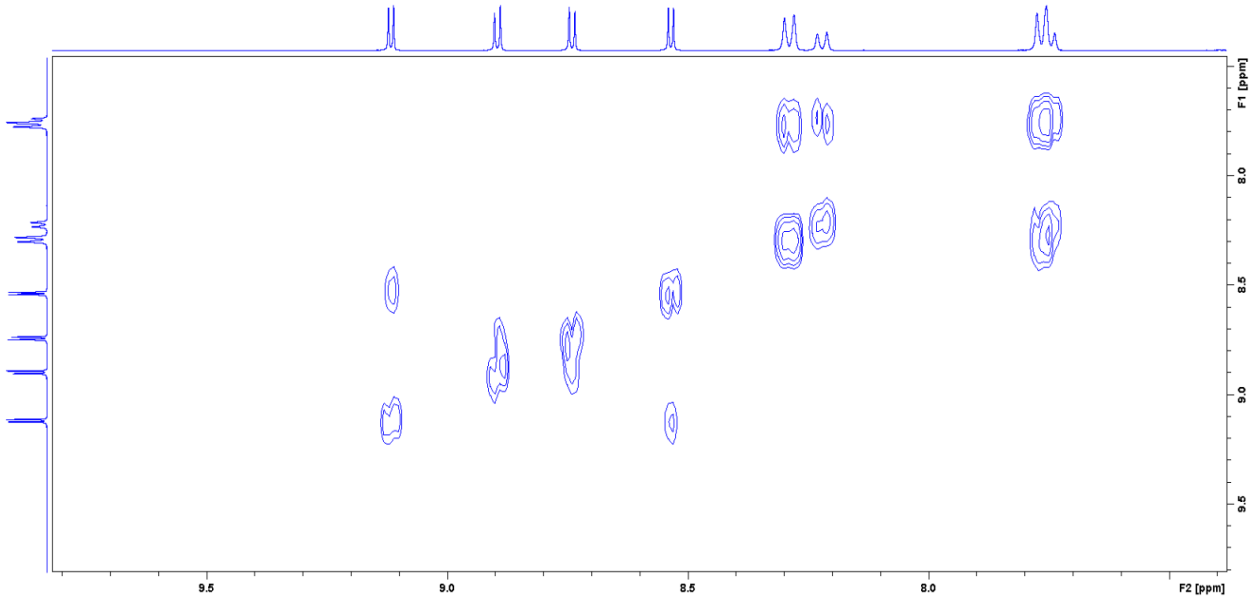

Figure S25. Expanded view of the aromatic area of **4b**.

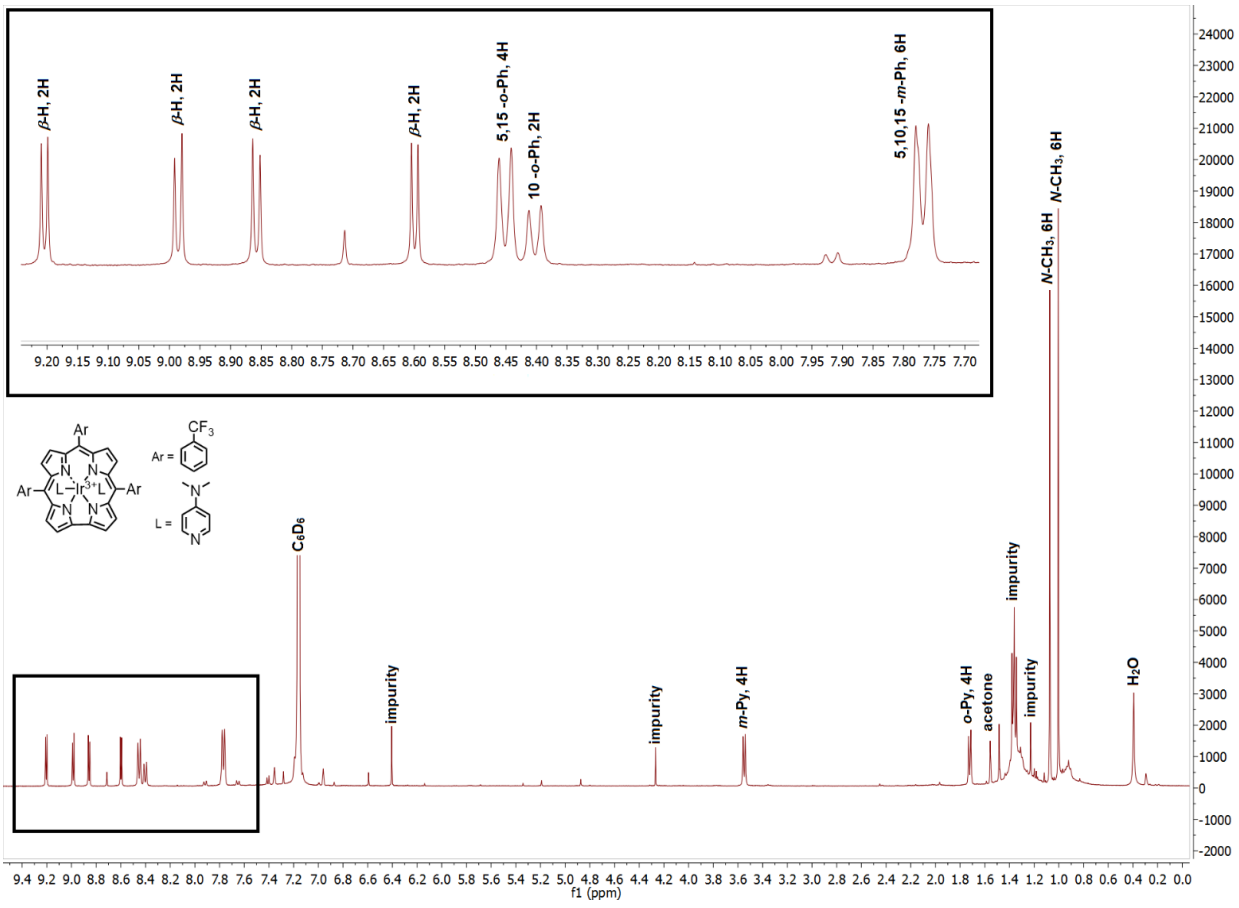

Figure S26. ^{1}H NMR spectrum of Ir[T*p*CF$_3$PC]dmap$_2$ (**4c**).

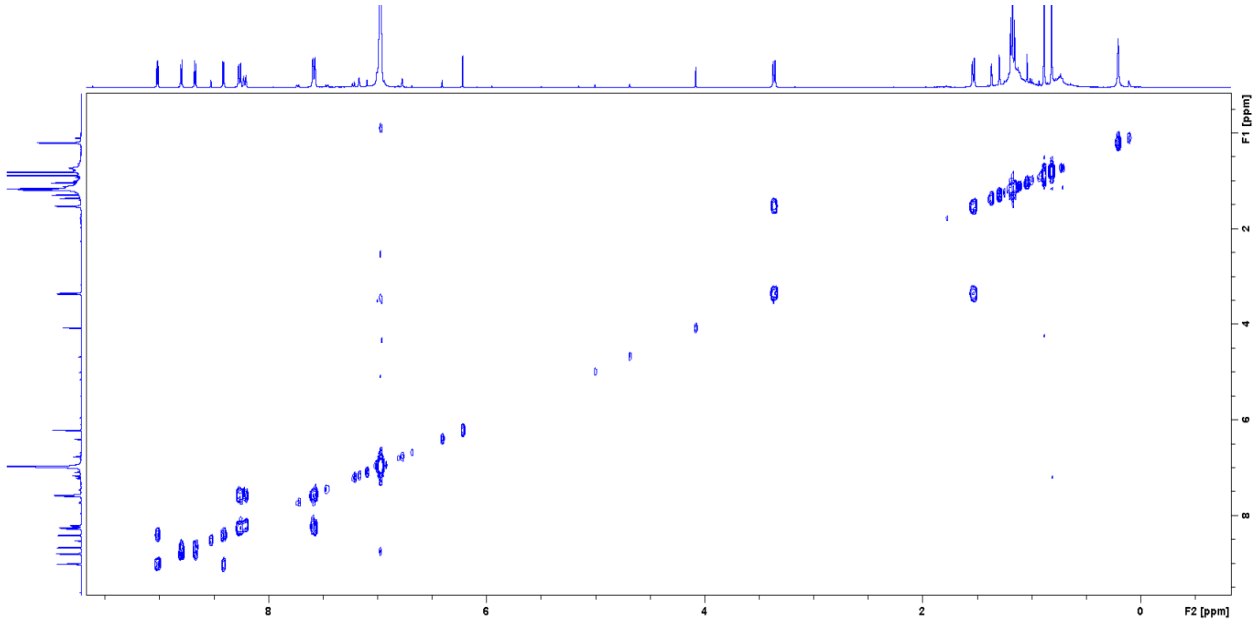

Figure S27. COSY spectrum of **4c**.

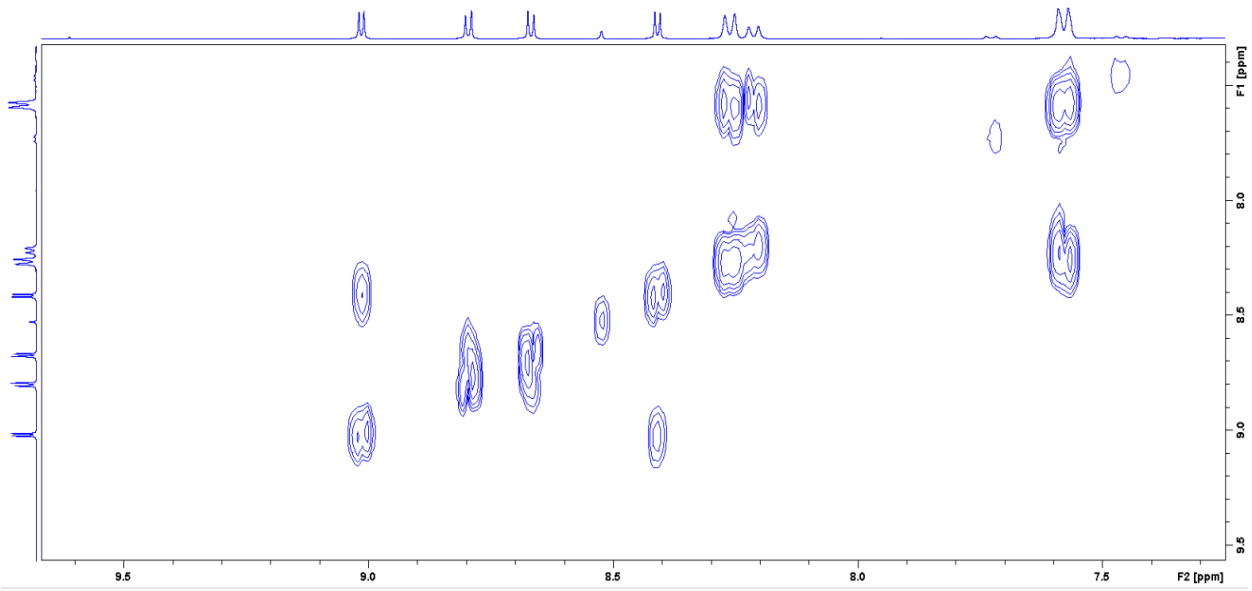

Figure S28. Expanded view of the aromatic area of **4c**.

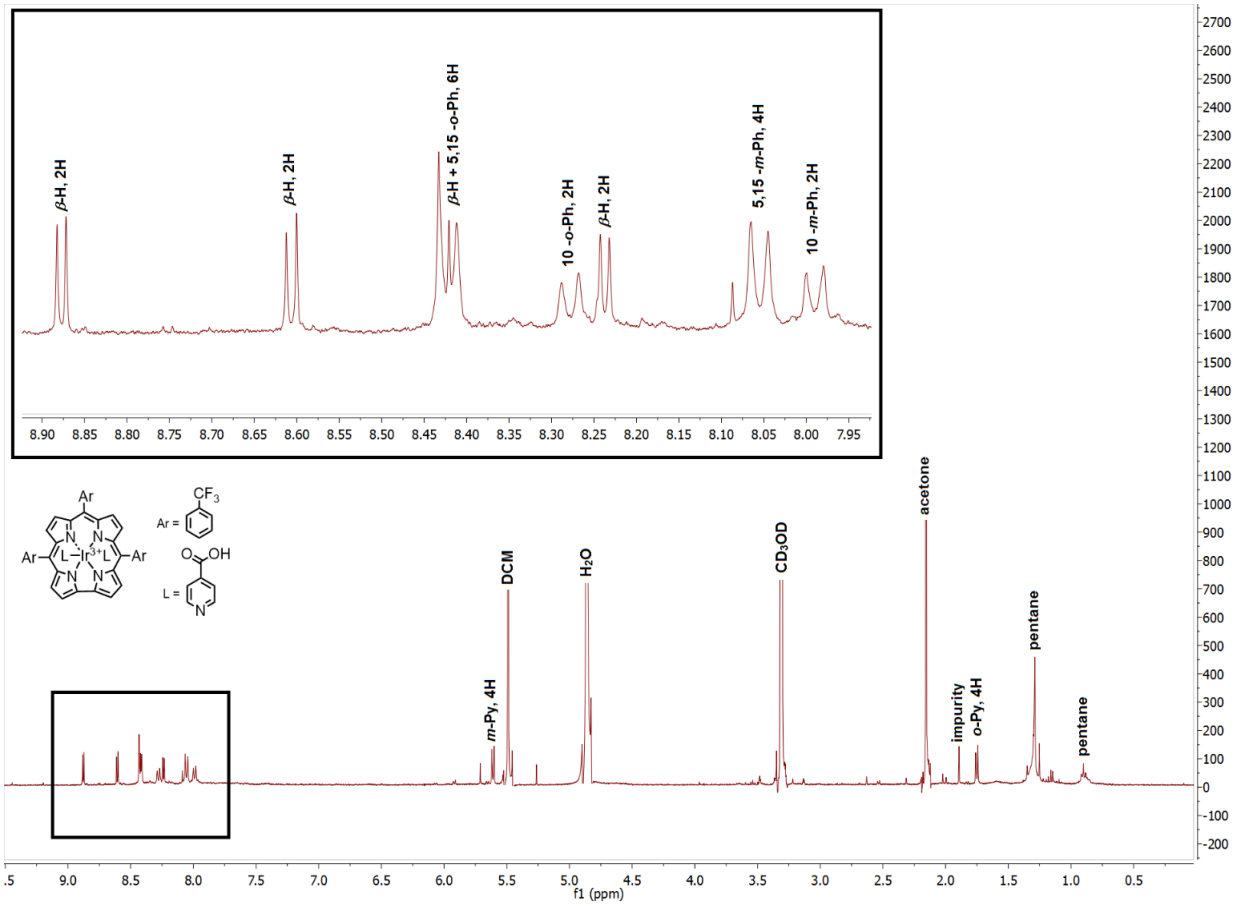

Figure S29. ^{1}H NMR spectrum of Ir[T*p*CF_3PC]4-picolinic $acid_2$ (**4d**).

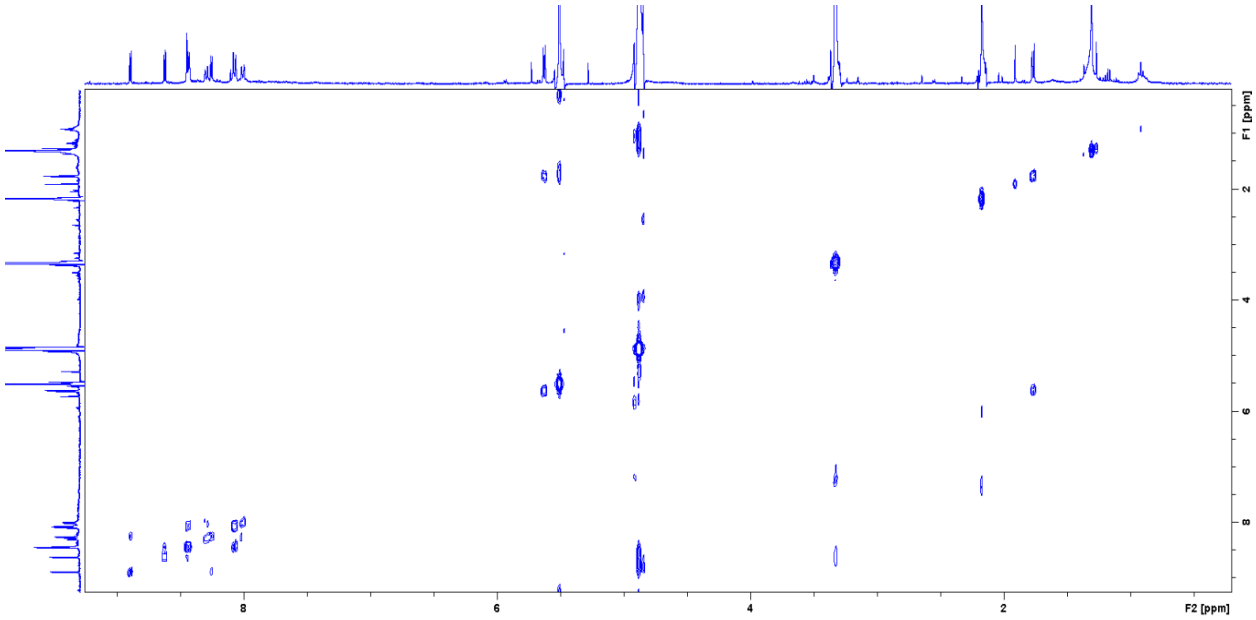

Figure S30. COSY spectrum of **4d**.

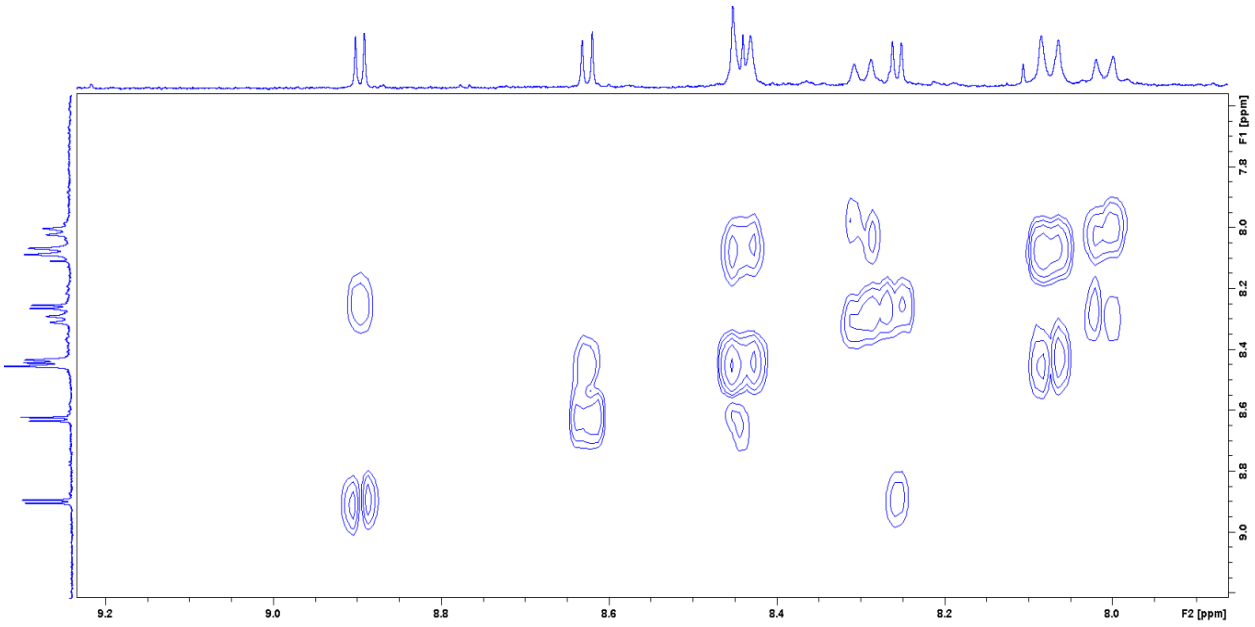

Figure S31. Expanded view of the aromatic area of **4d**.

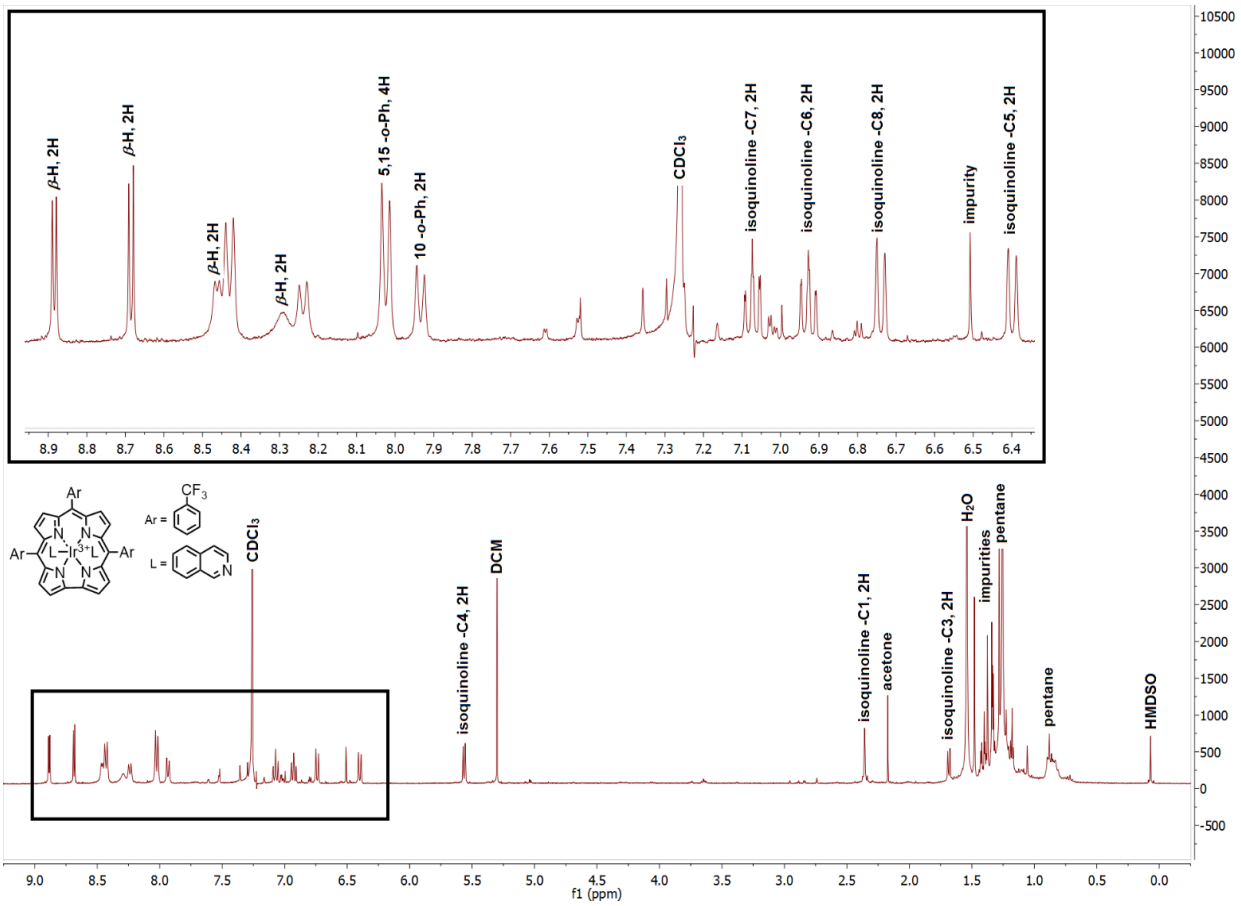

Figure S32. ^{1}H NMR spectrum of Ir[T*p*CF_3PC]isoquinoline$_2$ (**4e**).

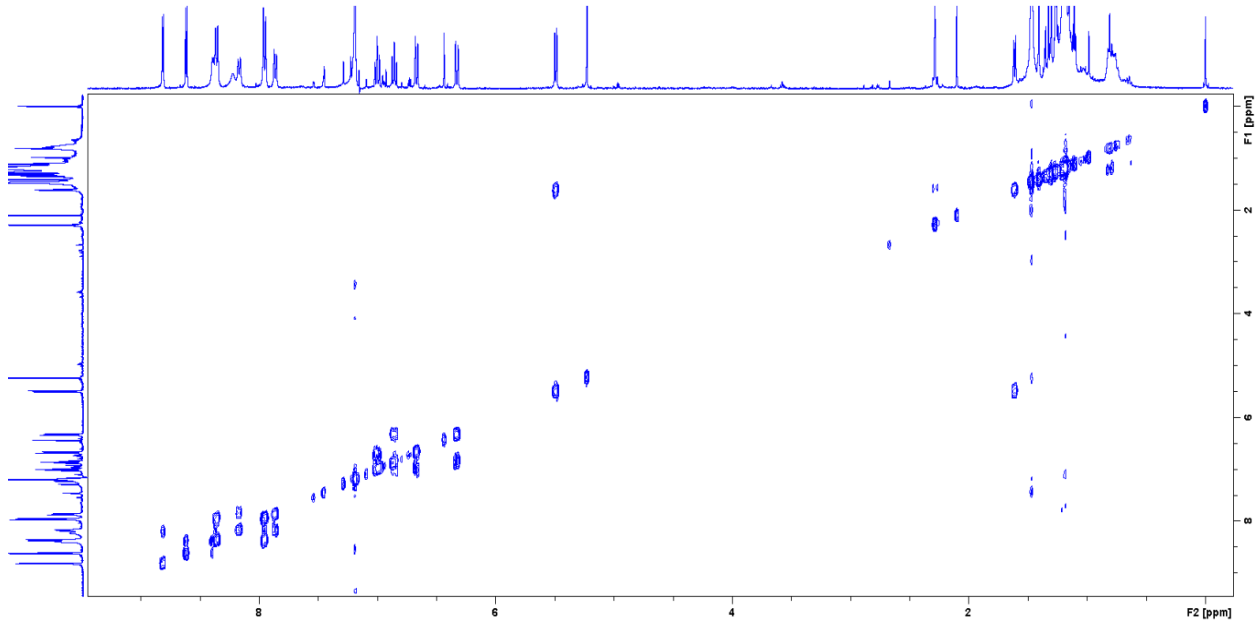

Figure S33. COSY spectrum of **4e**.

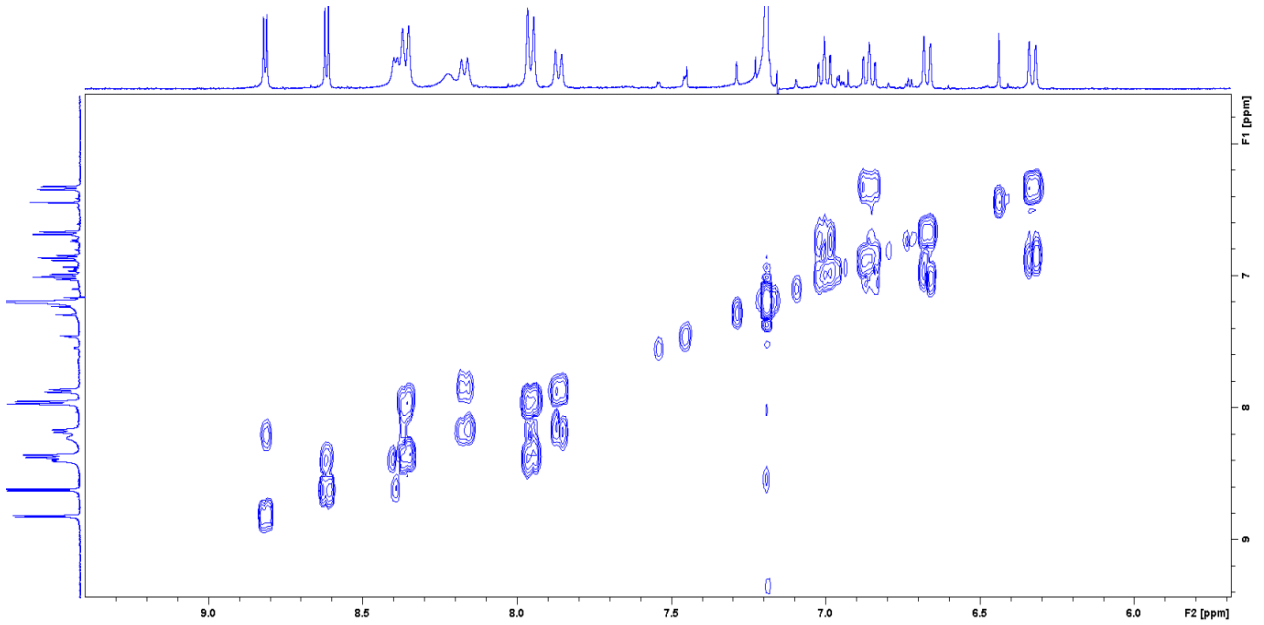

Figure S34. Expanded view of the aromatic area of **4e.**

Mass spectra

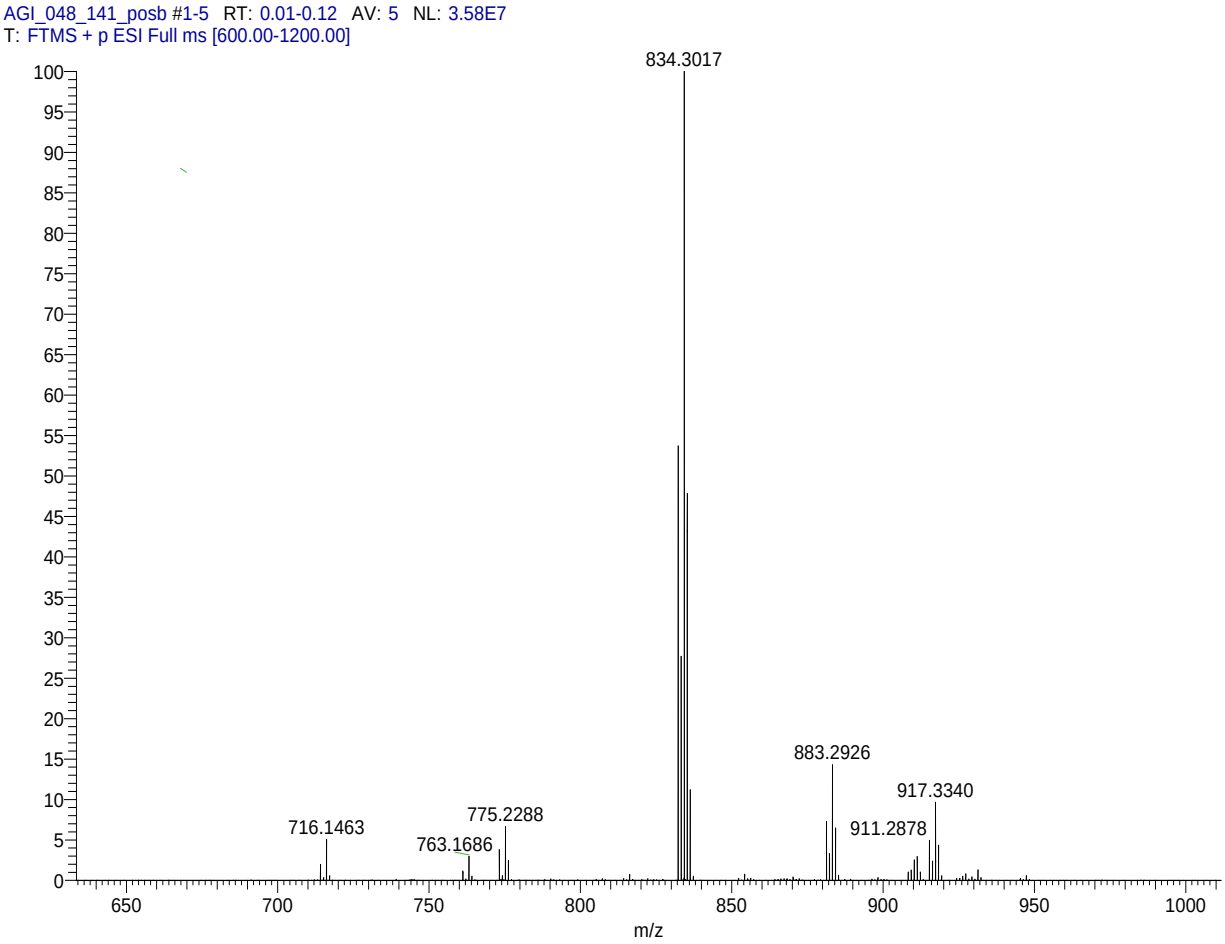

Figure S35. (a) Mass spectrum of Ir[TPC]tma$_2$ (**1a**).

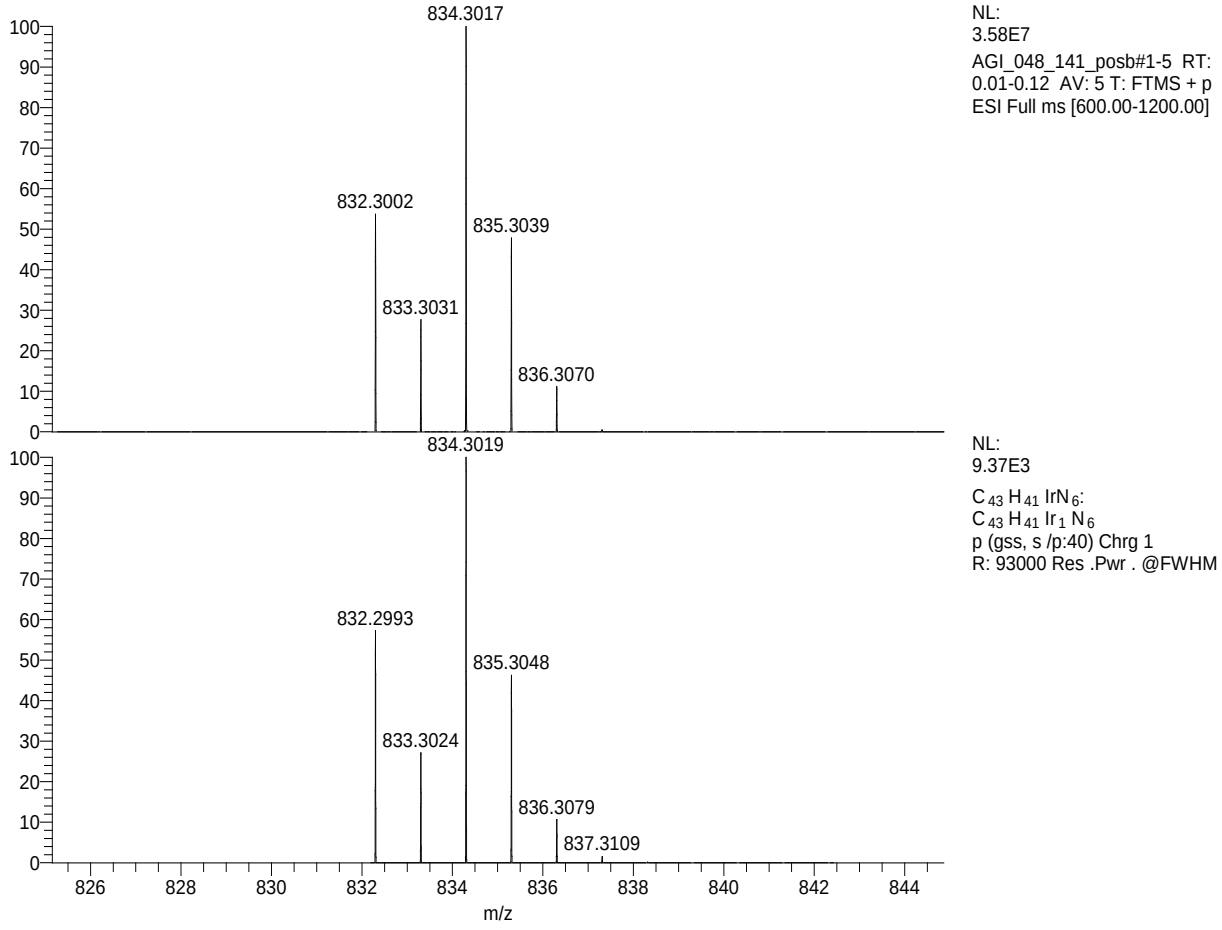

Figure S36. Expanded view of **1a**.

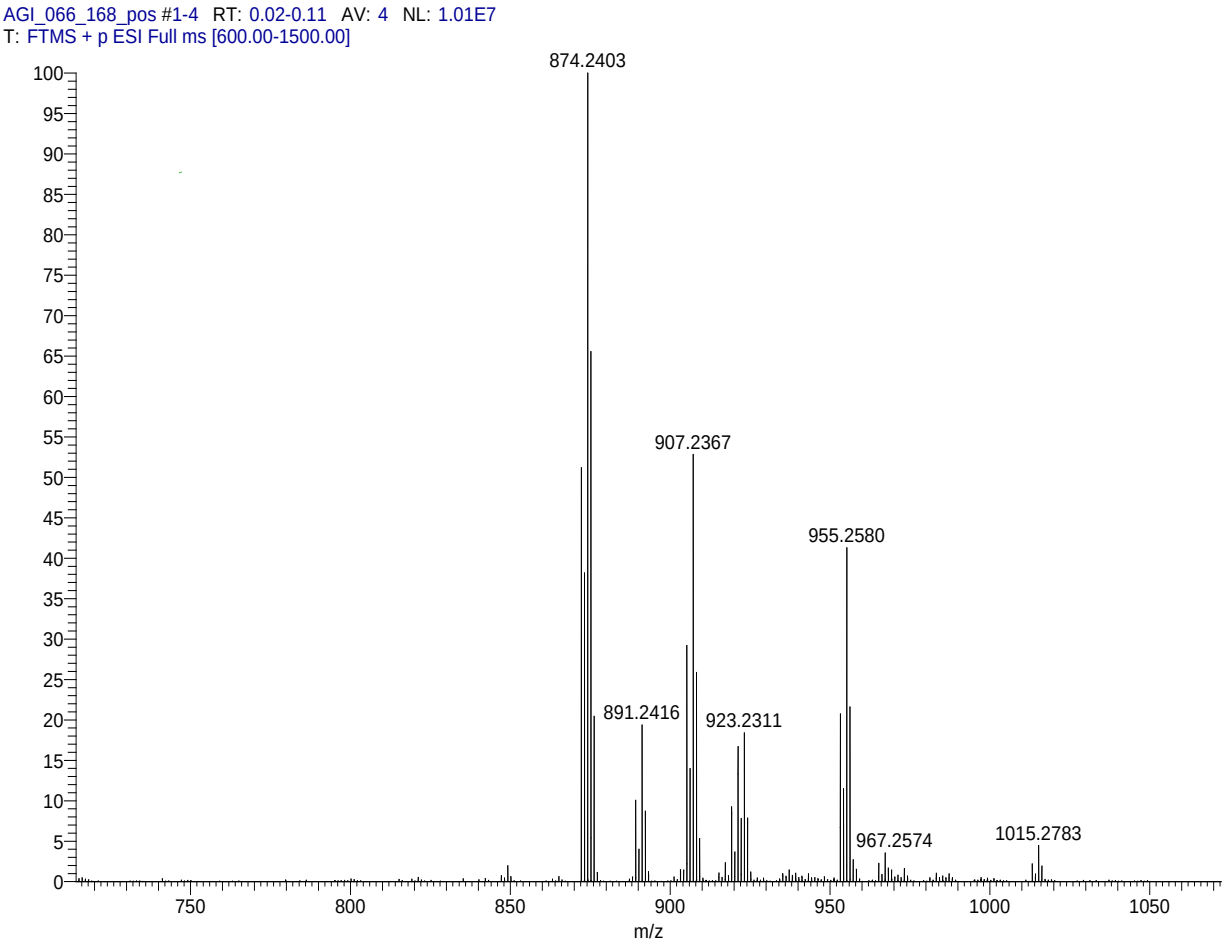

Figure S37. Mass spectrum of Ir[TPC]py_2 (**1b**).

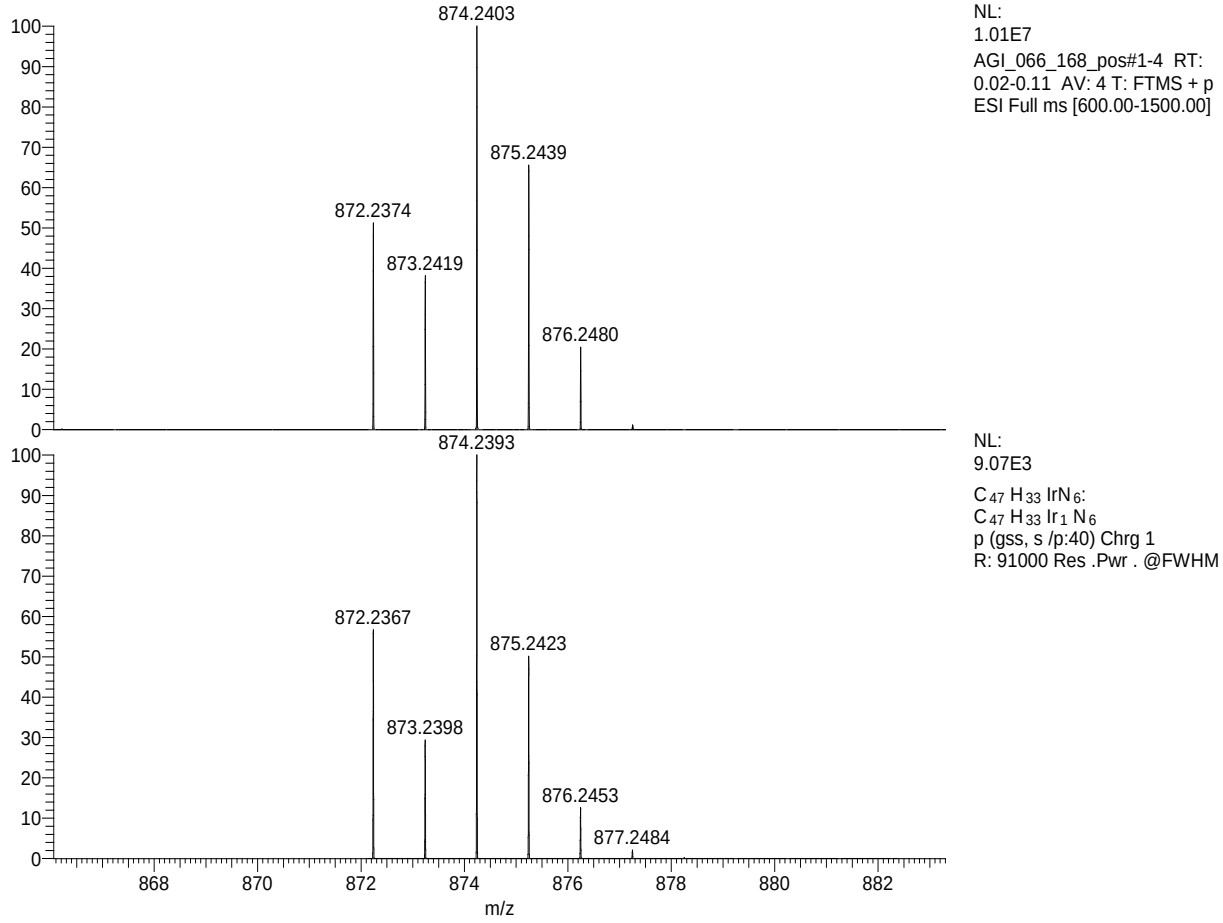

Figure S38. Expanded view of **1b**.

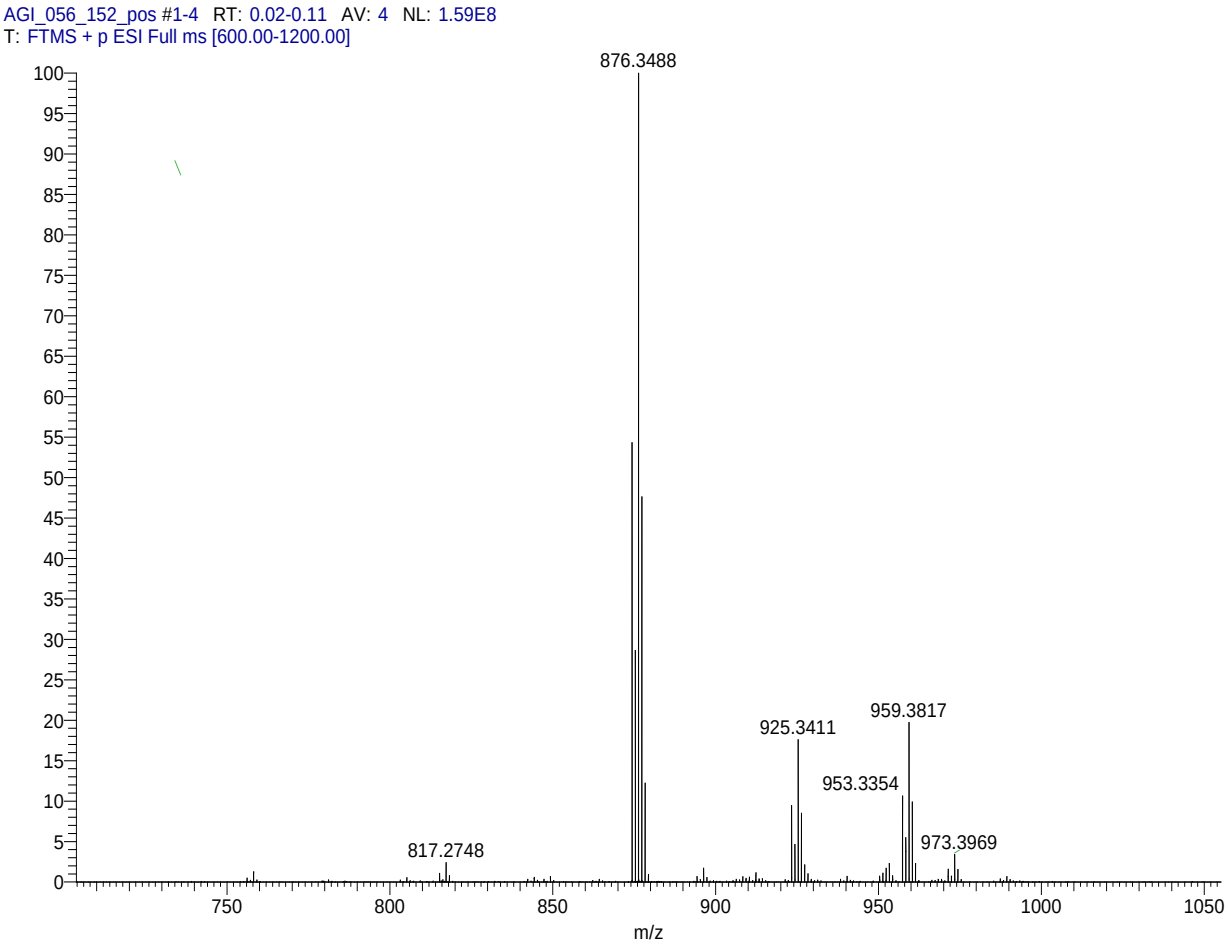

Figure S39. Mass spectrum of Ir[T*p*MePC]tma$_2$ (**2a**).

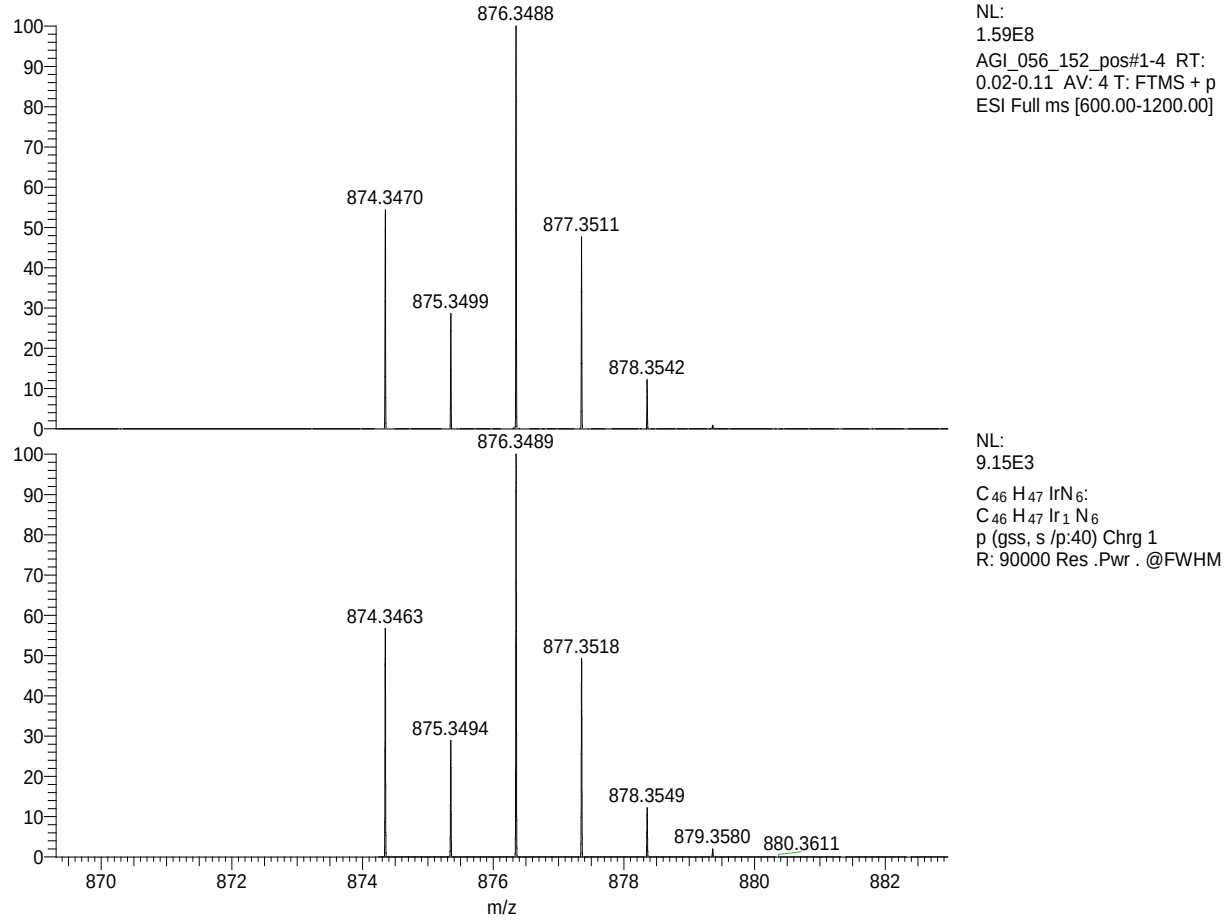

Figure S40. Expanded view of **2a**.

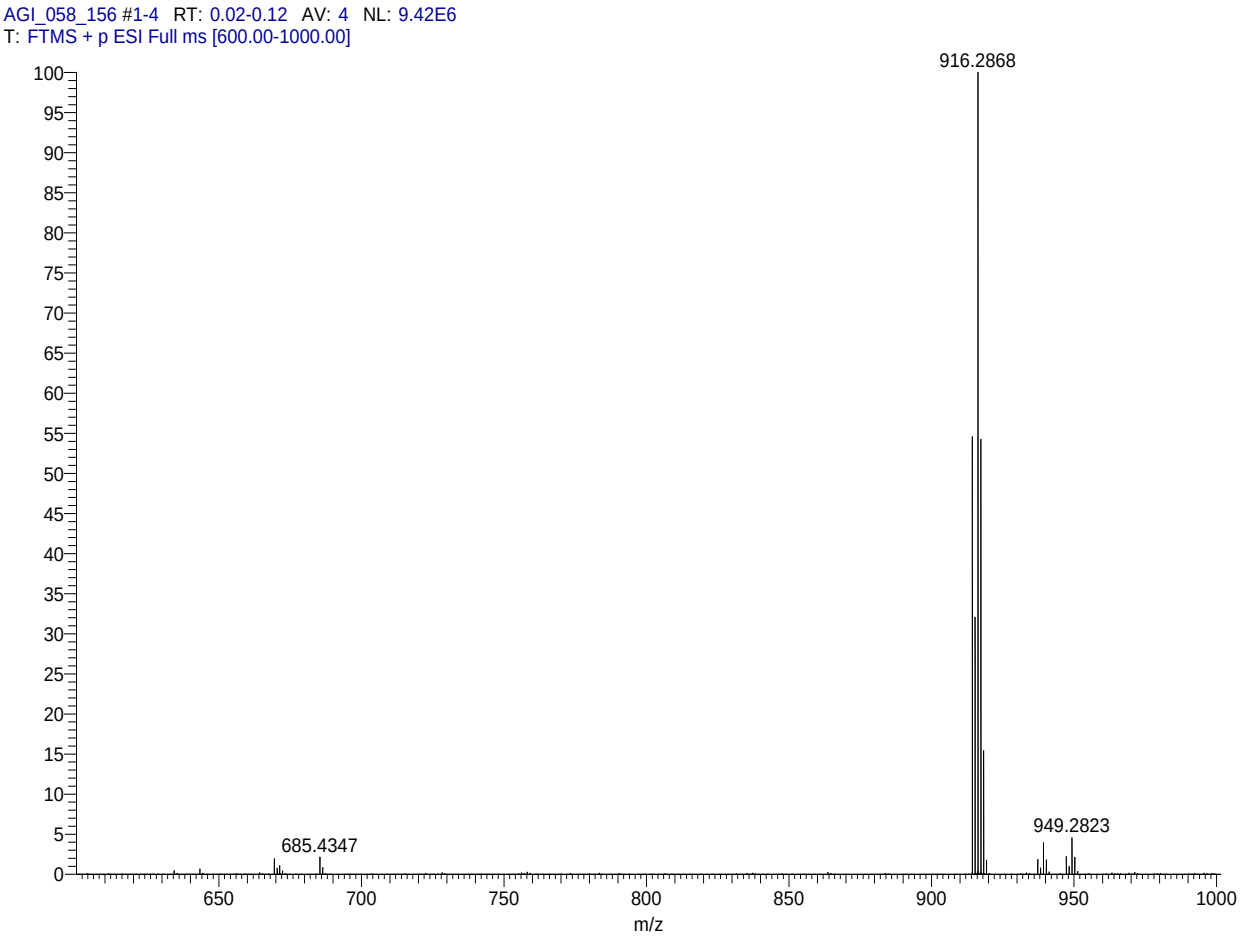

Figure S41. Mass spectrum of Ir[T*p*MePC]py_2 (**2b**).

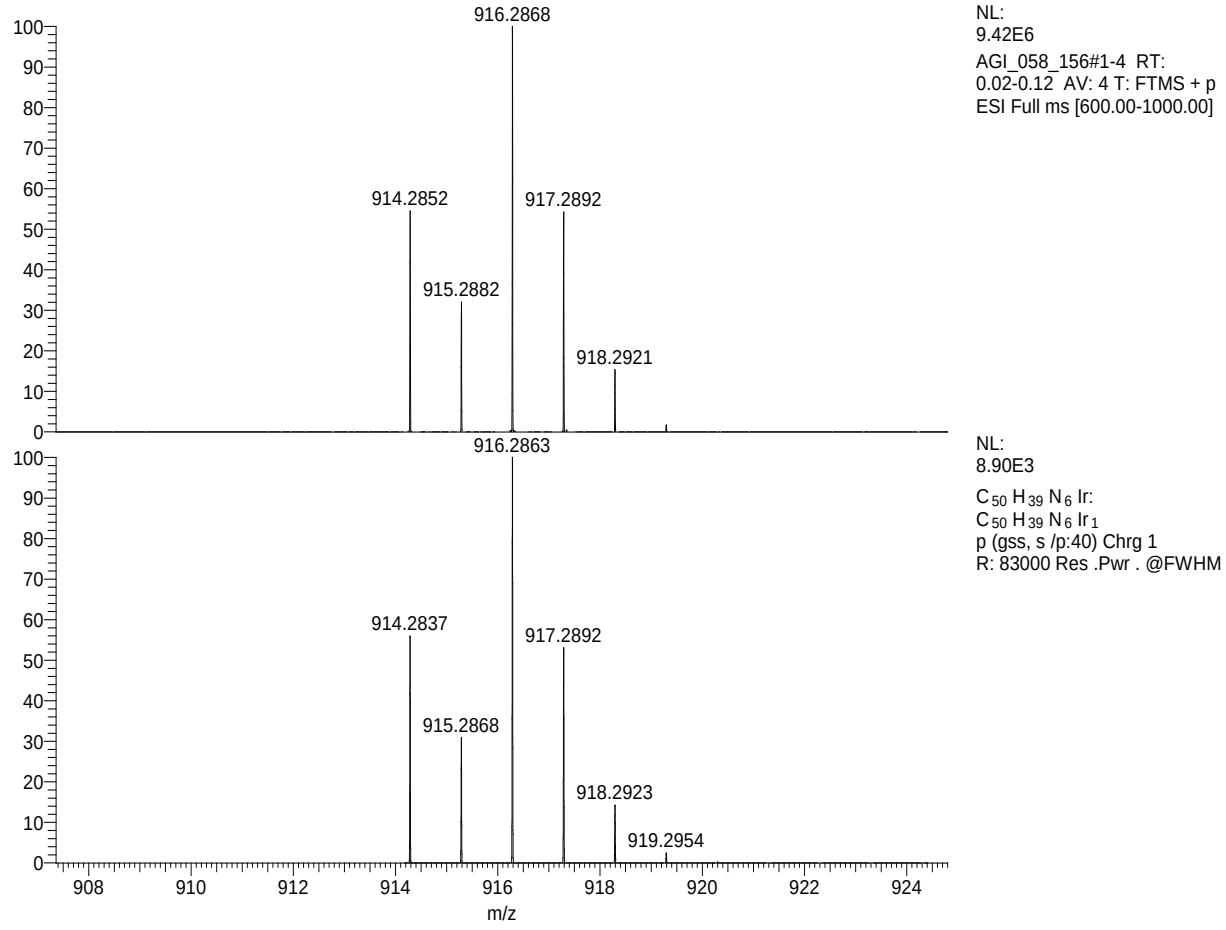

Figure S42. Expanded view of **2b**.

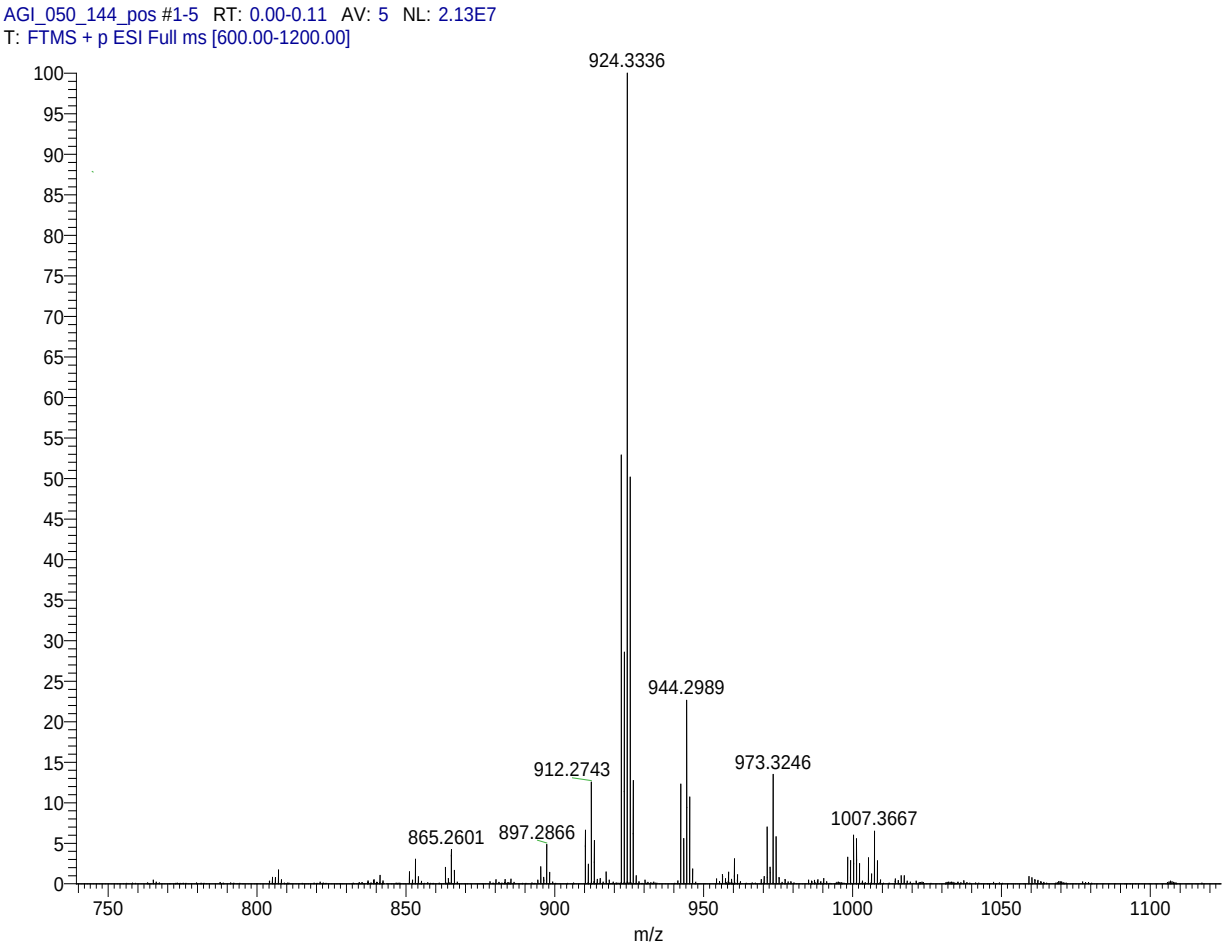

Figure S43. Mass spectrum of Ir[T*p*OMePC]tma$_2$ (**3a**).

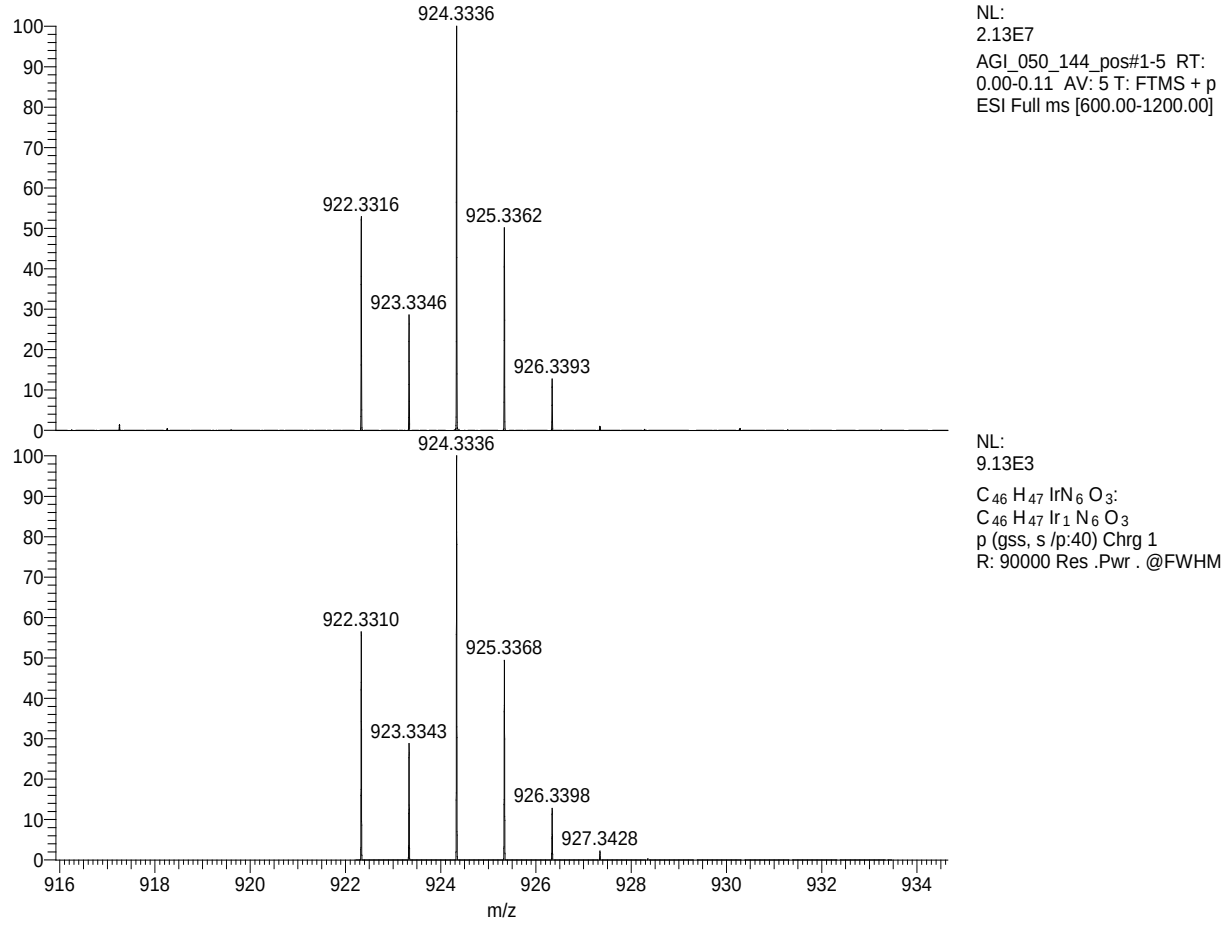

Figure S44. Expanded view of **3a**.

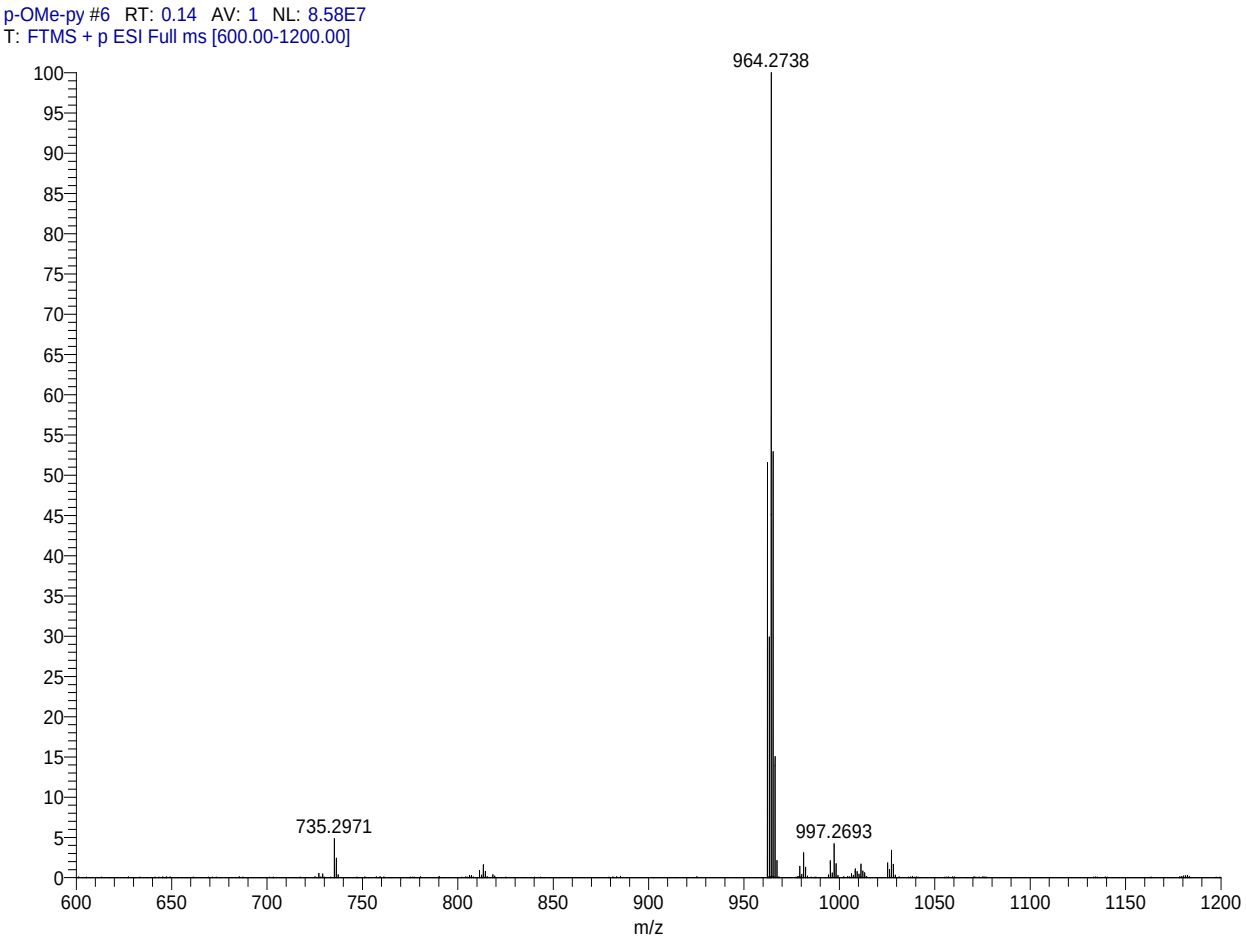

Figure S45. Mass spectrum of Ir[T*p*OMePC]py$_2$ (**3b**).

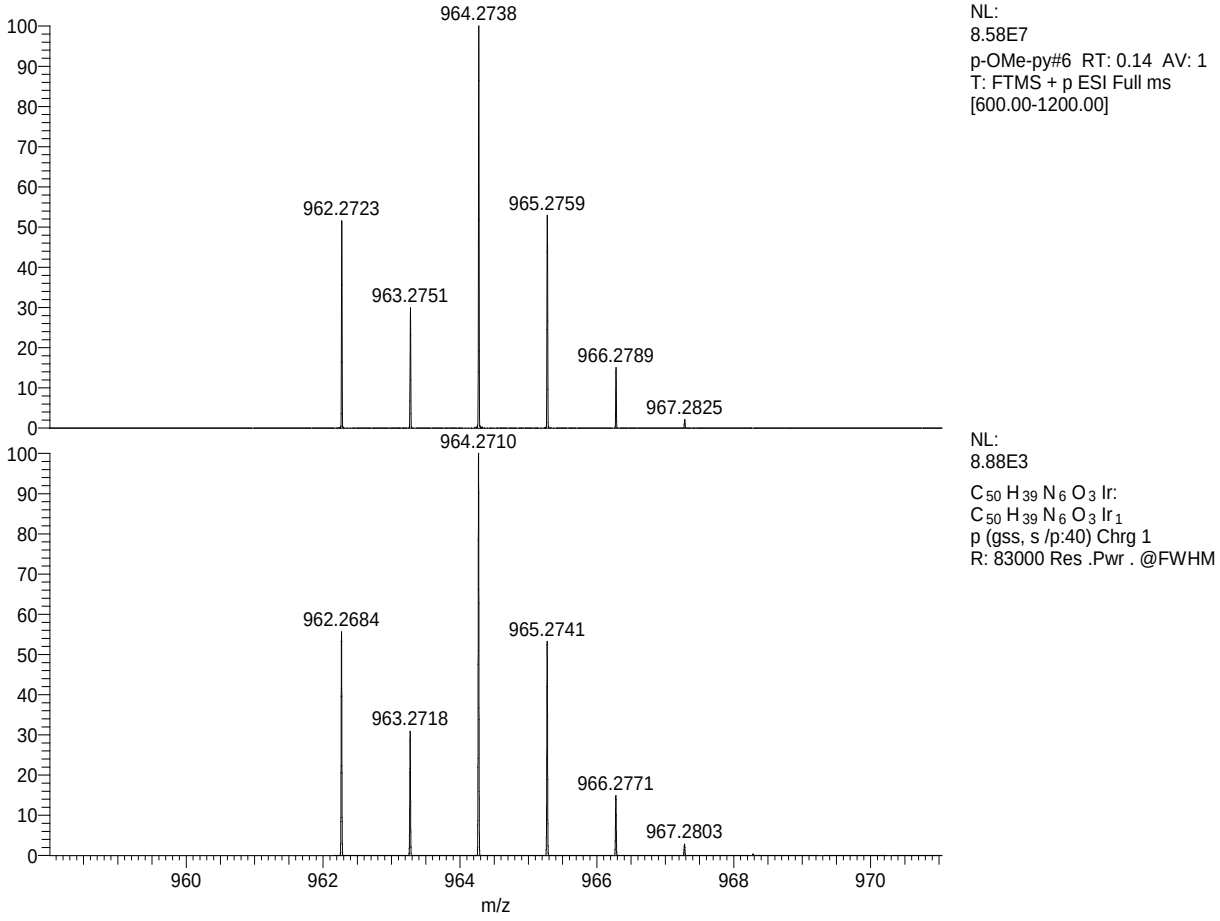

Figure S46. Expanded view of **3b**.

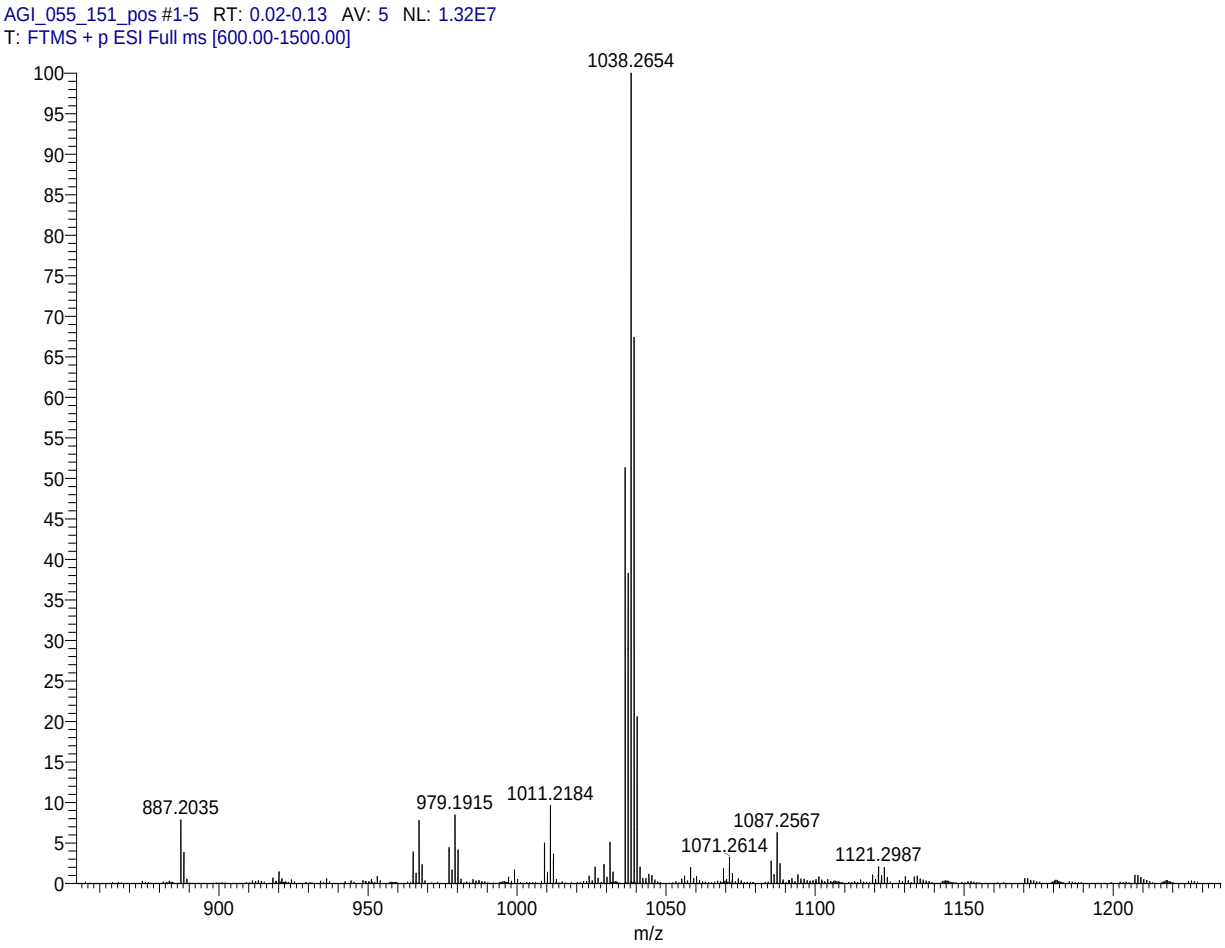

Figure S47. Mass spectrum of Ir[T*p*CF_3PC]tma_2 (**4a**).

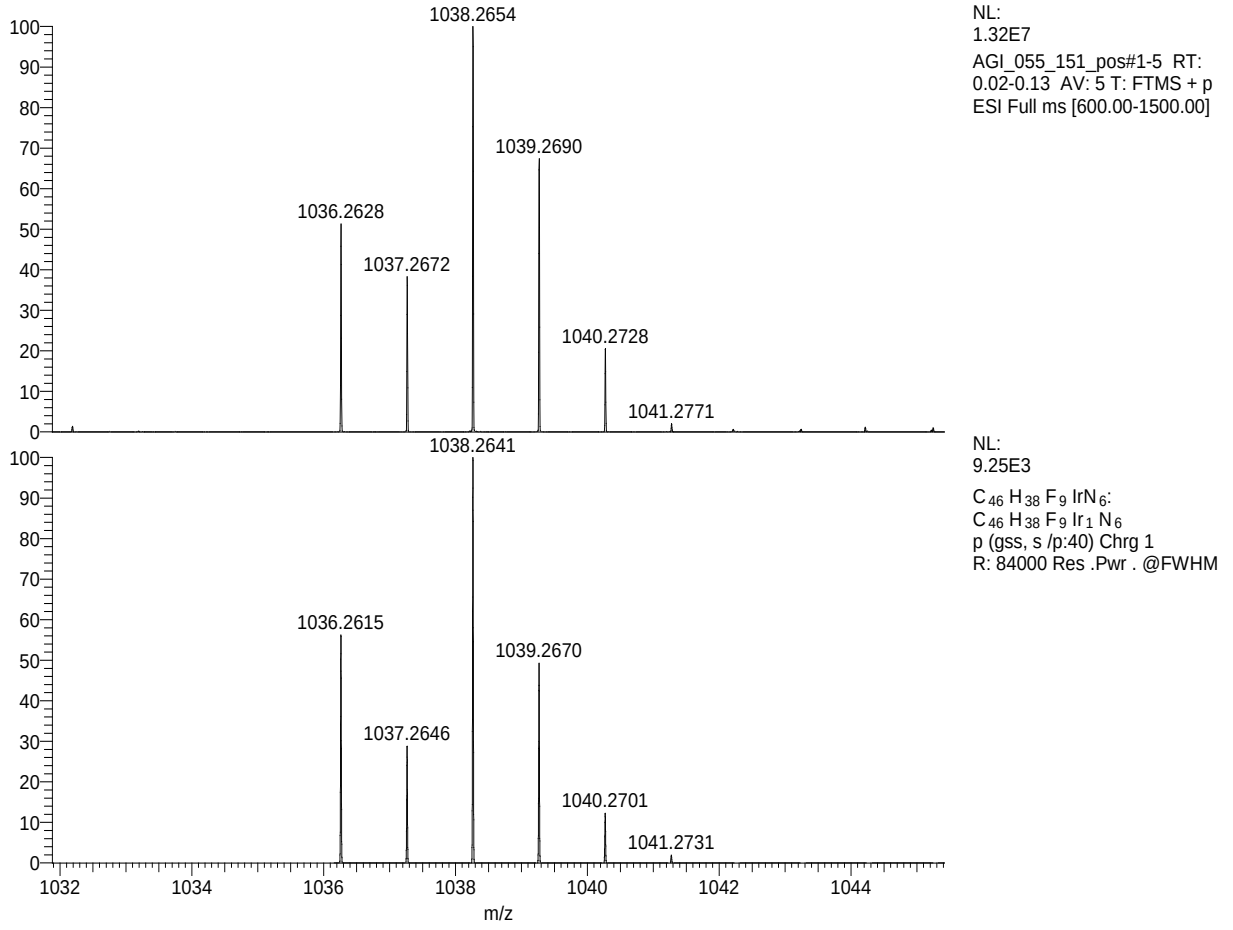

Figure S48. Expanded view of **4a**.

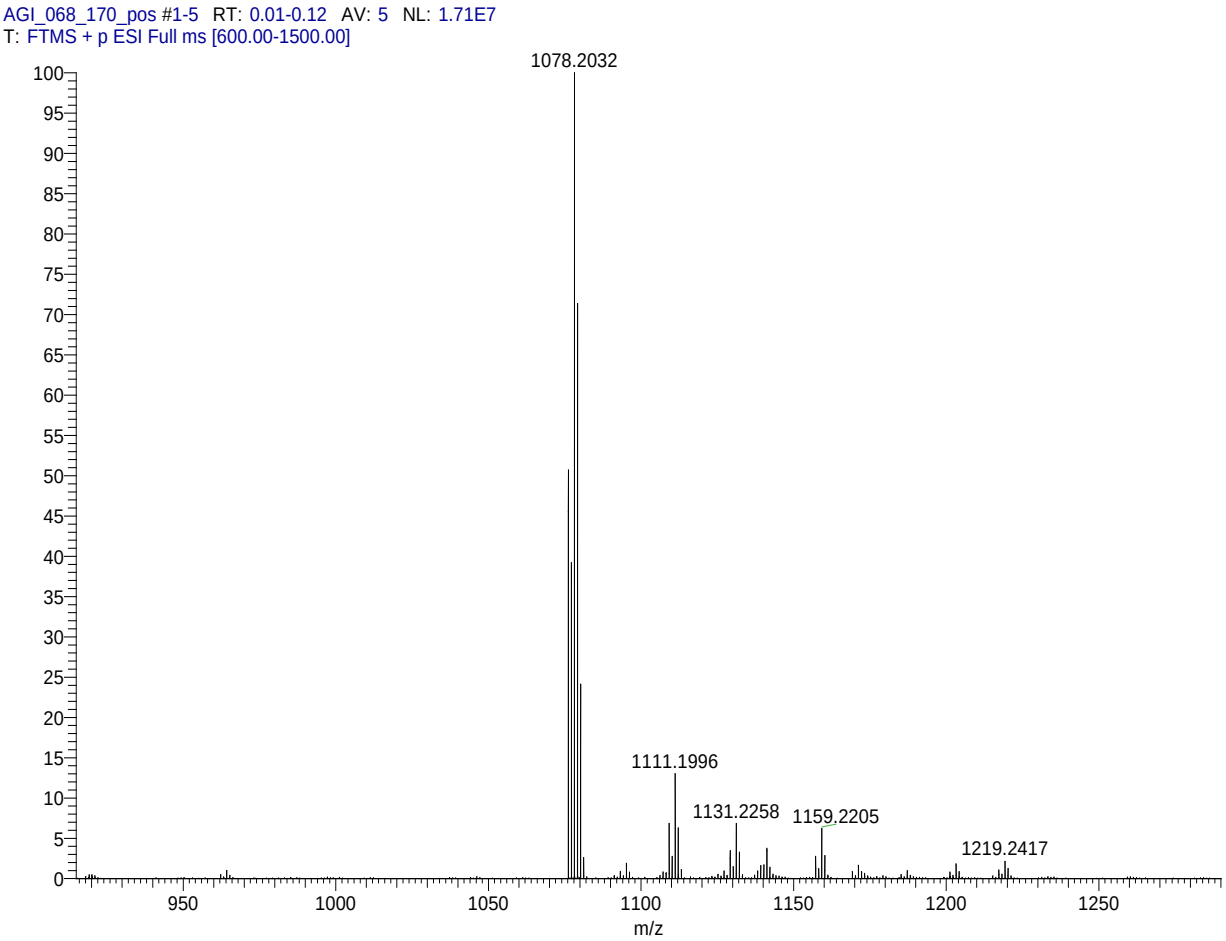

Figure S49. Mass spectrum of Ir[T*p*CF_3PC]py_2 (**4b**).

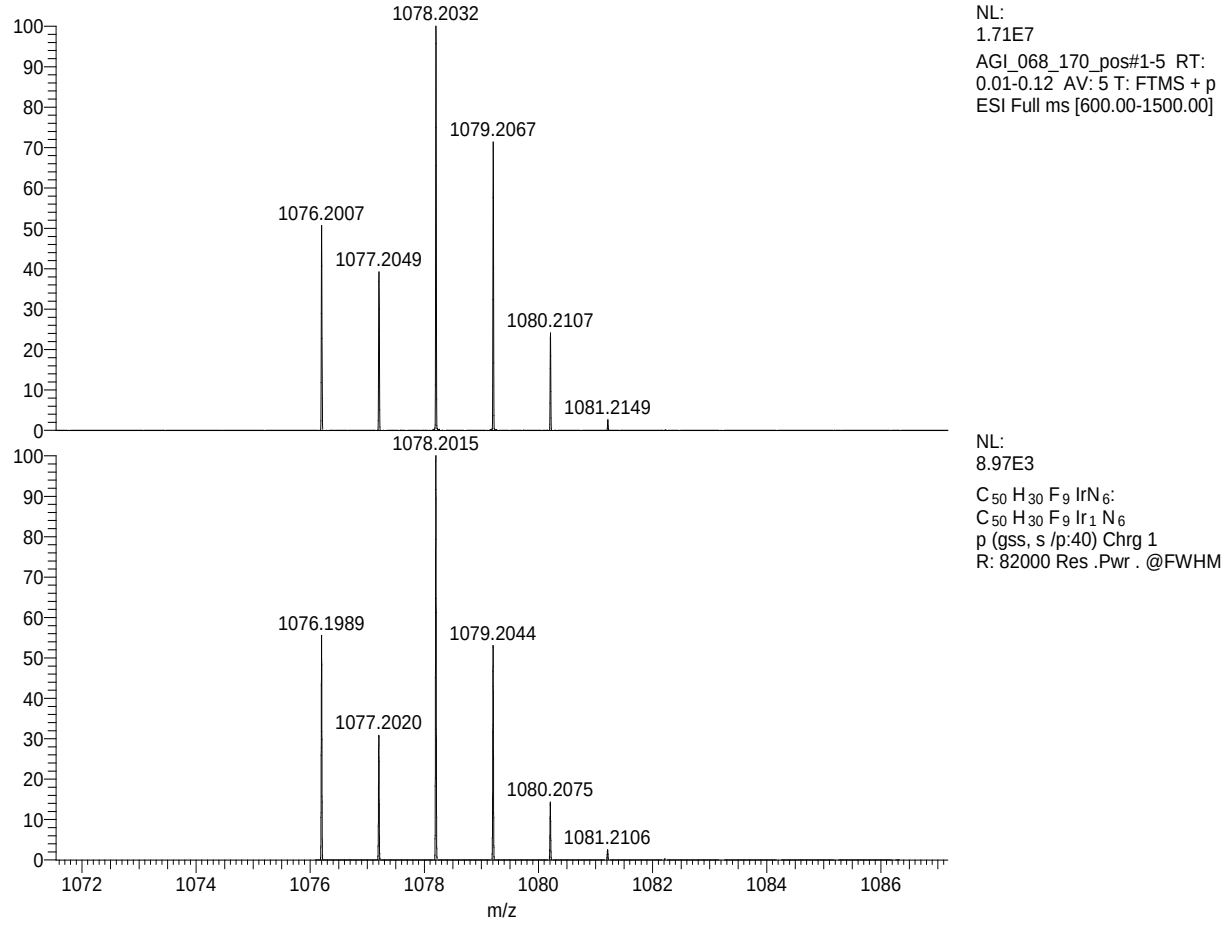

Figure S50. Expanded view of **4b**.

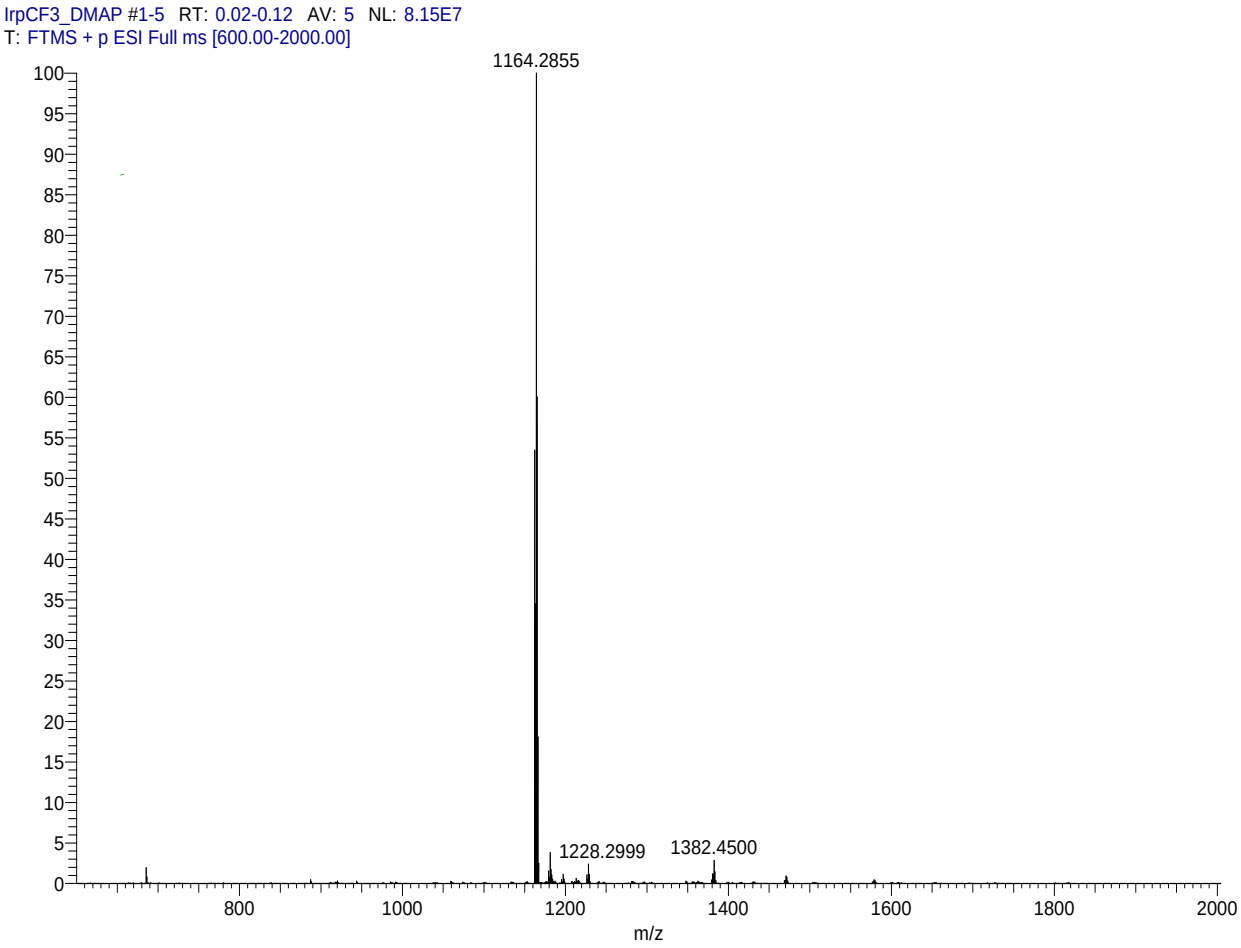

Figure S51. Mass spectrum of Ir[T*p*CF_3PC]$dmap_2$ (**4c**).

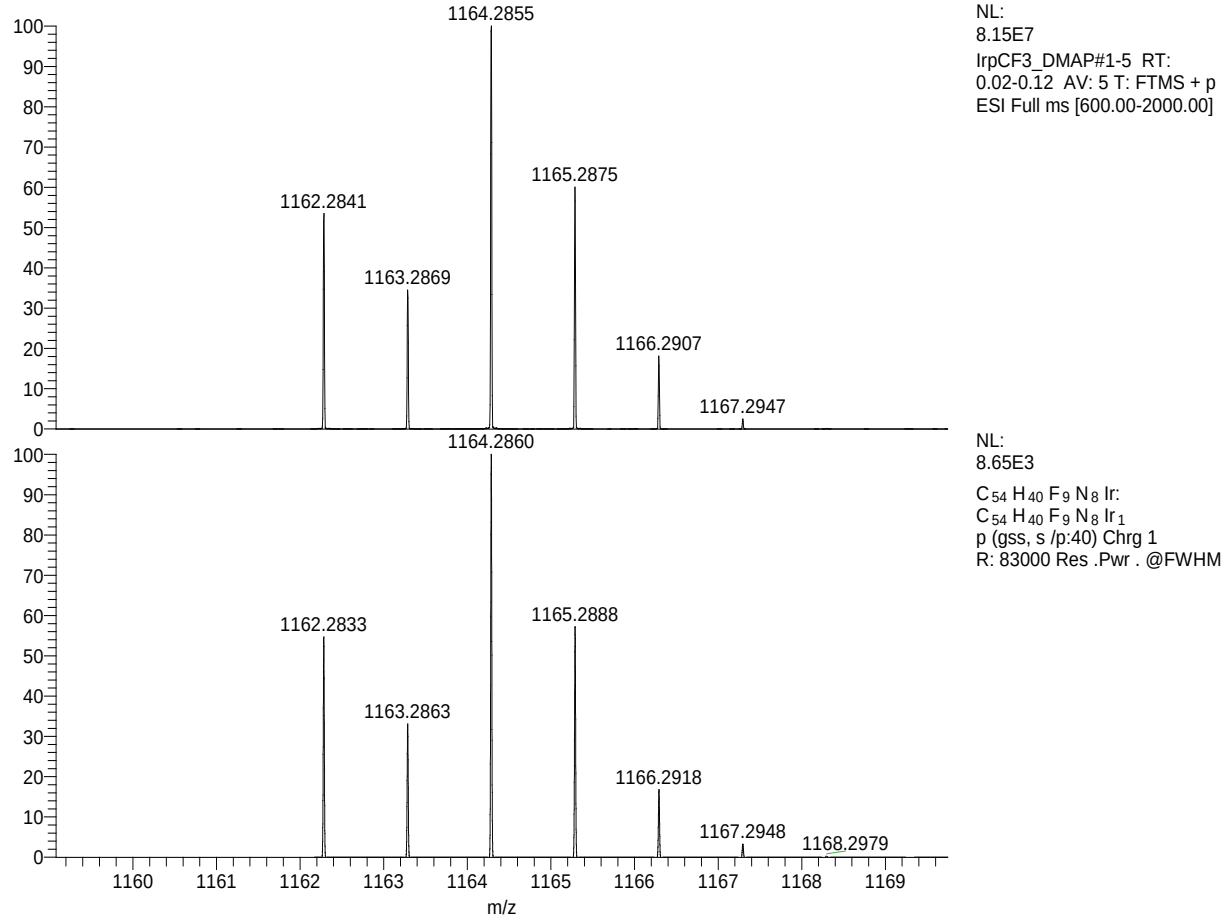

Figure S52. Expanded view of **4c**.

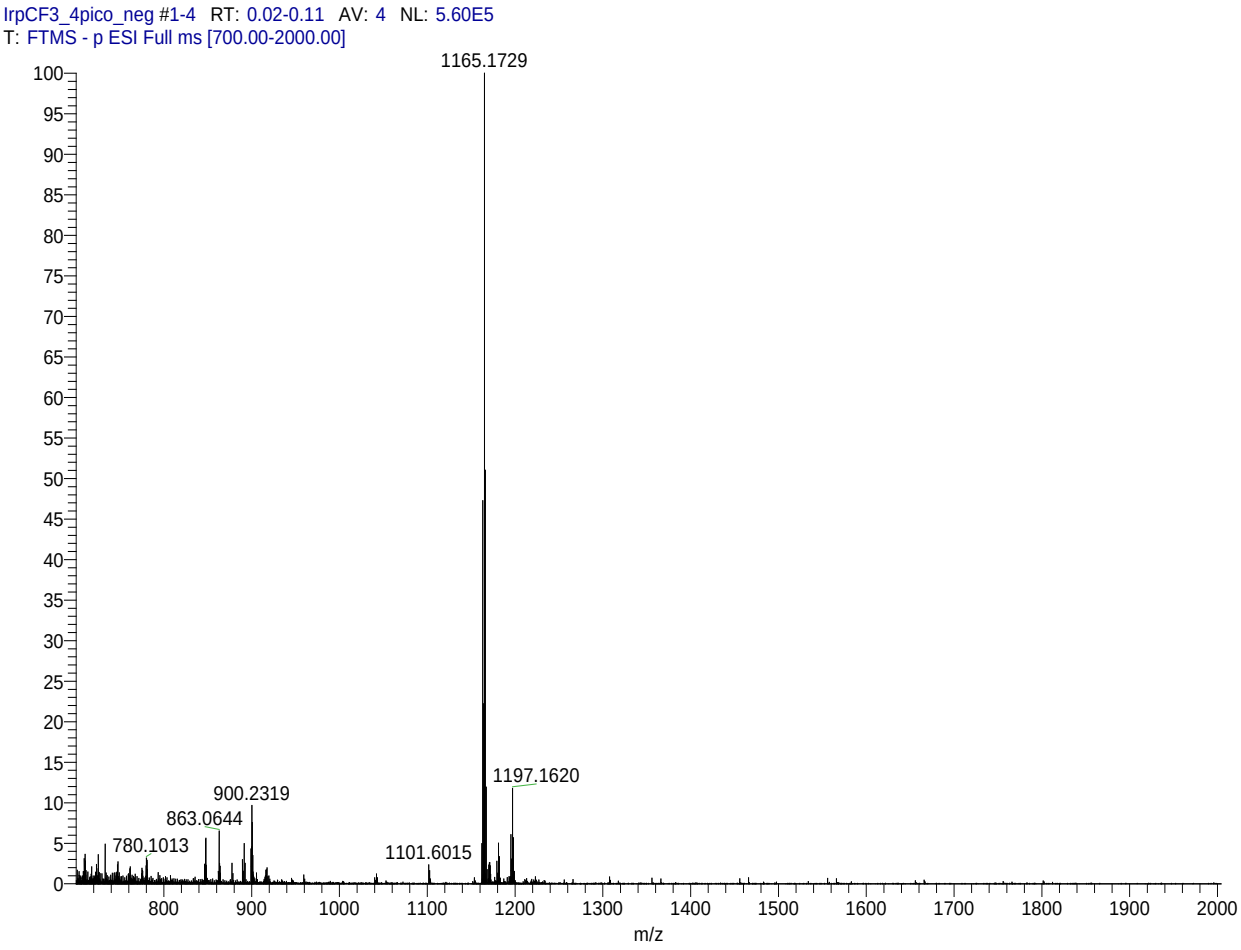

Figure S53. Mass spectrum of Ir[T*p*CF_3PC]4-picolinic $acid_2$ (**4d**).

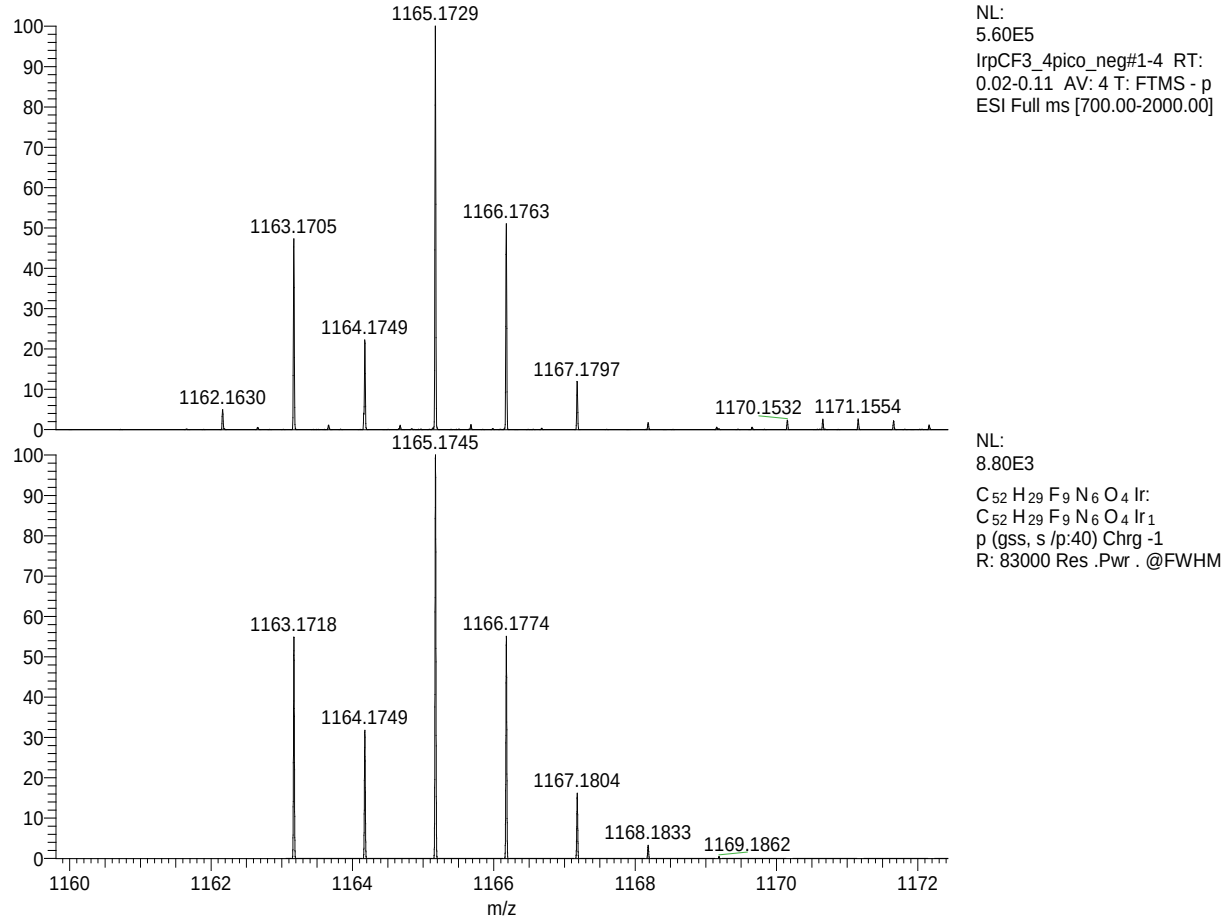

Figure S54. Expanded view of **4d**.

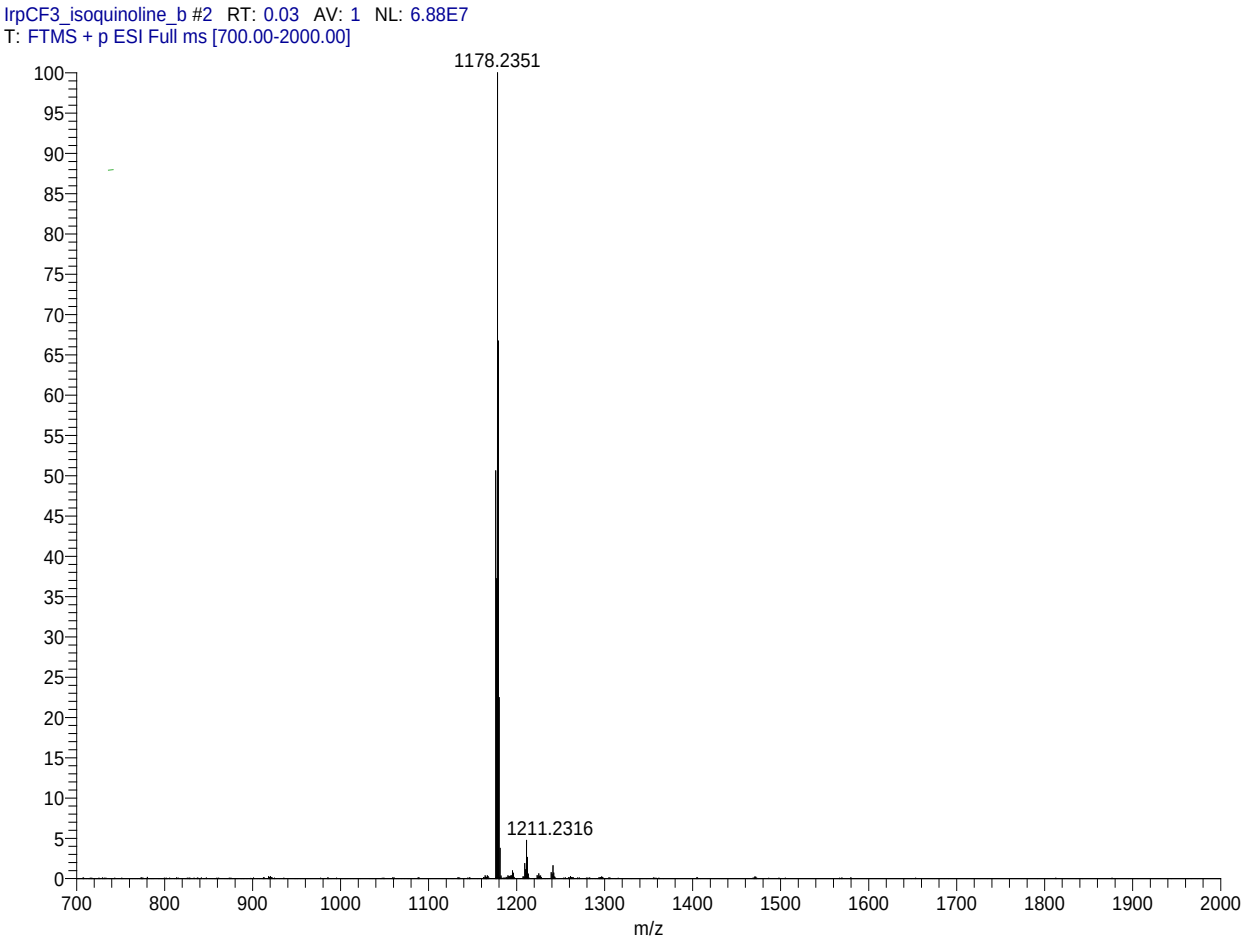

Figure S55. Mass spectrum of Ir[T*p*CF_3PC]isoquinoline$_2$ (**4e**).

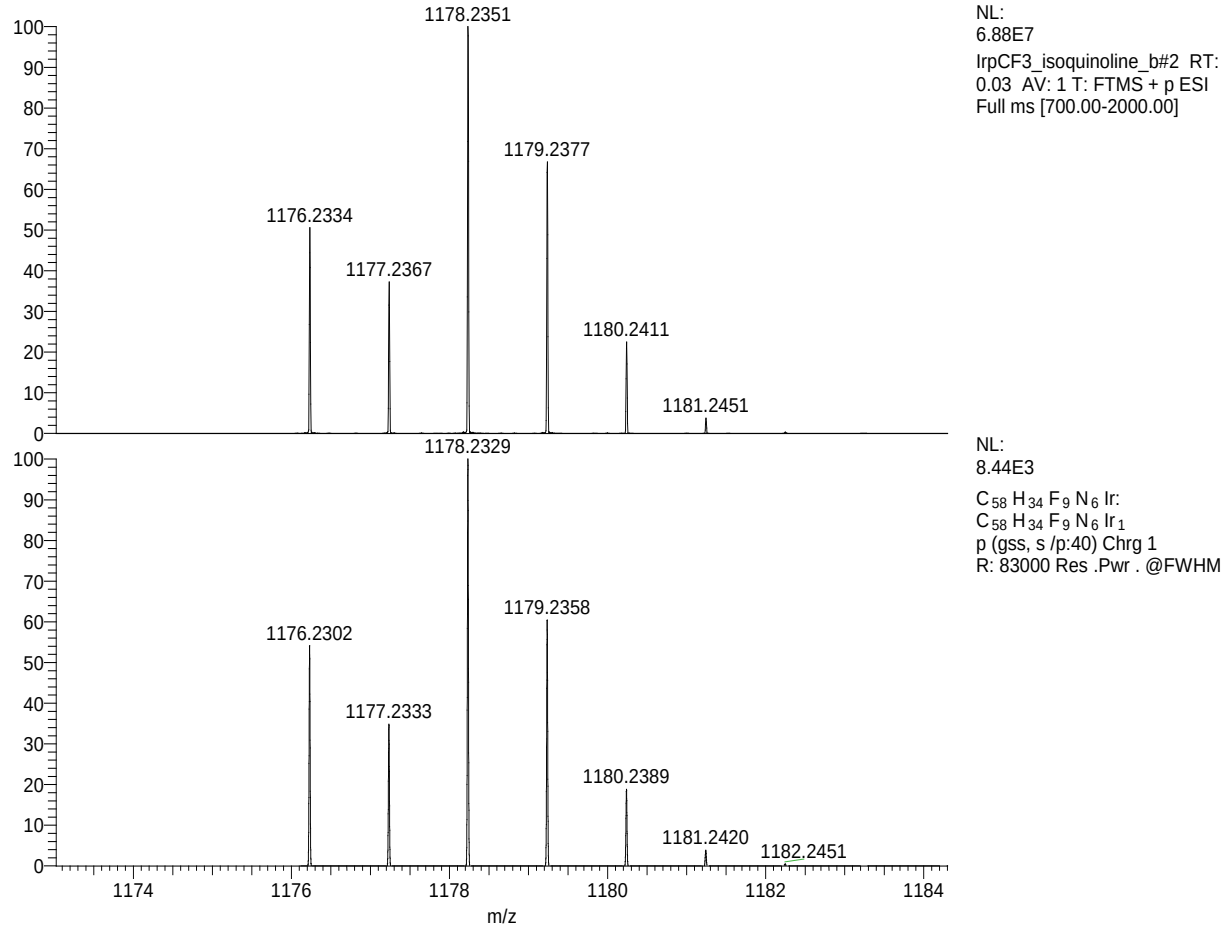

Figure S56. Expanded view of **4e**.

Conclusion

The ease of modulating electronic and photophysical properties of porphyrins and related macrocycles via metal complexation and peripheral substitution is one of their major attractive features, indeed one that has promoted their use in such diverse fields as catalysis, solar cells, photodynamic therapy, gas sensors, supramolecules, and nonlinear optics, among many others. Of particular importance are *β*-octabrominated porphyrins and corroles, since they are excellent precursors for further elaboration through transition-metal-catalyzed cross-coupling reactions such as the Suzuki reaction. The present thesis was inspired by the question whether polyiodinated porphyrin and corrole derivatives might be superior in this respect, reacting faster and affording products that are not obtainable from *β*-octabrominated porphyrins and corroles.

Toward that end, I synthesized the first examples of a *β*-octaiodinated porphyrin and a *β*-octaiodinated corrole, unique sterically encumbered molecules (characterized via 4 single-crystal X-ray structure determinations) with remarkable spectroscopic properties.

As promising electron-rich substrates for electrophilic polyiodination, I also synthesized a series of six-coordinated Ir(III) corroles with a variety of nitrogen axial ligands, three of which were structurally characterized. Unfortunately, although the complexes indeed proved reactive, I could not isolate discrete Ir(III) polyiodocorroles as pure compounds. The iodine-free Ir(III) complexes were evaluated for their near-IR phosphorescence. Here too, the performance proved rather modest.

Toward the end of the allotted time for my degree, I obtained a single-crystal X-ray structure of a free-base *β*-octaiodo-*meso*-tetraarylporphyrin. Remarkably, the structure proved to be a *cis* porphyrin tautomer – only the second ever to be observed – stabilized as termolecular hydrogen-bonded complex with a pair of water/methanol solvent molecules. This discovery potentially opens the door for the synthesis and detailed spectroscopic studies of additional *cis* porphyrin tautomers.

Throughout my tenure as a PhD student, I was accorded full freedom to follow my nose and steer the project according to my own interests. Thus, although the original question as to whether polyiodinated porphyrins and corroles are superior synthons remains unanswered, I was able to structurally characterize several unique, fragile, and delicate molecules of great theoretical interest, which in my view, are no less of an intellectual achievement.

References

(1) Hamza, I.; Dailey, H. A. One ring to rule them all: Trafficking of heme and heme synthesis intermediates in the metazoans. *Biochimica et Biophysica Acta (BBA) - Molecular Cell Research* **2012**, *1823*, 1617-1632.

(2) Layer, G.; Reichelt, J.; Jahn, D.; Heinz, D. W. Structure and function of enzymes in heme biosynthesis. *Protein Science* **2010**, *19*, 1137-1161.

(3) Poulos, T. L. Heme Enzyme Structure and Function. *Chemical Reviews* **2014**, *114*, 3919-3962.

(4) Neya, S.; Quan, J.; Hata, M.; Hoshino, T.; Funasaki, N. A novel and efficient synthesis of porphine. *Tetrahedron Letters* **2006**, *47*, 8731-8732.

(5) Fliegl, H.; Sundholm, D. Aromatic Pathways of Porphins, Chlorins, and Bacteriochlorins. *The Journal of Organic Chemistry* **2012**, *77*, 3408-3414.

(6) Gouterman, M.: 1 - Optical Spectra and Electronic Structure of Porphyrins and Related Rings. In *The Porphyrins*; Dolphin, D., Ed.; Academic Press, 1978; pp 1-165.

(7) Sanders, J. K. M.; Bampos, N.; Clyde-Watson, Z.; Darling, S. L.; Hawley, J. C.; Kim, H.-J.; Mak, C. C.; Webb, S. J.: 15 - Axial Coordination Chemistry of Metalloporphyrins. In *The Porphyrin Handbook*; Kadish, K. M., Smith, K. M., Guilard, R. E., Eds.; Academic Press: San Diego, 2000; Vol. 3; pp 1.

(8) Furuta, H.; Asano, T.; Ogawa, T. "*N*-Confused Porphyrin": A New Isomer of Tetraphenylporphyrin. *Journal of the American Chemical Society* **1994**, *116*, 767-768.

(9) Chatterjee, T.; Shetti, V. S.; Sharma, R.; Ravikanth, M. Heteroatom-Containing Porphyrin Analogues. *Chemical Reviews* **2017**, *117*, 3254-3328.

(10) Chen, F.; Tanaka, T.; Hong, Y.; Kim, W.; Kim, D.; Osuka, A. *ortho*-Phenylene-Bridged Cyclic Oligopyrroles: Conformational Flexibilities and Optical Properties. *Chemistry – A European Journal* **2016**, *22*, 10597-10606.

(11) Bergonia, H. A.; Phillips, J. D.; Kushner, J. P. Reduction of porphyrins to porphyrinogens with palladium on carbon. *Analytical biochemistry* **2009**, *384*, 74-78.

(12) Hill, J. P.; Ariga, K.; Schumacher, A. L.; Karr, P. A.; D'Souza, F. Pyren-1-ylmethyl *N*-substituted oxoporphyrinogens. *Journal of Porphyrins and Phthalocyanines* **2007**, *11*, 390-396.

(13) Saito, S.; Osuka, A. Expanded Porphyrins: Intriguing Structures, Electronic Properties, and Reactivities. *Angewandte Chemie International Edition* **2011**, *50*, 4342-4373.

(14) Mack, J. Expanded, Contracted, and Isomeric Porphyrins: Theoretical Aspects. *Chemical Reviews* **2017**, *117*, 3444-3478.

(15) Bröring, M.; Köhler, S.; Kleeberg, C. Norcorrole: Observation of the Smallest Porphyrin Variant with a N_4 Core. *Angewandte Chemie International Edition* **2008**, *47*, 5658-5660.

(16) Shimizu, S. Recent Advances in Subporphyrins and Triphyrin Analogues: Contracted Porphyrins Comprising Three Pyrrole Rings. *Chemical Reviews* **2017**, *117*, 2730-2784.

(17) Ghosh, A.; Steene, E. High-valent transition metal centers and noninnocent ligands in metalloporphyrins and related molecules: a broad overview based on quantum chemical calculations. *JBIC Journal of Biological Inorganic Chemistry* **2001**, *6*, 739-752.

(18) Ghosh, A. Electronic Structure of Corrole Derivatives: Insights from Molecular Structures, Spectroscopy, Electrochemistry, and Quantum Chemical Calculations. *Chemical Reviews* **2017**, *117*, 3798-3881.

(19) Aviv, I.; Gross, Z. Corrole-based applications. *Chemical Communications* **2007**, 1987-1999.

(20) Zucca, P.; Rescigno, A.; Rinaldi, A. C.; Sanjust, E. Biomimetic metalloporphines and metalloporphyrins as potential tools for delignification: Molecular mechanisms and application perspectives. *Journal of Molecular Catalysis A: Chemical* **2014**, *388-389*, 2-34.

(21) Castillero, P.; Roales, J.; Lopes-Costa, T.; Sánchez-Valencia, J. R.; Barranco, A.; González-Elipe, A. R.; Pedrosa, J. M. Optical Gas Sensing of Ammonia and Amines Based on Protonated Porphyrin/TiO(2) Composite Thin Films. *Sensors (Basel, Switzerland)* **2017**, *17*, 24.

(22) Birel, Ö.; Nadeem, S.; Duman, H. Porphyrin-Based Dye-Sensitized Solar Cells (DSSCs): a Review. *Journal of Fluorescence* **2017**, *27*, 1075-1085.

(23) Singh, S.; Aggarwal, A.; Bhupathiraju, N. V. S. D. K.; Arianna, G.; Tiwari, K.; Drain, C. M. Glycosylated Porphyrins, Phthalocyanines, and Other Porphyrinoids for Diagnostics and Therapeutics. *Chemical Reviews* **2015**, *115*, 10261-10306.

(24) Sinha, W.; Sommer, M. G.; Deibel, N.; Ehret, F.; Sarkar, B.; Kar, S. Silver corrole complexes: unusual oxidation states and near-IR-absorbing dyes. *Chemistry (Weinheim an der Bergstrasse, Germany)* **2014**, *20*, 15920-15932.

(25) Mori, H.; Tanaka, T.; Osuka, A. Fused porphyrinoids as promising near-infrared absorbing dyes. *Journal of Materials Chemistry C* **2013**, *1*, 2500-2519.

(26) Keinan, S.; Therien, M. J.; Beratan, D. N.; Yang, W. Molecular Design of Porphyrin-Based Nonlinear Optical Materials. *The Journal of Physical Chemistry A* **2008**, *112*, 12203-12207.

(27) Beletskaya, I.; Tyurin, V. S.; Tsivadze, A. Y.; Guilard, R.; Stern, C. Supramolecular Chemistry of Metalloporphyrins. *Chemical Reviews* **2009**, *109*, 1659-1713.

(28) Orłowski, R.; Tasior, M.; Staszewska-Krajewska, O.; Dobrzycki, Ł.; Schilf, W.; Ventura, B.; Cyrański Michał, K.; Gryko Daniel, T. Hydrogen Bonds Involving Cavity NH Protons Drives Supramolecular Oligomerization of Amido-Corroles. *Chemistry – A European Journal* **2017**, *23*, 10195-10204.

(29) A. Shelnutt, J.; Song, X.-Z.; Ma, J.-G.; Jia, S.-L.; Jentzen, W.; J. Medforth, C.; J. Medforth, C. Nonplanar porphyrins and their significance in proteins. *Chemical Society Reviews* **1998**, *27*, 31-42.

(30) Conradie, J.; Ghosh, A. Energetics of Saddling versus Ruffling in Metalloporphyrins: Unusual Ruffled Dodecasubstituted Porphyrins. *ACS Omega* **2017**, *2*, 6708-6714.

(31) Guilard, R.; Perié, K.; Barbe, J.-M.; Nurco, D. J.; Smith, K. M.; Van Caemelbecke, E.; Kadish, K. M. Electrochemical and Spectroscopic Characterization of Manganese(III) Dodecaphenylporphyrin Derivatives and X-ray Structural Determination of Chloro(5,10,15,20-tetrakis(pentafluorophenyl)-2,3,7,8,12,13,17,18-octaphenylporphyrinato)-manganese(III). Formation of a Manganese(IV) Species by Ozone and Electrochemical Oxidation. *Inorganic Chemistry* **1998**, *37*, 973-981.

(32) Jentzen, W.; Ma, J.-G.; Shelnutt, J. A. Conservation of the Conformation of the Porphyrin Macrocycle in Hemoproteins. *Biophysical Journal* **1998**, *74*, 753-763.

(33) Senge, M. O. Prevention of out-of-plane macrocycle distortion by thallium in the sterically strained 2,3,7,8,12,13,17,18-octaethyl-5,10,15,20-tetranitroporphyrin. *Journal of the Chemical Society, Dalton Transactions* **1993**, 3539-3549.

(34) Barkigia, K. M.; Fajer, J.; Adler, A. D.; Williams, G. J. B. Crystal and molecular structure of (5,10,15,20-tetra-*N*-propylporphinato)lead(II): a "roof" porphyrin. *Inorganic Chemistry* **1980**, *19*, 2057-2061.

(35) Le Gac, S.; Fusaro, L.; Dorcet, V.; Boitrel, B. Formation and Dynamic Behavior of Mono- and Bimetallic Cadmium(II) Porphyrin Complexes: Allosteric Control of Coupled Intraligand Metal Migrations. *Chemistry - A European Journal* **2013**, *19*, 13376-13386.

(36) Halime, Z.; Michaudet, L.; Razavet, M.; Ruzie, C.; Boitrel, B. Synthesis, characterisation and properties of bismuth(iii) ester pendant arm picket porphyrins. *Dalton Transactions* **2003**, 4250-4254.

(37) Boyle, N. M.; Rochford, J.; Pryce, M. T. Thienyl—Appended porphyrins: Synthesis, photophysical and electrochemical properties, and their applications. *Coordination Chemistry Reviews* **2010**, *254*, 77-102.

(38) Nurco, D. J.; Medforth, C. J.; Forsyth, T. P.; Olmstead, M. M.; Smith, K. M. Conformational Flexibility in Dodecasubstituted Porphyrins. *Journal of the American Chemical Society* **1996**, *118*, 10918-10919.

(39) Li, X. Y.; Czernuszewicz, R. S.; Kincaid, J. R.; Spiro, T. G. Consistent porphyrin force field. 3. Out-of-plane modes in the resonance Raman spectra of planar and ruffled nickel octaethylporphyrin. *Journal of the American Chemical Society* **1989**, *111*, 7012-7023.

(40) Akiba, K.-y.; Nadano, R.; Satoh, W.; Yamamoto, Y.; Nagase, S.; Ou, Z.; Tan, X.; Kadish, K. M. Synthesis, Structure, Electrochemistry, and Spectroelectrochemistry of Hypervalent Phosphorus(V) Octaethylporphyrins and Theoretical Analysis of the Nature of the PO Bond in P(OEP)(CH2CH3)(O). *Inorganic Chemistry* **2001**, *40*, 5553-5567.

(41) Tozuka, A.; Ohgo, Y.; Ikezaki, A.; Taniguchi, M.; Nakamura, M. Electronic Structure of Highly Ruffled Low-Spin Iron(III) Porphyrinates with Electron Withdrawing Heptafluoropropyl Groups at the meso Positions. *Inorganic Chemistry* **2010**, *49*, 10400-10408.

(42) Senge, M. O.; Ema, T.; Smith, K. M. Crystal structure of a remarkably ruffled nonplanar porphyrin (pyridine)[5,10,15,20-tetra(tert-butyl)porphyrinato]zinc(II). *Journal of the Chemical Society, Chemical Communications* **1995**, 733-734.

(43) Ema, T.; Senge, M. O.; Nelson, N. Y.; Ogoshi, H.; Smith, K. M. 5,10,15,20-Tetra-tert-butylporphyrin and Its Remarkable Reactivity in the 5- and 15-Positions. *Angewandte Chemie International Edition in English* **1994**, *33*, 1879-1881.

(44) SENGE, M. O.; BISCHOFF, I.; NELSON, N. Y.; SMITH, K. M. Synthesis, Reactivity and Structural Chemistry of 5,10,15,20-Tetraalkylporphyrins. *Journal of Porphyrins and Phthalocyanines* **1999**, *03*, 99-116.

(45) Bhyrappa, P.; Purushothaman, B.; Vittal, J. J. Highly brominated porphyrins: synthesis, structure and their properties. *Journal of Porphyrins and Phthalocyanines* **2003**, *07*, 682-692.

(46) Hoshino, A.; Ohgo, Y.; Nakamura, M. Synthesis and inversion barriers of undeca- and dodeca-substituted saddle shaped porphyrin complexes. *Tetrahedron Letters* **2005**, *46*, 4961-4964.

(47) Palmer, J. H.; Day, M. W.; Wilson, A. D.; Henling, L. M.; Gross, Z.; Gray, H. B. Iridium Corroles. *Journal of the American Chemical Society* **2008**, *130*, 7786-7787.

(48) Paolesse, R.; Nardis, S.; Sagone, F.; Khoury, R. G. Synthesis and Functionalization of *meso*-Aryl-Substituted Corroles. *The Journal of Organic Chemistry* **2001**, *66*, 550-556.

(49) Capar, J.; Conradie, J.; Beavers, C. M.; Ghosh, A. Molecular Structures of Free-Base Corroles: Nonplanarity, Chirality, and Enantiomerization. *The Journal of Physical Chemistry A* **2015**, *119*, 3452-3457.

(50) Luobeznova, I.; Raizman, M.; Goldberg, I.; Gross, Z. Synthesis and Full Characterization of Molybdenum and Antimony Corroles and Utilization of the Latter Complexes as Very Efficient Catalysts for Highly Selective Aerobic Oxygenation Reactions. *Inorganic Chemistry* **2006**, *45*, 386-394.

(51) Einrem Rune, F.; Braband, H.; Fox, T.; Vazquez-Lima, H.; Alberto, R.; Ghosh, A. Synthesis and Molecular Structure of ^{99}Tc Corroles. *Chemistry – A European Journal* **2016**, *22*, 18747-18751.

(52) Einrem Rune, F.; Gagnon Kevin, J.; Alemayehu Abraham, B.; Ghosh, A. Metal–Ligand Misfits: Facile Access to Rhenium–Oxo Corroles by Oxidative Metalation. *Chemistry – A European Journal* **2015**, *22*, 517-520.

(53) Alemayehu Abraham, B.; Gagnon Kevin, J.; Terner, J.; Ghosh, A. Oxidative Metalation as a Route to Size-Mismatched Macrocyclic Complexes: Osmium Corroles. *Angewandte Chemie International Edition* **2014**, *53*, 14411-14414.

(54) Alemayehu, A. B.; Vazquez-Lima, H.; Gagnon, K. J.; Ghosh, A. Stepwise Deoxygenation of Nitrite as a Route to Two Families of Ruthenium Corroles: Group 8 Periodic Trends and Relativistic Effects. *Inorganic Chemistry* **2017**, *56*, 5285-5294.

(55) Thomas Kolle, E.; Conradie, J.; Hansen Lars, K.; Ghosh, A. A Metallocorrole with Orthogonal Pyrrole Rings. *European Journal of Inorganic Chemistry* **2011**, *2011*, 1865-1870.

(56) Alemayehu, A. B.; Gonzalez, E.; Hansen, L. K.; Ghosh, A. Copper Corroles Are Inherently Saddled. *Inorganic Chemistry* **2009**, *48*, 7794-7799.

(57) Thomas, K. E.; Vazquez-Lima, H.; Fang, Y.; Song, Y.; Gagnon, K. J.; Beavers, C. M.; Kadish, K. M.; Ghosh, A. Ligand Noninnocence in Coinage Metal Corroles: A Silver Knife-Edge. *Chemistry - A European Journal* **2015**, *21*, 16839-16847.

(58) Chen, W.; El-Khouly, M. E.; Fukuzumi, S. Saddle Distortion of a Sterically Unhindered Porphyrin Ring in a Copper Porphyrin with Electron-Donating Substituents. *Inorganic Chemistry* **2011**, *50*, 671-678.

(59) Brückner, C.; Barta, C. A.; Briñas, R. P.; Krause Bauer, J. A. Synthesis and Structure of [*meso*-Triarylcorrolato]silver(III). *Inorganic Chemistry* **2003**, *42*, 1673-1680.

(60) Nardis, S.; Paolesse, R.; Licoccia, S.; Fronczek, F. R.; Vicente, M. G. H.; Shokhireva, T. K.; Cai, S.; Walker, F. A. NMR and Structural Investigations of A Nonplanar Iron Corrolate: Modified Patterns of Spin Delocalization and Coupling in A Slightly Saddled Chloroiron(III) Corrolate Radical. *Inorganic Chemistry* **2005**, *44*, 7030-7046.

(61) Thomas, K. E.; Conradie, J.; Hansen, L. K.; Ghosh, A. Corroles Cannot Ruffle. *Inorganic Chemistry* **2011**, *50*, 3247-3251.

(62) Pomarico, G.; Tortora, L.; Fronczek, F. R.; Smith, K. M.; Paolesse, R. Selective nitration and bromination of surprisingly ruffled phosphorus corroles. *Journal of Inorganic Biochemistry* **2016**, *158*, 17-23.

(63) Fischer, H.: On haemin and the relationship between haemin and chlorophyll. Nobel Lecture 1930. In *Nobel Lectures, chemistry 1922-1941*; Elsevier: Amsterdam, 1966.

(64) Ste˛pień, M.; Latos-Graz.yński, L.: Aromaticity and Tautomerism in Porphyrins and Porphyrinoids. Springer Berlin Heidelberg: Berlin, Heidelberg; pp 1-71.

(65) Maity, D. K.; Bell, R. L.; Truong, T. N. Mechanism and Quantum Mechanical Tunneling Effects on Inner Hydrogen Atom Transfer in Free Base Porphyrin: A Direct ab Initio Dynamics Study. *Journal of the American Chemical Society* **2000**, *122*, 897-906.

(66) Furuta, H.; Ishizuka, T.; Osuka, A.; Dejima, H.; Nakagawa, H.; Ishikawa, Y. NH Tautomerism of *N*-Confused Porphyrin. *Journal of the American Chemical Society* **2001**, *123*, 6207-6208.

(67) Beenken, W.; Presselt, M.; Ngo, T. H.; Dehaen, W.; Maes, W.; Kruk, M. Molecular Structures and Absorption Spectra Assignment of Corrole NH Tautomers. *The Journal of Physical Chemistry A* **2014**, *118*, 862-871.

(68) Namuangruk, S.; Sirithip, K.; Rattanatwan, R.; Keawin, T.; Kungwan, N.; Sudyodsuk, T.; Promarak, V.; Surakhot, Y.; Jungsuttiwong, S. Theoretical investigation of the charge-transfer properties in different *meso*-linked zinc porphyrins for highly efficient dye-sensitized solar cells. *Dalton Transactions* **2014**, *43*, 9166-9176.

(69) Hush, N. S.; Dyke, J. M.; Williams, M. L.; Woolsey, I. S. Electronic spectra of metal corrole anions. *Journal of the Chemical Society, Dalton Transactions* **1974**, 395-399.

(70) Ghosh, A.; Wondimagegn, T.; Parusel, A. B. J. Electronic Structure of Gallium, Copper, and Nickel Complexes of Corrole. High-Valent Transition Metal Centers versus Noninnocent Ligands. *Journal of the American Chemical Society* **2000**, *122*, 5100-5104.

(71) Okura, I.: *Photosensitization of Porphyrins and Phtalocyanines*; CRC Press: London, 2001.

(72) Seybold, P. G.; Gouterman, M. Porphyrins: XIII: Fluorescence spectra and quantum yields. *Journal of Molecular Spectroscopy* **1969**, *31*, 1-13.

(73) I Y Quiroz-Segoviano, R.; N Serratos, I.; Rojas-González, F.; Tello-Solís, S.; Sosa-Fonseca, R.; Medina-Juárez, O.; Menchaca, C.; A García-Sánchez, M.: *On Tuning the Fluorescence Emission of Porphyrin Free Bases Bonded to the Pore Walls of Organo-Modified Silica*, 2014; Vol. 19.

(74) Uttamlal, M.; Sheila Holmes-Smith, A. The excitation wavelength dependent fluorescence of porphyrins. *Chemical Physics Letters* **2008**, *454*, 223-228.

(75) Harriman, A. Luminescence of porphyrins and metalloporphyrins. Part 1.-Zinc(II), nickel(II) and manganese(II) porphyrins. *Journal of the Chemical Society, Faraday Transactions 1: Physical Chemistry in Condensed Phases* **1980**, *76*, 1978-1985.

(76) Liu, X.; Mahammed, A.; Tripathy, U.; Gross, Z.; Steer, R. P. Photophysics of Soret-excited tetrapyrroles in solution. III. Porphyrin analogues: Aluminum and gallium corroles. *Chemical Physics Letters* **2008**, *459*, 113-118.

(77) Rogers, J. E.; Nguyen, K. A.; Hufnagle, D. C.; McLean, D. G.; Su, W.; Gossett, K. M.; Burke, A. R.; Vinogradov, S. A.; Pachter, R.; Fleitz, P. A. Observation and Interpretation of Annulated Porphyrins: Studies on the Photophysical Properties of *meso*-Tetraphenylmetalloporphyrins. *The Journal of Physical Chemistry A* **2003**, *107*, 11331-11339.

(78) Koren, K.; Borisov, S. M.; Saf, R.; Klimant, I. Strongly Phosphorescent Iridium(III)–Porphyrins – New Oxygen Indicators with Tuneable Photophysical Properties and Functionalities. *European Journal of Inorganic Chemistry* **2011**, *2011*, 1531-1534.

(79) Minaev, B.; Ågren, H. Theoretical DFT study of phosphorescence from porphyrins. *Chemical Physics* **2005**, *315*, 215-239.

(80) Alemayehu, A. B.; Day, N. U.; Mani, T.; Rudine, A. B.; Thomas, K. E.; Gederaas, O. A.; Vinogradov, S. A.; Wamser, C. C.; Ghosh, A. Gold Tris(carboxyphenyl)corroles as Multifunctional Materials: Room Temperature Near-IR

Phosphorescence and Applications to Photodynamic Therapy and Dye-Sensitized Solar Cells. *ACS Applied Materials & Interfaces* **2016**, *8*, 18935-18942.

(81) Borisov, S. M.; Alemayehu, A.; Ghosh, A. Osmium-nitrido corroles as NIR indicators for oxygen sensors and triplet sensitizers for organic upconversion and singlet oxygen generation. *Journal of Materials Chemistry C* **2016**, *4*, 5822-5828.

(82) Palmer, J. H.; Durrell, A. C.; Gross, Z.; Winkler, J. R.; Gray, H. B. Near-IR Phosphorescence of Iridium(III) Corroles at Ambient Temperature. *Journal of the American Chemical Society* **2010**, *132*, 9230-9231.

(83) Kou, J.; Dou, D.; Yang, L. Porphyrin photosensitizers in photodynamic therapy and its applications. *Oncotarget* **2017**, *8*, 81591-81603.

(84) Tripathi, V. S.; Lakshminarayana, G.; Nogami, M. Optical oxygen sensors based on platinum porphyrin dyes encapsulated in ORMOSILS. *Sensors and Actuators B: Chemical* **2010**, *147*, 741-747.

(85) Lemon, C. M.; Powers, D. C.; Brothers, P. J.; Nocera, D. G. Gold Corroles as Near-IR Phosphors for Oxygen Sensing. *Inorganic Chemistry* **2017**, *56*, 10991-10997.

(86) Fischer, H.; Zeile, K. Synthese des Hämatoporphyrins, Protoporphyrins und Hämins. *Justus Liebigs Annalen der Chemie* **2006**, *468*, 98-116.

(87) Rothemund, P. FORMATION OF PORPHYRINS FROM PYRROLE AND ALDEHYDES. *Journal of the American Chemical Society* **1935**, *57*, 2010-2011.

(88) Rothemund, P. A New Porphyrin Synthesis. The Synthesis of Porphin1. *Journal of the American Chemical Society* **1936**, *58*, 625-627.

(89) Rothemund, P.; Menotti, A. R. Porphyrin Studies. IV.1 The Synthesis of α,β,γ,δ-Tetraphenylporphine. *Journal of the American Chemical Society* **1941**, *63*, 267-270.

(90) Thomas, D. W.; Martell, A. E. Tetraphenylporphine and Some *para*-Substituted Derivatives1,2. *Journal of the American Chemical Society* **1956**, *78*, 1335-1338.

(91) Smith, K. M. Development of porphyrin syntheses. *New Journal of Chemistry* **2016**, *40*, 5644-5649.

(92) Adler, A. D.; Longo, F. R.; Shergalis, W. Mechanistic Investigations of Porphyrin Syntheses. I. Preliminary Studies on ms-Tetraphenylporphin. *Journal of the American Chemical Society* **1964**, *86*, 3145-3149.

(93) Adler, A. D.; Longo, F. R.; Finarelli, J. D.; Goldmacher, J.; Assour, J.; Korsakoff, L. A simplified synthesis for *meso*-tetraphenylporphine. *The Journal of Organic Chemistry* **1967**, *32*, 476-476.

(94) Lindsey, J. S.; Hsu, H. C.; Schreiman, I. C. Synthesis of tetraphenylporphyrins under very mild conditions. *Tetrahedron Letters* **1986**, *27*, 4969-4970.

(95) Lindsey, J. S.; MacCrum, K. A.; Tyhonas, J. S.; Chuang, Y. Y. Investigation of a Synthesis of meso-Porphyrins Employing High Concentration Conditions and an Electron Transport Chain for Aerobic Oxidation. *The Journal of Organic Chemistry* **1994**, *59*, 579-587.

(96) Boudif, A.; Momenteau, M. A new convergent method for porphyrin synthesis based on a '3 + 1' condensation. *Journal of the Chemical Society, Perkin Transactions 1* **1996**, 1235-1242.

(97) Gradillas, A.; del Campo, C.; Sinisterra, J. V.; Llama, E. F. Novel synthesis of 5,10,15,20-tetraarylporphyrins using high-valent transition metal salts. *Journal of the Chemical Society, Perkin Transactions 1* **1995**, 2611-2613.

(98) Nascimento, B. F. O.; Pineiro, M.; Rocha Gonsalves, A. M. d. A.; Ramos Silva, M.; Matos Beja, A.; Paixão, J. A. Microwave-assisted synthesis of porphyrins and metalloporphyrins: a rapid and efficient synthetic method. *Journal of Porphyrins and Phthalocyanines* **2007**, *11*, 77-84.

(99) Kitaoka, S.; Nobuoka, K.; Ishikawa, Y. Ionic liquids for tetraarylporphyrin preparation. *Tetrahedron* **2005**, *61*, 7678-7685.

(100) Nia, S.; Gong, X.; Drain, C. M.; Jurow, M.; Rizvi, W.; Qureshy, M. Solvent-free synthesis of *meso*- tetraarylporphyrins in air: product diversity and yield optimization. *Journal of Porphyrins and Phthalocyanines* **2010**, *14*, 621-629.

(101) Johnson, A. W.; Kay, I. T. 306. Corroles. Part I. Synthesis. *Journal of the Chemical Society (Resumed)* **1965**, 1620-1629.

(102) Conlon, M.; Johnson, A. W.; Overend, W. R.; Rajapaksa, D.; Elson, C. M. Structure and reactions of cobalt corroles. *Journal of the Chemical Society, Perkin Transactions 1* **1973**, 2281-2288.

(103) Boschi, T.; Licoccia, S.; Paolesse, R.; Tagliatesta, P.; Tehran, M. A.; Pelizzi, G.; Vitali, F. Synthesis and characterization of novel metal(III) complexes of corrole. Crystal and molecular structure of (2,3,7,8,12,13,17,18-octamethylcorrolato)(triphenylarsine) rhodium(III). *Journal of the Chemical Society, Dalton Transactions* **1990**, 463-468.

(104) Kin Tse, M.; Zhang, Z.; Shing Chan, K. Synthesis of an oxorhenium(V) corrolate from porphyrin with detrifluoromethylation and ring contraction. *Chemical Communications* **1998**, 1199-1200.

(105) Paolesse, R.; Mini, S.; Sagone, F.; Boschi, T.; Jaquinod, L.; J. Nurco, D.; M. Smith, K. 5,10,15-Triphenylcorrole: a product from a modified Rothemund reaction. *Chemical Communications* **1999**, 1307-1308.

(106) Gross, Z.; Galili, N.; Saltsman, I. The First Direct Synthesis of Corroles from Pyrrole. *Angewandte Chemie International Edition* **1999**, *38*, 1427-1429.

(107) Wasbotten, I. H.; Wondimagegn, T.; Ghosh, A. Electronic Absorption, Resonance Raman, and Electrochemical Studies of Planar and Saddled Copper(III) meso-Triarylcorroles. Highly Substituent-Sensitive Soret Bands as a Distinctive Feature of High-Valent Transition Metal Corroles. *Journal of the American Chemical Society* **2002**, *124*, 8104-8116.

(108) König, M.; Faschinger, F.; Reith, L. M.; Schöfberger, W. The evolution of corrole synthesis — from simple one-pot strategies to sophisticated ABC-corroles. *Journal of Porphyrins and Phthalocyanines* **2016**, *20*, 96-107.

(109) Gryko, D. T. A simple, rational synthesis of -substituted AB-corroles. *Chemical Communications* **2000**, 2243-2244.

(110) Gryko, D. T.; Jadach, K. A Simple and Versatile One-Pot Synthesis of *meso*-Substituted *trans*-A2B-Corroles. *The Journal of Organic Chemistry* **2001**, *66*, 4267-4275.

(111) Guilard, R.; Gryko, D. T.; Canard, G.; Barbe, J.-M.; Koszarna, B.; Brandès, S.; Tasior, M. Synthesis of Corroles Bearing up to Three Different Meso Substituents. *Organic Letters* **2002**, *4*, 4491-4494.

(112) Gryko, D. T.; Koszarna, B. Refined methods for the synthesis of *meso*-substituted A3- and *trans*-A2B-corroles. *Organic & Biomolecular Chemistry* **2003**, *1*, 350-357.

(113) Koszarna, B.; Gryko, D. T. Efficient Synthesis of *meso*-Substituted Corroles in a H_2O−MeOH Mixture. *The Journal of Organic Chemistry* **2006**, *71*, 3707-3717.

(114) Ooi, S.; Tanaka, T.; Osuka, A. Synthesis and Characterization of *cis*-A2B-Type *meso*-Triaryl-Substituted Corroles. *European Journal of Organic Chemistry* **2014**, *2015*, 130-134.

(115) Collman, J. P.; Decréau, R. A. Microwave-assisted synthesis of corroles. *Tetrahedron Letters* **2003**, *44*, 1207-1210.

(116) Zhan, H.-Y.; Liu, H.-Y.; Chen, H.-J.; Jiang, H.-F. Preparation of *meso*-substituted *trans*-A2B-corroles in ionic liquids. *Tetrahedron Letters* **2009**, *50*, 2196-2199.

(117) Barata, J. F. B.; Neves, M. G. P. M. S.; Faustino, M. A. F.; Tomé, A. C.; Cavaleiro, J. A. S. Strategies for Corrole Functionalization. *Chemical Reviews* **2017**, *117*, 3192-3253.

(118) Hiroto, S.; Miyake, Y.; Shinokubo, H. Synthesis and Functionalization of Porphyrins through Organometallic Methodologies. *Chemical Reviews* **2017**, *117*, 2910-3043.

(119) Smith, K. M.; Langry, K. C. Electrophilic substitution reactions of derivatives of deuteroporphyrin-IX : deuteriation and Vilsmeier formylation. *Journal of the Chemical Society, Perkin Transactions 1* **1983**, 439-444.

(120) Montforts, F.-P.; Scheurich, G.; Meier, A.; Haake, G.; Höper, F. An improved method for the preparation of formyldeuteroporphyrins - Synthesis of biologically relevant porphyrins. *Tetrahedron Letters* **1991**, *32*, 3477-3480.

(121) Paolesse, R.; Jaquinod, L.; Senge, M. O.; Smith, K. M. Functionalization of Corroles: Formylcorroles. *The Journal of Organic Chemistry* **1997**, *62*, 6193-6198.

(122) Saltsman, I.; Mahammed, A.; Goldberg, I.; Tkachenko, E.; Botoshansky, M.; Gross, Z. Selective Substitution of Corroles: Nitration, Hydroformylation, and Chlorosulfonation. *Journal of the American Chemical Society* **2002**, *124*, 7411-7420.

(123) Pereira, N.; Serra, A.; Pineiro, M.; Rocha Gonsalves, A.; Abrantes, A.; Laranjo, M.; Botelho, M. F.: *Synthetic porphyrins bearing β-propionate chains as photosensitizers for photodynamic therapy*, 2010; Vol. 14.

(124) Silviya Reeta, P.; Kandhadi, J.; Lingamallu, G. One-pot synthesis of *β*-carboxy tetra aryl porphyrins: potential applications to dye-sensitized solar cells. *Tetrahedron Letters* **2010**, *51*, 2865-2867.

(125) Saltsman, I.; Goldberg, I.; Gross, Z. One-step conversions of a simple corrole into chiral and amphiphilic derivatives. *Tetrahedron Letters* **2003**, *44*, 5669-5673.

(126) Dahal, S.; Krishnan, V. Charge transfer excited states of zinc(II) derivatives of *β*-substituted dinitrotetraphenylporphyrin. *Journal of Photochemistry and Photobiology A: Chemistry* **1995**, *89*, 105-112.

(127) Bartoli, J. F.; Battioni, P.; De Foor, W. R.; Mansuy, D. Synthesis and remarkable properties of iron *β*-polynitroporphyrins as catalysts for monooxygenation reactions. *Journal of the Chemical Society, Chemical Communications* **1994**, 23-24.

(128) Palacio, M.; Mouries-Mansuy, V.; Loire, G.; Le Barch-Ozette, K.; Leduc, P.; Battioni, P.; Mansuy, D.; M. Barkigia, K.; Fajer, J.: *A New General Method for Selective β-Polynitration of Porphyrins; Preparation and Redox Properties of Zn-Porphyrins Bearing*

One Through to Eight β-Nitro Substituents and X-Ray Structure of the First Zn β-Pernitro Porphyrin, 2000.

(129) Catalano, M. M.; Crossley, M. J.; Harding, M. M.; King, L. G. Control of reactivity at the porphyrin periphery by metal ion co-ordination: a general method for specific nitration at the *β*-pyrrolic position of 5,10,15,20-tetra-arylporphyrins. *Journal of the Chemical Society, Chemical Communications* **1984**, 1535-1536.

(130) Baldwin, J. E.; Crossley, M. J.; DeBernardis, J. Efficient peripheral functionalization of porphyrins. *Tetrahedron* **1982**, *38*, 685-692.

(131) Stefanelli, M.; Mastroianni, M.; Nardis, S.; Licoccia, S.; Fronczek, F. R.; Smith, K. M.; Zhu, W.; Ou, Z.; Kadish, K. M.; Paolesse, R. Functionalization of Corroles: The Nitration Reaction. *Inorganic Chemistry* **2007**, *46*, 10791-10799.

(132) Stefanelli, M.; Pomarico, G.; Tortora, L.; Nardis, S.; Fronczek, F. R.; McCandless, G. T.; Smith, K. M.; Manowong, M.; Fang, Y.; Chen, P.; Kadish, K. M.; Rosa, A.; Ricciardi, G.; Paolesse, R. *β*-Nitro-5,10,15-tritolylcorroles. *Inorganic Chemistry* **2012**, *51*, 6928-6942.

(133) Stefanelli, M.; Nardis, S.; Fronczek, F. R.; Smith, K. M.; Paolesse, R. Copper *β*-trinitrocorrolates. *Journal of porphyrins and phthalocyanines* **2013**, *17*, 10.1142/S1088424613500120.

(134) Dąbrowski Janusz, M.; Pereira Mariette, M.; Arnaut Luis, G.; Monteiro Carlos, J. P.; Peixoto Andreia, F.; Karocki, A.; Urbańska, K.; Stochel, G. Synthesis, Photophysical Studies and Anticancer Activity of a New Halogenated Water-Soluble Porphyrin. *Photochemistry and Photobiology* **2007**, *83*, 897-903.

(135) Monteiro, C. J. P.; Pereira, M. M.; Pinto, S. M. A.; Simões, A. V. C.; Sá, G. F. F.; Arnaut, L. G.; Formosinho, S. J.; Simões, S.; Wyatt, M. F. Synthesis of amphiphilic sulfonamide halogenated porphyrins: MALDI-TOFMS characterization and evaluation of 1-octanol/water partition coefficients. *Tetrahedron* **2008**, *64*, 5132-5138.

(136) García-Ortega, H.; Ribo, J. M.: *Meso and beta-pyrrole sulfonated porphyrins obtained by sulfonation of 5,15-bis(phenyl)porphyrin*, 2000; Vol. 4.

(137) Gross, Z.; Mahammed, A. Selective sulfonation and deuteration of free-base corroles. *Journal of Porphyrins and Phthalocyanines* **2002**, *06*, 553-555.

(138) Mahammed, A.; Goldberg, I.; Gross, Z. Highly Selective Chlorosulfonation of Tris(pentafluorophenyl)corrole as a Synthetic Tool for the Preparation of Amphiphilic Corroles and Metal Complexes of Planar Chirality. *Organic Letters* **2001**, *3*, 3443-3446.

(139) Naitana, M. L.; Nardis, S.; Lentini, S.; Cicero, D. O.; Paolesse, R. Widening the scope of the corrole sulfonation. *Journal of Porphyrins and Phthalocyanines* **2015**, *19*, 735-744.

(140) Zhang, C.; Suslick, K. S. Syntheses of boronic-acid-appended metalloporphyrins as potential colorimetric sensors for sugars and carbohydrates. *Journal of Porphyrins and Phthalocyanines* **2005**, *09*, 659-666.

(141) Sharma, R.; Gautam, P.; Misra, R.; Shukla, S. K. *β*-Substituted triarylborane appended porphyrins: photophysical properties and anion sensing. *RSC Advances* **2015**, *5*, 27069-27074.

(142) Hata, H.; Shinokubo, H.; Osuka, A. Highly Regioselective Ir-Catalyzed *β*-Borylation of Porphyrins via C−H Bond Activation and Construction of *β*−*β*-Linked Diporphyrin. *Journal of the American Chemical Society* **2005**, *127*, 8264-8265.

(143) Hiroto, S.; Hisaki, I.; Shinokubo, H.; Osuka, A. Synthesis of Corrole Derivatives through Regioselective Ir-Catalyzed Direct Borylation. *Angewandte Chemie International Edition* **2005**, *44*, 6763-6766.

(144) Homma, M.; Aoyagi, K.; Aoyama, Y.; Ogoshi, H. Electron deficient porphyrins. 1. Tetrakis(trifluoromethyl)porphyrin and its metal complexes. *Tetrahedron Letters* **1983**, *24*, 4343-4346.

(145) Terazono, Y.; Dolphin, D. Synthesis and Characterization of *β*-Trifluoromethyl-*meso*-tetraphenylporphyrins. *The Journal of Organic Chemistry* **2003**, *68*, 1892-1900.

(146) Liu, C.; Chen, Q. Y. Fluoroalkylation of Porphyrins: A Facile Synthesis of Trifluoromethylated Porphyrins by a Palladium-Catalyzed Cross-Coupling Reaction. *European Journal of Organic Chemistry* **2005**, *2005*, 3680-3686.

(147) Jin, L.-M.; Zeng, Z.; Guo, C.-C.; Chen, Q.-Y. Fluoroalkylation of Porphyrins: Synthesis and Reactions of *β*-Fluoroalkyltetraarylporphyrins. *The Journal of Organic Chemistry* **2003**, *68*, 3912-3917.

(148) Jin, L.-M.; Chen, L.; Yin, J.-J.; Guo, C.-C.; Chen, Q.-Y. Fluoroalkylation of porphyrins: Preparation and characterization of *meso*- and *β*-fluoroalkyl-5,15-diarylporphyrins. *Journal of Fluorine Chemistry* **2005**, *126*, 1321-1326.

(149) Jin, L.-M.; Chen, L.; Guo, C.-C.; Chen, Q.-Y. Copper-induced fluoroalkylation of porphyrins: solvent-dependent synthesis of fluoroalkyl chlorins and porphyrins from fluoroalkyl iodides. *Journal of Porphyrins and Phthalocyanines* **2005**, *09*, 109-120.

(150) Du, R.-B.; Liu, C.; Shen, D.-M.; Chen, Q.-Y.: *Partial Bromination and Fluoroalkylation of 5,10,15Tris(pentafluorophenyl)corrole*, 2009; Vol. 2009.

(151) Belykh, D. V.; Tarabukina, I. S.; Gruzdev, I. V.; Kodess, M. I.; Kutchin, A. V. Aminomethylation of chlorophyll a derivatives using bis(*N*,*N*-dimethylamino)methane. *Journal of Porphyrins and Phthalocyanines* **2009**, *13*, 949-956.

(152) Lavallee, D. K.; Xu, Z.; Pina, R. Synthesis and properties of new cationic-periphery porphyrins, tetrakis(*p*-(aminomethyl)phenyl)porphyrin and *N*-methyltetrakis(*p*-(aminomethyl)phenyl)porphyrin. *The Journal of Organic Chemistry* **1993**, *58*, 6000-6008.

(153) Ramos Catarina, I. V.; Graça Santana-Marques, M.; Ferrer-Correia, A. J.; Barata Joana, F. B.; Tomé Augusto, C.; Neves, M. G. P. M. S.; Cavaleiro, J. A. S.; Abreu Paulo, E.; Pereira Mariette, M.; Pais Alberto, A. C. C. Differentiation of aminomethyl corrole isomers by mass spectrometry. *Journal of Mass Spectrometry* **2012**, *47*, 516-522.

(154) de Souza, M. C.; Pedrosa, L. F.; Cazagrande, G. S.; Ferreira, V. F.; Neves, M. G. P. M. S.; Cavaleiro, J. A. S. From porphyrin benzylphosphoramidate conjugates to the catalytic hydrogenation of 5,10,15,20-tetrakis(pentafluorophenyl)porphyrin. *Beilstein Journal of Organic Chemistry* **2014**, *10*, 628-633.

(155) Whitlock, H. W.; Hanauer, R.; Oester, M. Y.; Bower, B. K. Diimide reduction of porphyrins. *Journal of the American Chemical Society* **1969**, *91*, 7485-7489.

(156) Pereira, M. M.; Abreu, A. R.; Goncalves, N. P. F.; Calvete, M. J. F.; Simoes, A. V. C.; Monteiro, C. J. P.; Arnaut, L. G.; Eusebio, M. E.; Canotilho, J. An insight into solvent-free diimide porphyrin reduction: a versatile approach for *meso*-aryl hydroporphyrin synthesis. *Green Chemistry* **2012**, *14*, 1666-1672.

(157) Mahammed, A.; Gross, Z. Aluminum corrolin, a novel chlorophyll analogue. *Journal of Inorganic Biochemistry* **2002**, *88*, 305-309.

(158) Tomé, A. C.; Neves, M. G. P. M. S.; Cavaleiro, J. A. S. Porphyrins and other pyrrolic macrocycles in cycloaddition reactions. *Journal of Porphyrins and Phthalocyanines* **2009**, *13*, 408-414.

(159) Barata, J. F. B.; Silva, A. M. G.; Faustino, M. A. F.; Neves, M. G. P. M. S.; Tomé, A. C.; Silva, A. M. S.; Cavaleiro, J. A. S. Novel Diels-Alder and Thermal [4+4] Cycloadditions of Corroles. *Synlett* **2004**, *2004*, 1291-1293.

(160) Onda, H.; Toi, H.; Aoyama, Y.; Ogoshi, H. Fluoropyrroles and tetrafluoroporphyrins. *Tetrahedron Letters* **1985**, *26*, 4221-4224.

(161) Leroy, J.; Bondon, A. *β*-Fluorinated Porphyrins and Related Compounds: An Overview. *European Journal of Organic Chemistry* **2008**, *2008*, 417-433.

(162) Woller, E. K.; DiMagno, S. G. 2,3,7,8,12,13,17,18-Octafluoro-5,10,15,20-tetraarylporphyrins and Their Zinc Complexes: First Spectroscopic, Electrochemical, and Structural Characterization of a Perfluorinated Tetraarylmetalloporphyrin. *The Journal of Organic Chemistry* **1997**, *62*, 1588-1593.

(163) Leroy, J.; Bondon, A.; Toupet, L.; Rolando, C. 2,3,7,8,12,13,17,18-Octafluoro-5,10,15,20-Tetraphenylporphyrin: First Synthesis and X-Ray Crystal Structure of the ZnII Complex. *Chemistry – A European Journal* **2006**, *3*, 1890-1893.

(164) Woller, E. K.; Smirnov, V. V.; DiMagno, S. G. A Straightforward Synthesis of 3,4-Difluoropyrrole. *The Journal of Organic Chemistry* **1998**, *63*, 5706-5707.

(165) Higashino, T.; Osuka, A. 2,3,17,18-Tetrahalohexaphyrins and the First Phlorin-type Hexaphyrins. *Chemistry – An Asian Journal* **2013**, *8*, 1994-2002.

(166) Liu, H.-Y.; Lai, T.-S.; Yeung, L.-L.; Chang, C. K. First Synthesis of Perfluorinated Corrole and Its MnO Complex. *Organic Letters* **2003**, *5*, 617-620.

(167) Steene, E.; Dey, A.; Ghosh, A. *β*-Octafluorocorroles. *Journal of the American Chemical Society* **2003**, *125*, 16300-16309.

(168) Dogutan, D. K.; McGuire, R.; Nocera, D. G. Electocatalytic Water Oxidation by Cobalt(III) Hangman *β*-Octafluoro Corroles. *Journal of the American Chemical Society* **2011**, *133*, 9178-9180.

(169) Wijesekera, T.; Matsumoto, A.; Dolphin, D.; Lexa, D. Perchlorinated and Highly Chlorinated *meso*-Tetraphenylporphyrins. *Angewandte Chemie International Edition in English* **2003**, *29*, 1028-1030.

(170) Autret, M.; Ou, Z.; Antonini, A.; Boschi, T.; Tagliatesta, P.; Kadish, K. M. Synthesis and electrochemistry of 2,3,7,8,12,13,17,18-octachloro-5,10,15,20-tetrakis (3,5-dichloro-2,6-dimethoxyphenyl)porphyrin (H_2tdcdmpp), [CoII(tdcdmpp)] and [M(tdcdmpp)Cl](M = FeIII or MnIII). *Journal of the Chemical Society, Dalton Transactions* **1996**, 2793-2797.

(171) Rumyantseva, V. D.; Aksenova, E. A.; Ponamoreva, O. N.; Mironov, A. F. Halogenation of metalloporphyrins. *Russian Journal of Bioorganic Chemistry* **2000**, *26*, 423-428.

(172) McHiri, C.; Amiri, N.; Jabli, S.; Roisnel, T.; Nasri, H. The (oxo)[(2,3,7,8,12,13,17,18-octachloro-5,10,15,20-tetrakis(4-tolylporphyrinato)]vanadium(IV): Synthesis, UV–visible, Cyclic voltammetry and X-ray crystal structure. *Journal of Molecular Structure* **2018**, *1154*, 51-58.

(173) Ngo, T. H.; Van Rossom, W.; Dehaen, W.; Maes, W. Reductive demetallation of Cu-corroles-a new protective strategy towards functional free-base corroles. *Organic & Biomolecular Chemistry* **2009**, *7*, 439-443.

(174) Mahammed, A.; Botoshansky, M.; Gross, Z. Chlorinated corroles. *Dalton Transactions* **2012**, *41*, 10938-10940.

(175) Traylor, T. G.; Tsuchiya, S. Perhalogenated tetraphenylhemins: stable catalysts of high turnover catalytic hydroxylations. *Inorganic Chemistry* **1987**, *26*, 1338-1339.

(176) Bhyrappa, P.; Krishnan, V. Octabromotetraphenylporphyrin and its metal derivatives: Electronic structure and electrochemical properties. *Inorganic Chemistry* **1991**, *30*, 239-245.

(177) Su, W.; Singh, K.; Rogers, J.; Slagle, J.; Fleitz, P. The relationship of structure and optical properties of haloporphyrins: A new way to synthesize porphyrin chromophores and the investigation of their optical properties. *Materials Science and Engineering: B* **2006**, *132*, 12-15.

(178) Tortora, L.; Nardis, S.; Fronczek, F. R.; Smith, K. M.; Paolesse, R. Functionalization of the corrole ring: the role of isocorrole intermediates. *Chemical Communications* **2011**, *47*, 4243-4245.

(179) Nardis, S.; Mandoj, F.; Paolesse, R.; Fronczek, F. R.; Smith, K. M.; Prodi, L.; Montalti, M.; Battistini, G. Synthesis and Functionalization of Germanium Triphenylcorrolate: The First Example of a Partially Brominated Corrole. *European Journal of Inorganic Chemistry* **2007**, *2007*, 2345-2352.

(180) Nardis, S.; Pomarico, G.; Stefanelli, M.; Lentini, S.; Cicero, D. O.; Fronczek, F. R.; Smith, K. M.; Paolesse, R. The scope of the *β*-halogenation of triarylcorroles. *Journal of Porphyrins and Phthalocyanines* **2016**, *20*, 465-474.

(181) Mahammed, A.; Gray, H. B.; Meier-Callahan, A. E.; Gross, Z. Aerobic Oxidations Catalyzed by Chromium Corroles. *Journal of the American Chemical Society* **2003**, *125*, 1162-1163.

(182) Wagnert, L.; Berg, A.; Stavitski, E.; Berthold, T.; Kothe, G.; Goldberg, I.; Mahammed, A.; Simkhovich, L.; Gross, Z.; Levanon, H. Exploring the photoexcited triplet states of aluminum and tin corroles by time-resolved Q-band EPR. *Applied Magnetic Resonance* **2006**, *30*, 591.

(183) Wagnert, L.; Rubin, R.; Berg, A.; Mahammed, A.; Gross, Z.; Levanon, H. Photoexcited Triplet State Properties of Brominated and Nonbrominated Ga(III)-Corroles as

Studied by Time-Resolved Electron Paramagnetic Resonance. *The Journal of Physical Chemistry B* **2010**, *114*, 14303-14308.

(184) Capar, J.; Berg, S.; Thomas, K. E.; Beavers, C. M.; Gagnon, K. J.; Ghosh, A. Improved syntheses of *β*-octabromo-*meso*-triarylcorrole derivatives. *Journal of Inorganic Biochemistry* **2015**, *153*, 162-166.

(185) Senge Mathias, O.; Kalisch Werner, W.; Bischoff, I. The Reaction of Porphyrins with Organolithium Reagents. *Chemistry – A European Journal* **2000**, *6*, 2721-2738.

(186) Krattinger, B.; Callot, H. J. Alkylation and Reduction of Porphyrins and *N*-Substituted Porphyrins: New Routes to Chlorins and Phlorins. *European Journal of Organic Chemistry* **1999**, *1999*, 1857-1867.

(187) Cheng, D. O.; LeGoff, E. Synthesis of substituted porphyrins. *Tetrahedron Letters* **1977**, *18*, 1469-1472.

(188) Ono, N.; Miyagawa, H.; Ueta, T.; Ogawa, T.; Tani, H. Synthesis of 3,4-diarylpyrroles and conversion into dodecaarylporphyrins; a new approach to porphyrins with altered redox potentials. *Journal of the Chemical Society, Perkin Transactions 1* **1998**, 1595-1602.

(189) Kadish, K. M.; Van Caemelbecke, E.; D'Souza, F.; Lin, M.; Nurco, D. J.; Medforth, C. J.; Forsyth, T. P.; Krattinger, B.; Smith, K. M.; Fukuzumi, S.; Nakanishi, I.; Shelnutt, J. A. Synthesis and Electrochemical Studies of a Series of Fluorinated Dodecaphenylporphyrins. *Inorganic Chemistry* **1999**, *38*, 2188-2198.

(190) Guilard, R.; P. Gros, C.; Bolze, F.; Jérôme, F.; Ou, Z.; Shao, J.; Fischer, J.; Weiss, R.; M. Kadish, K.: *Alkyl and Aryl Substituted Corroles. 1. Synthesis and Characterization of Free Base and Cobalt Containing Derivatives. X-ray Structure of (Me4Ph5Cor)Co(py)2*, 2001; Vol. 40.

(191) DiMagno, S. G.; Lin, V. S. Y.; Therien, M. J. Facile elaboration of porphyrins via metal-mediated cross-coupling. *The Journal of Organic Chemistry* **1993**, *58*, 5983-5993.

(192) Scrivanti, A.; Beghetto, V.; Matteoli, U.; Antonaroli, S.; Marini, A.; Mandoj, F.; Paolesse, R.; Crociani, B.: *Iminophosphine—Palladium(0) Complexes as Highly Active Catalysts in the Suzuki Reaction. Synthesis of Undecaaryl Substituted Corroles*, 2004; Vol. 35.

(193) Kawamata, Y.; Tokuji, S.; Yorimitsu, H.; Osuka, A. Palladium-Catalyzed *β*-Selective Direct Arylation of Porphyrins. *Angewandte Chemie International Edition* **2011**, *50*, 8867-8870.

(194) Tokuji, S.; Awane, H.; Yorimitsu, H.; Osuka, A. Direct Arylation of *meso*-Formyl Porphyrin. *Chemistry – A European Journal* **2012**, *19*, 64-68.

(195) Barona-Castaño, J.; Carmona-Vargas, C.; Brocksom, T.; de Oliveira, K. Porphyrins as Catalysts in Scalable Organic Reactions. *Molecules* **2016**, *21*, 310.

(196) Chowdhury, A.; Chowdhury, J.; Pal, P.; Pal, A. J. Light-emitting diodes from molecularly thin porphyrin derivative: Effect of molecular packing. *Solid State Communications* **1998**, *107*, 725-729.

(197) Vicente, M. d. G. H.; Smith, K. M. Syntheses and Functionalizations of Porphyrin Macrocycles. *Current organic synthesis* **2014**, *11*, 3-28.

(198) Suzuki, A.: Organoboron compounds in new synthetic reactions. In *Pure and Applied Chemistry*, 1985; Vol. 57; pp 1749.

(199) Almond-Thynne, J.; Blakemore, D. C.; Pryde, D. C.; Spivey, A. C. Site-selective Suzuki-Miyaura coupling of heteroaryl halides - understanding the trends for pharmaceutically important classes. *Chemical Science* **2017**, *8*, 40-62.

(200) Heck, R. F.; Nolley, J. P. Palladium-catalyzed vinylic hydrogen substitution reactions with aryl, benzyl, and styryl halides. *The Journal of Organic Chemistry* **1972**, *37*, 2320-2322.

(201) Stille, J. K. The Palladium-Catalyzed Cross-Coupling Reactions of Organotin Reagents with Organic Electrophiles [New Synthetic Methods (58)]. *Angewandte Chemie International Edition in English* **1986**, *25*, 508-524.

(202) Tamao, K.; Sumitani, K.; Kumada, M. Selective carbon-carbon bond formation by cross-coupling of Grignard reagents with organic halides. Catalysis by nickel-phosphine complexes. *Journal of the American Chemical Society* **1972**, *94*, 4374-4376.

(203) King, A. O.; Okukado, N.; Negishi, E.-i. Highly general stereo-, regio-, and chemo-selective synthesis of terminal and internal conjugated enynes by the Pd-catalysed reaction of alkynylzinc reagents with alkenyl halides. *Journal of the Chemical Society, Chemical Communications* **1977**, 683-684.

(204) Hatanaka, Y.; Hiyama, T. Cross-coupling of organosilanes with organic halides mediated by a palladium catalyst and tris(diethylamino)sulfonium difluorotrimethylsilicate. *The Journal of Organic Chemistry* **1988**, *53*, 918-920.

(205) Sonogashira, K. Development of Pd–Cu catalyzed cross-coupling of terminal acetylenes with sp2-carbon halides. *Journal of Organometallic Chemistry* **2002**, *653*, 46-49.

(206) Nakano, A.; Shimidzu, H.; Osuka, A. Facile regioselective *meso*-iodination of porphyrins. *Tetrahedron Letters* **1998**, *39*, 9489-9492.

(207) Lash Timothy , D.; Colby Denise , A.; Ferrence Gregory , M. Further Studies on the Synthesis of *meso*-Tetraarylazuliporphyrins under Lindsey−Rothemund Reaction Conditions and Their Conversion into Benzocarbaporphyrins. *European Journal of Organic Chemistry* **2003**, *2003*, 4533-4548.

(208) Lin, Q.; Bu, X.; Kong, A.; Mao, C.; Bu, F.; Feng, P. Heterometal-Embedded Organic Conjugate Frameworks from Alternating Monomeric Iron and Cobalt Metalloporphyrins and Their Application in Design of Porous Carbon Catalysts. *Advanced Materials* **2015**, *27*, 3431-3436.

(209) Müther, M.; Bill, E.; Trautwein, A. X.; Mandon, D.; Weiss, R.; Gold, A.; Jayaraj, K.; Austin, R. N. Spin coupling in distorted high-valent Fe(IV)-porphyrin radical complexes. *Hyperfine Interactions* **1994**, *91*, 803-808.

(210) Bray, B. L.; Mathies, P. H.; Naef, R.; Solas, D. R.; Tidwell, T. T.; Artis, D. R.; Muchowski, J. M. *N*-(Triisopropylsilyl)pyrrole. A progenitor "par excellence" of 3-substituted pyrroles. *The Journal of Organic Chemistry* **1990**, *55*, 6317-6328.

(211) Mattern, D. L. Direct aromatic periodination. *The Journal of Organic Chemistry* **1984**, *49*, 3051-3053.

(212) Limbach, H.-H.; Lopez, J. M.; Kohen, A. Arrhenius Curves of Hydrogen Transfers: Tunnel Effects, Isotope Effects and Effects of Pre-Equilibria. *Philosophical Transactions: Biological Sciences* **2006**, *361*, 1399-1415.

(213) Silvers, S. J.; Tulinsky, A. The crystal and molecular structure of triclinic tetraphenylporphyrin. *Journal of the American Chemical Society* **1967**, *89*, 3331-3337.

(214) Codding, P. W.; Tulinsky, A. Structure of tetra-*n*-propylporphine. Average structure for the free base macrocycle from three independent determinations. *Journal of the American Chemical Society* **1972**, *94*, 4151-4157.

(215) Chen, B. M. L.; Tulinsky, A. Redetermination of the structure of porphine. *Journal of the American Chemical Society* **1972**, *94*, 4144-4151.

(216) Tulinsky, A. THE STRUCTURE OF FREE BASE PORPHINE: AN AVERAGE OF THREE INDEPENDENT STRUCTURES*. *Annals of the New York Academy of Sciences* **1973**, *206*, 47-69.

(217) Almlöf, J. Ab initio calculations on porphin. *International Journal of Quantum Chemistry* **1974**, *8*, 915-924.

(218) Ghosh, A.; Almlöf, J.; Gassman, P. G. Ab initio SCF studies of basis set effects in free base porphin. *Chemical Physics Letters* **1991**, *186*, 113-118.

(219) Almlof, J.; Fischer, T. H.; Gassman, P. G.; Ghosh, A.; Haeser, M. Electron correlation in tetrapyrroles: ab initio calculations on porphyrin and the tautomers of chlorin. *The Journal of Physical Chemistry* **1993**, *97*, 10964-10970.

(220) Butenhoff, T. J.; Moore, C. B. Hydrogen atom tunneling in the thermal tautomerism of porphine imbedded in a n-hexane matrix. *Journal of the American Chemical Society* **1988**, *110*, 8336-8341.

(221) Butenhoff, T. J.; Chuck, R. S.; Limbach, H. H.; Moore, C. B. Vibrational photochemistry of porphine imbedded in a hexane-d14 Shpol'skii matrix. *The Journal of Physical Chemistry* **1990**, *94*, 7847-7851.

(222) Limbach, H.-H.; Hennig, J.; Gerritzen, D.; Rumpel, H. Primary kinetic HH/HD/DH/DD isotope effects and proton tunnelling in double proton-transfer reactions. *Faraday Discussions of the Chemical Society* **1982**, *74*, 229-243.

(223) Braun, J.; Koecher, M.; Schlabach, M.; Wehrle, B.; Limbach, H.-H.; Vogel, E. NMR Study of the Tautomerism of Porphyrin Including the Kinetic HH/HD/DD Isotope Effects in the Liquid and the Solid State. *Journal of the American Chemical Society* **1994**, *116*, 6593-6604.

(224) Ghosh, A.; Almloef, J. Structure and Stability of *cis*-Porphyrin. *The Journal of Physical Chemistry* **1995**, *99*, 1073-1075.

(225) Naito, W.; Yasuda, N.; Morimoto, T.; Shigeta, Y.; Takaya, H.; Hisaki, I.; Maeda, H. Doubly *N*-Methylated Porphyrinoids. *Organic Letters* **2016**, *18*, 3006-3009.

(226) Thomas Kolle, E.; McCormick Laura, J.; Vazquez-Lima, H.; Ghosh, A. Stabilization and Structure of the *cis* Tautomer of a Free-Base Porphyrin. *Angewandte Chemie International Edition* **2017**, *56*, 10088-10092.

(227) Plumridge, T. H.; Waigh, R. D. Water structure theory and some implications for drug design. *Journal of Pharmacy and Pharmacology* **2002**, *54*, 1155-1179.

(228) Xantheas, S. S. Cooperativity and hydrogen bonding network in water clusters. *Chemical Physics* **2000**, *258*, 225-231.

(229) Snor, W.; Liedl, E.; Weiss-Greiler, P.; Karpfen, A.; Viernstein, H.; Wolschann, P. On the structure of anhydrous *β*-cyclodextrin. *Chemical Physics Letters* **2007**, *441*, 159-162.

(230) Stachowicz, A.; Styrcz, A.; Korchowiec, J.; Modaressi, A.; Rogalski, M. DFT studies of cation binding by *β*-cyclodextrin. *Theoretical Chemistry Accounts* **2011**, *130*, 939-953.

(231) Capar, J.; Zonneveld, J.; Berg, S.; Isaksson, J.; Gagnon, K. J.; Thomas, K. E.; Ghosh, A. Demetalation of copper undecaarylcorroles: Molecular structures of a free-base undecaarylisocorrole and a gold undecaarylcorrole. *Journal of Inorganic Biochemistry* **2016**, *162*, 146-153.

(232) Berg, S.; Thomas, K. E.; Beavers, C. M.; Ghosh, A. Undecaphenylcorroles. *Inorganic Chemistry* **2012**, *51*, 9911-9916.

(233) Vestfrid, J.; Botoshansky, M.; Palmer, J. H.; Durrell, A. C.; Gray, H. B.; Gross, Z. Iodinated Aluminum(III) Corroles with Long-Lived Triplet Excited States. *Journal of the American Chemical Society* **2011**, *133*, 12899-12901.

(234) Vestfrid, J.; Goldberg, I.; Gross, Z. Tuning the Photophysical and Redox Properties of Metallocorroles by Iodination. *Inorganic Chemistry* **2014**, *53*, 10536-10542.

(235) Sudhakar, K.; Mahammed, A.; Fridman, N.; Gross, Z. Iodinated cobalt corroles. *Journal of Porphyrins and Phthalocyanines* **2017**, *21*, 900-907.

(236) Soll, M.; Sudhakar, K.; Fridman, N.; Müller, A.; Röder, B.; Gross, Z. One-Pot Conversion of Fluorophores to Phosphorophores. *Organic Letters* **2016**, *18*, 5840-5843.

(237) Thomassen, I. K.; Vazquez-Lima, H.; Gagnon, K. J.; Ghosh, A. Octaiodoporphyrin. *Inorganic Chemistry* **2015**, *54*, 11493-11497.

(238) Rieke, R. D. Preparation of Organometallic Compounds from Highly Reactive Metal Powders. *Science* **1989**, *246*, 1260.

(239) Anding, B. J.; Ellern, A.; Woo, L. K. Olefin Cyclopropanation Catalyzed by Iridium(III) Porphyrin Complexes. *Organometallics* **2012**, *31*, 3628-3635.

(240) Shi, C.; Mak, K. W.; Chan, K. S.; Anson, F. C. Enhancement by surfactants of the activity and stability of iridium octaethyl porphyrin as an electrocatalyst for the four-electron reduction of dioxygen. *Journal of Electroanalytical Chemistry* **1995**, *397*, 321-324.

(241) Gärtner, F.; Denurra, S.; Losse, S.; Neubauer, A.; Boddien, A.; Gopinathan, A.; Spannenberg, A.; Junge, H.; Lochbrunner, S.; Blug, M.; Hoch, S.; Busse, J.; Gladiali, S.; Beller, M. Synthesis and Characterization of New Iridium Photosensitizers for Catalytic Hydrogen Generation from Water. *Chemistry – A European Journal* **2012**, *18*, 3220-3225.

(242) Cui, H.; Wang, Y.; Wang, Y.; Fan, Y.-Z.; Zhang, L.; Su, C.-Y. A stable and porous iridium(iii)-porphyrin metal-organic framework: synthesis, structure and catalysis. *CrystEngComm* **2016**, *18*, 2203-2209.

(243) Dairo, T. O.; Woo, L. K. Scope and Mechanism of Iridium Porphyrin-Catalyzed S–H Insertion Reactions between Thiols and Diazo Esters. *Organometallics* **2017**, *36*, 927-934.

(244) Cheung, C. W.; Fung, H. S.; Lee, S. Y.; Qian, Y. Y.; Chan, Y. W.; Chan, K. S. Reactivity Studies of Iridium(III) Porphyrins with Methanol in Alkaline Media. *Organometallics* **2010**, *29*, 1343-1354.

(245) Sinha, W.; Ravotto, L.; Ceroni, P.; Kar, S. NIR-emissive iridium(iii) corrole complexes as efficient singlet oxygen sensitizers. *Dalton Transactions* **2015**, *44*, 17767-17773.

(246) Palmer, J. H.; Mahammed, A.; Lancaster, K. M.; Gross, Z.; Gray, H. B. Structures and Reactivity Patterns of Group 9 Metallocorroles. *Inorganic Chemistry* **2009**, *48*, 9308-9315.

(247) Sheldrick, G. SHELXT - Integrated space-group and crystal-structure determination. *Acta Crystallographica Section A* **2015**, *71*, 3-8.

(248) Sheldrick, G. M. Crystal structure refinement with SHELXL. *Acta Crystallographica. Section C, Structural Chemistry* **2015**, *71*, 3-8.

Paper A

Paper B

Paper C